COORDINATION CHEMISTRY AND SOLUTION BEHAVIOUR OF GOLD(I) COMPLEXES

A thesis submitted to meet the requirements for the degree

PHILOSOPHIAE DOCTOR

in the

Department of Chemistry

Faculty of Natural and Agricultural Sciences

at the

University of the Free State

by

Zolisa Agnes Sam

Promoter

Prof. A. Roodt

November 2007

“How much better is to get wisdom than gold and to get understanding rather to be chosen than silver”

Proverbs 16:16

ACKNOWLEDGEMENTS

I would like to express my sincere gratitude to the Almighty Father for this precious life that He has given me and from whom we receive all grace:

There is a journey in this world
That I must take
And sometimes
There are victories to be won
Lord, give me power
Every hour
As I go through.

My sincere appreciation also goes to:

- Prof. Andreas Roodt for the supervision of the study and offering of valuable insights on the content of this project.

- Dr. Fanie Muller for his help with crystallography and the concepts involved.

- My grandmother (Mrs. E.L. Mateza, all praise to the Lord for giving us you as a blessing in the family), my parents (Mr. H.M. and Mrs. N.N. Sam), my sister Bulelwa and the entire family for their undying love and courageous support.

- Buyiswa Jacobs and Nomandla Vela for your friendship and for all the enjoyable times shared.

- My postgraduate colleagues at the Department of Chemistry for the inspiration and motivation.

- MINTEK's Project AuTek for financial assistance.

- Sofi Elmroth, the Swedish International Development Agency (SIDA), the Swedish Cancer Society and the Swedish Research Council (SKCE) for my research done at Lund University in Sweden.

- Prof. Connie Medlen and her group at the Pharmacology department, University of Pretoria.

Zolisa Sam

TABLE OF CONTENTS

ABSTRACT viii

OPSOMMING xi

LIST OF PUBLICATIONS FROM THIS STUDY xiv

ABBREVIATIONS AND SYMBOLS xv

CHAPTER 1

INTRODUCTION AND AIMS 1

1.1 Introduction 1
1.2 Research aims 5

CHAPTER 2

THEORY AND APPLICATIONS OF GOLD COMPLEXES 9

2.1 Introduction 9
2.2 Gold phosphine complexes and organometallic compounds 11
2.2.1 Introduction 11
2.2.2 Gold(I) phosphine complexes 12
2.2.3 Gold(III) phosphine complexes 14
2.2.4 Gold(I) ferrocenylphosphine complexes 15
2.2.5 Water-soluble phosphines 19
2.3 Chemotherapeutic applications of precious metals 23
2.3.1 Introduction 23
2.3.2 Inflammatory disorders 27
2.3.3 Gold(I) medicinal compounds 27
2.4 Reaction mechanisms in gold chemistry 31
2.5 Catalytic applications of gold 33

CHAPTER 3

MONODENTATE GOLD(I) SYSTEMS AND THEIR INTERACTION WITH LIGANDS AND CYCLODEXTRINS 43

3.1 Introduction 43

3.1.1 General Au(I) applications 43

3.1.2 Applications of cyclodextrins in drug delivery 44

3.2 Experimental 48

3.3 Synthesis of compounds and complexes 48

3.3.1 Synthesis of compounds 48

3.3.1.1 1,3,5-triaza-7-phosphatricyclo[3.3.1.$1^{3,7}$]decane (PTA) 48

3.3.1.2 (PTAMe)I 49

3.3.1.3 [Au(THT)Cl] 49

3.3.2 Synthesis of gold(I) complexes with PTA as ligand 50

3.3.2.1 [Au(PTA)Cl] 50

3.3.2.2 [Au(PTAMe)Cl]SO_3CF_3 50

3.3.2.3 [Au(PTA)SCN] 50

3.3.2.4 [Au(PTA)$SC(NH_2)_2$]Cl 51

3.3.2.5 [Au(PTA)$SC(NH_2)(NH(CH_3))$]Cl 51

3.3.3 Synthesis of gold(I) complexes with tertiary phosphine ligands 51

3.3.3.1 [Au(PEt_3)Cl] 51

3.3.3.2 [Au($AsEt_3$)Cl] 52

3.3.3.3 [Au(PPh_3)Cl] 52

3.3.4 Synthesis of auranofin analogues 53

3.3.4.1 Auranofin 53

3.3.4.2 PTA-auranofin 53

3.3.4.3 2,3,4,6-tetra-*O*-acetyl-1-thio-β-D-glucopyranosato (1-methyl-1,3,5-triaza-7-phosphatricyclo[3.3.1.$1^{3,7}$] decanium-*P*) gold(I) 54

3.3.4.4 2,3,4,6-tetra-*O*-acetyl-1-thio-β-D-glucopyranosato (triethylarsine) gold(I) 54

3.3.4.5 2,3,4,6-tetra-*O*-acetyl-1-thio-β-D-glucopyranosato (triphenylphosphine) gold(I) 55

3.3.5 Synthesis of 'host-guest' compounds with cyclodextrins 55

3.3.5.1 PTA-β-cyclodextrin inclusion complex 55

3.3.5.2 Attempted synthesis of auranofin-β-cyclodextrin inclusion complex 55
3.4 X-ray crystallography and inclusion complexes 56
3.4.1 PTA-β-cyclodextrin inclusion complex 58
3.4.2 Attempted X-ray crystal structure of auranofin inclusion complex into β-cyclodextrin 65
3.5 Equilibrium studies of chloride substitution from [Au(PTA)Cl] complexes with different S-donor ligands 69
3.5.1 Experimental 69
3.5.2 Spectroscopic studies of [Au(PTA)Cl] with various ligands 70
3.5.2.1 ^{31}P NMR study of chloride substitution by SCN^- from [Au(PTA)Cl] 70
3.5.2.2 ^{31}P NMR spectroscopic study of chloride substitution by thiourea from [Au(PTA)Cl] 72
3.5.2.3 ^{31}P NMR spectroscopic study of chloride substitution by methyl thiourea from [Au(PTA)Cl] 73
3.5.2.4 Summary of equilibrium constant determinations when the chloride is substituted by S-donor ligands from [Au(PTA)Cl] 75
3.5.2.5 ^{31}P NMR spectroscopic study of the effect of additional PTA on [Au(PTA)Cl] 75
3.6 Studies of inclusion of PTA and related gold(I) compounds into β-cyclodextrin 77
3.6.1 Experimental 77
3.6.2 NMR equilibrium study of PTA inclusion into β-cyclodextrin 78
3.6.2.1 ^{1}H NMR equilibrium constant determination of PTA inclusion into β-cyclodextrin 78
3.6.2.2 ^{31}P NMR equilibrium constant determination of PTA inclusion into β-cyclodextrin 79
3.6.3 ^{31}P NMR study of $(PTAMe)^+$ inclusion into β-cyclodextrin 81
3.6.4 ^{31}P NMR study of [Au(PTAMe)Cl]I inclusion into β-cyclodextrin 82
3.6.5 ^{31}P NMR study of inclusion of PPh_3 into β-cyclodextrin 84
3.6.6 ^{31}P NMR study of $[Au(dppe)_2]Cl$ inclusion into β-cyclodextrin 85
3.7 Conclusions 87

CHAPTER 4

CRYSTALLOGRAPHIC STUDY OF FERROCENYL P-DONOR GOLD(I) COMPLEXES 93

4.1 Introduction 93

4.2 Experimental 95

4.3 Synthesis of compounds and complexes 95

4.3.1 Synthesis of reactants and ligands 95

4.3.1.1 [Au(THT)Cl] 95

4.3.1.2 (*S*)-*N*,*N*-dimethyl-1-[(*R*)-1',2-bis(diphenylphosphino) ferrocenyl] ethylamine 96

4.3.1.3 (*R*)-1-[(*S*)-1',2-bis(diphenylphosphino)ferrocenyl] ethylacetate 96

4.3.1.4 Diphenylferrocenylphosphine 96

4.3.2 Synthesis of bis(diphenylphosphino) ferrocene Au(I) complexes 97

4.3.2.1 [$(AuCl)_2$(μ-dppf)] 97

4.3.2.2 [$(AuSCN)_2$(μ-dppf)] 97

4.3.2.3 [AuCl(μ-dppf)] 98

4.3.3 Synthesis of gold(I) complexes containing modified bis(diphenylphosphino) ferrocenyl ligands 98

4.3.3.1 [$(AuCl)_2$(μ-dppf-$CH(CH_3)N(CH_3)_2$)] 99

4.3.3.2 [$(AuSCN)_2$(μ-dppf-$CH(CH_3)N(CH_3)_2$)] 99

4.3.3.3 [AuCl(μ-dppf-$CH(CH_3)N(CH_3)_2$)] 100

4.3.3.4 [$(AuCl)_2$(μ-dppf-$CH(CH_3)$OAc)] 100

4.3.3.5 [$(AuSCN)_2$(μ-dppf-$CH(CH_3)$OAc)] 100

4.3.3.6 [AuCl(μ-dppf-$CH(CH_3)$OAc)] 101

4.3.4 Synthesis of the diphenylferrocenylphosphine gold(I) complex 101

4.3.4.1 [$Au(PPh_2Fc)Cl$] 101

4.4 X-ray structure determinations of ferrocene-type dinuclear gold(I) complexes 102

4.4.1 Crystal structure of [$(AuCl)_2$(μ-dppf-$CH(CH_3)N(CH_3)_2$)] 104

4.4.2 Crystal structure of [$(AuSCN)_2$(μ-dppf-$CH(CH_3)N(CH_3)_2$)] 107

4.4.3 Crystal structure of [$(AuCl)_2$(μ-dppf-$CH(CH_3)$OAc)] 110

4.4.4 Crystal structure of [$(AuSCN)_2$(μ-dppf-$CH(CH_3)$OAc)] 114

4.4.5 Crystal structure of [$(AuSCN)_2$(μ-dppf)] 119

4.5 Structural parameter correlations of similar gold(I) and other metal ferrocenyl complexes 122

CHAPTER 5

BIOCHEMICAL ACTIVITY OF AURANOFIN ANALOGUES 131

5.1 Introduction 131
5.2 Biological studies of auranofin and analogues 133
5.2.1 Cell assays 133
5.2.2 Chemiluminescence assays 133
5.3 Experimental 134
5.3.1 General 134
5.3.2 Cell line tests 135
5.3.3 Isolation of neutrophils and sample preparation for chemiluminescence studies 136
5.3.3.1 Isolation of neutrophils 136
5.3.3.2 Preparation of different samples for chemiluminescence experiments 137
5.4 Results and discussion 139
5.4.1 Cell line tests 139
5.4.2 Chemiluminescence assays 140
5.5 Conclusion 145
5.5.1 Cell line studies 145
5.5.2 Chemiluminescence studies 146

CHAPTER 6

SUBSTITUTION REACTIONS OF GOLD(I) TERTIARY PHOSPHINE COMPLEXES 148

6.1 Introduction 148
6.2 Experimental 149
6.2.1 Equilibrium studies 149
6.2.2 Kinetic studies 151
6.3 Results and discussion 152
6.3.1 Substitution of chloride from tertiary phosphine dinuclear gold(I) complexes by various entering ligands 152
6.3.1.1 Stability of the [$(AuCl)_2$(μ-dppf-$CH(CH_3)OAc$)] complex 152
6.3.1.2 Reaction of [$(AuCl)_2$(μ-dppf-$CH(CH_3)OAc$)] with L-cysteine 153

6.3.1.3 Substitution of chloride from [$(AuCl)_2$(μ-dppf-$CH(CH_3)OAc$)] with SCN^- 155
6.3.2 Stability evaluations of the gold(I) phosphine complexes by ^{31}P NMR 157
6.3.2.1 Stability of the [$(AuCl)_2$(μ-dppf-$CH(CH_3)N(CH_3)_2$)] complex as monitored by ^{31}P NMR 158
6.3.2.2 Stability of the [$(AuCl)_2$(μ-dppf-$CH(CH_3)OAc$)] complex as monitored by ^{31}P NMR 158
6.3.2.3 Stability of the [$Au(PPh_2Fc)Cl$] complex as monitored by ^{31}P NMR 159
6.3.3 ^{31}P NMR equilibrium studies of the chloride substitution from tertiary phosphine gold complexes by SCN^- 160
6.3.3.1 Stability of the [$(AuCl)_2$(μ-dppf-$CH(CH_3)OAc$)] complex with excess SCN^- as monitored by ^{31}P NMR 161
6.3.3.2 Study of equilibrium of chloride substitution by SCN^- from [$(AuCl)_2$(μ-dppf-$CH(CH_3)OAc$)] 162
6.3.3.3 Study of equilibrium of chloride substitution by SCN^- from [$(AuCl)_2$(μ-dppf-$CH(CH_3)N(CH_3)_2$)] 163
6.3.3.4 Study of equilibrium of chloride substitution by SCN^- from [$Au(PPh_2Fc)Cl$] 165
6.3.3.5 Study of equilibrium of chloride substitution by SCN^- from [$Au(PPh_3)Cl$] 166
6.3.4 Summary of equilibrium constant determinations 168
6.3.5 Kinetic investigations of S-donor ligand substitutions on mononuclear gold(I) phosphine complexes 168
6.3.5.1 Stability of the [$Au(PPh_3)Cl$] complex 169
6.3.5.2 Fast reaction kinetics of chloride substitution with SCN^- from the [$Au(PPh_3)Cl$] complex 169
6.3.6 Reaction scheme and rate law of mononuclear Au(I)-P complexes of the type [$Au(PPh_3)Cl$] 171
6.3.7 Substitution reactions of tertiary phosphine gold(I) complexes with ligands 172
6.3.7.1 Rate constant determinations when chloride is substituted from [$Au(PPh_3)Cl$] with SCN^- 173
6.3.7.2 Rate constant determinations when chloride is substituted from [$Au(PPh_3)Cl$] with dimethyl thiourea 175
6.4 Conclusions 177

CHAPTER 7

EVALUATION OF STUDY **182**

7.1 Introduction 182

7.2 Scientific relevance 182

7.3 Future aspects 186

APPENDIX **187**

A. Supplementary data for Chapter 3 and Chapter 6 188

A.1 Crystal data of PTA-β-Cyclodextrin 188

A.2 Crystal data of 2,3,4,6-tetra-*O*-acetyl-1-thio-β-D-glucopyranosato (triethylphosphine)gold(I) (auranofin) 199

A.3 Supplementary material for equilibrium constant determinations reported in Chapter 3 203

A.4 Supplementary material for equilibrium constant determinations reported in Chapter 6 205

A.5 Supplementary material for rate constant determinations reported in Chapter 6 205

A.6 Derivation of equations used in the equilibrium constant determinations for Chapters 3 and 6 207

A.6.1 Equation used when mononuclear gold(I) complexes are reacted with various ligands 207

A.6.2 Equation used when dinuclear gold(I) complexes are reacted with various ligands 209

A.6.3 Equation used when guest ligands and gold(I) complexes are included into β-cyclodextrin 212

B. Supplementary crystallographic data for Chapter 4 215

B.1 Crystal data of $[(AuCl)_2(\mu\text{-dppf-CH}(CH_3)N(CH_3)_2)]$ 215

B.2 Crystal data of $[(AuSCN)_2(\mu\text{-dppf-CH}(CH_3)N(CH_3)_2)]$ 221

B.3 Crystal data of $[(AuCl)_2(\mu\text{-dppf-CH}(CH_3)OAc)]$ 227

B.4 Crystal data of $[(AuSCN)_2(\mu\text{-dppf-CH}(CH_3)OAc)]$ 238

B.5 Crystal data of $[(AuSCN)_2(\mu\text{-dppf})]$ 244

ABSTRACT

The aim of this study was to extend the knowledge base of gold(I) coordination chemistry and investigate the substitution behaviour of these complexes with sulphur-donor ligands. The water-soluble and air-stable ligand 1,3,5-triaza-7-phosphatricyclo[3.3.1.1^{3,7}]decane (PTA) with low steric demand was employed in the synthesis of the various complexes in this study. The [Au(PTA)Cl] complex was reacted with S-donor ligands such as SCN^-, thiourea and methyl thiourea and the equilibrium constant determination was done using ^{31}P NMR by monitoring the chemical shift change when stoichiometric amounts of the ligand are added to the [Au(PTA)Cl] solution. The equilibrium constants obtained were 0.070(6), 4.191(1) and 6.734(3) for SCN^-, thiourea and methyl thiourea as entering ligands, respectively.

The X-ray crystal structure of the inclusion of the PTA 'guest' molecule into the 'host' β-cyclodextrin (β-CD) was determined. The PTA-β-CD·8H_2O inclusion compound crystallises in the monoclinic space group $P2_1$ with eight solvent water molecules in an asymmetric unit and was refined to a final *R* value of 4.35%. The packing within the PTA-β-CD·8H_2O inclusion compound is of a 'herring-bone' type motif. An attempt to include auranofin {[Au(PEt_3)(Sgluc)]; Sgluc = thioglucose} into the cavity of the β-cyclodextrin resulted in only auranofin crystallising without being included. However, since the data collection for the auranofin compound was done at 100 K, careful observations in parameters such as selected torsion and bond angles were noted to have 1-4° changes as compared to the known auranofin structure investigated at room temperature, which clearly indicated a phase change and a new polymorph at 100 K. The pure auranofin compound investigated in this study crystallises in the monoclinic space group $P2_1$ and was refined to a final *R* value of 1.59%.

Further study of the interactions of β-cyclodextrin with PTA and related ligands and gold(I) complexes in this study was investigated with NMR spectroscopy. This was done by the determination of the equilibrium constant when these complexes are included into the β-cyclodextrin. The equilibrium constants calculated for PTA, $(PTAMe)^+$ and PPh_3 were 8.7(1) x 10^2 and 23(4) and 10(6) M^{-1}, respectively, while for the [Au(PTAMe)Cl] and [Au$(dppe)_2$]Cl equilibrium constants of 23(5) and 6(1) M^{-1} were

obtained. The PTA ligand clearly showed the largest 'host-guest' stability. The solubility of the phenyl compounds, following the inclusion, was not improved that much as compared to the PTA compounds which may be due to steric hindrance and orientation of the phenyl groups being too large to be incorporated into the β-cyclodextrin. This phenomenon is also noted in the unsuccessful incorporation of auranofin which may be due the orientation of the ethyl groups into β-cyclodextrin.

In an attempt to increase the solubility of these gold(I) complexes, bidentate P-donor ligand systems with a bridging ferrocene group, functionalised by hydrophilic moieties, were synthesised. These complexes were unambiguously characterised by X-ray crystallography. The following dinuclear gold(I) crystal structures are reported, with their general crystal data reported in parenthesis:

$[(AuCl)_2(\mu\text{-dppf-CH}(CH_3)N(CH_3)_2)]$ (Monoclinic, $P2_1/n$, R = 4.94%)

$[(AuSCN)_2(\mu\text{-dppf-CH}(CH_3)N(CH_3)_2)]$ (Triclinic, $P\bar{1}$, R = 5.76%)

$[(AuCl)_2(\mu\text{-dppf-CH}(CH_3)OAc)]$ (Orthorhombic, Pbca, R = 4.09%)

$[(AuSCN)_2(\mu\text{-dppf-CH}(CH_3)OAc)]$ (Triclinic, $P\bar{1}$, R = 4.36%)

$[(AuSCN)_2(\mu\text{-dppf})]$ (Monoclinic, $C2/c$, R = 2.36%)

The SCN^- ligand in the thiocyanato gold(I) dppf structures coordinated to the soft Au(I) metal centre *via* the softer S atom. An interesting factor was the isomorphism identified for the two $[(AuSCN)_2(\mu\text{-dppf-CH}(CH_3)N(CH_3)_2)]$ and $[(AuSCN)_2(\mu\text{-dppf-CH}(CH_3)OAc)]$ structures while the structure for the $[(AuSCN)_2(\mu\text{-dppf})]$ compound was interlinked by short Au…Au contacts of 2.9798(7) Å of which none were observed for the other structures.

Auranofin and its derivative compounds such as PTA-auranofin, PTAMe-auranofin and triethylarsine-auranofin were utilised and tested for biological activity against cancer cell lines. Furthermore, a preliminary chemiluminescence assay was done with the compounds at three different concentrations (0.3, 3.1 and 12.5 μM for each compound) to determine their effect on the chemiluminescence of isolated blood neutrophils. The auranofin compound was included in the investigations as reference. The A2780 human ovarian cancer cell lines are the most sensitive to all derivatives while the arsine-auranofin compound showed good activity against A2780 human ovarian cancer cell lines with an IC_{50} of only about 0.0076 μg/mL. Generally, auranofin and arsine-auranofin gave results closely related to each other with arsine-auranofin having higher toxicity to other cells whereas PTA-auranofin and PTAMe-auranofin showed more

correlation to each other and had less activity. For the preliminary chemiluminescence assays it can be mentioned that for all auranofin derivatives, at low concentrations the compounds act as stimulants to the neutrophil chemiluminescence activity and at higher concentrations the compounds act as inhibitors to neutrophil activity.

Complex substitution behaviour was observed for selected gold(I) dinuclear {[$(AuCl)_2$(μ-dppf-$CH(CH_3)OAc$)]} and mononuclear systems {[Au(PX)Cl]; X = Ph_3 or Ph_2Fc} when the chloride is substituted with ligands such as L-cysteine and SCN^- as studied by UV-Vis and ^{31}P NMR. Furthermore, fast reaction kinetics for the chloride substitution with ligands such as SCN^- and dimethylthiourea from the mononuclear [$Au(PPh_3)Cl$] complex was investigated with stopped-flow techniques. The overall rate constants for the substitutions from [$Au(PPh_3)Cl$] with SCN^- and dimethyl thiourea representing the forward reactions were obtained as k_1 = 13(1) and 2.17(1) x 10^3 $M^{-1}s^{-1}$ respectively. Thus, it was concluded that chloride substitution reactions on linear gold(I) systems are extremely fast reactions.

Keywords:

Gold(I) complexes; 1,3,5-triaza-7-phosphatricyclo[3.3.1.$1^{3,7}$]decane; β-cyclodextrin; substitution; S-donor ligands; equilibrium constant; ferrocenyl phosphine; X-ray crystal structure; auranofin.

OPSOMMING

Die doel van hierdie ondersoek was om die kennis tov die koordinasiechemie van goud(I) komplekse uit te brei deur die substitusiegedrag van ‘n reeks komplekse met swaweldonoratoomligande te ondersoek. Die wateroplosbare en lugstabiele ligand, 1,3,5-triaza-7-fosfatrisiklo[3.3.1.1^{3,7}]dekaan (PTA) wat ‘n klein steriese parameter het, is gebruik om enkele monomeriese komplekse te berei. Die [Au(PTA)Cl] kompleks is met S-donorligande soos SCN^-, tioureum en metieltioureum gereageer en die ewewigskonstantes vir die chloriedsubstitusie is mbv ^{31}P NMR bepaal deur die verandering in chemiese verskuiwing as ‘n funksie van bygevoegde ligand te bepaal. Ewewigskonstantes van 0.070(6), 4.191(1) en 6.734(3) is onderskeidelik vir SCN^-, tioureum en metieltioureum as inkomende ligande, verkry.

Die X-straalkristalstruktuur van die insluiting van die PTA gasentiteit in die β-siklodekstrien (β-CD) gasheer, is bepaal. Die PTA-β-CD·8H_2O insluitingkompleks kristalliseer in die monokliniese ruimtegroep met agt solvaatwatermolekule in ’n asimmetriese eenheid en het verfyn na ’n *R*-waarde van 4.35%, met ’n visgraattipe pakkingspatroon. In ’n poging om ook die auranofin {[Au(PEt_3)(Sgluk)]; Sgluk = tioglukose} binne die β-siklodekstrien as inslutingsproduk te verkry was onsuksesvol, en slegs die auranofinmolekuul het gekristalliseer. Nadat die kristaldata-opname by 100 K gedoen is, het dit geblyk dat daar betekenisvolle verskille in sekere bindingsparameters, van 1 tot 4° in sekere gevalle van die kamertemperatuuropname verskil, bestaan, en het bevestig dat ‘n nuwe polimorf van auranofin by 100 K bestaan. Die suiwer auranofin hier genoem kristalliseer in die monokliniese ruimtegroep $P2_1$ en het verfyn tot ‘n finale *R*-waarde van 1.59%.

Verdere interaksies van die β-siklodekstrien met PTA, verwante ligande en goud(I) komplekse, is met behulp van KMR spektroskopie ondersoek deur die ewewigskonstantes van hierdie prosesse te bepaal. Waardes van 8.7(1) x 10^2, 23(4) en 10(6) M^{-1} vir PTA, $(PTAMe)^+$ en PPh_3 onderskeidelik verkry, terwyl die [Au(PTAMe)Cl] en [Au$(dppe)_2$]Cl ewewigskonstantes van 23(5) en 6(1) M^{-1} gelewer het. Die PTA insluitingskompleks was dus duidelik die stabielste. Die oplosbaarheid van die verbindings is nie noemenswaardig deur die byvoeging van die sikliese suiker verbeter

nie, moontlik as gevolg van steriese faktore en gepaardgaande swak interaksie met die β-siklodekstrien, terwyl die etielgroepe in auranofin waarskynlik soortgelyke afstotende eienskappe vertoon.

In ‘n poging om die oplosbaarheid van hierdie fosfienkomplekse te verbeter, is bimetaalkomplekse met ferroseenbrugligande gesintetiseer. Hidrofiliese water-oplosbare entiteite is aan die ferroseengroep geheg. Hierdie komplekse is eenduidig met behulp van X-straalkristallografie gekarakteriseer, en is soos volg (algemene kristaldata in hakies):

$[(AuCl)_2(\mu$-dppf-$CH(CH_3)N(CH_3)_2)]$ (Monoklinies, $P2_1/n$, R = 4.94%)

$[(AuSCN)_2(\mu$-dppf-$CH(CH_3)N(CH_3)_2)]$ (Triklinies, $P\bar{1}$, R = 5.76%)

$[(AuCl)_2(\mu$-dppf-$CH(CH_3)OAc)]$ (Ortorombiies, Pbca, R = 4.09%)

$[(AuSCN)_2(\mu$-dppf-$CH(CH_3)OAc)]$ (Triklinies, $P\bar{1}$, R = 4.36%)

$[(AuSCN)_2(\mu$-dppf)] (Monoklinies, $C2/c$, R = 2.36%)

Die SCN^- ligand in die tiosianato goud(I) dppf strukture koordineer aan die sagte Au(I) metaalsenter via die sagte swawelatoom. ‘n Interessante waarneming is dat die twee $[(AuSCN)_2(\mu$-dppf-$CH(CH_3)N(CH_3)_2)]$ en $[(AuSCN)_2(\mu$-dppf-$CH(CH_3)OAc)]$ strukture isomorf aanmekaar is, terwyl die $[(AuSCN)_2(\mu$-dppf)] verbinding intermolekulêre Au…Au kontakafstande van 2.9798(7) Å, wat nie in enige van die ander strukture bestaan nie, toon.

Auranofin en sy derivate soos die genoemde PTA-auranofin, PTAMe-auranofin en trietielarsienauranofin se biologiese aktiwiteit teen kankerselle is bepaal. Hierdie verbindings se chemiluminisensie is by drie konsentrasies (0.3, 3.1 en 12.5 μM vir elke verbinding) ook evalueer om die effek van inhibering op geïsoleerde bloedneutrofiele te bepaal met auranofin as verwysing. Die A2780 menslike ovariumkanker sellyne was die mees sensitiefste en die arsien-auranofin het baie goeie aktiwiteit getoon met ‘n IC_{50} van slegs 0.0076 μg/mL. In die algemeen het auranofin en arsien-auranofin soortgelyke resultate gelewer, maar die arsienkompleks het groter toksisiteit teen ander selle getoon. PTA-auranofin en PTAMe-auranofin, aan die ander kant, het baie laer aktiwiteit getoon. In die chemiluminesensiemetings het al die auranofinverbindings by lae konsentrasies as neurofiliese stimulante opgetree maar as inhibeerders by hoër konsentrasies.

OPSOMMING

Komplekse substitusiegedrag van die chloriedligand is waargeneem vir geselekteerde goud(I) bimetaal {[$(AuCl)_2$(μ-dppf-$CH(CH_3)OAc$)]} en monokernige {[Au(PX)Cl]; X = Ph_3 of Ph_2Fc} komplekse met ligande L-sisteïn en SCN^- soos deur UV-sigbare en ^{31}P KMR bestudeer. Baie vinnige reaksietempo's is vir die chloriedsubstitusie van die [$Au(PPh_3)Cl$] kompleks met ligande soos SCN^- en dimetieltioureum met behulp van stopvloeispektrofotometrie waargeneem. Die tempokonstantes vir die voorwaartse reaksies vir hierdie chloriedsubstitusie deur SCN^- en dimetieltioureum is k_1 = 13(1) en 2.17(1) x 10^3 $M^{-1}s^{-1}$ onderskeidelik, bepaal. Dit is dus duidelik dat hierdie tipe reaksies baie vinnig plaasvind.

Sleutelwoorde:

Goud(I) komplekse; 1,3,5-triaza-7-fosfatrisiklo[3.3.1.$1^{3,7}$]dekaan; β-siklodekstrien; substitusie; S-donor ligande; ewewigskonstante; ferrosenielfosfien; X-straal kristalstruktuur; auranofin.

LIST OF PUBLICATIONS FROM THIS STUDY

1. [$(AuSCN)_2$(μ-dppf-$CH(CH_3)N(CH_3)_2$)]: Z.A. Sam, S.K.C. Elmroth, A. Roodt, A.J. Muller, *Acta Cryst.*, 2006, **E62**, m1699.

2. [$(AuCl)_2$(μ-dppf-$CH(CH_3)N(CH_3)_2$)]: Z.A. Sam, Å. Oskarsson, S.K.C. Elmroth, A. Roodt, *Acta Cryst.*, 2005, **E61**, m2090.

ABBREVIATIONS AND SYMBOLS

δ	chemical shift
ν	stretching frequency on IR
Ac	acetyl
Ar	aryl
^{t}Bu	*tert*-butyl
β-CD	β-cyclodextrin
CO	carbonyl
Cp	η^5-C_5H_5
Cy	cyclohexyl
CyS^-	cysteinato
d	doublet
dd	doublet of doublets
D-H…A	donor, acceptor hydrogen interaction
dien	diethylenetriamine
DMARDs	disease modifying anti-rheumatic drugs
DNA	deoxyribonucleic acid
dppe	1,2-bis(diphenylphosphino)ethane
dppf	1,1'-bis(diphenylphosphino)ferrocene
dt	doublet of a triplet
dq	doublet of a quartet
EDTA	Ethylenediaminetetraacetic acid
Et	ethyl
Fc	ferrocenyl
Hz	Hertz
^{i}Pr	isopropyl
IR	infra-red
K	equilibrium constant
k_{obs}	observed pseudo first-order rate constant
L	neutral ligand
L,L-Bid	bidentate ligand

m	multiplet
Me	methyl
MRI	magnetic resonance imaging
nbd	norbornadiene
$^{n}J_{x-y}$	n^{th}-order coupling between nuclei x and y
NMR	nuclear magnetic resonance
OEt	ethoxy
OTf	triflate
o-tolyl	*ortho*-tolyl
PGM	platinum group metal
Ph	phenyl
ppm	parts per million – Unit of chemical shift
PTA	1,3,5-triaza-7-phosphatricyclo[3.3.1.1^{3,7}]decane
q	quartet
R	monoanionic ligand (R = H^-, Me^- or Ph^-)
s	singlet
SMe_2	dimethyl sulphide
T	temperature
t	triplet
td	triplet of doublets
THT	tetrahydrothiophene
TMEDA	*N*,*N*,*N*',*N*'-tetramethylethylenediamine
tt	triplet of triplets
Tu	thiourea
UV-Vis	ultraviolet-visible

1 INTRODUCTION AND AIMS

1.1 INTRODUCTION

Since earlier times humans have long been aware of the use of gold, and man has linked the lustre of gold with the warm, life-giving light of the sun. Gold is perhaps the most beautiful of the chemical elements and has been known and treasured by man since times began. In its massive and pure form, it is a soft, yellow metal with the highest ductility and malleability of any element. The beauty and rarity of gold has led to its employment in jewellery, coinage and as a standard for monetary systems throughout the world. Since gold is such a soft metal, it is usually alloyed to give it more strength. In these alloys, the term carat is used to express the amount of gold present, 24 carats being pure gold. Gold also has high thermal and electrical conductivity, hence its use in electronics. The high cost necessitates the use of very thin films, formed by electroplating on a base metal support, for gold switching devices. Electrolysis of solutions containing $[Au(CN)_2]^-$ is widely used to recover gold from solution (electrowinning)[1], *i.e*. in the mining industry. The process is also used to deposit gold coverings for electrons (*e.g*. printed circuit boards, electrical connectors) and recently for hip and shoulder joint replacement surgery.

The most in depth area of study of the coordination chemistry of gold revolves around organometallic chemistry[2,3,4], unusual oxidation states and stereochemistries[5,6], bioinorganic chemistry of gold with reference to the treatment of rheumatoid arthritis (chrysotherapy)[7,8,9], and the synthesis and properties of gold clusters and other complexes with gold-metal bonds[5,10]. Research on gold has also been assisted by the applications of spectroscopic techniques and the routine determination of structures by X-ray crystallography. Gold compounds are most readily classified according to the oxidation state of the metal which exist from state –I to +V. The metal shows a definite preference for two oxidation states namely +I and +III. Oxidation state –I is known in compounds like CsAu while the +II and +IV states are very rare for gold and the +V state only occurs in fluoride complexes like AuF_5 and $[AuF_6]^-$, which are very powerful oxidising agents[11].

The chemistry of metallic gold has been highly valued since the earlier times but its chemical compounds have not been thoroughly studied as compared to those of other rare metals. The phenomenon of gold in medicine dates back to antiquity with early physicians using gold preparations to treat a variety of ailments. Throughout ancient history most major civilisations attributed medicinal character to gold.

Bioinorganic chemistry with medicinal applications is an ever developing field. This offers the potential for the design of new therapeutic and diagnostic agents and a review on gold drug mechanisms has been published[12] and hence there is a great potential in transition metals for employment in medicine for the treatment and understanding of diseases which are currently refractory as illustrated in Fig. 1.1.

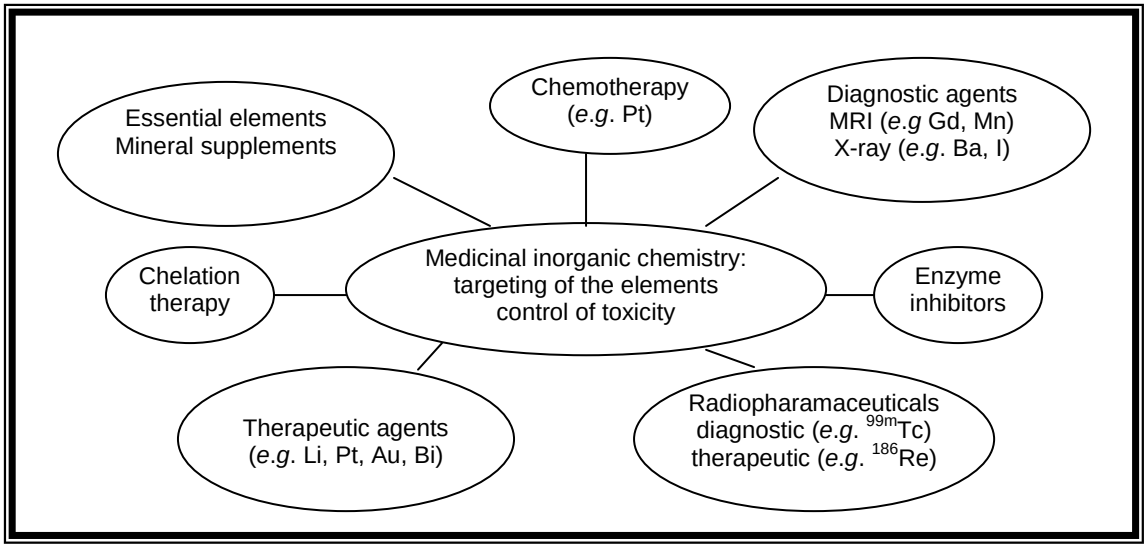

Figure 1.1 Elements employed in some of the key areas in bioinorganic chemistry[13].

Chrysotherapy, the use of gold compounds in medicine, refers to the fact that gold compounds, usually gold thiolates, are used clinically in the alleviation of the symptoms associated with rheumatoid arthritis. Koch demonstrated the bacteriostatic effects of $[Au(CN)_2]^-$ thereby providing a scientific basis for the pharmacological activity of gold compounds, such as gold thiolates, which have been used in the treatment of rheumatoid arthritis[14]. Recent areas of interest with respect to gold compounds have been their potential anti-tumour activity and perhaps more recently their anti-HIV activity[15].

The treatment of a variety of cancers by cisplatin, *cis*-$[Pt(NH_3)_2Cl_2]$, has instigated the on-going investigations of alternative metal-based drugs. The initial discovery of the anti-tumour activity of platinum complexes was made by Barnett Rosenberg's[16]

research group in the 1960's. They were studying the effects of an electric current passed over platinum electrodes immersed in a solution containing *Escherichia coli* cells that were growing in the presence of an ammonium chloride buffer. Interesting enough was that cell growth continued but division of the cells was greatly inhibited. It was found from tests that followed that the platinum had reacted with NH_4Cl to form an active compound, *cis*-$[Pt(NH_3)_2Cl_2]$ (cisplatin) of which the synthesis[17] and structure were well known at the time. Tests were done on cisplatin proving that it has beneficial effects on the treatment of cancer[18,19]. The biological activity results from binding to the DNA, thus inhibiting replication. Today, cisplatin is used in combination with other anticancer agents and is effective against testicular and ovarian carcinomas, bladder cancer and tumours of the head and neck.

Anti-cancer drugs have many side effects, like renal toxicity for cisplatin, which then restrict them to limited doses. Damage to bone marrow causes anaemia, which is an inability to fight infections and a tendency to internal bleeding. Other side effects include vomiting, diarrhoea, nausea, hair loss and neurological complications. Another drawback that can be encountered in using drugs is the fact that the tumour can develop resistance to other drugs after the first administration.

In an attempt to reduce the toxic side effects new research investigations were made and a new gold complex, 2,3,4,6-tetra-*O*-acetyl-1-thio-β-D-glucopyranosato (triethylphosphine) gold(I) (auranofin, Fig. 1.2) was developed.

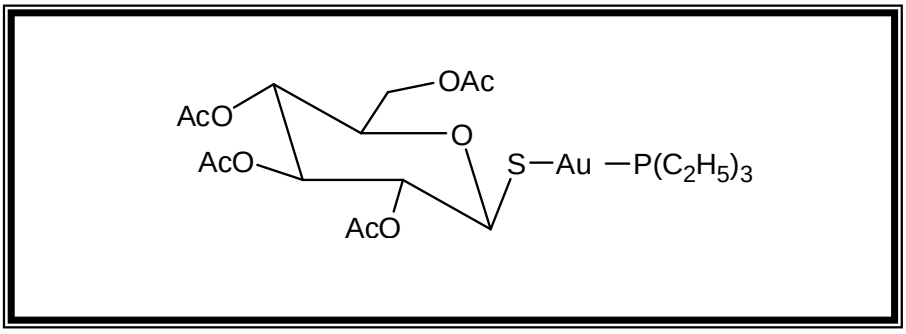

Figure 1.2 A drawing representing the structure of auranofin.

Auranofin is an experimental chrysotherapeutic agent shown by the research groups involved[20,21] to be clinically effective in the treatment of rheumatoid arthritis when administered orally. They showed that auranofin exhibited a unique pharmacological profile when compared with the earlier injectable gold preparations, gold sodium thiomalate (Myochrisin) and gold thioglucose (Solganol). Auranofin is a lipid-soluble,

linear, two-coordinate complex. It is monomeric and has been well characterised including a structure determined by X-ray crystallography[22]. There were still some toxic side effects however, including severe gastrointestinal problems which are not present with other gold drugs and therefore, modification of the drug in an attempt to eliminate these side effects would be useful and of prime importance.

An important discovery in the area of water-soluble phosphine ligands was that of the 1,3,5-triaza-7-phospha-tricyclo[3.3.1.1^{3,7}]decane (PTA)[23] ligand. This ligand is stable in air, water-soluble and has low steric demand. It has good electron donating capabilities and a small cone angle, which induces less steric strain at the metal centre and can also be functionalised with methyl or other R-groups at the nitrogen atom sites. The interest shown in PTA as a ligand is mainly from its catalytic utilisation and in addition, also possible medical applications. The ability of this phosphine to form stable organic derivatives[24] which leave the donor ability of the phosphorus atom intact, suggests that fine tuning of useful properties of the metal complexes may be possible.

The employment of organometallic ligands such as ferrocenylphosphines provides a convenient route to the synthesis of heterometallic complexes and further evaluation of systems with the Au-P bond. Added to this is the known anticancer activity of 1,1'-bis(diphenylphosphino)ferrocenes and their bis(gold(I)) complexes[25].

Pharmaceutical industries employed cyclodextrins and their derivatives in drugs for complexation, as additives or tablet ingredients to improve physical and chemical properties or to enhance bioavailability of poorly soluble drugs[26,27]. The 'host-guest' chemistry displayed by the cyclodextrins is an interesting potential field to study with gold complexes incorporating *e.g.* PTA as a ligand to evaluate the possibility of reducing side effects of the drug. The cyclodextrins and their chemically modified derivatives have been the subject of numerous investigations of which recent interest in the use of these cyclodextrins for various purposes has generated a number of papers containing information pertinent to the synthesis and reactions of these useful compounds[28]. Principal applications of cyclodextrins have been on the area of enzyme modelling and catalysis[29,30] (to improve the selectivity of reactions as well as for the separation and purification of industrial-scale products). The widespread utilisation of cyclodextrins in pharmaceutical, food, chemical and other industrial areas[31] has also been noted. In the food cosmetics, toiletry and tobacco industries, cyclodextrins have been widely used either for the stabilisation of flavours and fragrances or for the elimination of undesired tastes or microbial contaminations[32].

1.2 RESEARCH AIMS

As mentioned above, the recent history of metal-containing anti-tumour agents began with the detection of anti-tumour properties for the inorganic compound, *cis*-diamminedichloro platinum(II)[16] (cisplatin, *cis*-[$Pt(NH_3)_2Cl_2$]) in the late 1960's. Platinum complexes are now amongst widely used drugs for the treatment of cancer[33,34]. The orally active Au(I) complex auranofin has a well defined linear two-coordinate structure[35]. The discovery that auranofin had activity against HeLa cells *in vitro* and P388 leukemia cells *in vivo*[36] led to the wide research in the development of other gold based complexes.

The current study commenced by conducting thorough literature research gathering applicable theoretical information and thus formulating practical work. As mentioned above, much research with regard to the coordination chemistry and biological activity of metal complexes is necessary to understand the *in vivo* behaviour thereof.

The prime aim of this study therefore was to extend the knowledge base of gold(I) coordination chemistry. The stepwise aims of the research for this study can thus be formulated as follows:

- Synthesis of gold(I) complexes containing 1,3,5-triaza-7-phospha-tricyclo[3.3.1.$1^{3,7}$] decane (PTA) and its alkylated analogue, sulphur donor ligands *e.g*. SCN^-, thiourea and its methylated analogue and biological ligands such as L-cysteine, methionine, *etc*.

- Investigate stability and reactivity of the complexes in various media and evaluating the mechanism and rates of substitution or decomposition reactions.

- Synthesis and characterisation of gold(I) complexes with monodentate and bidentate ferrocene type ligands for improved solubility due to functionality. Comparison of the gold ferrocenyl complexes when stoichiometric amounts of ligand to amount of gold are varied *i.e.* 1:1 and 1:2 complexes.

- Study of solid and solution states by NMR, UV-Vis and X-ray crystallography and detailed characterisation of the complexes.

- Synthesis of auranofin and its analogues using PTA and methylated PTA and interchanging the phosphine moiety of the auranofin with triethylarsine forming the arsine analogue.

- Study of inclusion interactions of the synthesised gold(I) complexes and related compounds with cyclodextrins for possible stability, protection in biological environment and increased solubility.

- Evaluate the biochemical activity of selected compounds towards arthritis, selected cancer strains and tuberculosis, where relevant.

[1] (a) F. Simon, *Gold Bull.,* 1993, **26**, 14.
(b) C. Bocking, I.R. Christie, *Interdisc. Sci. Rev.,* 1992, **17**, 239.

[2] H. Schmidbaur, 'Gold-Organic Compounds', Gmelin Handbook, Springer-Verlag, Berlin, 1980.

[3] R.J. Puddephatt, In 'Comprehensive Organometallic Chemistry'; G. Wilkinson, F.G.A. Stone, E.W. Abel, Eds.; Pergamon, 1982, chap 15.

[4] G.K. Anderson, *Adv. Organomet. Chem.,* 1982, **20**, 39.

[5] H. Schmidbaur, K.C. Dash, *Adv. Inorg. Chem. Radiochem.,* 1982, **25**, 239.

[6] P.G. Jones, *Gold Bull.,* 1981, **14**, 102; 1981, **14**, 159; 1983, **16**, 114.

[7] 'Bioinorganic Chemistry of Gold Coordination Compounds'; B.M. Sutton, R.G. Franz, Eds.; Smith, Kline and French, Philadelphia, 1983.

[8] A.J. Lewis, D.T. Walz, *Prog. Med. Chem.,* 1982, **19**, 1.

[9] D.H. Brown, W.E. Smith, *Chem. Soc. Rev.,* 1980, **9**, 217.

[10] J.J. Steggerda, J.J. Bour, J.W.A. van der Velden, *Recl. Trav. Chim. Pays-Bas,* 1982, **101**, 164.

[11] K. Leary, N. Bartlett, *J. Chem. Soc., Chem Commun.,* 1972, 903.

[12] S.L. Best, P.J. Sadler, *Gold Bull.,* 1996, **29**, 87.

[13] Z. Guo, P.J. Sadler, *Angew. Chem. Int. Ed.,* 1999, **38**, 1512.

[14] R. Koch, *Deutsche med. Wochenschr.,* 1927, **16**, 756.

[15] T. Okada, B.K. Patterson, S.-Q. Ye, M.E. Gurney, *Virology,* 1993, **192**, 631.

[16] B. Rosenberg, L. van Camp, J.E. Trosko, V.H. Mansour, *Nature,* 1969, **22**, 385.

[17] M. Peyrone, *Ann. Chem. Pharm.,* 1844, **LI**, 1.

[18] 'Platinum Coordination Complexes in Cancer Chemotherapy'; M.P. Hacker, E.B. Douple, I.H. Krakoff, Eds.; Martinus Nijhoff: Boston, 1984.

[19] J. Reedijk, P.H.M. Lohman, *Pharm. Week. Sci. Ed.*, 1985, **7**, 173.

[20] A.E. Finkelstein, D.T. Walz, U. Batista, M. Mixraji, F. Roisman, A. Misher, *Ann. Rheum. Dis.,* 1976, **35**, 251.

[21] F.E. Berglof, K. Berglof, D.T. Walz, *J. Rheum.,* 1978, **5**, 68.

[22] D.T. Hill, B.M. Sutton, *Cryst. Struct. Commun.,* 1980, **9**, 679.

[23] D.J. Daigle, A.B. Pepperman Jr., S.L. Vail, *J. Heterocyclic Chem.,* 1974, **17**, 407.

[24] D.J. Daigle, A.B. Pepperman Jr., *J. Heterocyclic Chem.,* 1975, **12**, 579.

[25] C.K. Mirabelli, B.D. Jensen, M.R. Mattern, C. Mei Sung, S.-M. Mong, D.T. Hill, S.W. Dean, P.S. Schein, R.K. Johnson, S.T. Crooke, *Anti-Cancer Drug Des.,* 1987, **1**, 223.

[26] T.S. Jones, D.J.W. Grant, J. Hadgraft, G. Tarr, *Acta Pharm. Tech.,* 1984, **30**, 263.

[27] J. Szejtli, 'Controlled Drug Bioavailability'; W.F. Smolen, L.A. Ball, Eds.; Wiley-VCH, Weinheim, 1985.

[28] D. Hreczuk-Hirst, D. Chicco, L. German, R. Duncan, *Int. J. Pharm.,* 2001, **230**, 57.

[29] M.L. Bender, M. Komiyama, 'Cyclodextrin Chemistry', Springer-Verlag, Berlin, 1978.

[30] I. Tabushi, *Acc. Chem. Res.,* 1982, **15**, 66.

[31] J. Szejtli, 'Cyclodextrin Technology', Kluwer Academic Publishers, Boston, 1988.

[32] M. Okada, *New Food Ind. (Jpn.),* 1984, **26**, 22.

[33] 'Platinum and Other Coordination Complexes in Cancer Chemotherapy 2'; H.M. Pinto, J.H. Schornagel, Eds.; Plenum, New York, 1996.

[34] 'Cisplatin - Chemistry and Biochemistry of a Leading Anticancer Drug'; B. Lippert, Ed.; Wiley-VCH, Weinheim, 1999.

[35] B.M. Sutton, *ACS Symp. Ser.,*1983, **209**, 371.

[36] T.M. Simon, D.H. Kunishima, G.J. Vibert, A. Lorber, *Cancer Res.,* 1981, **41**, 94.

2 THEORY AND APPLICATIONS OF GOLD COMPLEXES

2.1 INTRODUCTION

Living organisms range from simple unicellular organisms to sophisticated multi-cellular and highly organised animals such as humans. Within each cell there is a complex, interactive series of chemical reactions involving both the synthesis of new molecules and breakdown of others[1]. Within this plethora of biochemical and physiological events inorganic elements play a vital and fundamental role. Metals, and hence inorganic chemistry, are therefore essential for the normal functioning of living organisms. Metals have also structural, communication and active functional roles. Most of the elements of the Periodic Table up to and including bismuth (Z = 83) are potentially useful in the design of new drugs and diagnostic agents[2,3,4].

Gold has been labelled one of the most beautiful of the chemical elements and has been treasured by man since earlier times[5]. For millennia, the human species has cherished the colour and lustre, the malleability and durability of the metal that would never tarnish. It can be cast and stamped, drawn into thin wires or foils, dispersed into colourful colloids, alloyed with many other metals and re-purified. From the studies of the solar spectrum the abundance of gold in the sun is found to be 0.04 ppm, but in the Earth's crust it is on average about 0.004 ppm. Thus, gold is probably more abundant in the core than in the crust, where concentration by a factor of about 10^3 is necessary before economic extraction is feasible. Gold in nature is usually present in metallic form and concentration of gold has been done in two ways. The first gives rise to alluvial gold and consists of the weathering of auriferous rocks which have been for example washed into river beds. The alluvial gold, once discovered, is often easy to extract as grains by simple gravity concentration *i.e*. panning. The most significant gold fields are found in South Africa, where the gold is present as thin veins in quartz rocks along with iron pyrites like chalcopyrite ($CuFeS_2$) or arsenopyrite (FeAsS). This type of gold is known as reef gold and is present as microscopic particles, which makes extraction more difficult than for alluvial gold. It was found that deposits with silver and other rare

metals often occur in volcanic regions controlled by major fault zones and thus in these regions concentration of gold takes place by hydrothermal metamorphism from basic rocks and deposition in sedimentary rocks[6].

In its bulk form gold is a soft with characteristic yellow colour metal but when finely divided can be purple, ruby red or blue. Thus reduction of gold compounds by $SnCl_2$ gives the colloid known as 'Purple of Cassius', which has been used as a colouring agent for enamel and glass. This is believed to be a colloid mixture of hydrated tin(IV) oxide and gold formed by reducing $[AuCl_4]^-$ with tin(II) chloride resulting, in the formation of a purple or ruby-red precipitate. Interestingly enough, the 16th century alchemist and the great Swiss medical iconoclast Paracelsus preceded the work on colloidal gold of the 17th century Andreus Cassius ('Purple of Cassius') and it was in fact Paracelsus who inspired Michael Faraday to form the first pure solutions of colloidal gold around 1857 which led to the recognition that there is a correlation between the colloidal size of gold and its colour.

Gold also has the highest ductility and malleability of any element. The gold metal is not attacked by either oxygen or sulphur at any temperature however it does react with tellurium at high temperatures to form $AuTe_2$ and reacts with all the halogens. It dissolves in aqueous solutions containing a good ligand for gold and an oxidising agent, thus for example gold will not dissolve in either hydrochloric nor nitric acid but dissolves readily in *aqua regia* to give tetrachloroauric(III) acid, $H[AuCl_4]$.

Throughout ancient history most major civilisations attributed medicinal character to gold and a historical perspective of the use of gold or gold compounds is available in literature[7]. Civilised humans have long been aware of the use of gold for the treatment of ailments, but the earliest recorded medical use of gold can be traced back to the Chinese in 2500 BC. In medieval Europe alchemists had numerous recipes for an elixir known as *aurum potabile*. Furthermore, gold was advocated by Nicholas Culpepper in the seventeenth century for ailments caused by a decrease in the vital spirits, e.g. melancholy, fainting, fevers and falling sickness, and a mixture of gold chloride and sodium chloride ($Na[AuCl_4]$) was used to treat syphilis[8,9].

2.2 GOLD PHOSPHINE COMPLEXES AND ORGANOMETALLIC COMPOUNDS

2.2.1 Introduction

Gold chemistry is largely characterised by the oxidation states +I and +III, with Au^{+} and Au^{3+} having the electron configurations [Xe]$4f^{14}5d^{10}$ and [Xe]$4f^{14}5d^{8}$, respectively[10,5]. Gold(I) can form linear, trigonal planar or tetrahedral complexes in which the hybridisation at gold can be considered to be *sp* (linear), sp^2 (trigonal planar) or sp^3 (tetrahedral) respectively, using 6*s* and one or more of the 6*p* orbitals of gold in bonding. This is however oversimplified since the 5*d* orbitals of gold are also involved in bonding to some extent.

Gold(I) complexes usually have coordination number two, with linear stereochemistry and thus are coordinatively unsaturated 14-electron complexes[11]. Occasionally, gold(I) complexes are three-coordinate species with trigonal planar stereochemistry and four-coordinate with tetrahedral stereochemistry[12,13]. Only the four-coordinate gold(I) complexes are coordinatively saturated with gold displaying the 18-electron configuration while the linear and trigonal gold(I) complexes have two and one vacant 6*p* orbital(s), respectively[14].

Gold(III) complexes have a strong preference for four coordination with square planar stereochemistry. In these complexes gold displays the 16-electron configuration with the $6p_z$ orbital vacant. In organometallic derivatives, this is the mostly common stereochemistry for stable gold(III) complexes. Coordination numbers five and six are known for inorganic gold(III) complexes, and both three- and five-coordinate organogold(III) complexes have been proposed as reaction intermediates. Organogold compounds may be widely classified according to the number of electrons donated by the carbon-donor ligand[15]. Historically, the first organogold compound studies were the dimeric halogen-bridged dialkylgold(III) halides and the coordination chemistry of these complexes was developed early by Gibson and his co-workers[16].

2.2.2 Gold(I) phosphine complexes

A large number of tertiary phosphine complexes of gold(I) are known[17] and were intensively studied since the early 1970's and will be only briefly discussed here. The possibilities of coordination numbers between two and four have been explored, though the use of bulky ligands is less essential than with the isoelectronic $M(PR_3)_2$ (M = Pd, Pt) compounds and the coordination numbers depends on both steric and electronic factors[18]. The most common method of preparation is by the reduction of $[AuCl_4]^-$ with the corresponding tertiary phosphine as shown in Eq. 2.1.

$$[AuCl_4]^- + 2PR_3 \rightarrow [Au(PR_3)Cl] + PR_3Cl_2 + Cl^- \quad (2.1)$$

An alternative method to the above would be the more cheaply *in situ* preparation with 2,2'-thiodiethanol with the intermediate being reacted by a tertiary phosphine ligand as shown in Eq. 2.2.

$$[AuCl_4]^- + 2(HOCH_2CH_2)_2S \rightarrow AuCl[S(CH_2CH_2OH)_2] + (HOCH_2CH_2)_2SO + Cl^- + 2HCl \quad (2.2)$$

As an example using Eq. 2.1, is the preparation of $[Au(PPh_3)Cl]$[19] of which the mechanism has been studied[20] and is shown in Eq. 2.3 and 2.4.

$$[AuCl_4]^- + PPh_3 \rightarrow [Au(PPh_3)Cl_3] + Cl^- \quad (2.3)$$

$$[Au(PPh_3)Cl_3] + PPh_3 \rightarrow [Au(PPh_3)Cl] + PPh_3Cl_2 \quad (2.4)$$

However, the analogous reaction with triphenylarsine or triphenylstibine follows a different mechanism in which the first step involves the reduction of $[AuCl_4]^-$ to $[AuCl_2]^-$ as illustrated below.

$$[AuCl_4]^- + AsPh_3 \rightarrow [AuCl_2]^- + [AsPh_3Cl_2] \quad (2.5)$$

$$[AuCl_2]^- + AsPh_3 \rightarrow [Au(AsPh_3)Cl] + Cl^- \quad (2.6)$$

The difference probably arises because the tertiary phosphine is a better ligand for gold(I) but a weaker reducing agent than triphenylarsine or triphenylstibine[20]. Other tertiary phosphine gold, arsine and stibine complexes that can be prepared in a similar way, include $[Au(PPh_3)X]$ (X = Br, I), $[Au(MPh_3)Cl]$ (M = As, Sb)[21], $[Au(AsMe_3)Cl]$[22] and

$[Au(PCy_3)Cl]$[23]. Another method of preparation of the gold(I) phosphines is from other gold(I) complexes, most frequently a more weakly bound ligand like tetrahydrothiophene (THT), the precursor being reacted with a tertiary phosphine ligand[24,25] as illustrated in Eq. 2.7 and 2.8.

$$[Au(SMe_2)Cl] + PPh_3 \rightarrow [Au(PPh_3)Cl] + SMe_2 \quad (2.7)$$

$$[Au(cyclooctene)Cl] + P(OMe)_3 \rightarrow [AuP(OMe)_3Cl] + cyclooctene \quad (2.8)$$

It is also possible to prepare complexes directly from the gold(I) halides or by substitution at the phosphorus centre[26] as presented in Eq. 2.9 and 2.10.

$$AuCl + PCl_3 \rightarrow [Au(PCl_3)Cl] \quad (2.9)$$

$$[Au(PCl_3)Cl] + 3MeOH \rightarrow [AuP(OMe)_3Cl] + 3HCl \quad (2.10)$$

In some cases, one tertiary phosphine may replace another[27,28] as indicated in Eq. 2.11 and 2.12.

$$[Au(PMe_3)Me] + PEt_3 \rightarrow [Au(PEt_3)Me] + PMe_3 \quad (2.11)$$

$$2[Au(PEt_3)Cl] + 2Et_2PCH_2CH_2SH \rightarrow \quad (2.12)$$

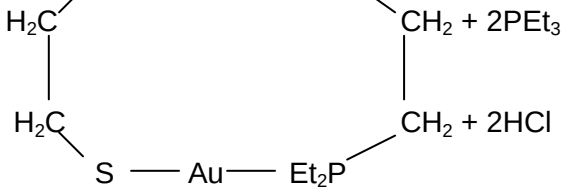

In most cases the structure of gold(I) phosphine complexes show linear coordination and examples include $[Au(PPh_3)X]$ (X = Cl, Br, I, NO_3, SCN[29], Ph[30], CN, Me, CF_3[31], *etc*.), $[Au(PR_3)Cl]$[32] (R_3 = Cy_3, $PhCy_2$, PMe_3, PEt_3, PCl_3, $P(PhO)_3$ and $P(tolyl)_3$), $[Au(PPr^i_3)C_5H_5]$ and $[Au(AsPh_3)X]$ (X = Cl, Br).

Complexes with more than one phosphine have been prepared by changing the stoichiometry of the reaction mixture where the complex formed in the solution is dependant upon the cone angle of the phosphine. Thus $[Au(PPh_3)_2SCN]$ is three-coordinate, while because of the bulky nature of tricyclohexylphosphine, $[Au(PCy_3)_2]SCN$ is two-coordinate[33]. Of many other similar structures determined include $[Au(PPh_3)_2X]$ (X = Cl, Br, I, NCS) and $[Au(PPh_3)_3]SCN$ (X = BPh_4) which are

three-coordinate and $[Au(PPh_3)_3X]$ (X = Cl, SCN), $[Au(PPh_2Me)_4]PF_6$, $[Au(PPh_3)_4]BPh_4$ and $[Au(SbPh_3)_4]ClO_4$ which are four-coordinate[34]. It is observed that the three-coordinate complexes are trigonal planar when all the ligands are the same or slightly distorted in $[Au(PPh_3)_2X]$, while the four-coordinated complexes are distorted tetrahedra.

2.2.3 Gold(III) phosphine complexes

Complexes of the form $[Au(PR_3)X_3]$ are usually prepared by oxidation of the gold(I) derivative $[Au(PR_3)X]$ with the corresponding halogen. By using a similar route one can prepare mixed halide complexes as shown in Eq. 2.13[35,36].

$$[Au(PEt_3)Cl] + I_2 \rightarrow [Au(PEt_3)(I)_2Cl] \qquad (2.13)$$

The complexes $[Au(PPh_3)Cl_3]$ and $[Au(PPh_3)Me_3]$ were found to have a distorted square planar stereochemistry and the electronic structure of $[Au(PMe_3)Me_3]$ has been evaluated by photoelectron spectroscopy[37]. Also, halogen oxidation of gold(I) complexes can yield products involving reaction of phosphine substituents or give binuclear gold(III) complexes as presented in Eq. 2.14 and 2.15.

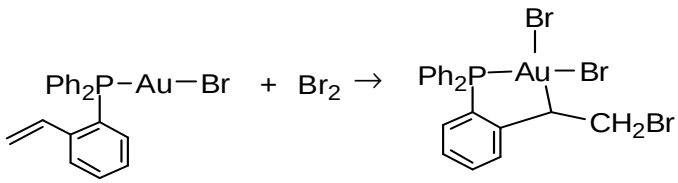

(2.14)

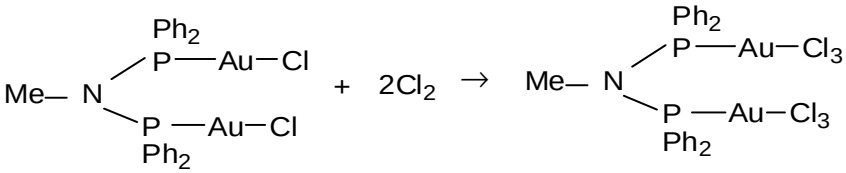

(2.15)

It is known in literature that oxidation of the tetrahedral derivatives $[Au(L,L\text{-}Bid)_2]^+$ where L,L-Bid = *o*-$C_6H_4(AsMe_2)_2$ or *o*-$C_6H_4(PMe_2)_2$, gives gold(III) complexes based on $[Au(L,L\text{-}Bid)_2]^{3+}$. However, this square planar unit binds to added halides to give $[Au(L,L\text{-}Bid)_2X]^{2+}$, presumed to have square pyramidal structure, or $[Au(L,L\text{-}Bid)_2X_2]^+$, with tetragonally distorted octahedral structure[38]. With the arsine derivative, the neutral complex $[Au(C_6F_5)_3\{(AsMe_2)_2(o\text{-}C_6H_4)\}]$ has only one of the arsine centres coordinated and the stereochemistry is distorted square planar[39].

2.2.4 Gold(I) ferrocenylphosphine complexes

The use of ferrocenyl phosphines as ligands in coordination chemistry has been widely studied and well reviewed[40]. The employment of organometallic ligands such as ferrocenylphosphines provides a convenient route to the synthesis of heterometallic complexes. The catalytic potential is emphasised in view of the developing influence of homogeneous catalysis in organic synthesis, manipulation of materials and production of fine chemicals. The use of these ferrocenyl phosphines as ligands in coordination chemistry has enlarged the scope of metal complexes in the design of catalysts[41], drugs[42,43] and materials[44]. Added to this is the utilisation of the 1,1'-bis(diphenylphosphino)ferrocene (dppf, Fig. 2.1) of which recent interest is the anti-tumour activity of bis(diphenylphosphines) and their bis(gold(I)) complexes[45]. The interest in diphosphine ligands and their complexes as therapeutic agents[46,47,48] has been extended to the complexes of ferrocenyl phosphines such as dppf. This can be extended to as many cyclopentadienyl complexes which display anti-tumour activity and cytotoxicity[49].

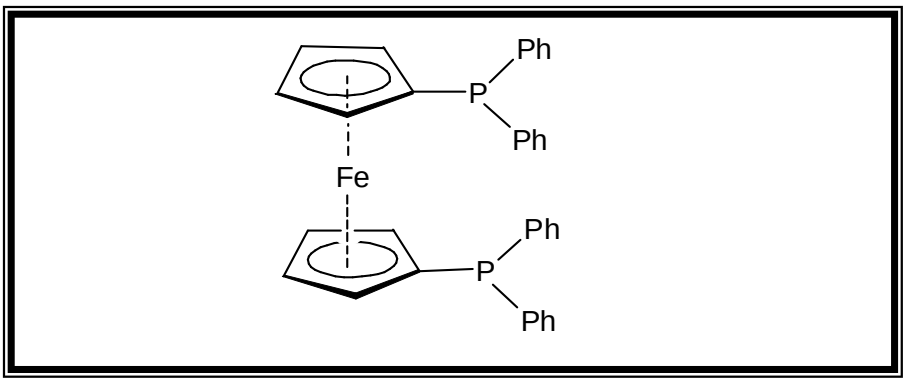

Figure 2.1 Structural representation of the 1,1'-bis(diphenylphosphino)ferrocene complexed-ligand (dppf).

The synthesis of the bidentate ferrocenyl ligand dppf was documented in the mid 1960's and was accomplished by the lithiation of ferrocene with *n*-butyllithium, followed by condensation with chlorodiphenylphosphine[50]. A higher yield could be obtained in the presence of *N*,*N*,*N*',*N*'-tetramethylethylenediamine (TMEDA)[51]. The development of this ferrocenyl diphosphine as a coordinating ligand stems from its chemical uniqueness and industrial importance.

The 1,1'-bis(diphenylphosphino)ferrocene ligand coordinates to a metal centre in various coordination modes as presented in Fig. 2.2. To relieve the strain induced by the complex formation, the Cp rings can twist about the Cp(centroid)-Fe-Cp(centroid) axis, see Fig 2.3.

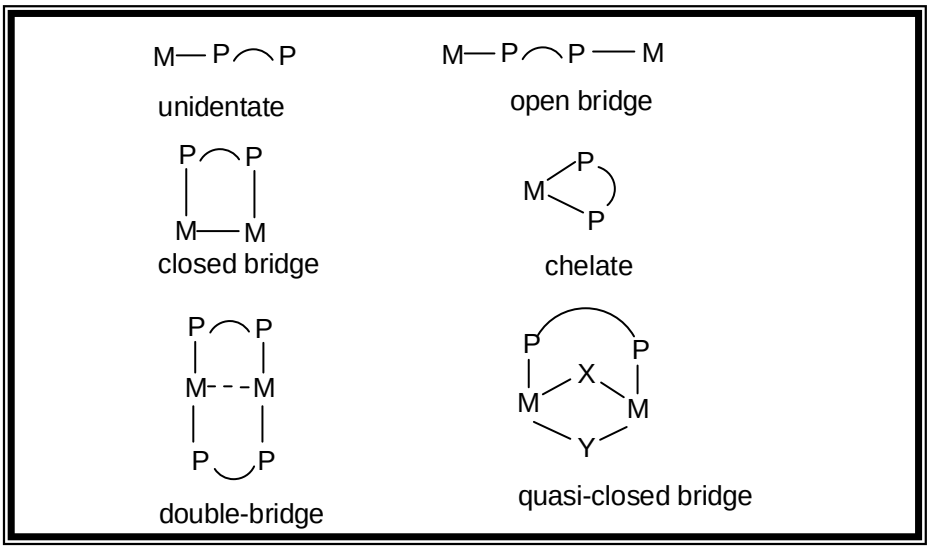

Figure 2.2 Illustration of the coordination modes for the dppf ligand with a metal(M)[52].

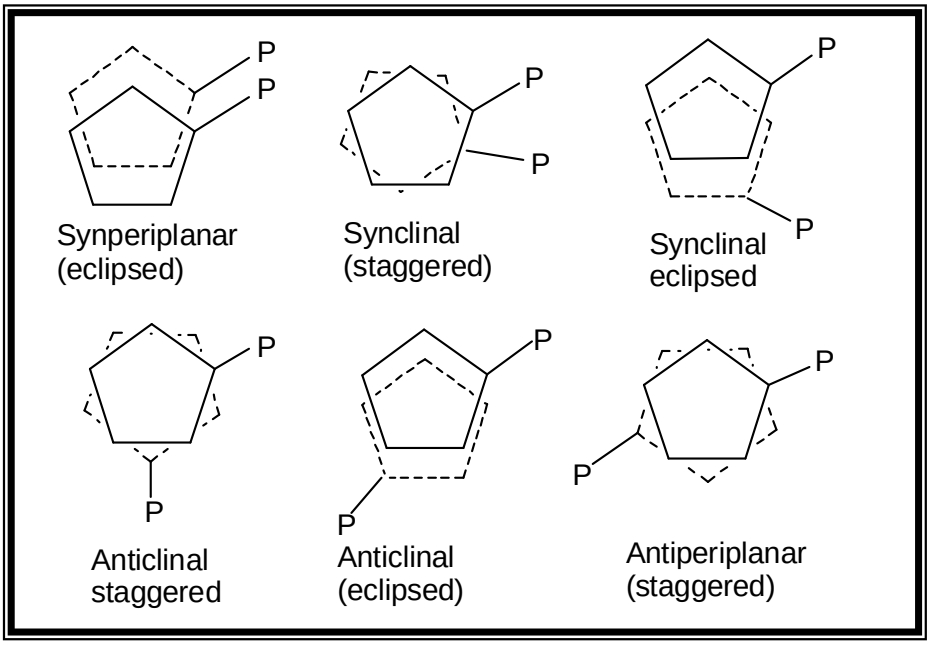

Figure 2.3 Ideal conformations of the dppf ligand arising from Cp…Fe…Cp torsional twist[52].

The dppf ligand is capable of undergoing coordination to a variety of transition metals *e.g*. the halo complexes of the late transition metals, carbonyl complexes of Group 6, 7 and 8 metals and the Group 5 metalates, with $[NEt_4][M(CO)_4(dppf\text{-}P,P')]$ (M = V, Ta)[53]

as an example. Complexes with dppf as a ligand are generally prepared by the direct reaction with binary compounds[54] or other primary forms of metallic Lewis acids[55]. For carbonyl complexes, substitution reactions by photolysis, thermolysis and chemically induced decarbonylation are usually the employed methods.

In many of the coordinated complexes with dppf, the complexed-ligand usually functions as a phosphine donor although occasionally, direct Fe→M is observed[56]. Lower coordination geometries such as trigonal planar can also be stabilised by the dppf ligand as displayed in the [Au(dppf-*P*,*P*')(dppf-*P*)]Cl complex[57]. It was observed that this complex readily rearranges to give [Au(dppf-*P*,*P*')$_2$]Cl in solution, presumably via a dibridged intermediate [Au(dppf-*P*,*P*')(μ-dppf)]$_2^{2+}$. The monobridged derivatives of the latter, [M$_2$(dppf-*P*,*P*')$_2$(μ-dppf)]$^{2+}$ (M = Cu; Ag; Au[58], Fig. 2.4) have been recently characterised structurally.

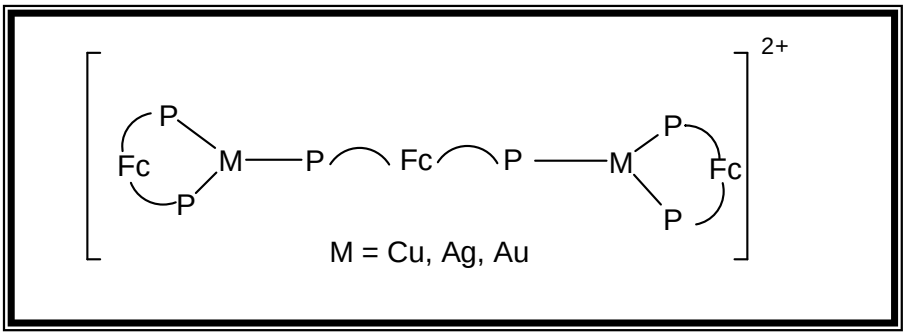

Figure 2.4 Monobridged derivative of the Au-dppf complex.

Linear dinuclear gold complexes found in literature include [Au$_2$X$_2$(μ-dppf)] (X = Cl[57], NO_3[58], CN[59]). Dppf can also act as a chelating or bridging ligand and of special interest is the quasi-closed bridging system in the [Rh$_2$(μ-S-^{t}Bu)$_2$(CO)$_2$(μ-dppf)][60] complex, see Fig. 2.5 in which the sterically demanding dppf ligand coexists with two bridging ligands of much smaller size. The structural determination of these complexes with varying geometries easily demonstrates the flexibility of the dppf as a ligand.

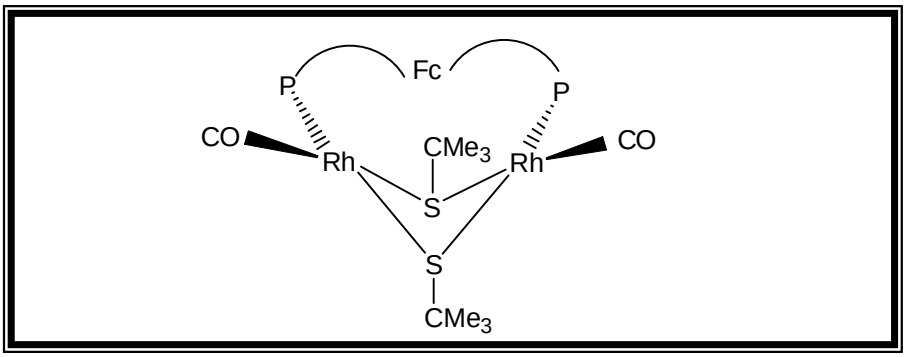

Figure 2.5 Quasi-closed bridging system in the [Rh$_2$(μ-S-^{t}Bu)$_2$(CO)$_2$(μ-dppf)] complex.

There has been an increasing interest in electroactive polymers, seemingly dppf polymers play an important role in this regard where an example found in literature is the isolation of polymeric $[AuCl(\mu\text{-dppf})]_n$[58]. Employment of these organometallic polymers based on the dppf ligand can find useful applications in materials science and homogeneous catalysis.

The interest in the bisphosphine ligands and their complexes as anti-tumour drugs or other therapeutic agents[61] has recently been extended to the complexes of ferrocenyl phosphines such as dppf. By the usage of mice-bearing ip P388 leukemia as model, both dppf and $[Au_2Cl_2(\mu\text{-dppf})]$ were shown to exhibit anti-tumour effects[42]. In general, complexes of the type $[ML_2(dppf)]^{2+}$ (M = Pd, Pt) with labile ligands L and free dppf are known to be active antiproliferating agents[62]. Literature indicates that the anti-tumour activity of $[Cu_2(dppf)_2(\mu\text{-dppf})][BF_4]_2$ is found to be comparable to that of cisplatin[63].

Chiral ferrocenylphosphine ligands have been employed in asymmetric catalysis and among the various types of asymmetric reactions, a chiral catalyst would be the preferred choice, provided the reactions proceed with high stereoselectivity forming the desired enantiomeric isomer in high yields[64]. A typical example of a simple chiral ferrocenyl phosphine is indicated in Fig. 2.6 and these phosphines have characteristic features that include having functional groups (X) at the ferrocenylmethyl position on the side chain.

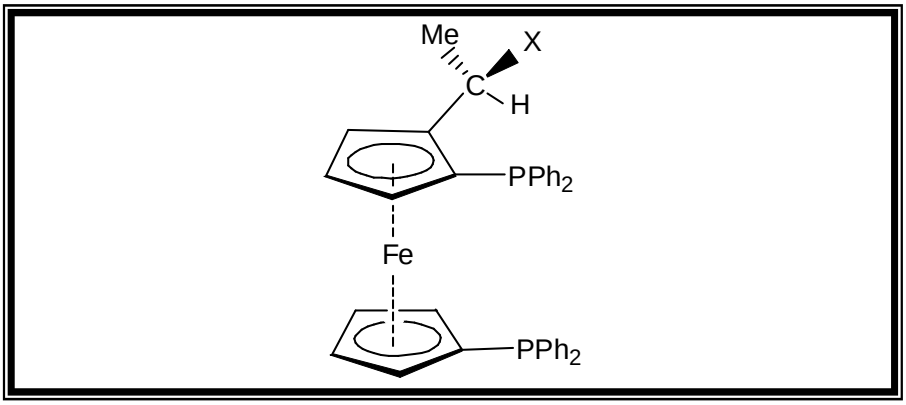

Figure 2.6 A simple chiral ferrocenylphosphine[65].

The functional groups on the side chain of the ligand are controlled by the ferrocenyl and methyl groups on the chiral carbon centre to face towards the reaction site on the catalyst coordinated with the phosphorus atoms on the ferrocenylphosphine ligand and they interact with a functional group on a substrate in a catalytic asymmetric reaction. With the secondary interaction[66] between functional groups and the reacting substrate,

the ferrocenylphosphines hence induce high enantioselectivity in a variety of asymmetric catalytic reactions.

Both the mono and biphosphines can be prepared from *N,N*-dimethyl-1-ferrocenylethylamine, which is the source of chirality. Chiral ferrocenylphosphines were first prepared by Hayashi and Kumada in the mid 1970's[67] and the asymmetric ortho-lithiation of optically resolved *N,N*-dimethyl-1-ferrocenylethylamine with butyllithium reported by Ugi and co-workers[68] was conveniently used for their preparation as presented in Scheme 2.1.

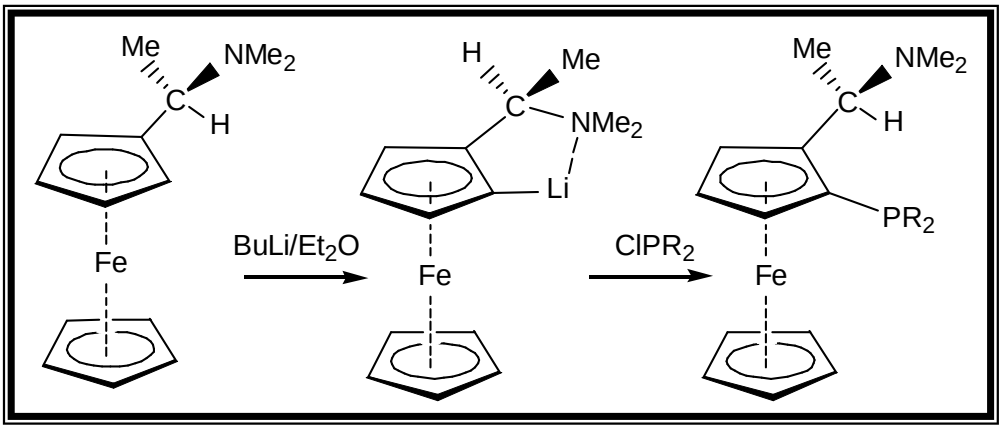

Scheme 2.1 Basic preparation route of the chiral ferrocenylphosphines.

Catalytic reactions found in the literature include the gold(I)-catalysed aldol reactions of enolates with aldehydes to give optically active β-hydroxycarbonyl compounds[69]. Catalytic asymmetric reactions yielding high enantioselectivity include the effect observed in the rhodium-catalysed asymmetric hydrogenation of α-(acylamino)acrylic acids and/or their analogues leading to the hydrogenation products of over 90% *ee*[70]. However, few of them displayed this high enantioselectivity in other types of catalytic asymmetric reactions[71].

2.2.5 Water-soluble phosphines

The ability of organophosphines to stabilise low metal oxidation states and to influence both steric and electronic properties of the catalytic species makes them very important ligands used in organometallic chemistry. In homogeneous catalysis, this can be very useful in order to change the activity or selectivity of the catalyst. The development of transition metal reagents for use in aqueous solvent systems offers advantages for a wide variety of chemical systems ranging from large scale industrial processes to fine

organic synthesis. The low water-solubility of most organometallic compounds has confined the study of their chemistry to organic media[72]. The use of water-soluble reagents for chemical manufacture can simplify catalyst-product separation and is also interesting because of the economy and the safety of using water as a solvent. Most water-soluble phosphines have ligands with hydrophilic functional groups and are mainly used in the field of catalysis. The solubility of the catalysts in water can be induced by modifying the phosphine structure by introducing polar substituents such as hydroxyl or amino functional groups or ionic groups such as sulphonate, carboxylate and ammonium functionalities. Of these the sulphonic acid group, $-SO_3^-$, is used most frequently since it can be easily attached to already available phosphines containing phenyl groups. A review article[73] that describes a large number of compounds prepared from such phosphines, in some cases comparing catalytic activities of their complexes with those of the more typical, non-functionalised phosphines is available as general reference. Unfortunately, hydroxyl group-containing ligands often do not exhibit significantly enhanced water-solubility while phosphines containing amino or carboxyl groups are soluble only in acidic or basic media, respectively.

Compounds containing sulphonated triphenylphosphines have been studied extensively[74]. These ligands containing the sulphonic acid moiety can therefore be grouped together with those that contain a charge like the quaternary ammonium ions (Amphos) or phosphonium ions as hydrophilic functional groups. The amount of impurities from oxidation products can be reduced with the new developed methods of sulphonation[75].

Examples of water-soluble monodentate aryl phosphines are the sulphonated analogues of PPh_3, namely the monosulphonated TPPMS and the tri-sulphonated TPPTS (Fig. 2.7). An example of a cationic water-soluble phosphine that has been synthesised and characterised is (2-diphenylphosphinoethyl)trimethylammonium iodide, amphos iodide[76]. Its metal carbonyl substitution complexes include iron, molybdenum and tungsten complexes as iodide salts, showing greatly enhanced solubility in polar solvents. Amphos ($PPh_2CH_2CH_2NMe_3^+$, Fig. 2.7) acts as a typical tertiary phosphine, with its electron donor properties slightly lower than those of $PPh_2(CH_3)$ and PPh_3. Amphos iodide is synthesised in high yields from 2-dimethylaminethyldiphenylphosphine, ($PPh_2CH_2CH_2N(CH_3)_2$), by oxidation to the phosphine oxide with hydrogen peroxide, alkylation at nitrogen with CH_3I followed by reduction with $HSiCl_3$ to give the air stable phosphine. The indefinite charged functional groups induce high water-solubility to the ligands which makes sulphonated ligands

very versatile in aqueous/organic biphasic catalysis. The problem of catalyst separation still exists however, if substrates with low solubility in the organic phase are used.

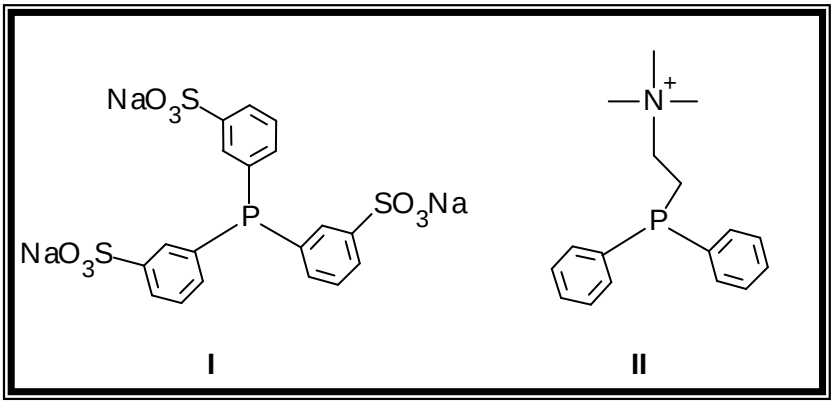

Figure 2.7 Examples of water-soluble phosphines; **I**, TPPTS and **II**, Amphos.

An important discovery in the area of water-soluble phosphine ligands was that of 1,3,5-triaza-7-phosphatricyclo[3.3.1.1^{3,7}]decane (PTA, Fig. 2.8)[77].

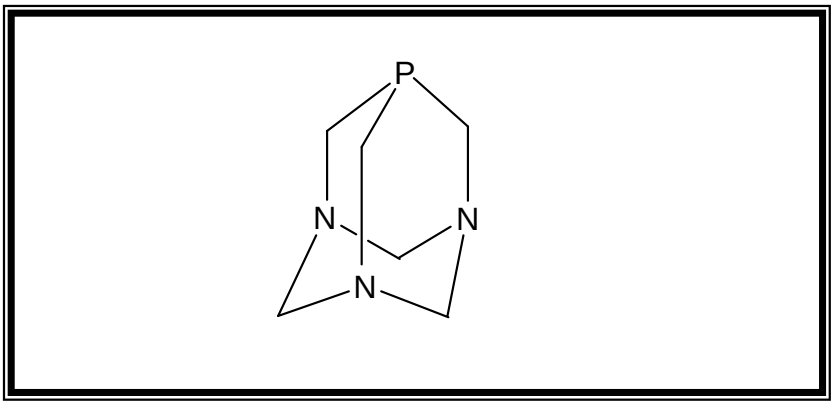

Figure 2.8 The 1,3,5-triaza-7-phosphatricyclo[3.3.1.1^{3,7}]decane ligand.

This ligand is stable in air, water-soluble and has low steric demand. It has good electron donating capabilities and a small cone angle, which induces less steric strain at the metal centre. The small cone angle of 118° further suggests that this phosphine should be a good substitute for trimethylphosphine[78]. The ligand can also be functionalised with methyl or other R-groups at the nitrogen atom sites. The interest shown in PTA as a ligand is mainly from its catalytic utilisation and in addition, also possible medical applications. This ligand is also of interest by virtue of its ability to form hydrogen bonds with both counter-ions and water molecules and in addition, PTA can be either protonated by HX or methylated at one of the nitrogen sites to form [PTAH]X and [PTA(CH_3)]I[79], respectively.

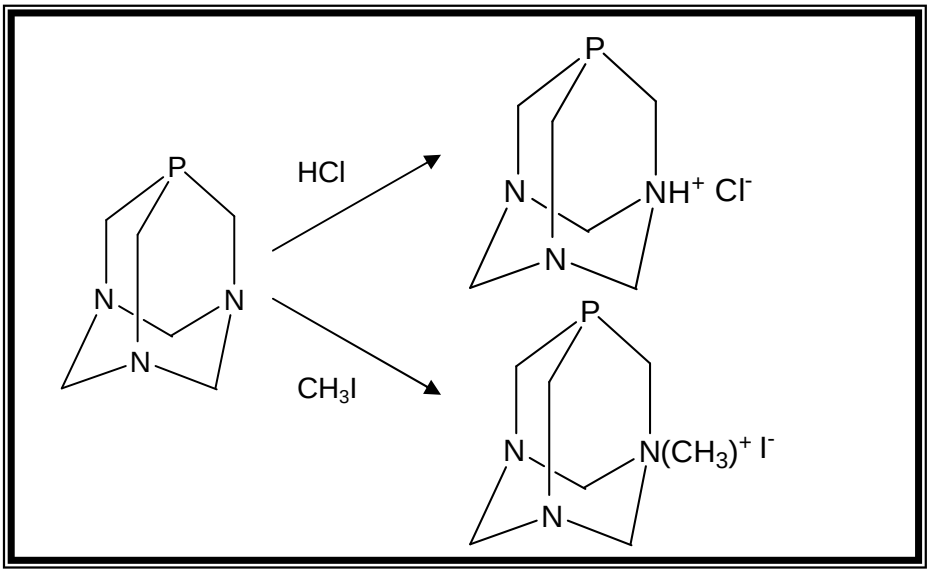

Figure 2.9 Protonation and methylation of PTA. An illustration of protonation when PTA is coordinated to a metal complex is given in literature[80].

Not much attention has been devoted to PTA coordination chemistry with copper or silver. In contrast, PTA was found to be a useful ligand in gold chemistry[81] and earlier research was stimulated by the intention to prepare water-soluble phosphine gold complexes which should show unusual reactivity patterns and self-aggregating properties. This latter feature, establishing short Au…Au interactions, provided an additional motivation to study these compounds as low energy luminescent materials. Among the first gold complexes with PTA was the two-coordinate, mono substituted PTA-gold complex [Au(PTA)Cl][82] which was synthesised by reacting the dimethylsulphide complex [Au(SMe_2)Cl] with PTA. The [Au(PTA)Br] or [Au(PTA)I] analogues were prepared by halide exchange upon mixing the [Au(PTA)Cl] complex with KBr or KI respectively and also the [Au(PTAMe)] complex was prepared through the reaction of [Au(PTA)Cl] with MeLi[82]. Reaction of [Au(PTA)Cl] with MeOTf in CH_2Cl_2 at -35 °C results in the formation of the methylated PTA complex, [Au(PTAMe)Cl]OTf in good yields[82]. The [Au(PTA)Cl] complex can be protonated by HCl yielding [Au(PTAH)Cl]Cl of which alternatively this can be prepared from (PTAH)Cl with [Au(THT)Cl]. Similarly, the protonated [Au(PTAH)Br]Br complex could be prepared from dissolving [Au(PTA)Br] in HBr. In contrast, when the same protocol is used for the synthesis of the iodide derivative the diiodo [Au(PTAH)I][Au($I)_2$] was formed[83].

Gold(I) complexes featuring more than one coordinated PTA ligand are also known. These include the di-substituted [Au($PTA)_2$]Cl complex[84], which was subsequently used to synthesise the [Au($PTA)_2$][Au($CN)_2$] complex[85]. The four-coordinate [Au($PTA)_3$Cl]

was prepared by stirring together [Au(THT)Cl] with three separate portions of PTA in a 1:2 MeCN/MeOH mixture[84]. Coordination of more than one alkylated PTA ligands to gold has also been achieved and the complex $[Au(PTAEt_3)I]I_3$[86] was prepared. Fully coordinated gold(I) complexes with either PTA or $(PTAMe)^+$ have also been reported[87].

Rhodium(I) carbonyl complexes containing the methylated PTA, $[RhI(CO)(PTAMe)]I^-$ and $[RhI(CO)(PTAMe)_3]I^-\cdot 4H_2O$, have also been prepared[88]. These complexes are stable in air in the solid state but when in solution they are oxidised with the loss of the carbonyl ligand and formation of water-insoluble complexes. The carbonyl stretching frequencies of these complexes suggest that the methylated PTA ligand possess stronger π-acceptor properties than most alkyl- and aryl-phosphines. These rhodium complexes were also found to be active catalysts for the water-gas shift reaction and they catalyse hydroformylation and carboxylation of alkenes as well as the hydrogenation of aldehydes and compounds containing a C=C bond[89]. Water-soluble ruthenium(II) and rhodium(I) phosphine complexes catalyse the hydrogenation of aqueous HCO_3^- to HCO_2^- under mild conditions. PTA has also been employed in ruthenium complexes, $[Ru(PTA)_4Cl_2]$ together with $[Ru(m\text{-}TPPMS)_2Cl_2]_2$ and $[Rh(m\text{-}TPPMS)_3Cl]$ complexes. These are precursors that have shown catalytic activity, in the hydrogenation of CO_2 and bicarbonate in aqueous solutions or in water/$CaCO_3$ suspensions in the absence of amine or other additives and under mild conditions[90].

2.3 CHEMOTHERAPEUTIC APPLICATIONS OF PRECIOUS METALS

2.3.1 Introduction

Since the *cis*-$[Pt(NH_3)_2Cl_2]$ complex (cisplatin) was a vast success on this regard, a brief introduction on the activity and mechanism of the complex and related compounds is discussed below. The treatment of a variety of cancers by cisplatin, *cis*-$[Pt(NH_3)_2Cl_2]$, has influenced the search for other alternative metal-containing anti-tumour drugs[91,92].

The classic discovery of *cis*-$[Pt(NH_3)_2Cl_2]$ and its anti-tumour activity by Rosenberg[93], of which the synthesis[94] and structure were well known at the time, led continuous research to determine its mechanism of action and to account for the fact that only the *cis* isomer was active. Research indicated that cisplatin has beneficial effects on the

treatment of cancer[95,96] and its activity stems from the fact that it inhibits replication through binding to the DNA. Nowadays, cisplatin is used in combination with other anticancer agents and is effective against a variety of cancers.

Cisplatin cannot be taken orally due to the hydrolysis action of the gastric juices in the stomach and therefore it is injected in the blood where it is bound to plasma protein. Some is excreted renally and some is transported in the blood as uncharged *cis*-$[Pt(NH_3)_2Cl_2]$ molecules which pass through the cell wall unchanged. It is believed that cisplatin is not active in its normal form, therefore once through the cell wall it is converted to the actual drug.

The *cis*-$[Pt(NH_3)_2Cl_2]$ complex undergoes hydrolysis to *cis*-$[Pt(NH_3)_2(H_2O)Cl]^+$ and more slowly to *cis*-$[Pt(NH_3)_2(H_2O)_2]^{2+}$ owing to the lower intracellular Cl^- concentrations as compared to the higher chloride concentration outside the cell. The hydrolysis of the chloride is outlined in Eq. 2.16 and 2.17 followed by deprotonation (Eq. 2.18 and 2.19).

$$cis\text{-}[Pt(NH_3)_2Cl_2] + H_2O \rightarrow Cl^- + cis\text{-}[Pt(NH_3)_2(H_2O)Cl]^+ \quad (2.16)$$

$$cis\text{-}[Pt(NH_3)_2(H_2O)Cl]^+ + H_2O \rightarrow Cl^- + cis\text{-}[Pt(NH_3)_2(H_2O)_2]^{2+} \quad (2.17)$$

$$cis\text{-}[Pt(NH_3)_2(H_2O)_2]^{2+} \rightleftharpoons cis\text{-}[Pt(NH_3)_2(H_2O)(OH)]^+ + H^+ \quad (2.18)$$

$$cis\text{-}[Pt(NH_3)_2(H_2O)(OH)]^+ \rightleftharpoons cis\text{-}[Pt(NH_3)_2(OH)_2] + H^+ \quad (2.19)$$

The platinum complex is more reactive when the chloride dissociates because water is a better leaving group than Cl^-. Coordination of water to platinum lowers its p*K*a, thereby causing the hydroxo products to form as well[97,98]. Since the hydroxo groups in the above-mentioned complexes are not reactive towards substitution, it is believed that the aqua species reacts with DNA.

In addition, the rate of hydrolysis of the first chloro ligand in *trans*-$[Pt(NH_3)_2Cl_2]$ is expected to be much more rapid than that of the second due to the classic *trans* effect. The positively charged platinum complexes are electrostatically attracted to the negatively charged DNA helix. The surface of the DNA double helix is characterised by major and minor grooves of which the backbone of each strand is made up of deoxy-ribose phosphodiester units. Cisplatin has been known to generate interesting adducts

with DNA mainly by forming intrastrand cross-links by joining two adjacent guanine groups or adjacent guanine and adenine groups, which occupy the *cis* position, formerly utilised by Cl^-.

There are also other ways of cisplatin binding to DNA namely interstrand cross-links and DNA-protein cross-links, Fig. 2.10.

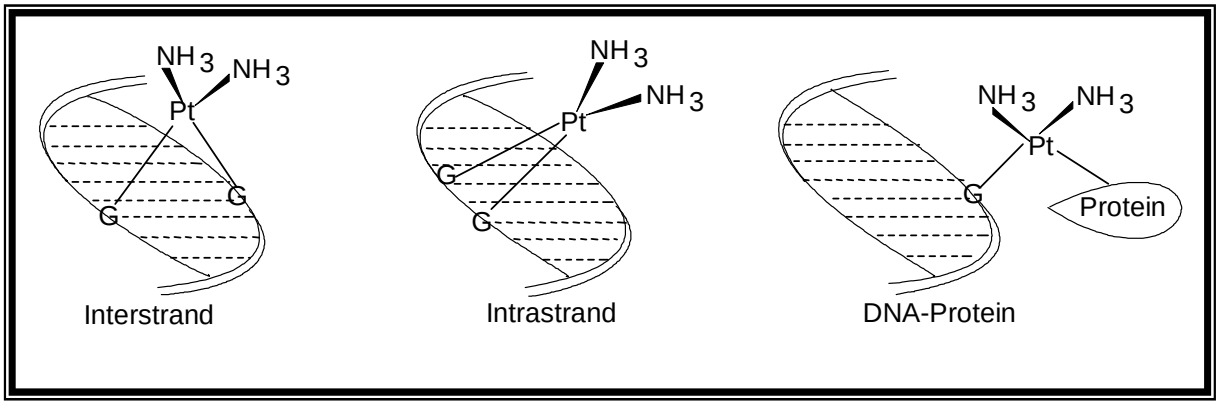

Figure 2.10 Possible ways of binding of *cis*-$[Pt(NH_3)_2Cl_2]$ to DNA.

The need to replace two Cl^- ligands explains why species like chlorodiethylenetriammineplatinum(II), $([Pt(dien)Cl]^+$, Fig. 2.11), with only one labile chloride are inactive. Due to the different geometry of *trans*-$[Pt(NH_3)_2Cl_2]$ molecules, they bind to DNA differently from cisplatin through these interstrand cross-links.

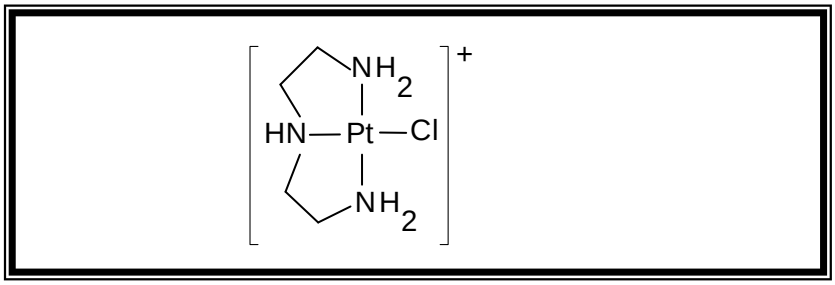

Figure 2.11 Structure of chlorodiethylenetriammineplatinum(II).

Binding of cisplatin to the N7 atoms of the two neighbouring guanosine nucleosides in the DNA, when it forms the 1,2-intrastrand cross-links, disrupts the orderly stacking of the bases thus bending the DNA helix and causing it to unwind by some degree, resulting in the distortion of the helix. These cross-links are believed to block DNA replication which results in the death of the tumour cell.

Fig. 2.12 shows another way of coordination of cisplatin to the DNA, where it binds to the same guanine molecule, although this form of binding is of little significance. It is very fascinating to suggest that this mode of binding is important to the anti-tumour activity of cisplatin since the *trans* isomer cannot form such a closed ring chelate involving the guanine N(7)-O(6) positions. The alkylation at the O(6) site has also been postulated as the most relevant in causing mutation in cells when alkylating agents are employed.

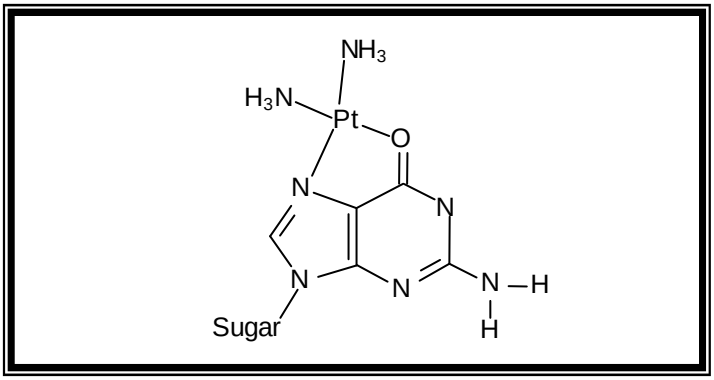

Figure 2.12 Bifunctional binding of cisplatin to guanine.

The study and the understanding of these mechanisms involved in the binding of platinum complexes to DNA is very important in designing better and more effective metal based drugs with less side effects. This goes for more than chemotherapy and includes treatment of other diseases like arthritis.

Other platinum complexes[99] that are known as second generation platinum anti-tumour drugs are illustrated in Fig. 2.13.

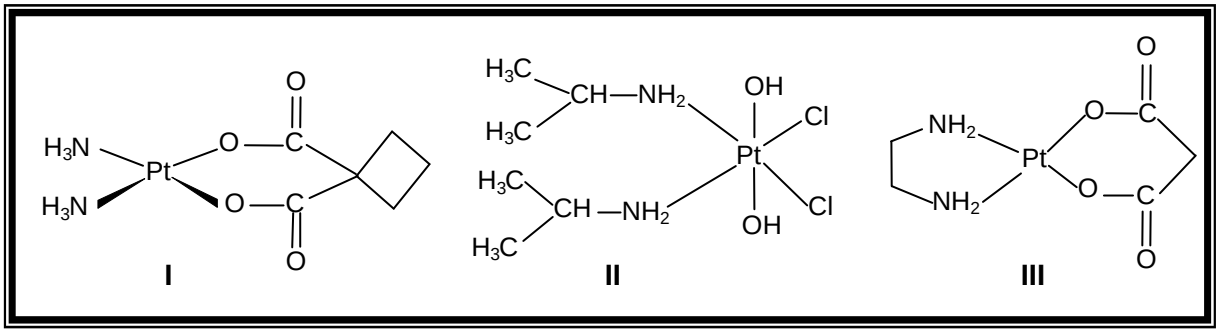

Figure 2.13 Platinum compounds studied for anti-tumour activity. **I**, Carboplatin; **II**, *cis*-dichloro-*trans*-dihydroxy-*cis*-bis(isopropylamine)platinum(IV), (Iproplatin); **III**, Malonatoplatinum.

Carboplatin, (*cis*-diammine(1,1-cyclobutanedicarboxylato)platinum(II)), displays similar activity to that of cisplatin but is less toxic and is used to treat ovarian tumours.

Although it causes less nausea, it has a side effect of lowering platelet levels. Iproplatin contains platinum(IV) in an octahedral coordination sphere and is an example of a platinum complex containing organic ligands but lacks carbon-metal bonds.

2.3.2 Inflammatory Disorders

Rheumatoid arthritis is a chronic inflammatory disease characterised by a progressive erosion of the joints and surrounding tissues but also affects other organ systems within the body resulting in deformities, immobility and a great deal of pain. It is an autoimmune disease in which the immune system of the body attacks against itself[100]. Rheumatoid arthritis is a specific type of arthritis that causes inflammation of the joints due to abnormalities in the body's own defence against infection, *i.e*. the immune system, and because of the immunological failure the immune system attacks its own cells. The immune system is a complex, multi-component system which is solely controlled by an intricate, interactive network of intercellular protein messenger molecules called cytokines. In rheumatoid arthritis, there is a breakdown of this control and an auto-immune response is directed towards self components known as autoantigens. Its cause is unknown but infectious, genetic and hormonal factors may play a role. Areas that may be affected include the joints of the hands, wrists, neck, jaw, elbows, feet and ankles.

2.3.3 Gold(I) Medicinal Compounds

Anti-cancer drugs have side effects, like renal toxicity for cisplatin, which then restrict them to limited doses. Damage to bone marrow causes anaemia, which is an inability to fight infections and a tendency to internal bleeding. Other side effects include vomiting, diarrhoea, nausea, hair loss and neurological complications. Another drawback that can be encountered in using drugs is the fact that the tumour can develop resistance to other drugs after the first administration.

The biological use of gold can be traced back in early years and it was until Koch's observation in 1890 that gold cyanide inhibited the growth of tuberculosis bacilli which represented the beginning of gold pharmacology and the design of new gold drugs. This also led to favourable observations on the use of gold in arthritis *e.g*. the use of gold(I) thiomalate in the treatment of rheumatoid arthritis. The problem with most gold-

based drugs is that complete structural characterisation had not been accomplished in detail. Most gold complexes used medically are thiol complexes (Fig. 2.14).

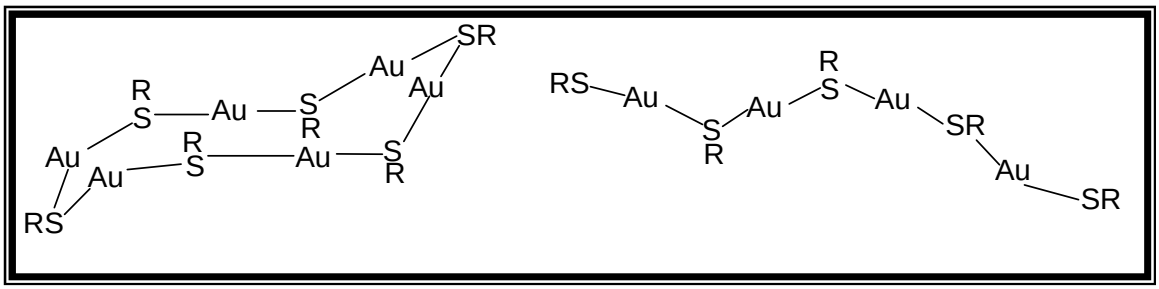

Figure 2.14 Structure of gold(I) thiolates.

Gold(I) thiolates were first introduced in 1929 as therapeutic agents for rheumatoid arthritis. The 1:1 gold thiolates have not yet been crystallised but NMR, mass spectrometric and X-ray scattering studies showed that they are not monomeric and are built up of ring and chain structures. The early gold compounds employed for the treatment of rheumatoid arthritis were gold thiolates[101] namely sodium aurothiomalate (myochrisin) and aurothioglucose (solganol), Fig. 2.15. These drugs were believed to be oligomeric or polymeric in nature.

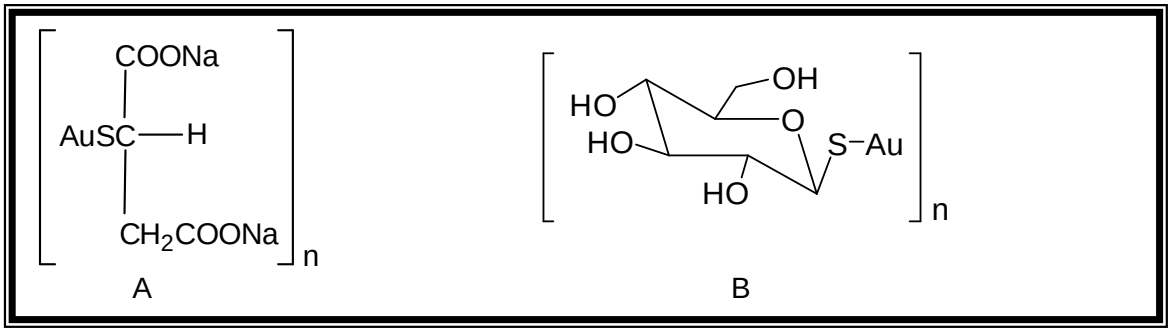

Figure 2.15 Structures of myochrisin (sodium aurothiomalate, A) and solganol (aurothioglucose, B).

Both drugs are water-soluble and were administered by intramuscular injections at weekly intervals in doses of ≈50 mg per week for several months[102]. Drugs like myochrisin took six weeks to three months to produce measurable improvements in rheumatoid arthritis in man which would result in several grams of gold remaining in the body long after therapy is completed. This causes the gold to be distributed to other tissues of the body like kidneys, spleen, liver and bone marrow where it accumulates and gives rise to nephrotoxicity, a major side effect. Other adverse reactions include mouth ulcers, skin reactions and blood disorders[103].

There has been much research on the efficacy of gold drugs in rheumatoid arthritis[104,105] and it is then generally accepted that these drugs have more effect as disease modifying anti-rheumatic drugs (DMARDs)[106]. Gold drugs have been employed to treat several other rheumatic diseases including psoriatic arthritis[107], a form of arthritis associated with psoriasis, juvenile arthritis, palindromic rheumatism and discoid lupus erythematosus[108]. Gold therapy has also been investigated as a treatment for various inflammatory skin disorders such as psoriasis[109], pemphigus[110] and urticaria[111]. The potential anti-tumour activity of gold compounds has been demonstrated in a number of experimental models[112,113]. In an attempt to reduce the toxic side effects new research investigations were made and a gold complex, 2,3,4,6-tetra-*O*-acetyl-1-thio-β-D-glucopyranosato(triethylphosphine) gold(I) (auranofin, Fig. 2.16) was developed.

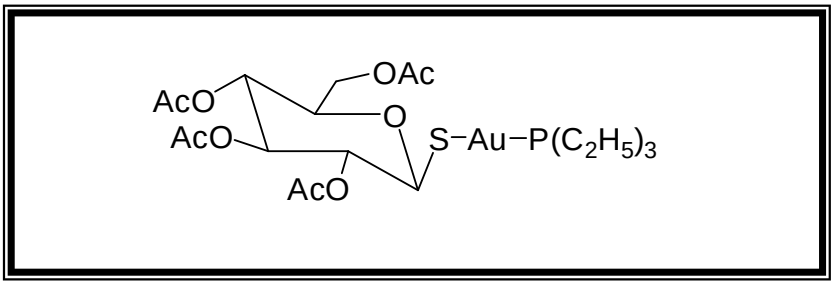

Figure 2.16 An illustrated drawing of auranofin.

The complex 2,3,4,6-tetra-*O*-acetyl-1-thio-β-D-glucopyranosato(triethylphosphine) gold(I) was shown to be cytotoxic towards HeLa cells and was also active against the P388 leukaemia *in vivo*, a standard and well documented primary screen for anti-cancer activity. Auranofin is an experimental chrysotherapeutic agent shown by the research groups involved[114,115] to be clinically effective in the treatment of rheumatoid arthritis when administered orally. They showed that auranofin exhibited a unique pharmacological profile when compared with the earlier injectable gold preparations, gold sodium thiomalate (Myochrisin) and gold thioglucose (Solganol). Auranofin is a lipid-soluble and linear, two-coordinate complex by virtue of the presence of a phosphine ligand of which the coordination at the gold centre is P-Au-S. It is monomeric and has been well characterised, including a structure determined by X-ray crystallography[116]. Research has indicated the design and testing of gold complexes for anti-tumour activity over the past decade[117,92,61]. The discovery that auranofin had activity against HeLa cells *in vitro* and P388 leukemia cells *in vivo*[118] led to screening of other auranofin analogues but their spectrum of activity was limited[119]. The oligomeric gold(I) thiolates were found to be inactive and also auranofin was inactive in subsequent tests using solid tumour models.

In this study an attempt was made to use auranofin and some of its analogues which were prepared by changing the phosphine moiety in the original auranofin with water-soluble phosphine ligands such as the PTA and PTAMe and also tertiary ligands *e.g*. triethylarsine for biological testing against cancer cell lines. Also, a chemiluminescence assay is done with the compounds at various concentrations to determine the effect they have on the chemiluminescence of isolated blood neutrophils. The preparation of auranofin compounds is presented in Chapter 3 while the experiments done with these compounds on cell assays and chemiluminescence are presented in Chapter 5.

Research in literature has also been focused on the μ-[bis(diphenylphosphine)ethane] digold complexes such as $[(AuCl)_2(dppe)]$[120], Fig 2.17. The dppe ligand is anti-tumour active on its own but the digold complexes were shown to have increased activity. These complexes rearrange to give tetrahedral complexes of the type $[Au(dppe)_2]^+$ (Fig. 2.17) which are of equal, if not greater, activity than their precursors[121]. The tetrahedral rearrangement is more favourable since the chelate effect stabilises the compound and the phosphine ligand is more inert to substitution by potential thiolate ligands that could be encountered in a biological environment. The suggested mechanism of action for the $[Au(dppe)_2]Cl$ complex was the formation of DNA-protein cross-links[122] and the inability of gold(I) affinity for O- and N-containing ligands resulting in poor reactivity with the DNA bases.

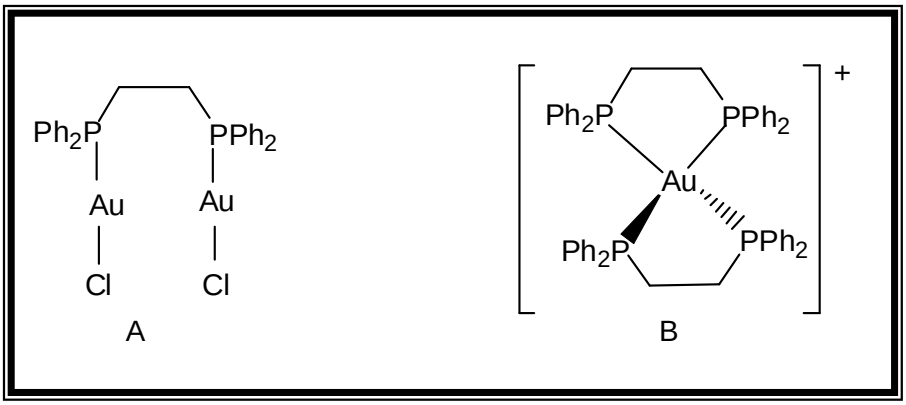

Figure 2.17 Illustrative structures of $[(AuCl)_2dppe]$ as a bridged compound (A, dppe = diphenylphosphino ethane) and its chelate gold complex (B).

Though $[Au(dppe)_2]Cl$ had marked activity against peritoneal cancer cells, this compound failed to enter clinical trials due to problems with cardiotoxicity highlighted during pre-clinical toxicology studies[123]. Generally, there were still some toxic side effects however, including severe gastrointestinal problems which are not present with

other gold drugs and therefore, modification of the drug in an attempt to eliminate these side effects would be useful and of prime importance.

2.4 REACTION MECHANISMS IN GOLD CHEMISTRY

Ligand substitution reactions of linear gold(I) complexes generally occur rapidly[124] but there has been little detailed study of the mechanism. However, a classical example is that of the exchange of tertiary phosphine ligands in methyl(tertiary phosphine) gold(I) complexes (Eq. 2.20) which has been studied by NMR techniques where an associative mechanism was proposed.

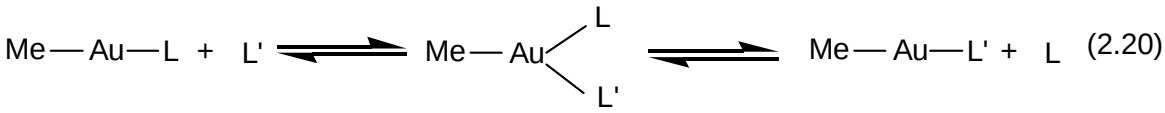

(2.20)

L, L' = tertiary phosphine

The intermediate is presumed to be a trigonal planar species which is analogous to the stable trigonal planar $[Au(PPh_3)_2Cl]$. These NMR phenomena can be understood in terms of a rapid ligand exchange process at the CH_3Au centre, the rate of which is strongly dependant on the concentration of the free ligand. With phosphine concentrations greater than 1%, the exchange reaction becomes rapid enough to reduce the preexchange lifetime value beyond the experimental limit[125] which is estimated to be 2.5×10^{-2} at 30 °C. The associative mechanisms of gold(I) exchange reactions have been characterised by second-order associative rate laws and negative entropies of activation for the reactions. The exchange of cyanide for 1-methylpyridiniumthione (mpt) is second order in both directions[126] with rate constants for the forward reaction as 1.8 $M^{-1}s^{-1}$.

Interestingly, it was observed that trimethyl(tertiary phosphine) gold(III) complexes underwent a similar exchange with free phosphine ligands. However, the reactions were much slower than for the gold(I) complexes. Bidentate and multidentate ligands often reduce the thermodynamic driving force for ligand exchange and/or increase the activation energy leading to slower reactions. This then results for example in greater stability of dppe and its complexes in aqueous solutions[122]. Ligand exchange reactions of gold(I) halides[127] *e.g.* for the stepwise conversion of $[AuCl_4]^-$ into $[AuBr_4]^-$ have second order rate constants of 63.3 $M^{-1}s^{-1}$ for the initial step of ligand exchange. With evidence, the activation energy for the formation of a five-coordinate gold(III)

intermediate is considerably higher than for the trigonal gold(I) species[128]. Ligand exchange reactions with other transition metals such as Pt and Pd have also been studied[129].

Oxidation-reduction reactions form part of the aqueous chemistry of gold compounds[130]. The aquated ions $[Au(H_2O)_n]^{+}$ and $[Au(H_2O)_4]^{+3}$, analogous to those found for many transition metal and main group cations, can be readily reduced to elemental gold.

$$Au^{+1} + e^{-} \rightarrow Au(0) \qquad E_0 = +1.68 \text{ volts} \qquad (2.21)$$

$$Au^{+3} + 3e^{-} \rightarrow Au(0) \qquad E_0 = +1.42 \text{ volts} \qquad (2.22)$$

The large and positive E_0 values suggest that mild reducing agents are able to induce the reduction of gold(III) to gold(I). As an example $[AuCl_4]^{-}$ slowly reacts with water to release elemental oxygen. The reduction potentials are sensitive to the choice of ligands and considerable stabilization of either oxidation state is possible[131,132].

$$[AuCl_2]^{-} + e^{-} \rightarrow Au(0) + 2Cl^{-} \qquad E_0 = +1.15 \text{ volts} \qquad (2.23)$$

$$[AuBr_2]^{-} + e^{-} \rightarrow Au(0) + 2Br^{-} \qquad E_0 = +0.959 \text{ volt} \qquad (2.24)$$

$$[Au(SCy)_2]^{-} + e^{-} \rightarrow Au(0) + 2CyS^{-} \qquad E_0 = -0.14 \text{ volt} \qquad (2.25)$$

(CyS^{-} = cysteinato)

$$[Au(CN)_2]^{-} + e^{-} \rightarrow Au(0) + 2CN^{-} \qquad E_0 = -0.48 \text{ volt} \qquad (2.26)$$

$$[AuCl_4]^{-} + 3e^{-} \rightarrow Au(0) + 4Cl^{-} \qquad E_0 = +1.00 \text{ volt} \qquad (2.27)$$

$$[AuBr_4]^{-} + 3e^{-} \rightarrow Au(0) + 4Br^{-} \qquad E_0 = +0.854 \text{ volt} \qquad (2.28)$$

$$[Au(CN)_4]^{-} + 3e^{-} \rightarrow Au(0) + 4CN^{-} \qquad E_0 = -0.10 \text{ volt} \qquad (2.29)$$

The E_0 value for $[AuBr_4]^{-}$ is significantly less than that for the free Au^{+3}, but still sufficiently positive that it remains a powerful oxidant. The negative potential of $[Au(SCy)_2]^{-}$ indicates a significant stabilisation of the +1 oxidation state by the coordinated thiolate ligands. Thus, gold(III) tetrahalide complexes remain powerful oxidising agents but gold(I) complexes can be stabilized by cyanide and thiolate ligands.

Reduction of gold(III) to gold(I) or gold(0) is often observed in biological systems where the reaction can be driven by naturally occurring reductants such as thioethers, thiols

or even disulphides. The reduction of gold(III) in cell culture media has been examined in literature[133].

2.5 CATALYTIC APPLICATIONS OF GOLD

For a long time, gold was considered to posses only low catalytic activity and therefore only its stoichiometric coordination and organometallic chemistry was investigated. Literature reports indicated that applications of gold as a catalyst were in heterogeneous catalysis[134]. Compared to the noble metals in Group 8 and the other metals in Group 11 of the periodic table, gold had found little application as a heterogeneous catalyst. The low catalytic activity of gold is due to the *d*-band being filled, with the result that gold is unable to chemisorb small molecules. Gold has a completely filled 5d electron shell and its lone 6s electron experiences less screening from the nucleus through the 5d electrons compared to alkali metals, resulting in a significantly higher ionisation potential. Although gold has been sparingly used in heterogeneous catalysis previously[135] but recently a change of paradigm has thus taken place[136].

The use of gold as a catalyst is desirable when it has a similar activity as for a more expensive catalyst, when it shows a higher activity or selectivity than less expensive catalysts and when a new chemical transformation is possible using the gold catalyst. The recent surge of new interest in catalysis by gold[137] has led researchers to investigate the effects of adding other metals to the gold. Hence gold is combined with platinum group metals (PGM's) for a number of reactions with potential for industrial applications. One of the major uses of gold/platinum group metal catalysis was on the vinyl acetate monomer production[138] (used in the production of emulsion paint and glues), which showed that the addition of gold to palladium can improve the rate of production. Other literature reports on the surface science of Au/PGM catalysts include a review paper[139] while some groups have studied the bimetallic Au/Ru catalysts supported on α-Fe_2O_3 for the water gas shift reaction[140].

Research on the chemical synthesis of gold colloids is widely reported in literature[141]. The development of new gold based nanostructures creates interesting possibilities in fields such as sensors and biological scaffolds[142,143].

The utilisation of gold in homogeneous catalysis is a relatively new field of transition metal catalysis but with growing interest. Homogeneous catalysis includes all reactions in which the substrates and the catalyst are in the same state. As there are few highly volatile gold compounds, most of these reactions are conducted in the liquid phase with liquid or dissolved substrates and a dissolved catalyst. Homogeneous catalysis in the solid state, which is part of the solvent-free reactions quite essential in the field of green chemistry, has not been explored with gold yet and in this context the non-toxicity of gold which helps to avoid environmental problems is also of importance.

Recently, the benefits of gold as a homogeneous catalyst for the synthesis of fine chemicals have been reported[144]. Homogeneous gold-catalysed reactions have become an interesting field to study[145,146] of which many of the investigations into the catalytic reactivity of gold focus on the tendency of both gold(III) and gold(I) complexes to activate alkynes towards nucleophilic addition[147,145]. The field is primarily dominated by oxidation reactions, addition of nitrogen-, oxygen- or carbon-containing nucleophiles to C-C multiple bonds and C-C bond forming reactions. Gold salts utilised in homogeneous catalysis have a unique ability to active C-C multiple bonds as soft Lewis acids allowing for the formation of new C-C, C-O, C-N and C-S bonds by nucleophilic attack at these activated substrates. Also, gold is responsible catalyst for the activation of C-H bonds in compounds thus forming nucleophiles which can react with various electrophiles[148,149]. The overall and wide spectrum potential of the recent interesting advances in gold catalysis and current developments have been illustrated in a book of abstracts and references therein of the Gold 2006[150] conference held in Limerick.

[1] S.P. Fricker, *Transition Met. Chem.,* 1996, **21**, 377.

[2] P.J. Sadler, *Adv. Inorg. Chem.,* 1991, **36**, 1.

[3] N.J. Birch, P.J. Sadler, *Inorg. Biochem.,* 1981, **2**, 315.

[4] N.J. Birch, P.J. Sadler, *Inorg. Biochem.,* 1981, **3**, 372.

[5] R.J. Puddephatt, 'The Chemistry of Gold', Elsevier, Amsterdam, 1978.

[6] (a) N.A. Shilo, *Earth Sci. Rev.,* 1971, **7**, 215.
(b) W.S. Fyfe, R.W. Henley, *Miner. Sci. Eng.,* 1973, **5**, 295.

[7] W.F. Kean, F. Forestier, Y. Kassam, W.W. Buchanan, P.J. Rooney, *Semin. Arthritis Rheum.,* 1985, **14**, 180.

[8] G.J. Higby, *Gold Bull.,* 1982, **15**, 130.

[9] R.V. Parish, *Interdisc. Sci. Rev.,* 1992, **17**, 221.

[10] F.A. Cotton, G. Wilkinson, 'Advanced Inorganic Chemistry', 4th Ed., Wiley, New York, 1980.

[11] R.J. Puddephatt, In 'Comprehensive Organometallic Chemistry'; G. Wilkinson, F.G.A. Stone, E.W. Abel, Eds.; Pergamon, 1982, chap 15.

[12] R.C. Elder, E.H.K. Zeiher, M. Onady, R.R. Whittle, *J. Chem. Soc., Chem. Commun.,* 1981, 900.

[13] P.G. Jones, *Z. Naturforsch., Teil B,* 1982, **37**, 937.

[14] G. Wilkinson, R.D. Gillard, J.A. McCleverty, 'Comprehensive Organometallic Chemistry', Vol 5, Pergamon Press, 1987.

[15] G.E. Coates, M.L.H. Green, K. Wade, 'Organometallic Compounds', Methuen, London, 1968, Vol. 2.

[16] W.J. Pope, C.S. Gibson, *J. Chem. Soc.,* 1907, 2061.

[17] C.A. McAuliffe (Ed.), in 'Transition Metal Complexes of Phosphorus, Arsenic and Antimony Ligands', MacMillan, London, 1973.

[18] (a) C.C. Colburn, W.E. Hill, C.A. McAuliffe, R.V. Parish, *J. Chem. Soc., Chem. Commun.,* 1979, 218.
(b) R.V. Parish, O. Parry, C.A. McAuliffe, *J. Chem. Soc., Dalton Trans.,* 1981, 2098.
(c) A.K.H. Al-Sa'ady, C.A. McAuliffe, K. Moss, R.V. Parish, R. Fields, *J. Chem. Soc., Dalton Trans.,* 1984, 491.

[19] L. Malatesta, L. Naldini, G. Simonetta, F. Cariati, *Coord. Chem. Rev.,* 1966, **1**, 255.

[20] R. Roulet, N.Q. Lan, W.R. Mason, G.P. Fenske, *Helv. Chim. Acta,* 1973, **56**, 2405.

[21] A.D. Westland, *Can. J. Chem.,* 1969, **47**, 4135.

[22] D.A. Duddell, P.L. Goggin, R.J. Goodfellow, M.G. Norton, J.G. Smith, *J. Chem. Soc. A,* 1970, 545.

[23] J. Bailey, *J. Inorg. Nucl. Chem.,*1973, **35**, 1921.

[24] L.G. Vaughan, *U.S. Pat,* 3,661,959,1972.

[25] D.A. Couch, S.D. Robinson, *Inorg. Chim. Acta,* 1974, **9**, 39.

[26] H. Schmidbaur, R. Franke, *Chem. Ber.,* 1972, **105**, 2985.

[27] H. Schmidbaur, A. Shiotani, *Chem. Ber.,* 1971, **104**, 2821.

[28] (a) B.M. Sutton, J. Weinstock, *Chem. Abstr.,* 1976, **84**, 31242.
(b) B.M. Sutton, J. Weinstock, *Chem. Abstr.,* 1975, **82**, 86410.

[29] P.F. Barron, L.M. Engelhardt, P.C. Healy, J. Oddy, A.H. White, *Austr. J. Chem.,* 1987, **40**, 1545.

[30] X. Hong, K.-K. Cheung, C.-X. Guo, C.-M. Che, *J. Chem. Soc., Dalton Trans.,* 1994, 1867.

[31] U. Flärke, H.-J. Haupt, P.G. Jones, *Acta Cryst.,* 1996, C**52**, 609.

[32] (a) J.A. Muir, M.M. Muir, L.B. Pulgar, P.G. Jones, G.M. Sheldrick, *Acta Cryst.,* 1985, C**41**, 1174.
(b) H. Schmidbaur, G. Weidenhiller, A.A.M. Aly, O. Steigelmann, G. Müller, *Z. Naturforsch, Teil B,* 1989, **44**, 1503.
(c) H. Schmidbaur, G. Weidenhiller, O. Steigelmann, G. Müller, *Chem. Ber.,* 1990, **123**, 285.
(d) J.A. Muir, S.I. Cuadrado, M.M. Muir, *Acta Cryst.,* 1991, C**47**, 1072.
(e) P.G. Jones, *J. Cryst. Spect. Res.,* 1992, **22**, 397.
(f) K. Angermaier, E. Zeller, H. Schmidbaur, *J. Organomet. Chem.,* 1994, **472**, 371 and references therein.
(g) B. Weissbart, L.J. Larson, M.M. Olmstead, C.P. Nash, D.S. Tinti, *Inorg. Chem.,* 1995, **34**, 393 and references therein.

[33] J.A. Muir, M.M. Muir, E. Lorca, *Acta Cryst.,* 1980, B**36**, 931.

[34] (a) P.G. Jones, *J. Chem. Soc., Chem. Commun.,* 1980, 1031.
(b) P.G. Jones, *Acta Cryst,* 1992, B**48**, 1487.
(c) P.G. Jones, G.M. Sheldrick, J.A. Muir, M.M. Muir, L.B. Pulgar, *J. Chem. Soc., Dalton Trans.,* 1982, 2123.
(d) J.A. Muir, M.M. Muir, S. Arias, C.F. Campana, S.K. Dwight, *Acta Cryst.,* 1982, B**38**, 2047.

[35] G. Banditelli, A.L. Bandini, F. Bonati, R.G. Goel, G. Minghetti, *Gazz. Chim. Ital.,* 1982, **112**, 539.

[36] F.G. Mann, D. Purdie, *J. Chem. Soc.,* 1940, 1235.

[37] (a) J. Stein, J.P. Fackler Jr., C. Paparizos, H.W. Chen, *J. Am. Chem. Soc.,* 1981, **103**, 2192.

(b) G.M. Bancroft, T.C.S. Chan, R.J. Puddephatt, *Inorg. Chem.,* 1983, **22**, 2133.

(c) G. Bandoli, D.A. Clemente, G. Marangoni, L. Cattalini, *J. Chem. Soc., Dalton Trans.,* 1973, 886.

[38] (a) C.M. Harris, R.S. Nyholm, *J. Chem. Soc.,* 1957, 63.

(b) L.F. Warren, M.A. Bennett, *Inorg. Chem.,* 1976, **15**, 3126.

(c) V.F. Duckworth, N.C. Stephenson, *Inorg. Chem.,* 1969, **8**, 1661.

[39] H. Schmidbaur, *Angew. Chem. Int. Ed. Engl.,* 1983, **22**, 907.

[40] W.R. Cullen, J.D. Woollins, *Coord. Chem. Rev.,* 1981, **39**, 1.

[41] A. Togni, S.D. Pastor, *J. Org. Chem.,* 1990, **55**, 1649.

[42] D.T. Hill, G.R. Girard, F.L. McCabe, R.K. Johnson, P.D. Stupik, J.H. Zhang, W.M. Reiff, D.S. Eggleston, *Inorg. Chem.,* 1989, **28**, 3529.

[43] A. Holton, R.M.G. Roberts, J. Silver, *J. Organomet. Chem*., 1991, **418**,107.

[44] T. Hayashi, T. Mise, M. Fukushima, M. Kagotani, N. Nagashima, Y. Hamada, A. Matsumoto, S. Kawakami, M. Konishi, K. Yamamoto, M. Kumada, *Bull. Chem. Soc. Jpn.,* 1980, **53**, 1138.

[45] C.K. Mirabelli, B.D. Jensen, M.R. Mattern, C. Mei Sung, S.-M. Mong, D.T. Hill, S.W. Dean, P.S. Schein, R.K. Johnson, S.T. Crooke, *Anti-Cancer Drug Des.,* 1987, **1**, 223.

[46] S.J. Berners-Price, P.J. Sadler in 'Platinum and Other Metal Coordination Compounds in Cancer Chemotherapy', Martinus Nijhoff, Boston, 1988, p. 527 and references therein.

[47] C.K. Mirabelli, D.T. Hill, L.F. Faucette, F.L. McCabe, G.R. Girard, D.B. Bryan, B.M. Sutton, J.O. Bartus, S.T. Crooke, R.K. Johnson, *J. Med. Chem.,* 1987, **30**, 2181.

[48] S.J. Berners-Price, R.K. Johnson, C.K. Mirabelli, L.F. Faucette, F.L. McCabe, P.J. Sadler, *Inorg. Chem.,* 1987, **26**, 3383.

[49] (a) P. Köpf-Maier, H. Köpf, E.W. Neuse, *J. Cancer Res. Clin. Oncol.,* 1984, **108**, 336.

(b) P. Köpf-Maier, H. Köpf, *Chem Rev.,* 1987, **87**, 1137.

(c) P. Köpf-Maier, H. Köpf, E.W. Neuse, *Angew. Chem. Int. Ed. Engl.,* 1984, **23**, 456.

[50] G.P. Sollot, J.L. Snead, S. Portnoy, W.R. Peterson Jr., H.E. Mertwoy, *Chem. Abstr.,* 1965, **63**, 18147b.

[51] (a) J.J. Bishop, A. Davison, M.L. Katcher, D.W. Lichtenberg, R.E. Merrill, J.C. Smart, *J. Organomet. Chem.,* 1971, **27**, 241.

(b) G. Mar, T. Hunt, *J. Chem. Soc. (C),* 1969, 1070.

[52] A. Togni, T. Hayashi, 'Ferrocenes: Homogeneous Catalysis, Organic Synthesis, Materials Science', VCH, New York, 1995.

[53] A.W. Rudie, D.W. Lichtenberg, M.L. Katcher, A. Davison, *Inorg. Chem.,* 1978, **17**, 2859.

[54] K.R. Mann, W.H. Morrison Jr., D.N. Hendrickson, *Inorg. Chem.,* 1974, **13**, 1180.

[55] I.R. Butler, W.R. Cullen, T.-J. Kim, S.J. Rettig, J. Trotter, *Organometallics,* 1985, **4**, 972.

[56] W.H. Morrison Jr., D.N. Hendrickson, *Inorg. Chem.,* 1972, **11**, 2912.

[57] A. Houlton, R.M.G. Roberts, J. Silver, R.V. Parish, *J. Organomet. Chem.,*1991, **418**, 269.

[58] L.-T. Phang, T.S.A. Hor, Z.-Y. Zhou, T.C.W. Mak, *J. Organomet. Chem.,* 1994, **469**, 253.

[59] P.M.N. Low, Y.K. Yan, H.S.O. Chan, T.S.A. Hor, *J. Organomet. Chem.,* 1993, **454**, 205.

[60] P. Kalck, C. Randrianalimanana, M. Ridmy, A. Thorez, H.T. Dieck, J. Ehlers, *New J. Chem.,* 1988, **12**, 679.

[61] S.J. Berners-Price, P.J. Sadler, *Struct. Bonding,* 1988, **70**, 27.

[62] V. Scarcia, A. Furlani, B. Longato, B. Corain, G. Pilloni, *Inorg. Chim. Acta,* 1988, **153**, 67.

[63] G. Pilloni, R. Graziani, B. Longato, B. Corain, *Inorg. Chim. Acta,* 1991, **190**, 165.

[64] (a) H. Brunner, *Synthesis,* 1988, 645.

(b) G. Consiglio, R.M. Waymouth, *Chem. Rev.,* 1989, **89**, 257.

(c) I. Ojima, N. Clos, C. Bastos, *Tetrahedron,* 1989, **45**, 6901.

(d) I. Ojima, 'Catalytic Asymmetric Synthesis', VCH Publishers, New York, 1993.

[65] T. Hayashi, *Pure Appl. Chem.,* 1988, **60**, 7.

[66] M. Sawamura, Y. Ito, *Chem. Rev.,* 1992, **92**, 857.

[67] T. Hayashi, K. Yamamoto, M. Kumada, *Tetrahedron Lett.,* 1974, 4405.

[68] D. Marquarding, H. Klusacek, G. Gokel, P. Hoffmann, I. Ugi, *J. Am. Chem. Soc.,* 1970, **92**, 5389.

[69] (a) Y. Ito, M. Sawamura, T. Hayashi, *J. Am. Chem. Soc.,* 1986, **108**, 6405.

(b) Y. Ito, M. Sawamura, T. Hayashi, *Tetrahedron Lett.,* 1987, **28**, 6215.

[70] J.D. Morrison, *Asymmetric Synthesis,* 1985, **5**, London: Academic Press.

[71] R. Noyori, H. Takaya, *Acc. Chem. Res.,* 1990, **23**, 345 and references therein.

[72] B.M. Novak, R.H. Grubbs, *J. Am. Chem. Soc.,* 1988, **110**, 7542.

[73] F. Joó, Z. Tóth, *J. Mol. Cat.,* 1980, **8**, 369.

[74] F. Joó, Z. Tóth, M.T. Breck, *Inorg. Chim. Acta,* 1977, **25**, L61.

[75] W.A. Herrmann, G.P. Albanese, R.B. Manetsberger, P. Lappe, H. Bahrman, *Angew. Chem. Int. Ed. Engl.,* 1995, **34**, 811.

[76] R.T. Smith, M.C. Baird, *Inorg. Chim. Acta,* 1982, **62**, 135.

[77] D.J. Daigle, A.B. Pepperman Jr., S.L. Vail, *J. Heterocyclic Chem.,* 1974, **17**, 407.

[78] S. Otto, A. Roodt, *Inorg. Chem. Commun.,* 2001, **4**, 49.

[79] D.J. Daigle, A.B. Pepperman Jr., S.L. Vail, *J. Heterocyclic Chem.,* 1974, **11**, 407.

[80] Z.A. Sam, A. Roodt, S. Otto, *J. Coord. Chem.,* 2006, **59**, 1025.

[81] A.D. Phillips, L. Gonsalvi, A. Romerosa, F. Vizza, M. Peruzzini, *Coord. Chem. Rev.,* 2004, **248**, 955.

[82] Z. Assefa, B.G. McBurnett, R.J. Staples, J.P. Fackler Jr., B. Assmann, K. Angermaier, H. Schmidbaur, *Inorg. Chem.,* 1995, **34**, 75.

[83] Z. Assefa, B.G. McBurnett, R.J. Staples, J.P. Fackler Jr., P. John, *Inorg. Chem.,* 1995, **34**, 4965.

[84] Z. Assefa, J.M. Forward, T.A. Grant, R.J. Staples, B.E. Hanson, A.A. Mohamed, J.P. Fackler Jr., *Inorg. Chim. Acta,* 2003, **352**, 31.

[85] Z. Assefa, M.A. Omary, B.G. McBurnett, A.A. Mohamed, H.H. Patterson, R.J. Staples, J.P. Fackler Jr., *Inorg. Chem.,* 2002, **41**, 6274.

[86] J.M. Forward, R.J. Staples, C.W. Liu, J.P. Fackler Jr., *Acta Cryst.,* 1997, C**53**, 195.

[87] J.M. Forward, Z. Assefa, R.J. Staples, J.P. Fackler Jr., *Inorg. Chem.,* 1996, **35**, 16.

[88] F.P. Pruchnik, P. Smoleñski, E. Galdecka, Z. Galdecki, *New J. Chem.,* 1998, 1395.

[89] F.P. Pruchnik, P. Smoleñski, E. Galdecka, Z. Galdecki, *Inorg. Chim. Acta,* 1999, **293**, 110.

[90] F. Joó, G. Laurenczy, L. Nádasdi, J. Elek, *Chem. Commun.,* 1999, 971.

[91] O.M. Ni Dhubhghaill, P.J. Sadler, 'Metal Complexes in Cancer Chemotherapy', ed. B.K. Keppler, VCH, Weinheim, 1993, p. 221.

[92] C.F. Shaw III, 'Metal Compounds in Cancer Therapy', ed. S.P. Fricker, Chapman and Hall, London, 1994, p. 46.

[93] B. Rosenberg, L. van Camp, J.E. Trosko, V.H. Mansour, *Nature,* 1969, **22**, 385.

[94] M. Peyrone, *Ann. Chem. Pharm.,* 1844, **LI**, 1.

[95] M.P. Hacker, E.B. Douple, I.H. Krakoff, Eds. 'Platinum Coordination Complexes in Cancer Chemotherapy', Martinus Nijhoff: Boston, 1984.

[96] J. Reedijk, P.H.M. Lohman, *Pharm. Week. Sci. Ed.*, 1985, **7**, 173.

[97] D.M. Orton, V.A. Gretton, M. Green, *Inorg. Chim. Acta,* 1993, **204**, 265.

[98] K.W. Lee, D.S. Martin, Jr., *Inorg. Chim. Acta,* 1976, **17**, 105.

[99] S.E. Sherman, S.J. Lippard, *Chem. Rev.,* 1987, **87**, 1153.

[100] C. Moncur, H.J. Williams, *Phys. Ther.,* 1995, **75**, 511.

[101] G.D. Champion, G.G. Graham, J.B. Ziegler, *Balliéré's Clin. Rheumatol.,* 1990, **4**, 491.

[102] N.L. Gottlieb, *J.Rheumatol.,* 1982, **9 (Suppl. 8)**, 99.

[103] R.V. Parish, S.M. Cottrill, *Gold Bull.,* 1987, **20**, 3.

[104] D.T. Felson, J.J. Anderson, R.F. Meenan, *Arthritis Rheum.,* 1990, **33**, 1449.

[105] M. Harth, *J. Rheumatol.,* 1993, **20**, 771.

[106] J. Bondeson, *Gen. Pharmac.,* 1997, **29**, 127.

[107] M.H. Pioro, J.M. Cash, *Rheum. Dis. Clin. North Am.,* 1995, **21**, 129.

[108] G.D. Champion, G.G. Graham, J.B. Ziegler, *Balliéré's Clin. Rheumatol.,* 1990, **4**, 491.

[109] R.E. Thomas, R.A. Papandrea, *Med. J. Aust.,* 1993, **158**, 720.

[110] B.A. Becker, A.A. Gaspari, *Dermatol. Clin.,* 1991, **11**, 429.

[111] A.D. Ormerod, *Drugs,* 1994, **48**, 717.

[112] C.F. Shaw III, In 'Metal Compounds in Cancer Therapy', edited by S.P. Fricker; Chapman and Hall, London, 1994, p. 46-64.

[113] O.M. Ni Dhubhghaill, P.J. Sadler, In 'Metal Complexes in Cancer Chemotherapy', edited by B.K. Keppler; VCH, Weinheim, 1993, 221.

[114] A.E. Finkelstein, D.T. Walz, U. Batista, M. Mixraji, F. Roisman, A. Misher, *Ann. Rheum. Dis.,* 1976, **35**, 251.

[115] F.E. Berglof, K. Berglof, D.T. Walz, *J. Rheum.,* 1978, **5**, 68.

[116] D.T. Hill, B.M. Sutton, *Cryst. Struct. Commun.,* 1980, **9**, 679.

[117] P.J. Sadler, M. Nasr, V.L. Narayanan, In 'Platinum Coordination Complexes in Cancer Chemotherapy'; M.P. Hacker, E.B. Douple, I.H. Krakoff, Eds.; Martinus Nijhoff Publishing, Boston, 1984, pp 209-304.

[118] (a) T.M. Simon, D.H. Kunishima, G.J. Vibert, A. Lorber, *Cancer*, 1979, **44**, 1965.
(b) T.M. Simon, D.H. Kunishima, G.J. Vibert, A. Lorber, *Cancer Res.*, 1981, **41**, 94.

[119] (a) C.K. Mirabelli, R.K. Johnson, C. Mei Sung, L. Faucette, K. Muirhead, S.T. Crooke, *Cancer Res.,* 1985, **45**, 32.
(b) C.K. Mirabelli, R.K. Johnson, D.T. Hill, L. Faucette, G.R. Girard, G.Y. Kuo, C. Mei Sung, S.T. Crooke, *J. Med. Chem.,* 1986, **29**, 218.

[120] S.J. Berners-Price, C.K. Mirabelli, R.K. Johnson, M.R. Mattern, F.L. McCabe, L. Faucette, C. Mei Sung, S.M. Mong, P.J. Sadler, S.T. Crooke, *Cancer Res.,* 1986, **46**, 5486.

[121] C.K. Mirabelli, R.K. Johnson, S.T. Crooke, M.R. Mattern, S.M. Mong, C. Mei Sung, G. Rush, S.J. Berners-Price, P.S. Jarrett, P.J. Sadler in M. Nicolini and G. Bandoli (Eds.), '5th International Symposium on Platinum and Other Metal Coordination Compounds in Cancer Chemotherapy', 1987, p319.

[122] S.J. Berners-Price, P.S. Jarrett, P.J. Sadler, *Inorg. Chem.,* 1987, **26**, 3074.

[123] G.D. Hoke, R.A. Macia, P.C. Meunier, P.J. Bugelski, C.K. Mirabelli, G.F. Rush, W.D. Matthews, *Toxicol. Appl. Pharmacol.,* 1989, **100**, 293.

[124] S. Komiya, T.A. Albright, R. Hoffmann, J.K. Kochi, *J. Am. Chem. Soc.,* 1971, **98**, 7255.

[125] H.S. Gutowsky, C.H. Holm, *J. Chem. Phys.,* 1956, **25**, 1228.

[126] P.N. Dickson, A. Wehrli, G. Geier, *Inorg. Chem.,* 1988, **27**, 2921.

[127] L.H. Skibsted, *Adv. Inorg. Bioinorg. Mech.,* 1986, **4**.137.

[128] A. Shiotani, H.-F. Klein, H. Schmidbaur, *J. Am. Chem. Soc.,* 1971, **93**, 1555.

[129] U. Frey, S. Elmroth, B. Moullet, L.I. Elding, A.E. Merbach, *Inorg. Chem.,* 1991, **30**, 5033.

[130] H. Schmidbaur, In 'Gold: Progress in Chemistry, Biochemistry and Technology', John Wiley & Sons, London, 1999.

[131] L.H. Skibsted, J. Bjerrum, *Acta Chem. Scand. A,* 1977, **31**, 155.

[132] A.S. Chernyak, L.F. Shestopalova, *Russ. J. Inorg. Chem., Engl. Transl.,* 1976, **21**, 464.

[133] P.J. Sadler et al., *J. Inorg. Biochem.,* 1995, **54**, 225.

[134] (a) B.J. Wood, H. Wise, *J. Catal.,* 1966, **5**, 135.
(b) R.S. Yolles, B.J. Wood, H. Wise, *J. Catal.,* 1971, **21**, 66.

[135] J. Schwank, *Gold Bull.,* 1983, **16**, 4.

[136] H. Schmidbaur, *Naturw. Rdsch.,* 1995, **48**, 443.

[137] (a) M. Haruta, *Gold Bull.,* 2004, **37**, 27.
(b) M. Cortie, R. Holliday, A. Laguna, B. Nieuwenhuys, D. Thompson, *Gold Bull.,* 2003, **36**, 144.

[138] W.D. Provine, P.L. Mills, J.J. Lerou, *Stud. Surf. Sci. Catal.,* 1996, **101**, 191.

[139] R. Meyer, C. Lemire, K. Shaikhutdinov, H.-J. Freund, *Gold Bull.,* 2004, **37**, 72.

[140] A. Venugopal, J. Aluha, D. Mogano, M.S. Scurrell, *Appl. Catal. A: Gen.,* 2003, **245**, 149.

[141] M.C. Daniel, D. Astruc, *Chem. Rev.,* 2004, **104**, 293.

[142] J. Gong, C. Shao, Y. Pan, F. Gao, L. Qu, *Mater. Chem. Phys.,* 2004, **86**, 156.

[143] M. Suliman Selim, R. Seoudi, A.A. Shabaka, *Mater. Lett.,* 2005, **59**, 2650.

[144] (a) G. Dyker, *Angew. Chem.,* 2000, **112**, 4407.
(b) G. Dyker, *Angew. Chem. Int. Ed. Engl.,* 2000, **39**, 4237.

[145] A.S.K. Hashmi, *Gold Bull.,* 2004, **37**, 51.

[146] D.J. Gorin, F.D. Kotse, *Nature,* 2007, **446**, 395.

[147] A.S.K. Hashmi, *Gold Bull.,* 2003, **36**, 3.

[148] M.T. Reetz, K. Sommer, *Eur. J. Org. Chem.,* 2003, 3485.

[149] C. Wei, C.-J. Li, *J. Am. Chem. Soc.,* 2003, **125**, 9584.

[150] GOLD2006 conference: New Industrial Applications of Gold, 2006, University of Limerick, Limerick, Ireland.

3 MONODENTATE GOLD(I) SYSTEMS AND THEIR INTERACTION WITH LIGANDS AND CYCLODEXTRINS

3.1 INTRODUCTION

3.1.1 General Au(I) applications

As discussed in Chapter 2, the treatment of diseases with gold complexes (called chrysotherapy) can be traced back since the beginning of times[1]. The mechanistic approach regarding the action of gold drugs is still a matter of interest and research, however they remain the most effective second line treatment for rheumatoid arthritis[2,3]. This led to the development of a gold complex called auranofin (2,3,4,6-tetra-*O*-acetyl-1-thio-β-D-glucopyranosato(triethylphosphine) gold(I)) by Smith, Kline and French laboratories. Auranofin was found to be an experimental chrysotherapeutic agent shown by groups of Finkelstein[4] and Berglof[5] and was clinically effective in the treatment of rheumatoid arthritis when administered orally. Research groups like Walz *et al*.[6] have shown that auranofin has a unique pharmacological profile when compared with the previously used gold drugs, myochrisin and solganol, which were administered by injection. Auranofin is a lipid-soluble, linear two-coordinate complex which has a potent action in treatment of rheumatoid arthritis and its structure has been characterised by X-ray diffraction[7].

Small cage-type ligands like 1,3,5-triaza-7-phosphatricyclo[3.3.1.1^{3,7}] decane (PTA) have very narrow cone angles at their donor centres and can thus be readily accommodated even at crowded coordination centres. Organometallic complexes containing phosphine ligands, such as PTA, are currently widely under investigation for their chemical behaviour[8,9,10,11]. The discovery and synthesis of PTA in early 1970's[12], geared a wide investigation into this tetrabasic ligand and has produced a multifunctional ligand with one donor site for the complexation of soft, low valent, late transition elements. Its ligand chemistry has been exploited to date in a limited number of cases[13,14,15] and its behaviour as a ligand for gold has now been probed.

PTA has a cone angle of 118° (similar to that of PMe_3)[16] thus has a low steric demand and by taking advantage of this reduced steric hindrance, stable platinum(II) complexes containing this ligand can be prepared. The PTA ligand is also of interest due to its solubility in aqueous media and ability to form hydrogen bonds with both counter-ions and water molecules. This ligand has been receiving much attention because of its remarkable characteristics since it is neutral, water-soluble, and is stable in air. Investigations on various transition elements containing these ligands are of importance in numerous fields, for example in catalysis[17], possible medical applications[18] *etc*. PTA was found to be an extremely important ligand in gold chemistry and this research was stimulated by the intention to prepare water-soluble phosphine gold(I) complexes.

The research described here has been aimed at manipulating and tailoring of the phosphine moiety coordinated to the gold in auranofin. Ligands, for example 1,3,5-triaza-7-phosphatricyclo[3.3.1.$1^{3,7}$]decane (PTA) and its alkylated analogue which is soluble in aqueous media was employed. This study also includes interchanging the phosphine moiety of the auranofin with triethylarsine forming the arsine analogue. Gold compounds with mixed phosphine/arsine ligands and the influence of the substitution of the phosphorus atom by arsenic have been investigated[19]. A fine tuning of selected physical and chemical properties can reduce poisonous side effects and this opens up new field worthy of chemical, biochemical, toxicological and structural interest. Therefore, the synthesis of auranofin, PTA-auranofin, PTAMe-auranofin and arsine-auranofin is described later in the chapter and the biochemical activity analysis of these complexes is reported in Chapter 5. In this chapter, the experimental details and the characterisation of the ligands and the complexes prepared are described. Characterisation was done using IR and NMR spectroscopy as well as X-ray crystallography, which will be discussed in more detail: (§ 3.4). Also presented in this chapter is the investigation of equilibria of substitution of chloride from gold complexes with ligands as well as equilibria from the interactions and inclusion of compounds and gold complexes into β-cyclodextrin by NMR techniques (§ 3.5 - 3.6).

3.1.2 Applications of cyclodextrins in drug delivery

Cyclodextrins, which are cyclic sugars, comprise a family of cyclic oligosaccharides obtained from starch by enzymatic degradation. These cyclic oligosaccharides consist of at least six glucopyranose units and although cyclodextrins with up to 12 glucose

residues are known[20]. Cyclodextrins composed of less than six glucose units are not known to exist due to steric hindrance[21] and the six-fold character of the starch helix[22]. The most common ones contain six, seven and eight such moieties and are called α-cyclodextrin (α-CD), β-cyclodextrin (β-CD) and γ-cyclodextrin (γ-CD), respectively. These cyclodextrins have been isolated by selective precipitation with appropriate organic compounds[23,24]. In this research study cyclodextrins are employed to induce water-solubility of the complexes prepared and to investigate structural properties of the inclusion complexes as well as 'host-guest' interactions.

Cyclodextrins have undoubtedly found applications in many areas in analytical and supramolecular chemistry, biological systems and so forth because of the versatile binding abilities, ease of modification, good solubilities in water and their importance in 'host-guest' chemistry[23]. The properties of cyclodextrins and their ability to accomodate a range of suitable organic, metal-organic and inorganic guest molecules and ions in solutions and in the solid state have been well documented[25]. They also have received a great deal of attention[26] as enzyme models. Cyclodextrins can serve as good models for non-covalent bonding, since they can accommodate guests that are small enough to fit into their cavities.

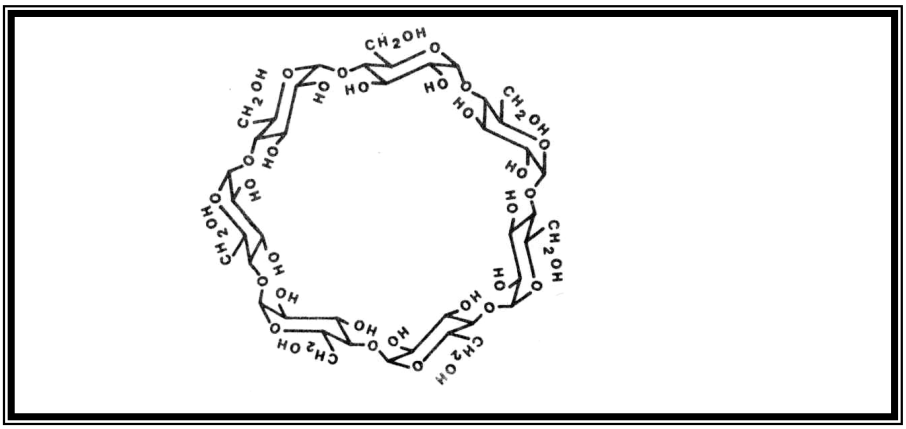

Figure 3.1 Illustration of β-cyclodextrin showing the cyclic sugar units joined by α-(1,4) linkages and in chair conformation[27].

Cyclodextrins are cyclic oligosaccharides consisting of α-(1,4)-linked D-glucopyranose units. All of the glucopyranoside building blocks are relatively rigid and exist in a $^4C_1$ chair conformation. The natural method of synthesis of cyclodextrins includes the enzymatic degradation of starch which affords a mixture of cyclic and linear maltooligosaccharides. According to literature[28] the enzymes used are cyclodextrin glucosyl transferases (CGTases) which are of bacterial origin, *e.g.* from *Bacillus*

macerans and *alcaliphilic bacilli*[29]. The isolation of a specific cyclodextrin is done by addition of selective precipitating agents[22] and the final product is the one that is continuously removed from the reaction mixture by selective precipitation. This results in remarkable yields and high homologous purity of cyclodextrins[30]. It is stated in literature that due to the biological origin of cyclodextrins, only the dextrorotatory enantiomers are formed, the levorotatory enantiomers could be obtained by synthetic procedures but an economical total synthesis does not appear feasible as yet[28]. For an example, the D-α-CD and D-γ-CD have been obtained from D-maltose in multi-step procedures[31].

The structures of cyclodextrins display a geometry which gives the overall shape of a truncated cone. The oligosaccharide ring forms a torus with the primary hydroxyl groups of the glucose residues lying on the narrow end of the torus. The secondary glucopyranose 2- and 3-hydroxyl groups are located on the wider end (Fig. 3.2). The number of glucose units determines the dimensions and the size of the cavity. The hydrogen atoms and glycosidic oxygen bridges in the cavity of the cyclodextrins are arranged in such a way that the nonbonding electron pairs of the glycosidic oxygen bridges are directed towards the inside of the cavity. This therefore gives the cyclodextrin a Lewis base character, by virtue of the resulting high electron density. This unique arrangement of the functional groups in cyclodextrin molecules results in the cavity being relatively hydrophobic compared to water while the external faces are hydrophilic. Also, a ring of hydrogen bond interaction is also formed intramolecularly between the 2-hydroxyl and the 3-hydroxyl groups of the adjacent glucose units, which enables the cyclodextrins to have remarkable rigid structures.

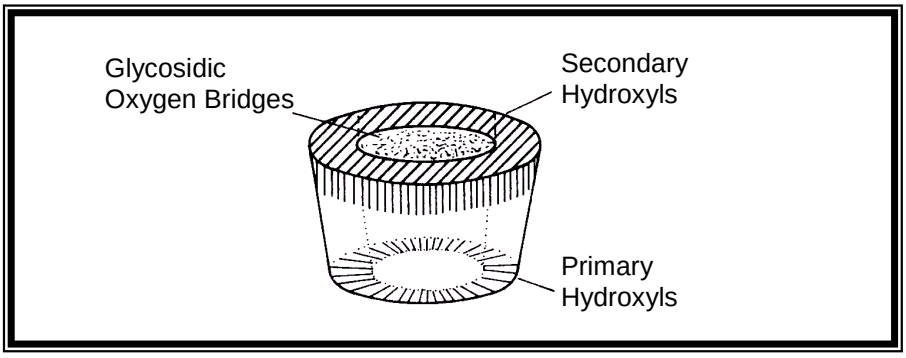

Figure 3.2 Functional structural scheme of β-cyclodextrin with the alignment of the hydroxyl groups and oxygen bridges thus forming a cone[27].

The structural features of cyclodextrins lead to their unique physical and chemical properties. These include the fact that they are water-soluble, with solubilities of 14.5,

1.85 and 23.2 g/100 mL for α-, β-, and γ-cyclodextrins respectively[27]. Cyclodextrins are stable in alkaline solutions but their stability in acidic medium can be susceptible to hydrolysis, depending on temperature and acidity, resulting in the breakdown of the cyclodextrin to glucose and a series of acyclic maltosaccharides[32].

The most striking characteristic of cyclodextrins is their interesting ability to form inclusion complexes with a wide variety of guest molecules; organic or inorganic compounds of neutral or ionic nature. It has been noted that the minimum requirement for the inclusion of the guest molecule to the host cyclodextrin is that the guest molecule must fit into the cavity, even if only partially. The guest molecule-cyclodextrin complex formation in solution is a dynamic equilibrium process and the stabilising binding forces involved in the process are:

- van der Waals interactions between the hydrophobic moiety of the guest molecules and the cyclodextrin cavity.
- Hydrogen bonding interactions between the polar functional groups of the guest molecules and the hydroxyl groups of the cyclodextrin.
- Release of water molecules from the cavity in the guest molecule-cyclodextrin complex formation process.
- Release of strain energy in the ring frame system of the cyclodextrin.

The stability of a 'host-guest' inclusion compound also depends on the polarity of the guest molecule where the stability of the complex is proportional to the hydrophobic character of the guest molecule. The complexation of inclusion compounds is usually done in aqueous medium and the stability of the compounds strongly depends on the nature of the medium used. The stability of the inclusion compounds has also been found to decrease with increasing temperature[33]. The complexing ability of the cyclodextrins can be modified by substitution of the hydrogen atom or hydroxyl groups of the primary or secondary hydroxyl groups in the cyclodextrin molecule or even splitting one or more C-C bonds through a periodate oxidation. This has therefore generated some articles on the use of chemically modified cyclodextrins[34,28,35].

Cyclodextrins and their applications in analytical chemistry have been widely reported in reviews[27]. Among these, applications of cyclodextrins include enzyme or drug modelling and delivery[36,37] and in 'host-guest' catalysis[38].

The overview of this project regarding cyclodextrins has thus been selected to investigate, in a combination with the gold drug model complexes, for possible application to increase solubility of ligands and transition metal complexes.

3.2 EXPERIMENTAL

All common laboratory reagents and chemicals used in the preparations were of reagent grade and distilled water was used in all experiments. All manipulations with air and moisture sensitive compounds were performed by means of standard Schlenk techniques[39] under argon gas. The following chemicals were commercially available: $HAuCl_4$ (Next Chimica); Tetrahydrothiophene (Merck); 1-thio-β-D-glucose tetraacetate (Aldrich); PEt_3, $AsEt_3$ (Strem); β-cyclodextrin (Fluka); Hexamine; $MeOSO_2CF_3$ (Fluka); PPh_3 (Merck). These reagents were used without further purification.

The characterisation of the complexes was done with ^1H and ^{31}P NMR (Varian Gemini 200 spectrometer operating at 300 and 121.5 MHz, respectively). The ^1H and ^{31}P NMR spectra were recorded at 25 °C in D_2O, DMSO, $CDCl_3$ or MeOD, where relevant. The ^1H NMR spectra were referenced relative to the residual relevant peaks while the ^{31}P NMR spectra were referenced relative to 85% H_3PO_4 as an external standard at 0.0 ppm. Infrared spectra were recorded as KBr disks using a DIGILAB Merlin FTIR spectrometer in the range 4000 - 500 cm^{-1}. The UV-Vis spectra were obtained on a CARY 50 CONC UV-Vis spectrophotometer with cell holders which were thermostated to within 0.1 °C.

3.3 SYNTHESIS OF COMPOUNDS AND COMPLEXES

3.3.1 Synthesis of compounds

3.3.1.1 1,3,5-triaza-7-phosphatricyclo[3.3.1.1^{3,7}]decane (PTA)

The procedure described is as according to that of Daigle[40]. To a beaker containing ice (12.4 g) and tetrakis(hydroxymethyl)phosphonium chloride (80% solution in water, 17 mL, 95 mmol), a solution of NaOH (50% w/w, 6.39 g) was slowly added while manually stirring. After the resulting clear colourless solution reached room temperature, formaldehyde (37%, 45 g, 0.55 mol) was added, followed by hexamethylenetetraamine

(14 g, 99.9 mmol) that was dissolved in the solution, which was subsequently allowed to stand overnight. The solution was then transferred to a large evaporating dish and placed in a hood for evaporation. It was allowed to stand until the solution became approximately 80% solid. The solid was then filtered on a Büchner funnel, washed with several volumes of cold ethanol and allowed to dry in air giving the desired product (6.0 g, 38%).

^{1}H NMR (D_2O): δ3.81 (d, 6H), 4.35 (dd, 6H) ppm; $^{31}P\{^{1}H\}$ NMR (D_2O): δ-95.7 (s) ppm.

^{1}H NMR (DMSO): δ3.93 (d, 6H), 4.42 (dd, 6H) ppm; $^{31}P\{^{1}H\}$ NMR (DMSO): δ-103.0 (s) ppm.

3.3.1.2 (PTAMe)I

The procedure is as described by Daigle and co-workers[40]. In a 250 mL round-bottomed flask fitted with a reflux condenser, PTA (600 mg, 3.8 mmol) and methyl iodide (552 mg, 3.8 mmol) were dissolved in 72 mL of acetone. Methyl iodide was weighed in a little amount of acetone to avoid evaporation. The mixture was then refluxed for 1h during which a white precipitate formed. The solution was filtered in air through a Büchner funnel and subsequently washed with acetone. This resulted in a crude yield of 914 mg of the methylammonium salt. The product was recrystallised in a 60 mL solution of methanol:ethylacetate (1:1) and upon cooling in an ice bath a white precipitate formed (638 mg, 56%).

^{1}H NMR (DMSO): δ2.60 (s), 3.33 (s), 3.71 - 4.97 ppm (complex set of peaks).

$^{31}P\{^{1}H\}$ NMR (DMSO): δ-85.85 (s) ppm.

3.3.1.3 [Au(THT)Cl]

The synthesis of this complex was done in the following procedure[41]. Tetrachloroauric acid hydrate, $HAuCl_4 \cdot 3H_2O$ (1.97 g, 5.0 mmol) was dissolved in an ice-cooled solution of absolute ethanol:water (25 mL: 5 mL). Tetrahydrothiophene (1 mL, 11.3 mmol) was then added dropwise to the solution for approximately 10 min with stirring. A yellow [$Au(THT)Cl_3$] precipitate appeared and this was subsequently reduced to the white [Au(THT)Cl] solid. After 20 min stirring at room temperature, the solid was filtered off, washed with ethanol (2 x 10 mL) and dried. The product was transferred to a storage flask and further dried in vacuum, (Yield = 1.45 g, 90%). The material was then stored in the fridge as it slowly decomposes in room temperature when dry.

^{1}H NMR ($CDCl_3$): δ2.181 (d, 4H), 3.402 (d, 4H) ppm.

3.3.2 Synthesis of gold(I) complexes with PTA as ligand

3.3.2.1 [Au(PTA)Cl]

To a stirred suspension of [Au(THT)Cl] (200 mg, 0.62 mmol) in 15 mL of MeOH:CH_3CN (2:1), solid PTA (98 mg, 0.62 mmol) was added in one portion. In about 2 minutes, a gelatinous white precipitate appeared which turned to a fine precipitate in approximately 15 minutes. After 2 hours of further stirring diethyl ether (7 mL) was added to precipitate the entire product. The precipitate was filtered, washed with cold ethanol and ether and dried under vacuum to give the desired product. (Yield = 185 mg, 76%.)

^{1}H NMR (DMSO): δ 4.42 (dd, PCH_2), 2.49 (s, NCH_2N_{eq}), 2.49 (s, NCH_2N_{ax}) ppm.

$^{31}P\{^1H\}$ NMR (DMSO): δ -51.08 (s) ppm.

3.3.2.2 [Au(PTAMe)Cl]SO_3CF_3

Method of synthesis is as found in literature[42]. A slurry of [Au(PTA)Cl] (2.26 g, 5.8 mmol) in CH_2Cl_2 (150 mL) was treated at -35 °C with $MeOSO_2CF_3$ (1 mL, 9 mmol). The mixture was allowed to warm to ambient temperature over a period of 4 hours. The solvent and other volatiles were removed in a vacuum and the residue gave a white solid (Yield = 2.70 g, 84%).

^{1}H NMR (DMSO): δ 2.73 (d, 3H, NCH_3) , 4.0 - 5.2 (m, 12H, CH_2) ppm.

$^{31}P\{^1H\}$ NMR (DMSO): δ -32.98 (s) ppm.

3.3.2.3 [Au(PTA)SCN]

This method of synthesis was according to the modified procedure found in literature[42]. A suspension of [Au(PTA)Cl] (0.1 g, 0.26 mmol) in boiling acetone (50 mL) was treated with a slurry of excess KSCN (0.1 g, 1.0 mmol) in 50 mL acetone. After 1h at reflux temperature and overnight stirring, the solvent was removed in a vacuum. The residue was extracted with boiling acetonitrile and the product precipitates from the solvent on cooling forming colourless crystals (80 mg, 76%).

^{1}H NMR (DMSO): δ 4.35 (d, PCH_2), 4.49 (s, NCH_2N_{eq}), 4.53 (s, NCH_2N_{ax}) ppm.

$^{31}P\{^1H\}$ NMR (DMSO): δ -47.1 (s) ppm.

IR (KBr): ν (SCN) 2064 cm^{-1}.

3.3.2.4 [Au(PTA)SC(NH_2)$_2$]Cl

These thiourea complexes were synthesised by modification of the procedure found in literature[43]. [Au(PTA)Cl] (0.1 g, 0.26 mmol) was suspended in 20 mL methanol. 3 equivalents of thiourea (0.070 g, 0.78 mmol) were added as a solid to the suspension. After the addition of the equivalents of the solid the solution turned colourless. The solution was stirred for a further 30 minutes, filtered and then kept in the fridge for crystallisation (85 mg, 71%).

^{1}H NMR (DMSO): δ4.33 (d, PCH_2), 4.48 (s, NCH_2N_{eq}), 4.52 (s, NCH_2N_{ax}), 7.56 (broad, CNH_2 peak) ppm.

^{31}P{^{1}H} NMR(DMSO) : δ-50.1 (s) ppm.

3.3.2.5 [Au(PTA)SC(NH_2)(NH(CH_3))]Cl

Complex was synthesised by modification of the procedure found in literature[43]. [Au(PTA)Cl] (0.1 g, 0.26 mmol) was suspended in 20 mL methanol. 3 equivalents of methyl thiourea (0.070 g, 0.78 mmol) were added as a solid to the suspension. After the addition of the equivalents of the solid the solution turned colourless. The solution was stirred for a further 30 minutes, filtered and then kept in the fridge for crystallisation. There were no crystals formed and the solution was evaporated to form a sticky oily product (63 mg, 47.6%).

^{1}H NMR (DMSO): δ4.34 (s, PCH_2), 4.47 (s, NCH_2N_{eq}), 4.51 (s, NCH_2N_{ax}) ppm.

^{31}P{^{1}H} NMR (DMSO): δ-49 (s) ppm.

3.3.3 Synthesis of gold(I) complexes with tertiary phosphine ligands

Complexes in § 3.3.3.1 - 3.3.3.2 were synthesised by following a similar procedure as found in literature[44].

3.3.3.1 [Au(PEt_3)Cl]

Monochlorotriethylphosphine gold was prepared by carefully adding a solution of triethylphosphine (6 mL, 40.7 mmol) in 20 mL ethanol to a well cooled stirred mixture of the tetrachloroauric acid hydrate (7.5 g, 19 mmol) in 20 mL ethanol. An orange product first separated and was rapidly replaced by the required white solid. The mixture was

shaken for 1 hour, diluted with water (50 mL) and the white product collected, washed with water and dried. Cooling and (in particular) the presence of alcohol appeared to be essential for such preparations (Yield = 4.64 g, 69%).

^{1}H NMR ($CDCl_3$): δ 1.12 - 1.23 (dt, 9H, ($CH_3CH_2)_3P$), 1.76 - 1.88 (dq, 6H, ($CH_3CH_2)_3P$) ppm.

$^{31}P\{^{1}H\}$ NMR ($CDCl_3$): δ 31.98 (s) ppm.

3.3.3.2 [Au($AsEt_3$)Cl]

A solution of triethylarsine (4 mL, 28.4 mmol) in 20 mL ethanol was added to a well cooled stirred mixture of the tetrachloroauric acid hydrate (4 g, 10 mmol) in 20 mL ethanol. An orange product first separated and was rapidly replaced by the required white solid. The mixture was shaken for 1 hour, diluted with water (50 mL) and the white product collected, washed with water and dried (Yield = 2 g, 50%). Yield can be improved if [Au(THT)Cl] is treated with $AsEt_3$ on a 1:1 ratio.

^{1}H NMR (MeOD): δ 0.12 (t, 9H, ($CH_3CH_2)_3As$), 0.64 (q, 6H, ($CH_3CH_2)_3As$) ppm.

3.3.3.3 [Au(PPh_3)Cl]

The procedure for the synthesis of the [Au(PPh_3)Cl] complex is as given in literature[45]. Triphenylphosphine (2.32 g, 8.8 mmol) was dissolved in 50 mL of absolute ethanol contained in a flask, with gentle warming to complete dissolution. A solution of hydrogen tetrachloroaurate (1.5 g, 4.4 mmol) in 10 mL ethanol was filtered, to remove any insoluble gold-containing material, into the stirred solution of triphenylphosphine. This gave a white precipitate. After stirring for 15 min, the white microcrystalline solid was collected on a fritted glass filter (Corning porosity 3), washed with ethanol (2 x 5 mL) and dried in vacuum to give [Au(PPh_3)Cl]. (Yield: 1.17 g, 54%).

^{1}H NMR ($CDCl_3$): δ 7.47 - 7.54 (m, 15H) ppm.

$^{31}P\{^{1}H\}$ NMR ($CDCl_3$): δ 33.15 (s) ppm.

IR (KBr): *v* 692(s), 748(m) (peaks indicating the presence of phenyl groups), 1102(m), 1434(s) (aromatic ring), 1479(w) cm^{-1}.

3.3.4 Synthesis of auranofin analogues

3.3.4.1 Auranofin

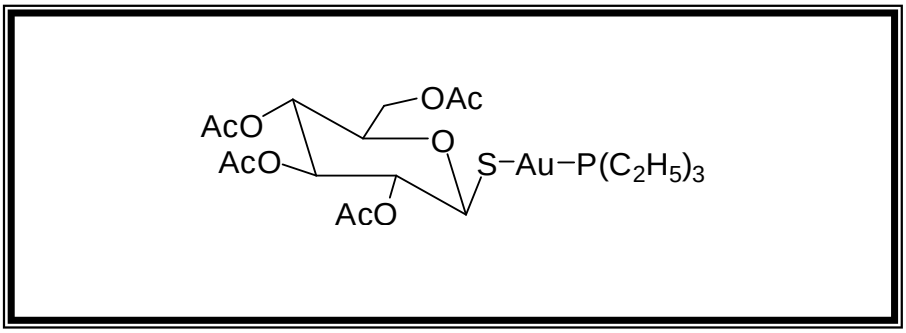

Figure 3.3 Illustration of the structure of 2,3,4,6-tetra-*O*-acetyl-1-thio-β-D-glucopyranosato(triethylphosphine)gold(I) (auranofin).

To a solution of 2,3,4,6-tetra-*O*-acetyl-1-thio-β-D-glucopyranose (500 mg, 1.37 mmol) in ethanol:H_2O (10 mL:2.5 mL) at 0 °C, a solution of K_2CO_3 (190 mg, 1.37 mmol) in water (1.25 mL) was added. This was followed by addition of [Au(PEt_3)Cl] (481 mg, 1.37 mmol) in EtOH:DCM (9 mL: 1.5 mL). The mixture was stirred at 0 °C for 1 hour and after that diluted with water. The solution was extracted with CH_2Cl_2 (5 x 50 mL), dried with $MgSO_4$, filtered and the solvent removed *in vacuo* to give an oily material. This was redissolved in methanol, put in the fridge to give a white solid (Yield = 350 mg, 38%). The crystals of the auranofin compound were obtained when the co-crystallisation of the auranofin-β-cyclodextrin inclusion compound was attempted by heating at 60 °C an aqueous solution of β-cyclodextrin with auranofin. The crystals were obtained as needles and are colourless. The compound crystallises in the monoclinic space group $P2_1$ with one molecule in an asymmetric unit. The crystal structure for the compound is discussed in § 3.4.2.

^{1}H NMR (DMSO): δ 1.54 (dt, 9H, (CH_3CH_2)$_3$P), 1.84 - 2.05 (m, (12H, OCOCH_3 (sugar) + 6H, (CH_3CH_2)$_3$P)), 4.0 (m, 7H (sugar)) ppm.

^{31}P{^{1}H} NMR (DMSO): δ 36.70 (s) ppm.

3.3.4.2 PTA-auranofin

PTA-auranofin = 2,3,4,6-tetra-*O*-acetyl-1-thio-β-D-glucopyranosato(1,3,5-triaza-7-phosphatricyclo[3.3.1.1^{3,7}]decane) gold(I).

A solution of K_2CO_3 (177 mg, 1.28 mmol) in water (1.2 mL) was added to a solution of 2,3,4,6-tetra-*O*-acetyl-1-thio-β-D-glucopyranose (468 mg, 1.28 mmol) in ethanol:H_2O (9 mL:2 mL) at 0 °C followed by addition of [Au(PTA)Cl] (500 mg, 1.28 mmol) in EtOH:DCM (7 mL:1 mL). The mixture was stirred at 0 °C for 1 hour and after that diluted with water (45 mL). The solution was extracted with CH_2Cl_2 (5 x 10 mL), dried with $MgSO_4$, filtered and the solvent removed in vacuo to give a white solid. (Yield ≈ 450 mg, 49%).

^{1}H NMR (D_2O): δ 2.0 (dd, 3H, OCOCH_3), 4.0 (dd, 2H), 4.2 (s, broad, H), 4.3 (s, 6H), 4.5 (dd, 6H), 4.6 (s, H); 4.8(t, H), 5.0 (t, H), 5.1 (dt, 2H) ppm.

^{31}P{^{1}H} NMR (D_2O): δ -44.98 (s) ppm.

3.3.4.3 2,3,4,6-tetra-*O*-acetyl-1-thio-β-D-glucopyranosato(1-methyl-1,3,5-triaza-7-phosphatricyclo[3.3.1.1^{3,7}]decanium-*P*) gold(I)

The complex was synthesised according to the procedure similar to the one of Bell *et al.*[46]. 1-thio-β-D-glucose tetraacetate (132 mg, 0.36 mmol) was added to a solution of [Au(PTAMe)Cl]SO_3CF_3 (200 mg, 0.36 mmol) in MeOH:CH_3CN (50 mL) solvent mixture. This solution mixture was stirred for 3 hours and the solution was evaporated under vacuum. The residue was washed with diethyl ether, dried to give a white product (170 mg, 54%).

^{1}H NMR (DMSO): δ 1.91 - 2.04 (q, 12H, OCOCH_3), 2.75 (d, 3H, NCH_3), 3.99 - 5.28 (m, (12H (MePTA) + 7H (sugar)) ppm.

^{31}P{^{1}H} NMR (DMSO): δ -31.93 (s, broad peak) ppm.

3.3.4.4 2,3,4,6-tetra-*O*-acetyl-1-thio-β-D-glucopyranosato(triethylarsine) gold(I)

To a solution of 1-thio-β-D glucose tetraacetate (185 mg, 0.5 mmol) in CH_2Cl_2 (15 mL), a solution of [Au($AsEt_3$)Cl] (200 mg, 0.5 mmol) in 10 mL of CH_2Cl_2 was added. The mixture was stirred for 3 hours and the solution was evaporated under a slow flow of nitrogen gas. The residue was washed with diethyl ether, dried to give a white product (285 mg, 78%).

^{1}H NMR (MeOD): δ 1.54 (t, 9H, (CH_3CH_2)$_3$As), 2.15 - 2.41 (m, (12H, OCOCH_3 (sugar) + 6H, (CH_3CH_2)$_3$As)), 4.0 (m, 7H (sugar)) ppm.

3.3.4.5 2,3,4,6-tetra-*O*-acetyl-1-thio-β-D-glucopyranosato(triphenylphosphine) gold(I)

To a solution of 1-thio-β-D glucose tetraacetate (74 mg, 0.2 mmol) in CH_2Cl_2 (5 mL), a solution of [Au(PPh_3)Cl] (100 mg, 0.2 mmol) in 10 mL of CH_2Cl_2 was added. The mixture was stirred for 3 hours and the solution was evaporated under a slow flow of nitrogen gas. The residue was washed with diethyl ether, dried to give a white product. ^{1}H NMR ($CDCl_3$): δ 1.90 - 2.06 (m, 12H, OCOCH_3), 3.77 (m, H, HCCH_2OAc), 4.11 - 4.23 (d;dd, 2H CH_2OAc), 5.11 - 5.18 (m, 4H), 7.43 - 7.51 (m, 15H) ppm.

3.3.5 Synthesis of 'host-guest' compounds with cyclodextrins

3.3.5.1 PTA-β-cyclodextrin inclusion complex

The crystals of the PTA-β-cyclodextrin (PTA-β-CD) inclusion compound suitable for X-ray analysis were obtained by a method of co-crystallisation by adding solid PTA to a solution of β-cyclodextrin in aqueous solutions with slight heating at 80 °C. Several stoichiometric amounts of PTA:CD were prepared in 1:1, 2:1 and 3:1 ratios respectively at concentrations of approximately 0.04 M to the β-cyclodextrin. The solutions were left at room temperature for slow cooling and crystal formation. Suitable crystals were obtained in the 3:1 PTA:CD batch. A single crystal of dimensions 0.3 x 0.15 x 0.06 mm was mounted with the mother solvent, to avoid crystal degradation, in a Lindemann capillary which had been filled with quick-setting glue. The crystals were obtained as needles and are colourless. The PTA-β-CD·8H_2O inclusion compound crystallises in the monoclinic space group $P2_1$ with eight solvent water molecules. The crystal structure for the compound is discussed in § 3.4.1.

3.3.5.2 Attempted synthesis of auranofin-β-cyclodextrin inclusion complex

The crystals of the auranofin compound (2,3,4,6-tetra-*O*-acetyl-1-thio-β-D-glucopyranosato(triethylphosphine) gold(I)) were obtained when the co-crystallisation of the auranofin-β-cyclodextrin inclusion compound was attempted by heating at 60 °C an aqueous solution of β-cyclodextrin with auranofin. Several stoichiometric amounts of auranofin:β-cyclodextrin were prepared in 1:1, 1:2 and 1:3 ratios at concentrations of

approximately 0.02 M to the β-cyclodextrin. The solutions were left at room temperature for slow cooling and crystal formation. Crystals were harvested in the 1:3 auranofin:β-cyclodextrin batch as described in the above paragraph and a single crystal of dimensions 0.098 x 0.115 x 0.428 mm was used. The crystals were obtained as needles and are colourless. The compound crystallises in the monoclinic space group $P2_1$ and was refined to a final R value of 1.59%. The crystal structure for the compound is further discussed in § 3.4.2.

3.4 X-RAY CRYSTALLOGRAPHY AND INCLUSION COMPLEXES

X-ray crystal structures for the PTA-β-cyclodextrin inclusion compound and auranofin are discussed. The preparation of these complexes was discussed above in § 3.3.5.1 and 3.3.5.2 respectively. The X-ray data sets were collected on the Bruker X8 Apex II 4K CCD area detector system using Mo radiation (λ = 0.71073 Å) by use of *omega* and *phi* scans at a low temperature of 100 K. For the PTA-β-cyclodextrin inclusion compound, a total of approximately 700 frames were collected using a frame width of 0.5° covering up to θ = 27.22° with completeness of 99.8% being achieved for the crystal, while for auranofin, a total of approximately 847 frames were collected covering up to θ = 25.50° with completeness of 96.5%. The first 50 frames were recollected at the end of each data collection to check for any decomposition since the first collection and it was found that both crystals were stable during the data collection. Absorption corrections were applied by use of the SADABS and SMART-NT programmes[47]. The structure was solved by the heavy atom method and was refined through full matrix least squares approximations using the SHELXS-97[48] and SHELXL-97[49] programs with F^2 being minimised. All non-hydrogen atoms were refined with anisotropic displacement parameters, while the hydrogen atoms were constrained to parent sites, using a riding model and were calculated as riding on the adjacent carbon atoms with bond distances: methylene C-H as 0.98 Å, methine C-H as 0.97 Å and methyl C-H as 0.96 Å. Hydrogen atom positions on the water solvent molecules were determined from the experimental data and Fourier maps. The molecular graphics were drawn using DIAMOND[50].

Presented below (Table 3.1) are the general crystal data and refinement parameters of the PTA-β-cyclodextrin inclusion compound, auranofin (obtained when inclusion of auranofin into β-cyclodextrin was attempted) and values for auranofin structure obtained from literature.

Table 3.1 Crystallographic data and refinement parameters for the PTA-β-cyclodextrin inclusion complex, auranofin (This work) and auranofin (Literature).

Compound	PTA-β-CD·8H_2O	Auranofin (This work)	Auranofin[7]
Empirical formula	C_{48} H_{98} N_3 O_{43} P	C_{20} H_{34} Au O_9 P S	C_{20} H_{34} Au O_9 P S
Formula weight	1436.26	678.47	
Temperature (K)	100(2)	100(2)	283-303
Wavelength (Å)	0.71073	0.71073	
Crystal system	Monoclinic	Monoclinic	Monoclinic
Space group	$P2_1$	$P2_1$	$P2_1$
a (Å) *b* (Å) *c* (Å)	15.0186 10.1662(4) 21.6633(10)	10.0262(5) 8.1336(3) 16.1497(7)	10.331(1) 8.231(1) 16.203(2)
α (°) β (°) γ (°)	90 107.9(2) 90	90 106.289(2) 90	90 105.31(1) 90
Volume(Å^3)	3147.5(2)	1264.13(10)	1328.9(3)
Z	2	2	2
D_c (g.cm^{-3})	1.515	1.782	1.70
μ (mm^{-1})	0.158	6.010	
F(000)	1532	672	
Crystal size	0.06, 0.15, 0.30	0.10, 0.12, 0.43	
θ range (°)	0.99 to 27.22	1.31 to 25.50	
Limiting indices	$-19 \le h \le 19$ $-13 \le k \le 13$ $-27 \le l \le 27$	$-12 \le h \le 12$ $-8 \le k \le 9$ $-15 \le l \le 19$	
Reflections collected / unique	70778 / 14022 [R_{int} = 0.0729]	8442 / 3591 [R_{int} = 0.0238]	4104 / 2496
Completeness to θ (°, %)	27.22, 99.8	25.50, 96.5	
T_{max} and T_{min}	0.993 and 0.970	0.553 and 0.440	
Refinement method	Full-matrix least-squares on F^2	Full-matrix least-squares on F^2	
Data / restraints / parameters	14022 / 1 / 968	3591 / 1 / 292	
Goodness-of-fit on F^2	1.044	1.157	
Final *R* indices [I>2σ(I)]	*R*1 = 0.0435, *wR*2 = 0.0879	*R*1 = 0.0159, *wR*2 = 0.0392	*R*1 = 0.029, *wR*2 = 0.035
R indices (all data)	*R*1 = 0.0622, *wR*2 = 0.0997	*R*1 = 0.0173, *wR*2 = 0.0633	
Absolute structure parameter	-0.01(10)	0.006(8)	
ρ_{max} and ρ_{min} (e.Å^{-3})	0.343 and -0.312	0.576 and -0.751	

$R = [(\Sigma\Delta F)/(\Sigma\Delta F_0)]$

$wR = \Sigma[w(F_0^2 - F_c^2)^2]/\Sigma[w(F_0^2)^2]^{1/2}$

3.4.1 PTA-β-cyclodextrin inclusion complex

The preparation and X-ray crystallographic characterisation of the PTA-β-cyclodextrin inclusion complex was discussed previously in § 3.3.5.1. The crystal data and refinement parameters PTA-β-cyclodextrin inclusion compound are presented in Table 3.1 while the supplementary material containing the complete lists of atomic coordinates, bond distances and angles, anisotropic displacement parameters as well as hydrogen coordinates is given in the Appendix, § A.1.

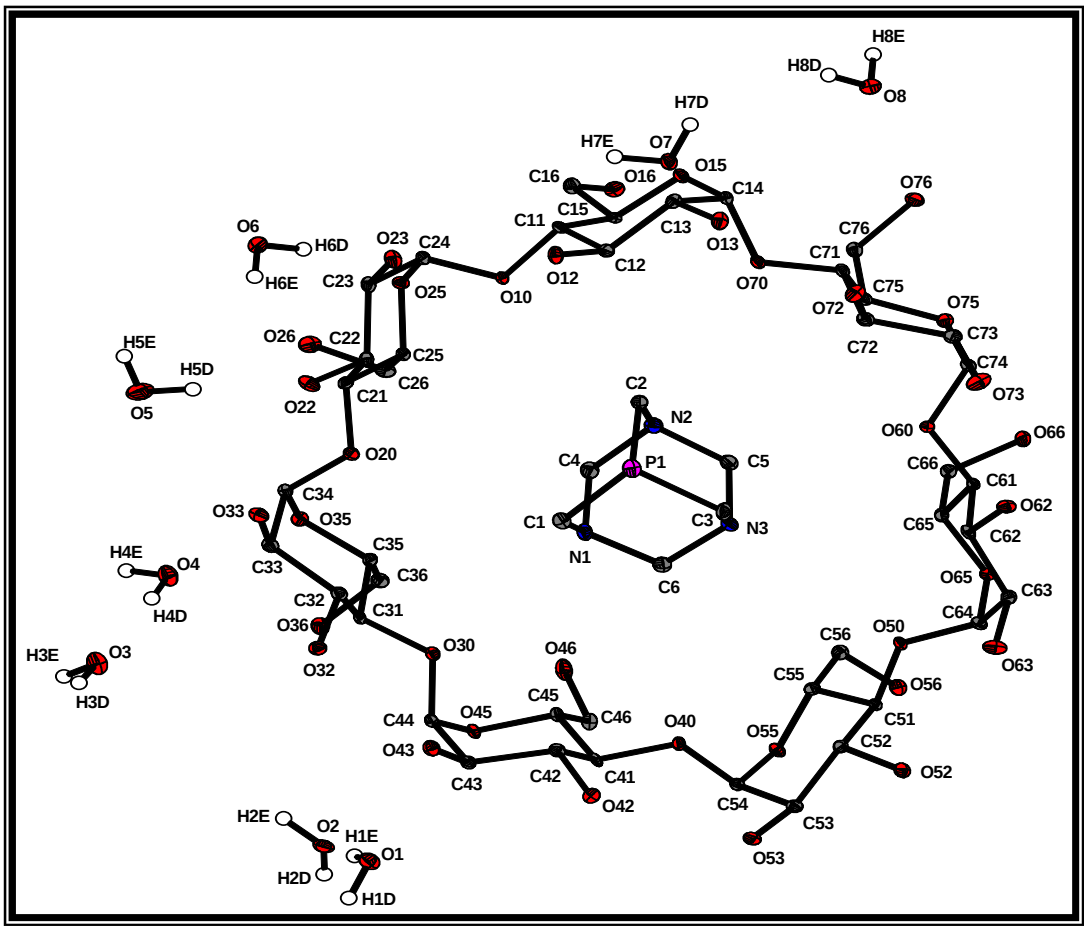

Figure 3.4 Molecular drawing of PTA-β-CD·8H_2O inclusion compound showing 'host-guest' chemistry and thermal displacement ellipsoids (30% probability). In the numbering scheme the first digit refers to the number of the sugar unit and the second one to the number of the atom in the unit. Hydrogen atoms except for water molecules are omitted for clarity.

In Fig. 3.4 above, it can be noted that all the glucose residues are in a $^4C_1$ chair conformation. The PTA ligand is situated inside the cavity of the β-cyclodextrin. Although as mostly observed in literature, that β-cyclodextrins tend to form dimers, the current PTA-β-cyclodextrin inclusion complex is a monomer and a 1:1 adduct.

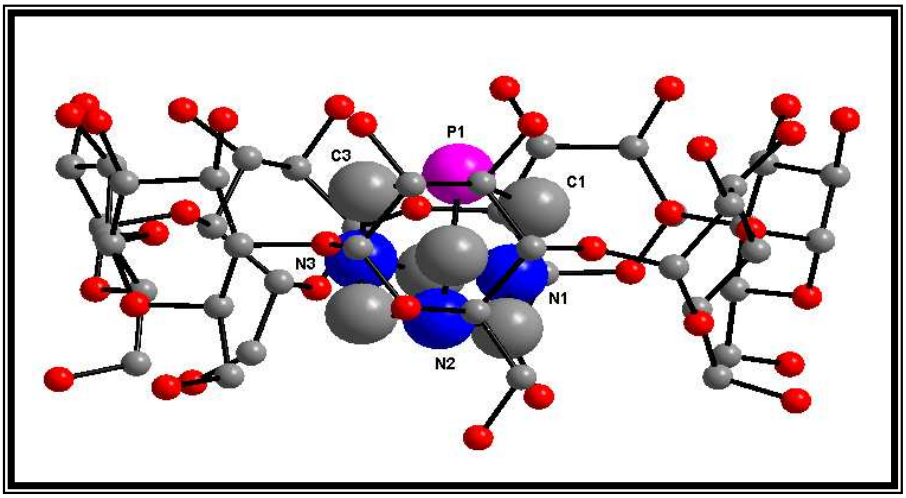

Figure 3.5 Molecular drawing of PTA-β-CD·8H_2O inclusion compound showing a side view of the complex to illustrate the cone form.

Fig. 3.5 above illustrates a molecular drawing showing the side view of the PTA-β-cyclodextrin inclusion compound. The diagram clearly confirms the 'host-guest' interaction of the PTA as a guest and the β-cyclodextrin acting as a host molecule. This therefore results in a 'cone' shaped compound with the PTA molecule held inside the β-cyclodextrin.

Table 3.2 Selected bond lengths and angles for the PTA guest molecule in the PTA-β-CD·8H_2O inclusion compound.

Bond lengths (Å)		Bond angles (°)	
C(1)-P(1)	1.867(3)	N(1)-C(1)-P(1)	114.5(2)
C(2)-P(1)	1.859(3)	N(2)-C(2)-P(1)	115.42(19)
C(3)-P(1)	1.863(3)	N(3)-C(3)-P(1)	115.16(19)
C(1)-N(1)	1.468(4)		
C(2)-N(2)	1.482(4)		
C(3)-N(3)	1.467(4)		

Selected bond distances and angles of choice for the PTA-β-cyclodextrin inclusion compound are listed in Tables 3.2 and 3.3 while the supplementary material containing the complete lists of atomic coordinates, bond distances and angles, anisotropic displacement parameters as well as hydrogen coordinates is given in the Appendix, § A.1. The C-P bond distances in the PTA guest molecule range from 1.859(3) - 1.867(3) Å while the C-N distances range from 1.462(4) - 1.482(4) Å. Also the C-P-C bond angles in the guest range from 94.42(13) - 96.05(14)° while its N-C-P angles range from 114.5 (2) - 115.42(19)° and N-C-N bond angles at approximately 114°. The cavity diameter of the cyclodextrin in the inclusion complex is 7.9 Å while the outer diameter is ≈14.2 Å.

Table 3.3 Comparison of selected bond lengths and angles for the sugar units in the PTA-β-CD·8H_2O inclusion compound, n = number of the sugar unit and chair conformations thereof evaluated by dihedral angles between planes: Plane 1 is defined by atoms C(n1)-C(n2)-C(n5), Plane 2 defined by C(n2)-C(n3)-O(n5)-C(n5) atoms and Plane 3 defined by C(n3)-C(n4)-O(n5) atoms.

Bond lengths (Å)							
	Sugar 1	Sugar 2	Sugar 3	Sugar 4	Sugar 5	Sugar 6	Sugar 7
C(n1)-C(n2)	1.507(4)	1.520(4)	1.513(4)	1.513(4)	1.533(4)	1.519(4)	1.524(4)
C(n2)-C(n3)	1.527(4)	1.512(4)	1.517(4)	1.520(4)	1.526(4)	1.516(4)	1.516(4)
C(n3)-C(n4)	1.524(4)	1.525(4)	1.525(4)	1.532(4)	1.526(4)	1.533(4)	1.517(4)
C(n1)-C(n5)	1.536(4)	1.515(4)	1.522(4)	1.528(4)	1.529(4)	1.527(4)	1.529(4)
C(n5)-C(n6)	1.514(4)	1.514(4)	1.505(4)	1.504(4)	1.503(4)	1.513(4)	1.517(4)
C(n4)-(On5)	1.414(3)	1.410(3)	1.411(3)	1.412(3)	1.403(3)	1.415(3)	1.399(3)
C(n5)-(On5)	1.441(3)	1.444(3)	1.441(3)	1.440(3)	1.443(3)	1.446(3)	1.434(3)
C(n2)-(On2)	1.430(3)	1.434(3)	1.427(3)	1.427(3)	1.429(3)	1.422(3)	1.415(3)
C(n3)-(On3)	1.416(3)	1.428(3)	1.427(3)	1.422(3)	1.422(3)	1.417(3)	1.417(4)
C(n6)-(On6)	1.420(3)	1.419(4)	1.429(3)	1.417(3)	1.426(3)	1.417(3)	1.431(3)
C(n1)-(On0)	1.438(3)	1.435(3)	1.430(3)	1.438(3)	1.440(3)	1.431(3)	1.435(3)
Bond angles (°)							
O(n5)-C(n5)-C(n6)-O(n6)	70.3(2)	-58.5(2)	-69.4(2)	72.9(2)	-60.3(2)	-74.3(2)	-52.2(2)
C((n+1)4)-O(n0)-C(n1)	118.0(2)	118.4(2)	117.3(2)	118.8(2)	118.5(2)	117.5(2)	119.2(2)*
C(n1)-C(n5)-C(n6)-O(n6)	-167.2(2)	61.5(3)	50.3(3)	-167.4(2)	61.1(3)	44.8(3)	71.0(3)
Plane 1-Plane 2	49.3(2)	52.18(19)	48.22(17)	53.20(17)	48.28(16)	51.50(22)	48.34(17)
Plane 2-Plane 3	54.06(17)	51.18(18)	52.98(18)	49.94(17)	53.23(19)	51.90(21)	50.40(15)
Plane 1-Plane 3	5.59(21)	1.07(23)	4.76(21)	3.26(23)	5.01(22)	0.88(13)	3.73(17)

* C(14)-O(70)-C(71)

The bond lengths and angles of importance for the sugar units in the PTA-β-cyclodextrin inclusion compound are presented in Table 3.3. Within the sugar units, the longest C-C bond distance is the C(11)-C(15) for sugar unit 1 at 1.536(4) Å while the shortest distance C(55)-C(56) at 1.503(4) Å is noted for sugar unit 5. The C(n2)-C(n3) bond distance bearing the C atoms bound to secondary OH-groups is longest for sugar units 1 and 5 while for the rest of the sugar units is approximately the same. The C(n3)-C(n4) bond distance is approximately the same for all sugars except for sugar 7 with a slightly shorter distance at 1.517(4) Å. The average bond distance for the C(n5)-C(n6) bearing the C atom bound to the methylene group in sugar units 1, 2, 6 and 7 is 1.515(4) Å while the similar average distance for sugar units 3, 4 and 5 is shorter at 1.504(4) Å. The longest C-O of the C(n2)-O(n2) and C(n3)-O(n3) bond distances indicative of the C atom bound to secondary OH-groups is 1.434(3) Å for sugar unit 2 whereas the shortest distance is noted at 1.415(3) Å for sugar unit 7. The C(n6)-O(n6) bond distance with the C atom bound to the methylene group is ≈1.43 Å for sugar units 3, 5 and 7 while it is ≈1.42 Å for sugar units 1, 2, 4 and 6.

The only significant differences between the various β-cyclodextrin complexes are in the orientation of these C(n6)-O(n6) bonds which are generally turned away from the centre of the β-cyclodextrin (for example in Fig. 3.4) with torsion angles O(n5)-C(n5)-C(n6)-C(n6) (Table 3.3) corresponding to the (-)*gauche* conformation. In the PTA-β-cyclodextrin inclusion compound two C(6)-O(6) bonds, for sugar units 1 and 4 are rotated inwards, more obvious for sugar 4, ((+)*gauche* conformation) to probably participate in hydrogen interactions with the PTA guest molecule. The angle formed by the glycosidic oxygen joining the two adjacent sugars (C((n+1)4)-O(n0)-C(n1)) is approximately the same for all sugar units with an average of 118.2(2)°. The dihedral angles between planes 1, 2 and 3 are also given in Table 3.3. As it is described in Table 3.3, plane 1 is defined by atoms C(n1)-C(n2)-C(n5), plane 2 defined by C(n2)-C(n3)-O(n5)-C(n5) atoms and plane 3 defined by C(n3)-C(n4)-O(n5) atoms and thus one would say that planes 1, 2 and 3 represent the 'back, 'bottom' and 'leg' portions of the chair conformations of the sugar units respectively. The dihedral angles between planes 1 and 2 and planes 2 and 3 are approximately the same for all sugar units. The differences are noted for the sugar units on the 'leg' portion of the chair which is represented by the dihedral angle between planes 1 and 3. The smallest dihedral angles are observed for sugar units 2 and 6 which are 0.88(13) and 1.07(23)° respectively while the largest is 5.59(21)° for sugar unit 1. The small dihedral angle may indicate that the chair-like structures of the sugar units are slightly changed to boat-like conformations.

Fig. 3.6 below indicates a packing diagram of the unit cell of the PTA-β-CD·8H_2O inclusion compound. Depending on the nature and size of the guest molecule, an inclusion complex may crystallise in three different forms of which two are of the cage type where the cavity of each cyclodextrin is blocked on both sides by adjacent cyclodextrin molecules in the crystal lattice. In the channel-type crystal structures, the cyclodextrin macrocycles are stacked like coins in a roll so that the cavities form infinite channels[51]. The PTA-β-CD·8H_2O inclusion compound investigated in this study packs in a herringbone-type cage. The β-cyclodextrin is known to form this type of cage complexes with water and small molecules but with larger guests, the preferred motif is a 'basket' formed between two β-cyclodextrin molecules hydrogen bonded with their secondary O(2)-O(3) hydroxyl groups. The guest molecules are located within these baskets which are stacked either collinearly to form channel-type structures or can be displaced sideways to different degrees which depends on the guest molecules and on the mode of hydration.

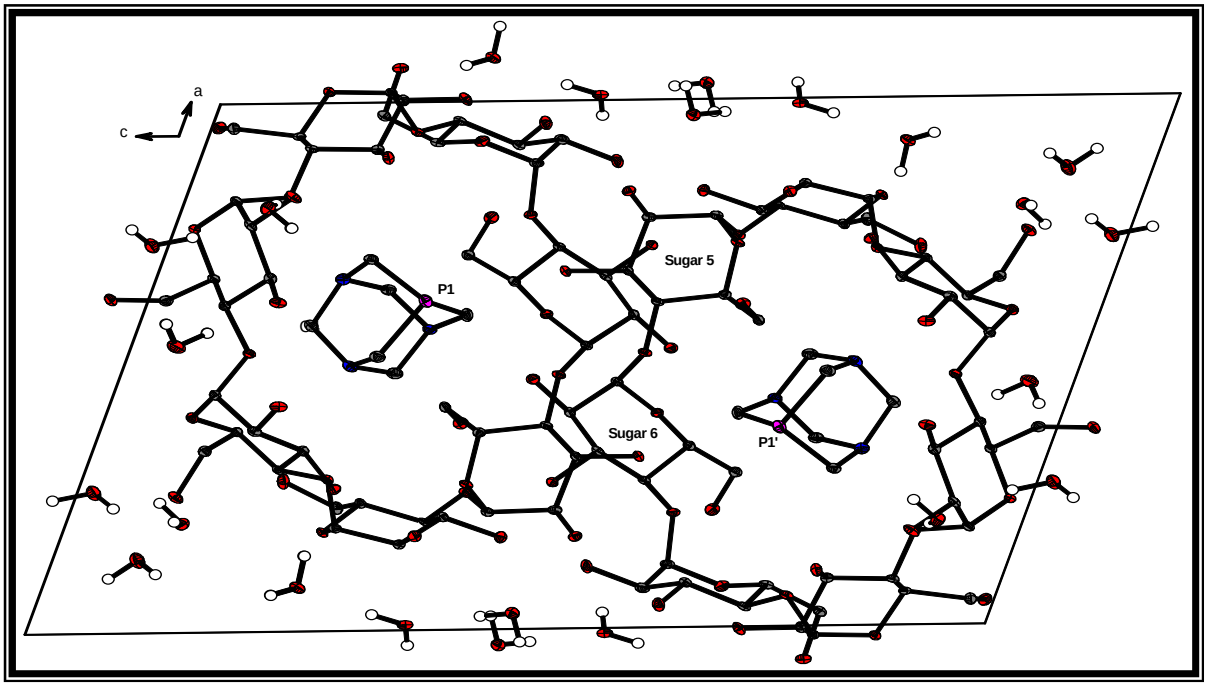

Figure 3.6 Packing diagrams of the PTA-β-CD·8H_2O inclusion compound along the b-axis showing complete packing of hydrated water molecules. Hydrogen atoms except for the water molecules are omitted for clarity. [Symmetry operator: P1' (1-x,0.5+y, 1-z)].

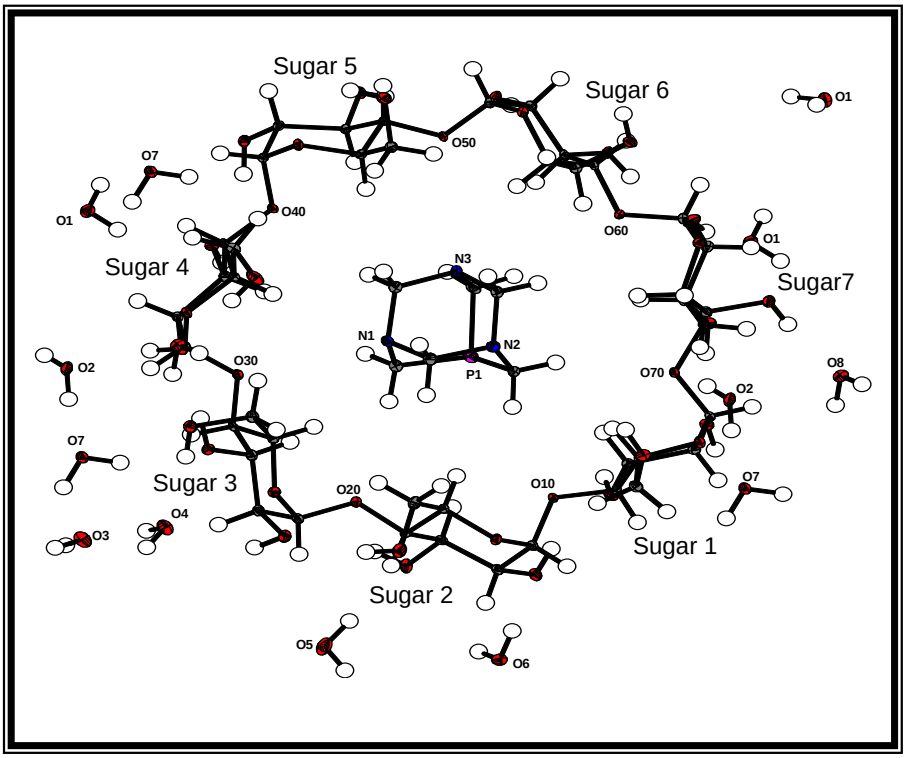

Figure 3.7 Molecular drawing of PTA-β-CD·8H_2O inclusion compound showing a sphere of water molecules surrounding the sugar units of the β-cyclodextrin host molecule.

Figure 3.7 above presents a molecular drawing of the PTA-β-CD·8H_2O inclusion compound showing a sphere of water molecules surrounding the sugar units of the β-cyclodextrin host molecule. On one side of the β-cyclodextrin host molecule there are primarily water molecules whereas on the other side not much water molecule interaction is observed. This indicates that sugar units 1, 2, 3, 4 and 7 interacts with a water 'half' sphere whilst sugar units 5 and 6 show interactions with another β-cyclodextrin molecule via the -OH interactions. As mentioned earlier, the oxygen atom O52 of the sugar unit 5 of the β-cyclodextrin molecule has a packing interaction with the phosphorus atom P1 of the PTA guest molecule.

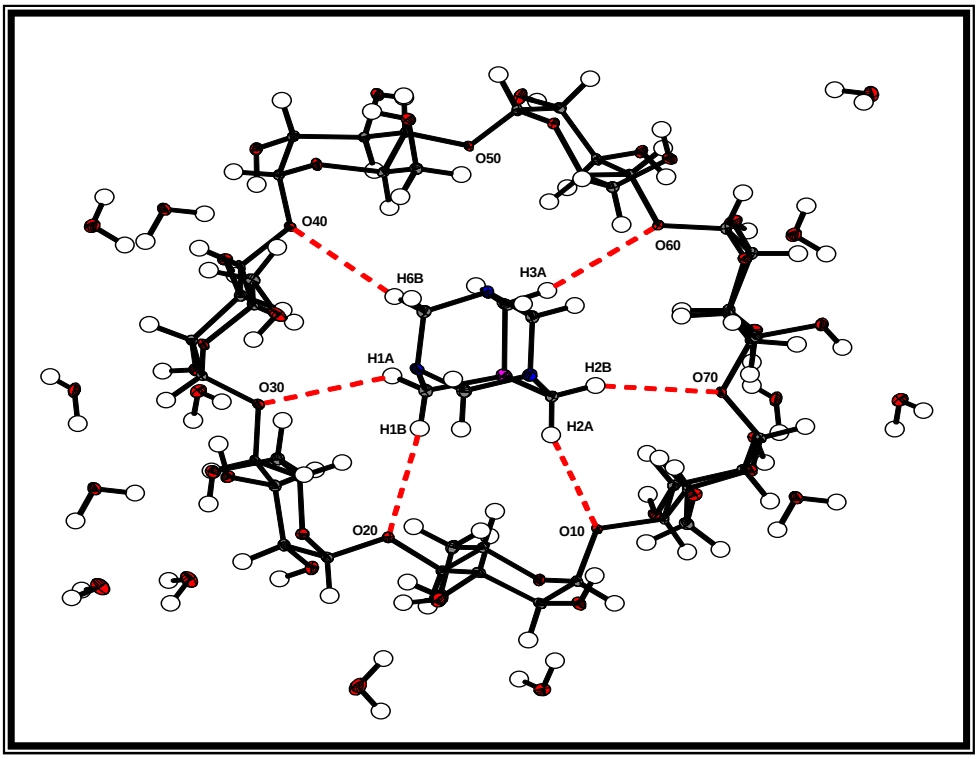

Figure 3.8 Illustration of hydrogen bonding interactions observed between the PTA guest molecule and glycosidic oxygen atoms of the host β-cyclodextrin molecule in PTA-β-CD·8H_2O inclusion compound. Hydrogen bondings are shown as fragmented lines.

Figure 3.8 shows the extended hydrogen bond network formed between the hydrogen atoms of the PTA guest molecule and the bridging glysosidic oxygen atoms of the β-cyclodextrin. Strong hydrogen bondings are observed between the atom pairs (C2, O10) and (C2, O70) with bond distances and angles of 2.594 Å, 154.04° and 2.678 Å, 159.78° respectively, with weaker interactions between the atom pairs (C6, O40); (C1, O20); (C3, O60) and (C1, O30) with bond distances and angles of 2.820 Å, 142.71°; 2.833 Å, 172.52°; 2.967 Å, 150.41° and 3.054 Å, 113.1° respectively.

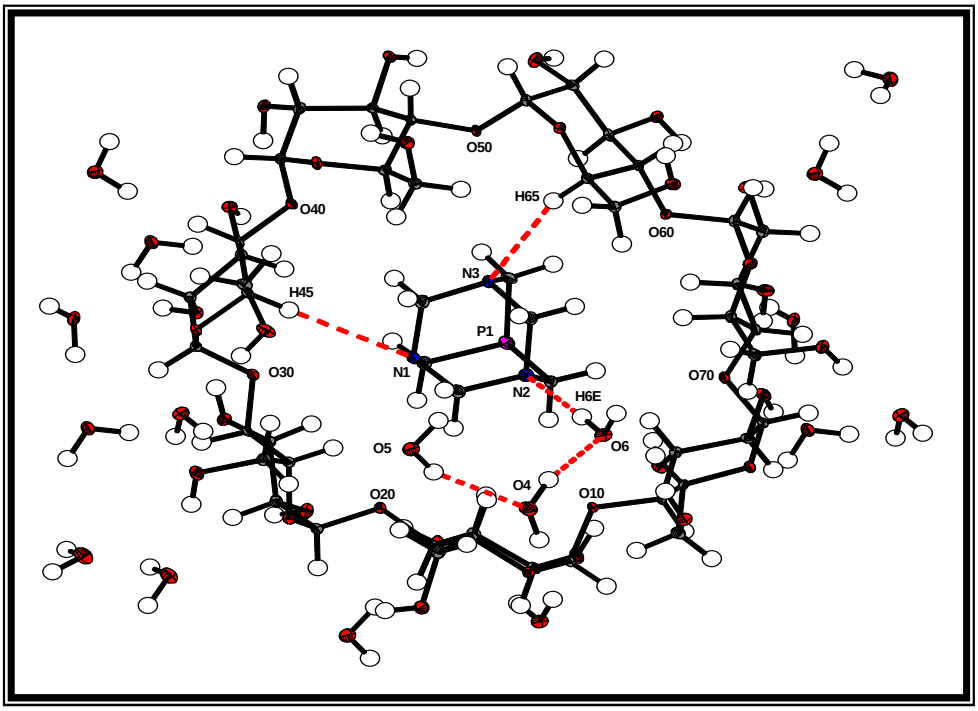

Figure 3.9 Illustration of hydrogen bonding interactions observed between the PTA guest molecule and hydrogen atoms of the host β-cyclodextrin molecule and also between the N atom of PTA guest molecule and hydrogen atoms of surrounding water molecules in PTA-β-CD·8H_2O inclusion compound. Hydrogen bondings are shown as fragmented lines.

Figure 3.9 shows the hydrogen bonding interactions formed between the nitrogen atoms in the PTA guest molecule and the hydrogen atoms of the β-cyclodextrin host molecule. Hydrogen bonding interactions are observed between the atom pairs (N3, C65) and (N1, C45) with bond distances and angles of 2.655 Å, 163.76° and 2.851 Å, 175.36° respectively representing bonding interactions observed between the nitrogen atoms of the PTA guest molecule and hydrogen atoms of the host β-cyclodextrin molecule. Other interactions include a hydrogen bonding between the atom pair (N2, O6) with the bond distance and angle of 1.943 Å, 175.15° representing an interaction between the nitrogen atom of the PTA guest molecule and a hydrogen atom of the surrounding water molecule. Thus the two nitrogen atoms of the PTA guest molecule N1 and N3 are involved in hydrogen interactions with hydrogen atoms of the β-cyclodextrin whilst the third N2 atom is blocked with water molecules. Also there are hydrogen bonding interactions between the water molecules as shown between atom pairs (O6, O4) and (O4, O5) with bond distances and angles of 1.882 Å, 166.54° and 2.157 Å, 146.51° respectively. There are no P-H interactions observed in the PTA-β-CD·8H_2O inclusion compound with the closest interaction for the phosphorus atom of

the PTA guest molecule being a packing interaction as represented by the atom pairs (P1, O52) (x,y-1,z) with the bond distance of 3.410 Å representing an interaction between the phosphorus atom of the PTA guest molecule and an oxygen atom of the adjacent β-cyclodextrin host molecule.

3.4.2 Attempted X-ray crystal structure of auranofin inclusion complex into β-cyclodextrin

The preparation and attempted inclusion of auranofin into β-cyclodextrin was discussed previously in § 3.3.5.2. As indicated previously in the section, only auranofin crystallised without being included into the β-cyclodextrin. The general crystal data and refinement parameters of the auranofin compound are given in Table 3.1 and the supplementary material containing complete lists of atomic coordinates, bond distances and angles, anisotropic displacement parameters as well as hydrogen coordinates is given in the Appendix, § A.2.

The structural representation of the compound is presented in Fig. 3.10.

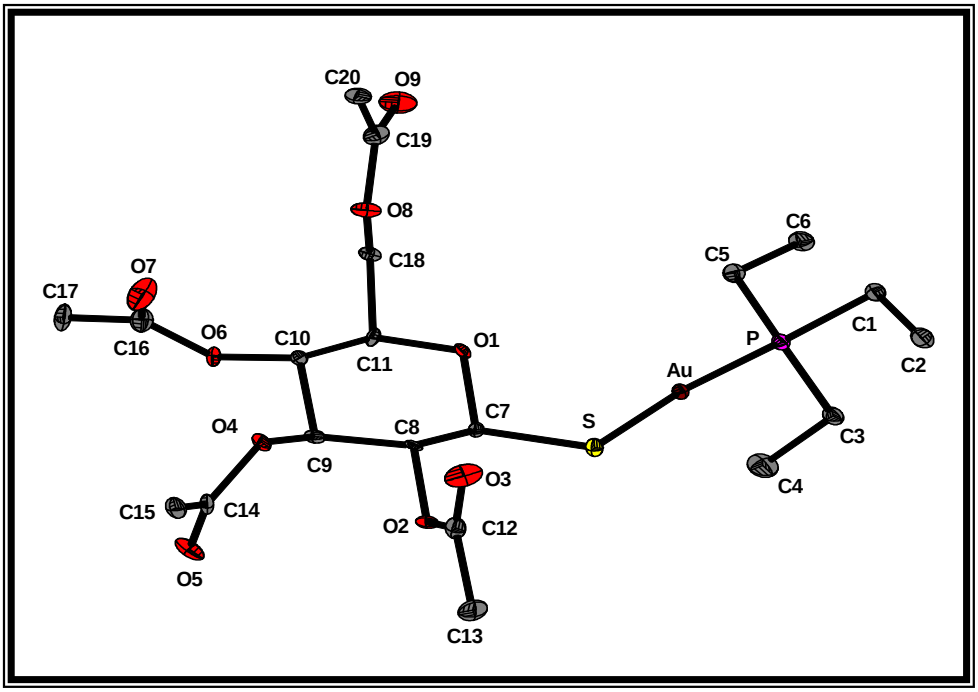

Figure 3.10 Molecular drawing of auranofin, showing the numbering scheme and thermal displacement ellipsoids (30% probability). Hydrogen atoms are omitted for clarity.

The structure of auranofin is known in literature[7] and the crystal structure obtained when the inclusion compound of auranofin and β-cyclodextrin was attempted, is included for comparison. The data for the current structure in this study was collected at low temperature, yielding more accurate bond parameters (Table 3.4). The auranofin structure shows that the gold centre is two-coordinated linearly to the phosphorus and sulphur ligands on either side. It has four acetyl groups coordinated in an equatorial manner on the glucopyranose ring. The glucopyranose ring of auranofin adopts the $^4C_1$ chair conformation with all groups attached orientated equatorially. The hydrogen atoms of the ring carbon atoms are in axial configuration. The anomeric C-S bond is in a β-configuration as proposed by Sutton in literature[52] on the basis of synthesis and optical rotation. The acetyl groups are approximately on the same plane as the adjacent O or C atoms. The O3, O5 and O7 atoms are arranged *cis* relative to the corresponding ring H atoms.

Table 3.4 Selected bond lengths and angles for auranofin and comparison with literature[7] values.

Bond lengths (Å)			Bond angles (°)		
	Auranofin (This work)	Auranofin (Literature)		Auranofin (This work)	Auranofin (Literature)
Au-P	2.264(1)	2.259(3)	P-Au-S	172.69(6)	173.6(1)
Au-S	2.302(1)	2.293(3)	Au-S-C(7)	105.6(2)	105.6(3)
S-C(7)	1.810(6)	1.788(9)	P-C(1)-C(2)	114.3(5)	115(1)
P-C(1)	1.823(7)	1.863(12)	P-C(3)-C(4)	112.9(5)	114(2)
P-C(3)	1.824(7)	1.787(14)	P-C(5)-C(6)	115.5(4)	117(1)
P-C(5)	1.822(7)	1.821(13)	Au-P-C(1)	112.5(2)	111.3(5)
C(7)-O(1)	1.436(7)	1.427(11)	Au-P-C(3)	111.4(2)	111.6(5)
C(11)-O(1)	1.435(7)	1.420(11)	Au-P-C(5)	116.0(2)	115.8(5)
C(7)-C(8)	1.529(8)	1.523(13)	Au-P-C(1)-C(2)	49.5(5)	47.270(9)
C(8)-C(9)	1.507(10)	1.521(14)	Au-P-C(3)-C(4)	55.0(5)	54.037(9)
C(9)-C(10)	1.520(8)	1.502(13)	Au-P-C(5)-C(6)	-178.8(4)	179.498(7)
C(10)-C(11)	1.536(9)	1.517(14)	Au-S-C(7)-O(1)	-49.4(4)	-51.405(8)
P…S'	4.916(4)[a]	5.006(17)[b]	Au-S-C(7)-C(8)	-165.4(3)	-169.287(6)
Au…Au'	6.375(3)[a]	6.498(14)[b]	C(8)-O(2)-C(12)-O(3)	5.4(10)	6.30(1)
S…P'	9.186(3)[a]	9.25(9)[b]	C(9)-O(4)-C(14)-O(5)	-11.3(10)	-9.26(1)

[a] Symmetry operator: atom' (1-x,0.5+y,1-z).
[b] Symmetry operator: atom' (-x,0.5+y,-z).

Selected bond lengths include Au-P, Au-S and S-C(7) = 2.264(1), 2.302(1), and 1.810(6) Å respectively. The average P-C bond distance is 1.823(7) Å. Selected angles that can be mentioned are P-Au-S and Au-S-C(7) = 172.69(6) and 105.6(2)° respectively. These parameters are approximately similar to those of the structure found in literature but with bond difference of 0.1 Å (Table 3.4). The average C-O bond distance for the pyranose ring is 1.436(7) Å. The C(10)-C(11) bond distance which is

1.536(9) Å is longer as compared to other C-C distances for the glucopyranose ring with the shortest such distance for C(8)-C(9) = 1.507(10) Å. The Au-S-C(7) bond angle is approximately orthogonal. The average Au-P-C bond angle is 113.3(2)°. The torsion angle Au-S-C(7)-O(1) is -49.4(4)° as compared to the Au-S-C(7)-C(8) torsion angle of -165.4(3)° which indicates that the Au atom is orientated preferentially towards the O(1) atom. This is also proved by the interatomic distance of 3.328(3) Å between Au and O(1) atoms compared to 4.678(5) Å between the Au and C(8) atoms. Supplementary material containing the complete lists of atomic coordinates, bond distances and angles, anisotropic displacement parameters as well as hydrogen coordinates is given in the Appendix, § A.2.

In Tables 3.1 and 3.4, a comparison of the parameters of the auranofin structure obtained from this work and one from the literature is also presented. Both structures crystallise under the same monoclinic $P2_1$ space group. The collection of data for the literature structure was done at ambient temperatures while for this work a low temperature study was done. The low temperature structure has shorter unit cell distances while the β unit cell angle is larger than for the literature values. The Au-P, Au-S and S-C(7) bond distances for the literature structure are slightly shorter while the P-C distances are comparable to each other. The C-C distances in the glucopyranose ring are also similar to each other. The P-Au-S and P-C-C bond angles for the structure done for this work are slightly shorter while Au-S-C(7) angles have similar values.

The packing diagram for the auranofin structure obtained in this study is given in Fig. 3.11. An illustration representing the superimposed auranofin structures is presented in Fig. 3.12. This clearly indicates a phase change and a new polymorph at 100 K. This observation is further manifested by the approximate 1-4° changes in selected torsion and bond angles, see Table 3.4, and also note Au…Au' *etc*. interactions in structures studied at 100 and 293 K. Further study of this phenomenon is beyond the scope of this PhD thesis but will be investigated in future work.

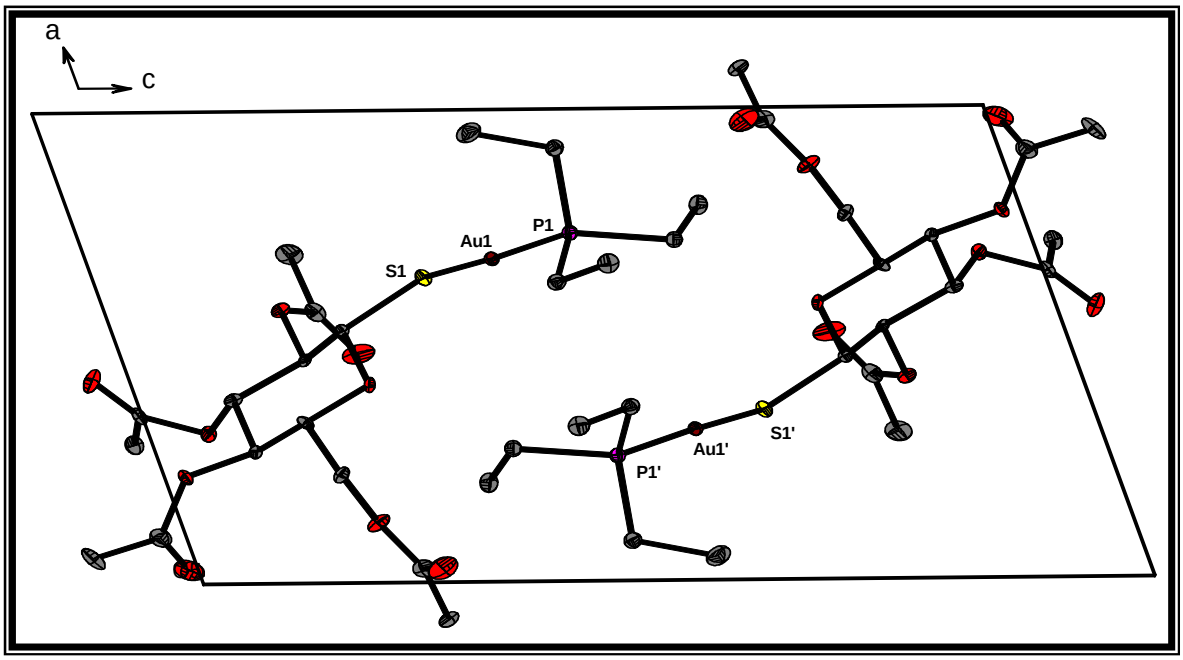

Figure 3.11 Packing diagrams of auranofin along the b-axis showing partial packing of the molecules in the unit cell. Shown also are thermal displacement ellipsoids (30% probability) and hydrogen atoms are omitted for clarity. [Symmetry operator: Au1' (1-x,0.5+y, 1-z)].

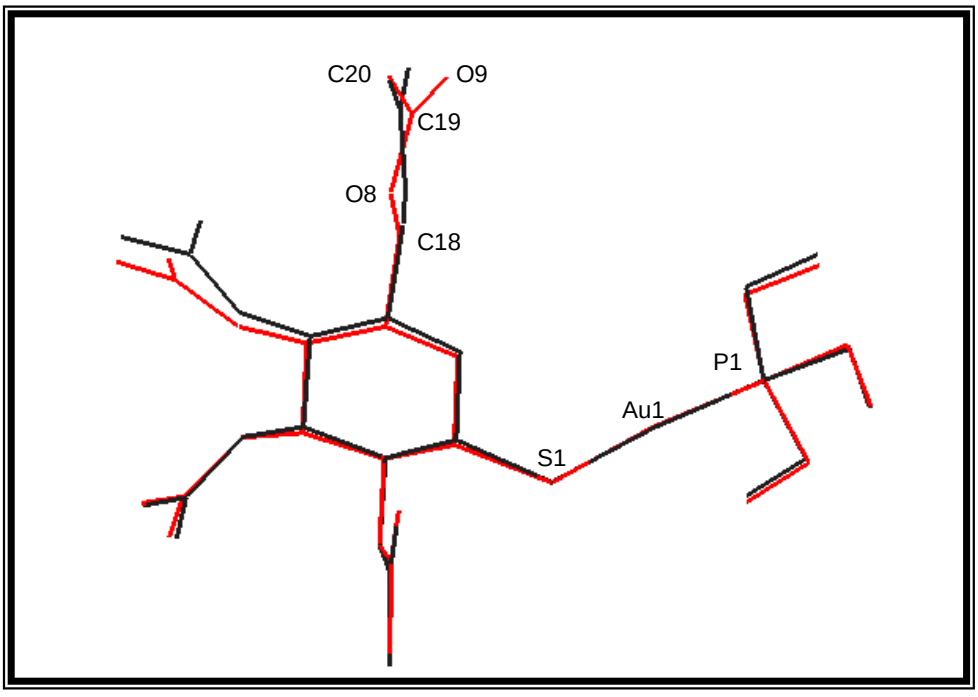

Figure 3.12 Superimposed wire frames of auranofin structures (red, this work) and (black, literature). Hydrogens are omitted for clarity.

3.5 EQUILIBRIUM STUDIES OF CHLORIDE SUBSTITUTION FROM [Au(PTA)Cl] COMPLEXES WITH DIFFERENT S-DONOR LIGANDS

The determination of the equilibrium constants when the [Au(PTA)Cl] complex is reacted with various sulphur donor ligands such as SCN^-, thiourea and methyl thiourea is discussed in this section. The thiocyanate is an ambidentate ligand which can bind to the central metal *via* the S or N atom therefore it appears useful for the purpose of this study to compare its ease of bonding with other S-donors such as thiourea analogues.

3.5.1 Experimental

The equilibrium constants obtained from reacting [Au(PTA)Cl] with the various ligands (L = SCN^-, thiourea, methyl thiourea) was determined using the following equation which also represents the equilibrium reaction process:

$$[Au(PTA)Cl] + L \underset{}{\overset{K_L}{\rightleftharpoons}} [Au(PTA)L] + Cl^- \qquad (3.1)$$

The equilibrium constant determination experiments were all conducted using freshly prepared gold complexes and ligand solutions, in DMSO solvent and at 25 °C. For equilibrium constant determinations the gold solutions were mixed with the different concentrations of the various halide solutions and the final concentrations for Au(I) and halide were thus as indicated in the various respective figure captions in the sections below.

The phosphorus NMR spectra for the gold complexes dissolved in DMSO were recorded on a 300 MHz Gemini spectrometer operating at 121.497 MHz for ^{31}P. The ^{31}P chemical shifts are reported as calibrated at 0 ppm relative to 85% H_3PO_4 as an internal standard in a capillary. The experiments were done by monitoring the change in the chemical shift by adding stoichiometric equivalents of the ligand and hence different ligand concentrations to the DMSO solution of the [Au(PTA)Cl] complex. Data analysis was conducted by means of Microsoft Excel 97 and the observed equilibrium constants were obtained from the chemical shift versus ligand concentration graphs using the least-squares program Scientist[53].

The equation used in fitting data and getting the plots of the chemical shift versus ligand concentration is presented as Eq. 3.2 and this model allows for the calculation of the uncoordinated ligand concentration at equilibrium. The derivation of the equation is given in the Appendix, § A.6.1.

$$\delta_{obs} = \frac{\delta_R[Cl^-] + \delta_P K_L[L]_f}{[Cl^-] + K_L[L]_f} \qquad (3.2)$$

K_L = Equilibrium constant, δ_R = chemical shift observed for the reactants, δ_P = chemical shift for the products and L_f = final ligand concentration.

3.5.2 Spectroscopic studies of [Au(PTA)Cl] with various ligands

The determination of the equilibrium constant when [Au(PTA)Cl] is reacted with ligands such as SCN^-, thiourea and methyl thiourea is discussed in § 3.5.2.1 - 3.5.2.3. In these reactions the ^{31}P NMR chemical shift change is monitored while stoichiometric amounts of the ligand are added.

3.5.2.1 ^{31}P NMR study of chloride substitution by SCN^- from [Au(PTA)Cl]

The determination of the equilibrium constant when the [Au(PTA)Cl] complex is reacted with the SCN^- ligand is discussed. Fig. 3.13 indicates the ^{31}P NMR chemical shift change when stoichiometric amounts of the ligand are added while fit of data in order to calculate the equilibrium constant using Eq. 3.2 is given in Fig. 3.14. The results for the calculated equilibrium constant are summarised in Table 3.5, § 3.5.2.4.

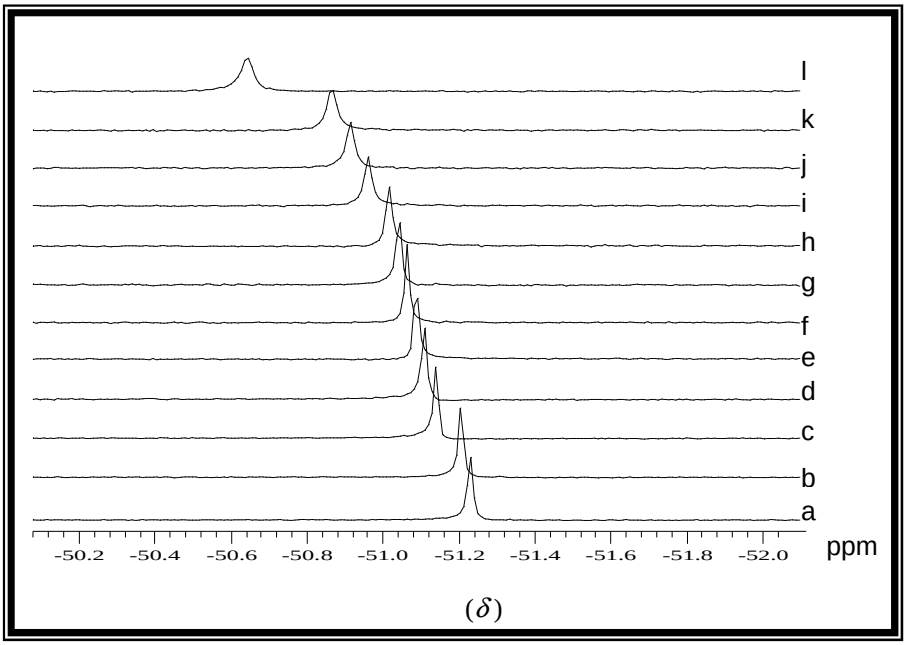

Figure 3.13 Overlay plot of the ^{31}P NMR spectra of [Au(PTA)Cl] with different amounts of SCN^- ligand added in DMSO. [Au] = 51.3 mM, 0 - 10 equivalents of SCN^- were added, [SCN^-] = 0 - 513 mM. Scans were taken at 25°C and a, b, c, d, e, f, g, h, i, j, k and l = 0.0, 0.1, 0.5, 1.0, 1.2, 1.5, 2.0, 2.5, 3.0, 4.0, 5.0 and 10.0 equivalents of SCN^- added respectively.

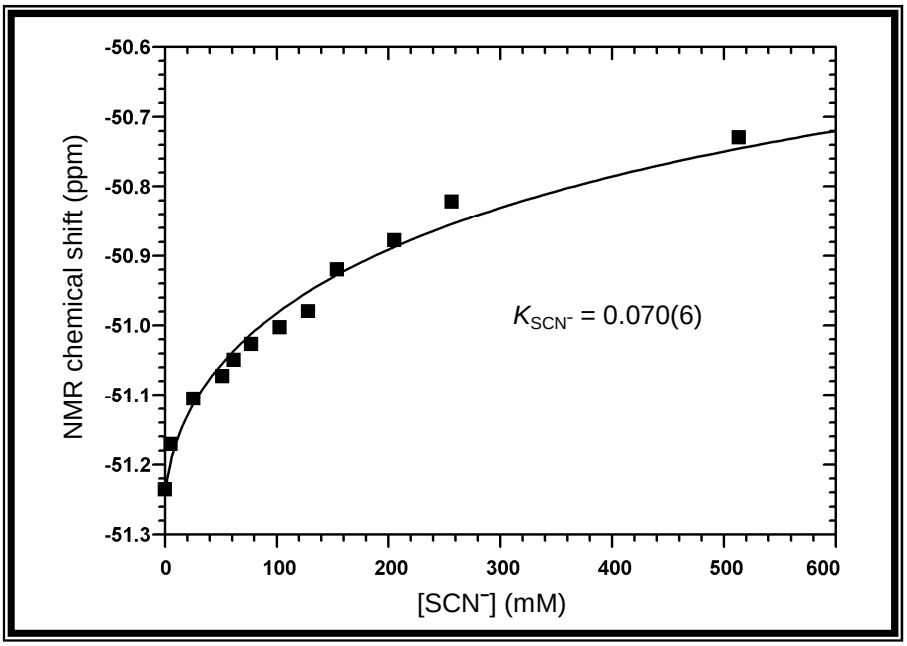

Figure 3.14 A graph showing the fit of data of the ^{31}P NMR chemical shift change (Fig. 3.13) to Eq. 3.2, when SCN^- concentration is varied in a solution of [Au(PTA)Cl] in DMSO. [Au] = 51.3 mM, [SCN^-] = 0 - 515 mM and T = 25 °C. Solid line represents fit of data to Eq. 3.2.

3.5.2.2 ^{31}P NMR spectroscopic study of chloride substitution by thiourea from [Au(PTA)Cl]

The determination of the equilibrium constant when the [Au(PTA)Cl] complex is reacted with thiourea is discussed. Fig. 3.15 indicates the ^{31}P NMR chemical shift change when stoichiometric amounts of the ligand are added while fit of data in order to calculate the equilibrium constant using Eq. 3.2 is given in Fig. 3.16. The results for the calculated equilibrium constant are summarised in Table 3.5, § 3.5.2.4.

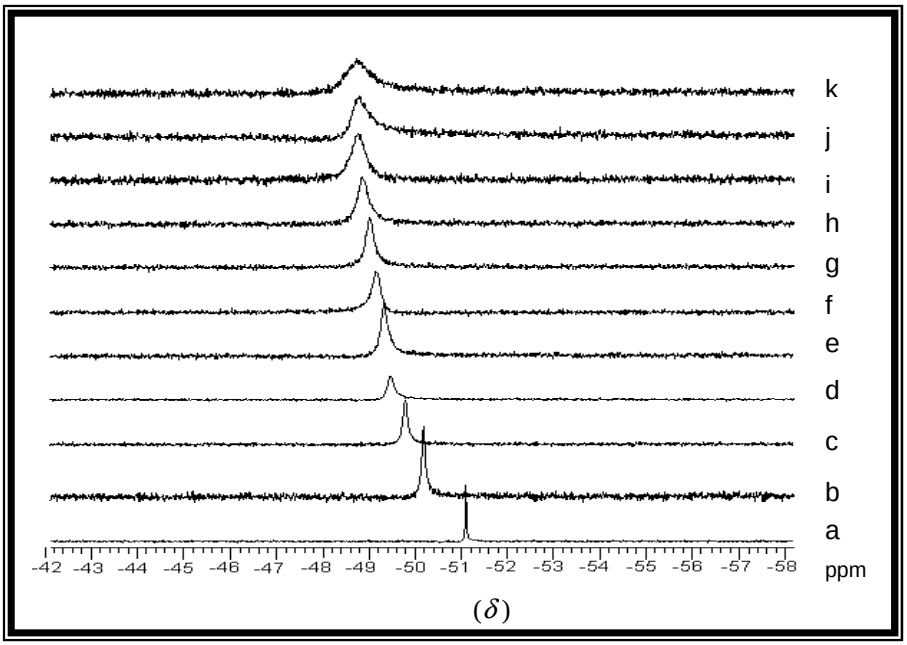

Figure 3.15 Overlay plot of the ^{31}P NMR spectra of [Au(PTA)Cl] with different amounts of the thiourea ligand added in DMSO. [Au] = 42.7 mM, 0 - 10 equivalents of thiourea were added, [Tu] = 0 - 427 mM. Scans were taken at 25 °C and a, b, c, d, e, f, g, h, i, j and k = 0.0, 0.1, 0.5, 1.0, 1.2, 1.5, 2.0, 3.0, 4.0, 5.0 and 10.0 equivalents of thiourea added respectively.

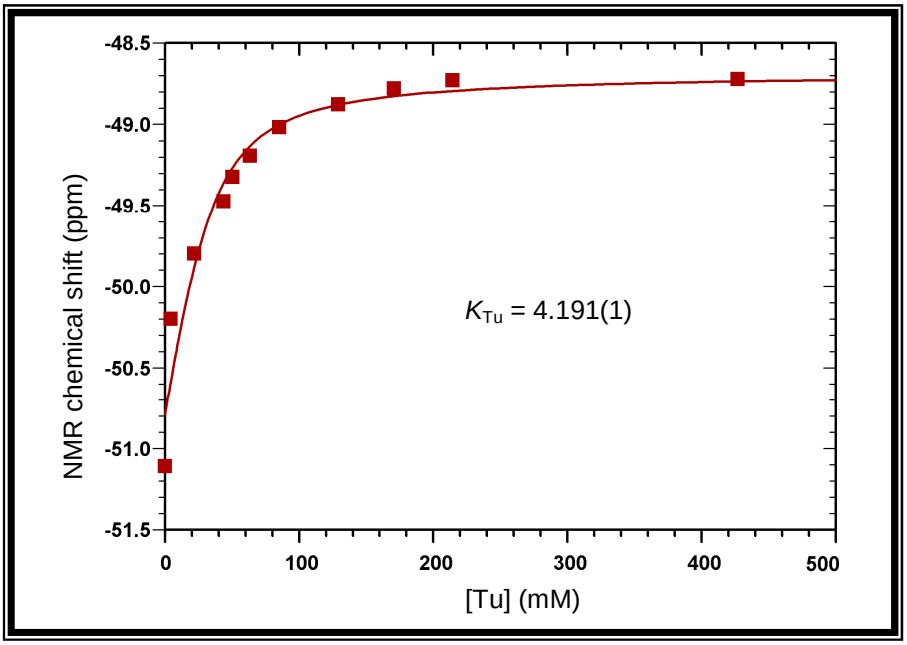

Figure 3.16 A graph showing the fit of data of the ^{31}P NMR chemical shift change (Fig. 3.15) to Eq. 3.2, when thiourea concentration is varied in a solution of [Au(PTA)Cl] in DMSO. [Au] = 42.7 mM, [Tu] = 0 - 430 mM and T = 25 °C. Solid line represents fit of data to Eq. 3.2.

3.5.2.3 ^{31}P NMR spectroscopic study of chloride substitution by methyl thiourea from [Au(PTA)Cl]

The determination of the equilibrium constant when the [Au(PTA)Cl] complex is reacted with methyl thiourea is discussed. Fig. 3.17 indicates the ^{31}P NMR chemical shift change when various amounts of the ligand are added while fit of data in order to calculate the equilibrium constant using Eq. 3.2 is given in Fig. 3.18. The results for the calculated equilibrium constant are summarised in Table 3.5, § 3.5.2.4.

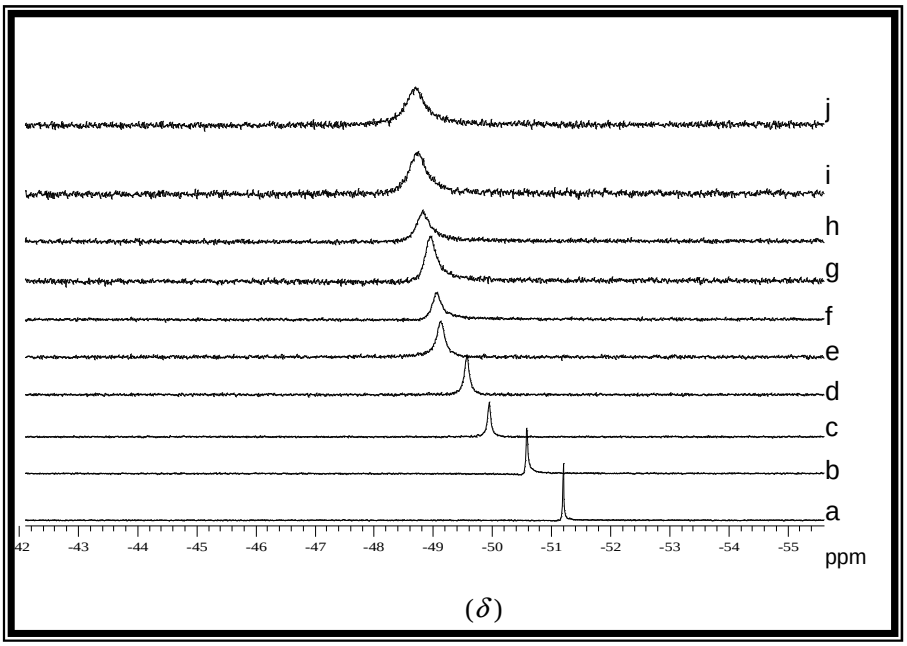

Figure 3.17 Overlay plot of the ^{31}P NMR spectra of [Au(PTA)Cl] with different amounts of the methyl thiourea ligand added in DMSO. [Au] = 51.3 mM, 0-10 equivalents of methyl thiourea were added, [MeTu] = 0 - 513 mM. Scans were taken at 25 °C and a, b, c, d, e, f, g, h, i and j = 0.0, 0.1, 0.5, 1.0, 1.2, 1.5, 2.0, 3.0, 4.0 and 5.0 equivalents of methyl thiourea added respectively.

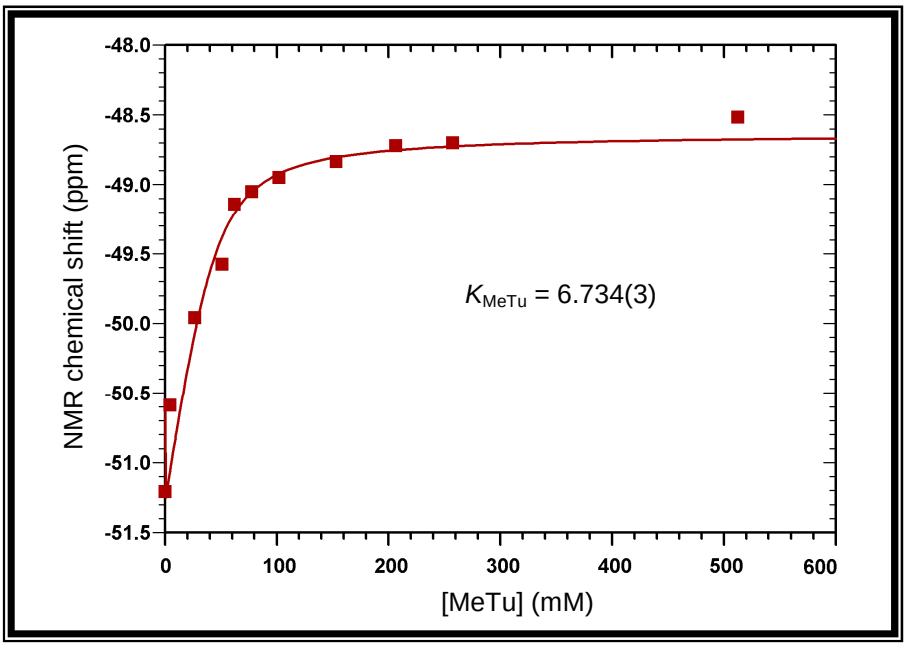

Figure 3.18 A graph showing the fit of data of the ^{31}P NMR chemical shift change (Fig. 3.17) to Eq. 3.2, when methyl thiourea concentration is varied in a solution of [Au(PTA)Cl] in DMSO. [Au] = 51.3 mM, [MeTu] = 0 - 515 mM and T = 25 °C. Solid line represents fit of data to Eq. 3.2.

3.5.2.4 Summary of equilibrium constant determinations when the chloride is substituted by S-donor ligands from [Au(PTA)Cl]

As indicated with the equilibrium results presented above (§ 3.5.2.1 - 3.5.2.3), it can be stated that the equilibrium constant was fairly accurately determined. For easy comparison, the summary of the results of the equilibrium constants determined for the reaction of the [Au(PTA)Cl] complex and a range of entering ligands L is presented in Table 3.5. When the [Au(PTA)Cl] complex is reacted with the sulphur donor ligands (L = SCN^-, thiourea, methyl thiourea), a change in the ^{31}P NMR chemical shift is observed. The spectra for the phosphorus NMR experiments showed that there is only one peak observed. The broadening of the signal at higher concentrations of the added ligand also indicates that some of the PTA is being substituted and that phosphine exchange could be taking place.

In Table 3.5 it is noted that the equilibrium constants for the thiourea and methyl thiourea are comparable. Figs. 3.16 and 3.18 indicate that the total conversion of the reactants to the products is at the stage when approximately 100 mmol of the ligands are added. However, in Fig. 3.14 for the thiocyanate ligand the deduction can be made that when 100 mmol of the ligand is added the conversion to the products is less than 50%, hence the small equilibrium constant value. Thus, the stability of the thiocyanate complex is two orders of magnitude lower as compared to the thiourea and methyl thiourea in spite of coordination *via* the S atom (See Chapter 4).

Table 3.5 Equilibrium constant values for the reactions of [Au(PTA)Cl] + L (L = SCN^-, thiourea, methyl thiourea) at 25 °C, calculated from the fit of data.

L	K_L [a]
SCN^-	0.070(6)
Thiourea	4.191(1)
Methyl thiourea	6.734(3)

[a] Obtained from Eq. 3.2 as derived in the Appendix, § A.6.1.

3.5.2.5 ^{31}P NMR spectroscopic study of the effect of additional PTA on [Au(PTA)Cl]

The reaction of [Au(PTA)Cl] with additional amounts of the PTA ligand is monitored by observing the peak change of the ^{31}P NMR chemical shift.

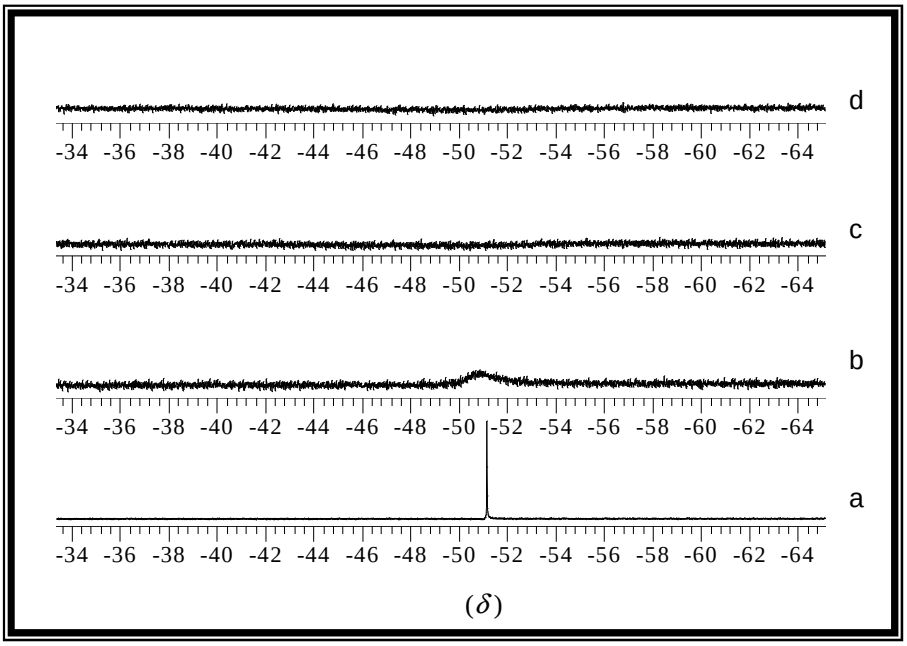

Figure 3.19 ^{31}P NMR spectra of [Au(PTA)Cl] with additional amounts of PTA, in DMSO. [Au] = 50 mM, scans were taken at 25 °C and a, b, c, and d = 0.0, 0.2, 0.5 and 1.0 equivalents of added PTA respectively.

The ^{31}P NMR spectra overlay graph when additional amounts of PTA were added to the [Au(PTA)Cl] complex is presented in Fig. 3.19. Upon addition of 0.2 equivalents of PTA is added to the complex, broadening of the phosphorus peak is observed. This may be due to the fast exchange of the free PTA ligand with the coordinated one in the [Au(PTA)Cl] complex. When additional equivalents of PTA of up to equimolar concentrations (d in Fig 3.19 as the complex is added, much broadening of the peak is observed. The chemical shift for the free PTA ligand in DMSO is observed at -103.03 ppm and when the full spectrum in Fig 3.19 was recorded there were no other peaks observed on this entire spectrum as it can be anticipated that the peak for the free PTA will be observed. This observation, *i.e*., the broadening of the ^{31}P NMR signal, was also seen in the studies described in § 3.5.2.1 - 3.5.2.3 above wherein the chloride was substituted with various ligands. It is therefore quite likely that the broadening observed previously could also be due to small amounts of PTA liberated upon substitution of the chloride thereby inducing fast PTA exchange in a parallel reaction.

3.6 STUDIES OF INCLUSION OF PTA AND RELATED GOLD(I) COMPOUNDS INTO β-CYCLODEXTRIN

In this section the properties of cyclodextrins and their ability to complex with suitable guest molecules in solution are investigated by the determination of equilibrium constants. Also, the study was done in order to increase solubility of the guest molecules in aqueous media for perhaps uses such as drug delivery as it is one of the prominent applications of cyclodextrins.

3.6.1 Experimental

The equilibrium constants (K_D) obtained from including various guest ligands (G) such as PTA and gold(I) complexes into β-cyclodextrin (β-CD) were determined using the following equation which also represents the equilibrium reaction process:

$$G + \beta\text{-CD} \rightleftharpoons[K_D] G\text{-}\beta\text{-CD} \qquad (3.3)$$

The equilibrium constant determination experiments were all conducted using freshly prepared gold complexes, ligand and β-cyclodextrin solutions, in DMSO solvent for the complexes and in aqueous media for PTA + β-cyclodextrin reactions and at 25 °C. The gold or ligand solutions were mixed with the different concentrations of β-cyclodextrin and the final concentrations for Au(I) or phosphine and β-cyclodextrin are thus as indicated in the various respective figure captions in the following sections. The ^{1}H and ^{31}P NMR spectra were recorded on a 300 MHz Gemini spectrometer operating at 300 and 121.45 MHz respectively. The ^{1}H NMR spectra were calibrated relative to the residual D_2O peak (4.63 ppm) while the ^{31}P chemical shifts are reported as calibrated at 0 ppm relative to 85% H_3PO_4 as an internal standard in a capillary. The observed equilibrium constants were obtained from the chemical shift versus ligand concentration graphs using the least-squares program Scientist[53]. The equation used in fitting data and getting the plots of the chemical shift versus β-cyclodextrin concentration is presented as Eq. 3.4.

The derivation of the equation is given in the Appendix, § A.6.3.

$$\delta_{obs} = \frac{\delta_R + \delta_P K_D[\beta\text{-CD}]}{1 + K_D[\beta\text{-CD}]} \quad (3.4)$$

K_D = Equilibrium constant, δ_R = chemical shift observed for the reactants, δ_P = chemical shift for the products and [β-CD] = final cyclodextrin concentration.

3.6.2 NMR equilibrium study of PTA inclusion into β-cyclodextrin

3.6.2.1 ^{1}H NMR equilibrium constant determination of PTA inclusion into β-cyclodextrin

The spectrum of the PTA ligand is shown in Fig. 3.20. As various equivalents of β-cyclodextrin were added to the PTA solution in DMSO, the change in the chemical shifts was observed. This hence allowed for the determination of the equilibrium constant by fitting of the chemical shift change data into Eq. 3.4 (Fig. 3.21).

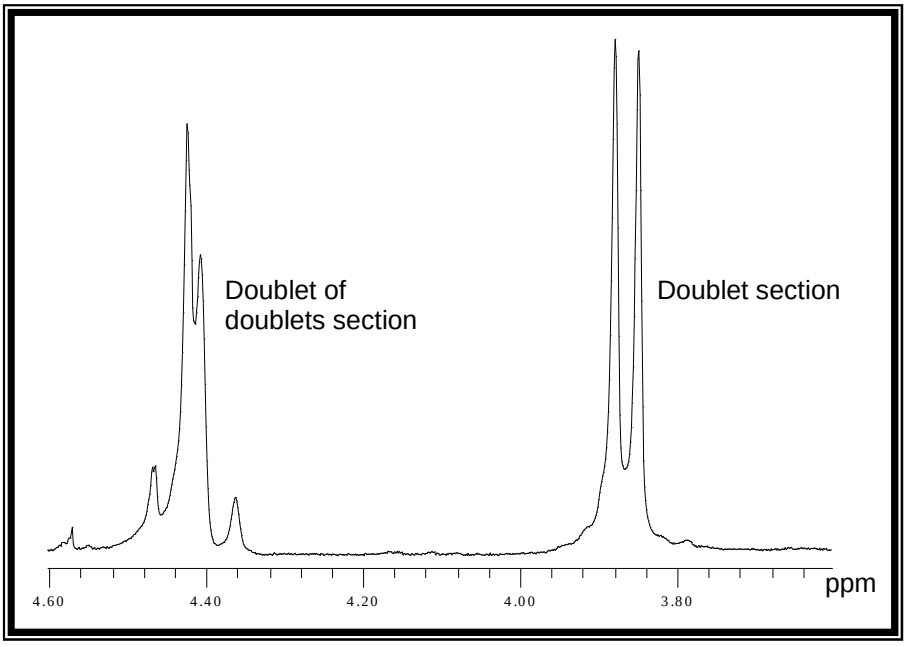

Figure 3.20 ^{1}H NMR spectrum of PTA in D_2O at 25 °C. [PTA] = 30 mM.

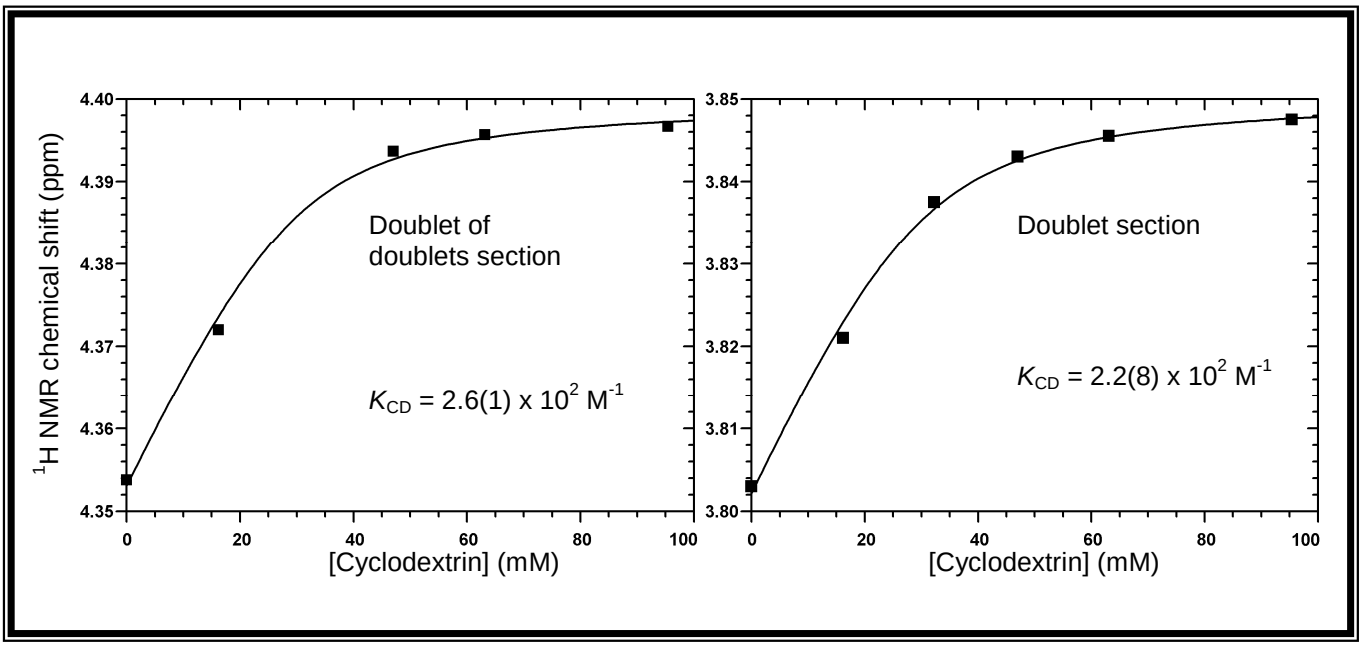

Figure 3.21 A plot of the ^{1}H NMR chemical shift change when β-cyclodextrin concentration is varied in a solution of PTA in D_2O. [PTA] = 30 mM, [β-cyclodextrin] = 0 - 100 mM and T = 25 °C. Solid line represents fit of data to Eq. 3.4.

3.6.2.2 ^{31}P NMR equilibrium constant determination of PTA inclusion into β-cyclodextrin

Stoichiometric amounts of β-cyclodextrin were added to PTA solution and the change of the chemical shift was monitored by ^{31}P NMR as presented in Fig. 3.22 while fit of data in order to calculate the equilibrium constant using Eq. 3.4 is given in Fig. 3.23.

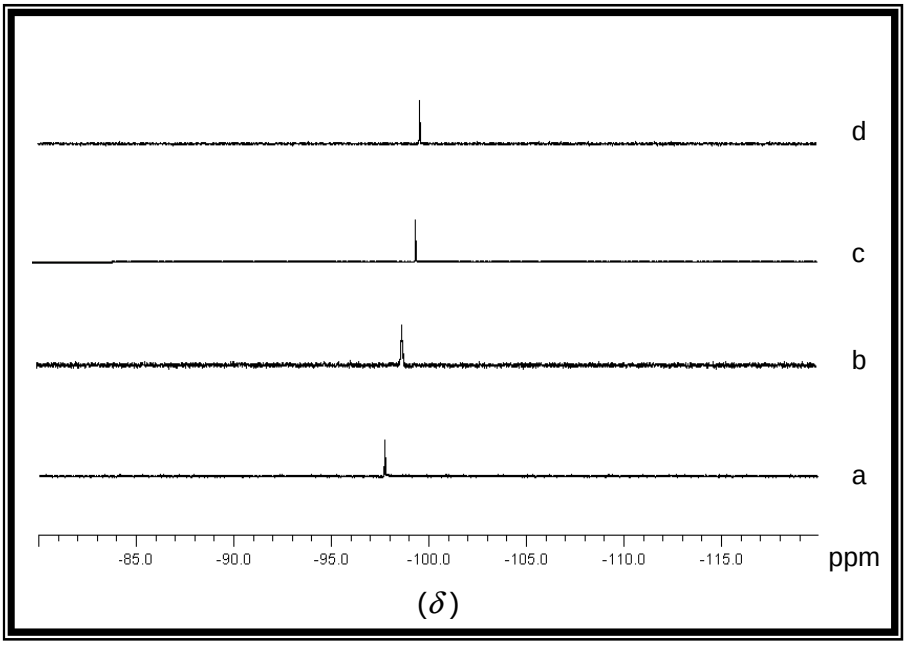

Figure 3.22 ^{31}P NMR spectra of PTA with different amounts β-cyclodextrin added in D_2O. [PTA] = 30 mM, scans were taken at 25 °C and a, b, c, and d = 0.0, 0.5, 1.0 and 2.0 equivalents of β-cyclodextrin added respectively.

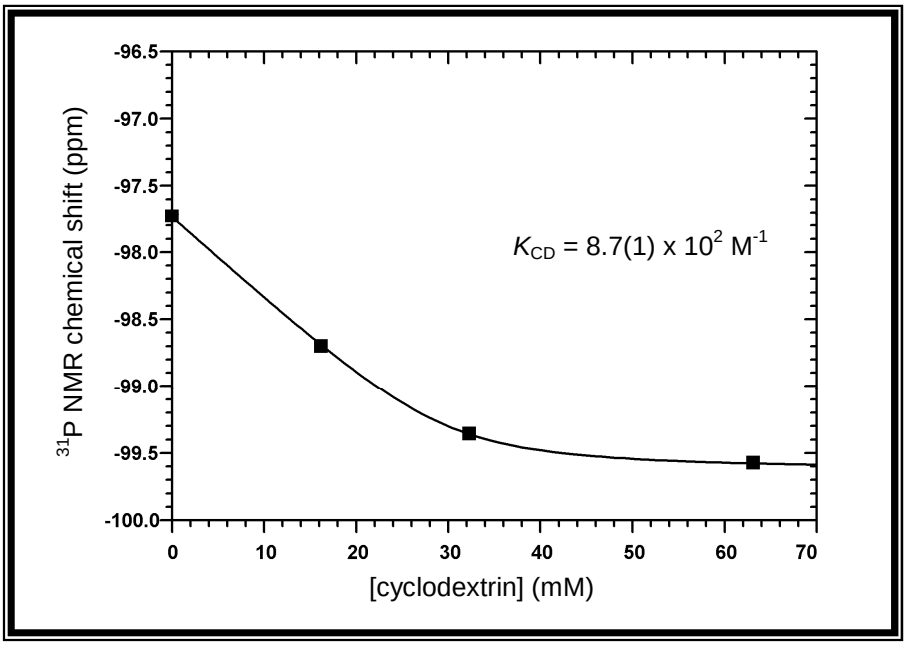

Figure 3.23 A plot of the ^{31}P NMR chemical shift change (Fig. 3.22) when β-cyclodextrin concentration is varied in a solution of PTA in D_2O. [PTA] = 30 mM, [β-cyclodextrin] = 0 - 65 mM and T = 25 °C. Solid line represents fit of data to Eq. 3.4.

3.6.3 ^{31}P NMR study of $(PTAMe)^+$ inclusion into β-cyclodextrin

The determination of the equilibrium constant when (PTAMe)I is included into β-cyclodextrin is discussed. Fig. 3.24 indicates the ^{31}P NMR chemical shift change when various amounts of β-cyclodextrin are added to the compound while fit of data in order to calculate the equilibrium constant using Eq. 3.4 is given in Fig. 3.25.

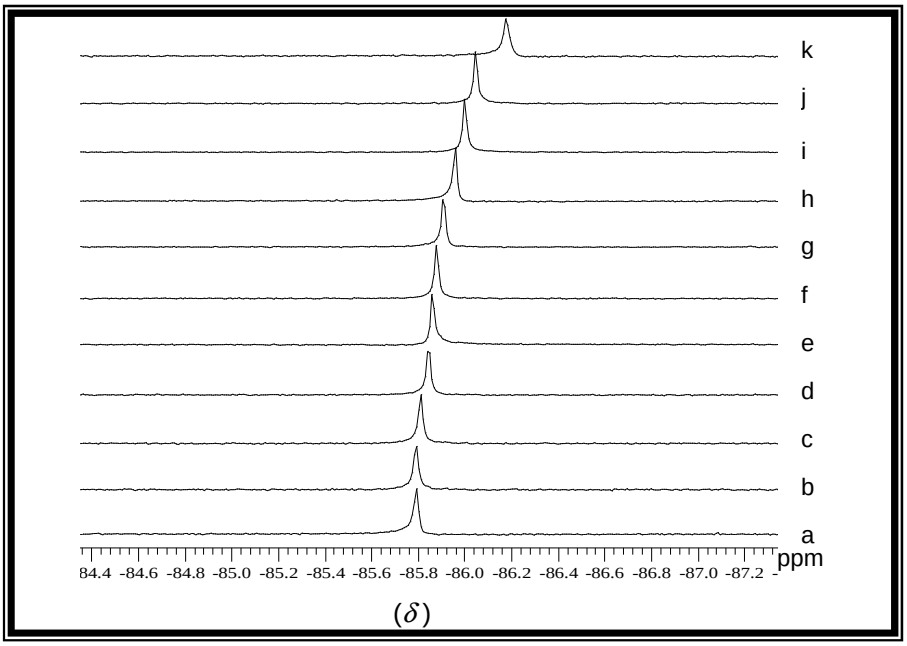

Figure 3.24 Overlay plot of the ^{31}P NMR spectra of (PTAMe)I with different amounts of β-cyclodextrin (β-CD) added in DMSO. [(PTAMe)I] = 54.8 mM, scans were taken at 25 °C and 0 - 10 equivalents of β-cyclodextrin were added respectively. [β-cyclodextrin] = 0 - 548 mM. a, b, c, d, e, f, g, h, i, j, k = 0.0, 0.1, 0.5, 1.0, 1.2, 1.5, 2.0, 3.0, 4.0, 5.0, 10.0 equivalents of β-cyclodextrin added respectively.

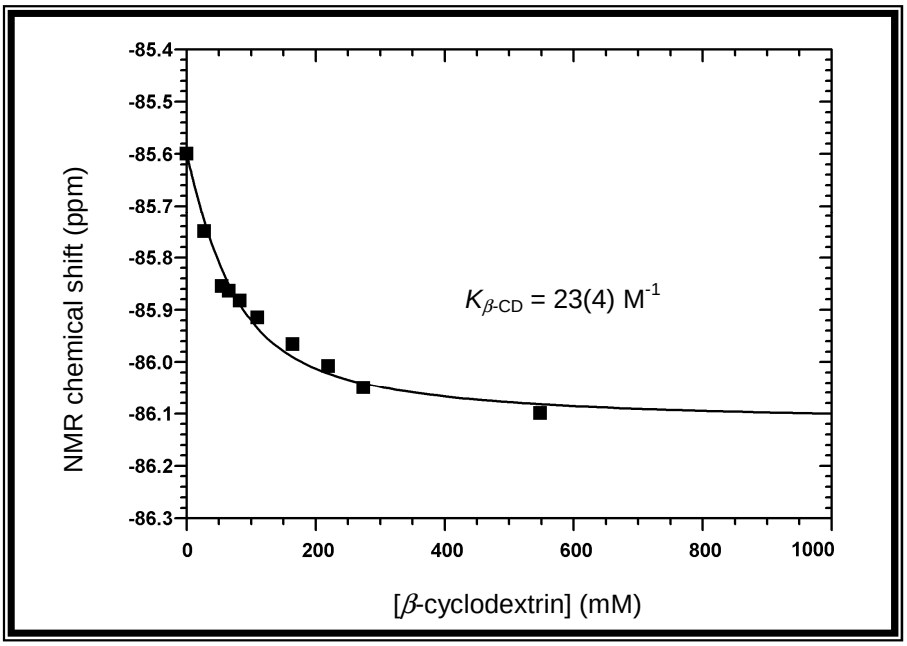

Figure 3.25 A graph showing the fit of data of the ^{31}P NMR chemical shift change (Fig. 3.24) to Eq. 3.4, when β-cyclodextrin concentration is varied in a solution of (PTAMe)I in DMSO. [(PTAMe)I] = 54.8 mM, [β-cyclodextrin] = 0 - 548 mM and T = 25 °C. Solid line represents fit of data to Eq. 3.4.

3.6.4 ^{31}P NMR study of [Au(PTAMe)Cl]I inclusion into β-cyclodextrin

The graphs showing the determination of the equilibrium constant when the various amounts of β-cyclodextrin are added to [Au(PTAMe)Cl]I are presented. Fig. 3.26 indicates the ^{31}P NMR chemical shift change when various amounts of the host β-cyclodextrin are added while fit of data in order to calculate the equilibrium constant using Eq. 3.4 is given in Fig. 3.27.

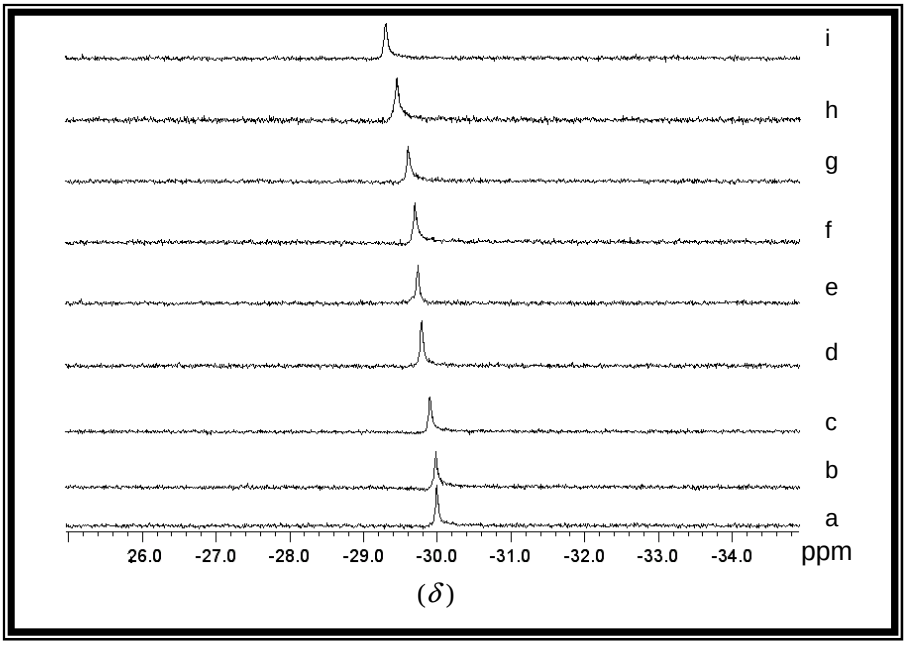

Figure 3.26 Overlay plot of the ^{31}P NMR spectra of [Au(PTAMe)Cl^{+}] with different amounts of β-cyclodextrin (β-CD) added in DMSO. [Au] = 16.6 mM, scans were taken at 25 °C and 0 - 5 equivalents of β-cyclodextrin were added sequentially, [β-cyclodextrin] = 0 - 83.1 mM. a, b, c, d, e, f, g, h, i = 0.0, 0.1, 0.5, 1.0, 1.2, 1.5, 2.0, 3.0, 4.0 equivalents of β-cyclodextrin added respectively.

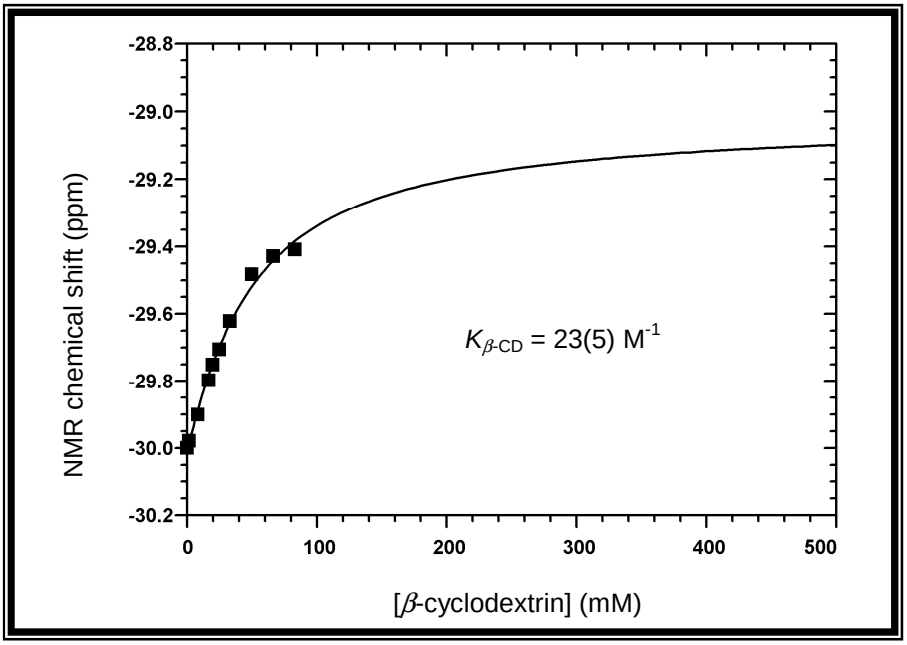

Figure 3.27 A graph showing the fit of data of the ^{31}P NMR chemical shift change (Fig. 3.26) to Eq. 3.4, when β-cyclodextrin concentration is varied in a solution of [Au(PTAMe)Cl^{+}] in DMSO. [Au] = 16.6 mM, [β-cyclodextrin] = 0 - 83.1 mM and T = 25 °C. Solid line represents fit of data to Eq. 3.4.

3.6.5 ^{31}P NMR study of inclusion of PPh_3 into β-cyclodextrin

The determination of the equilibrium constant when the PPh_3 complex is included into β-cyclodextrin is discussed. Fig. 3.28 indicates the ^{31}P NMR chemical shift change when various amounts of the β-cyclodextrin are added while fit of data in order to calculate the equilibrium constant using Eq. 3.4 is given in Fig. 3.29.

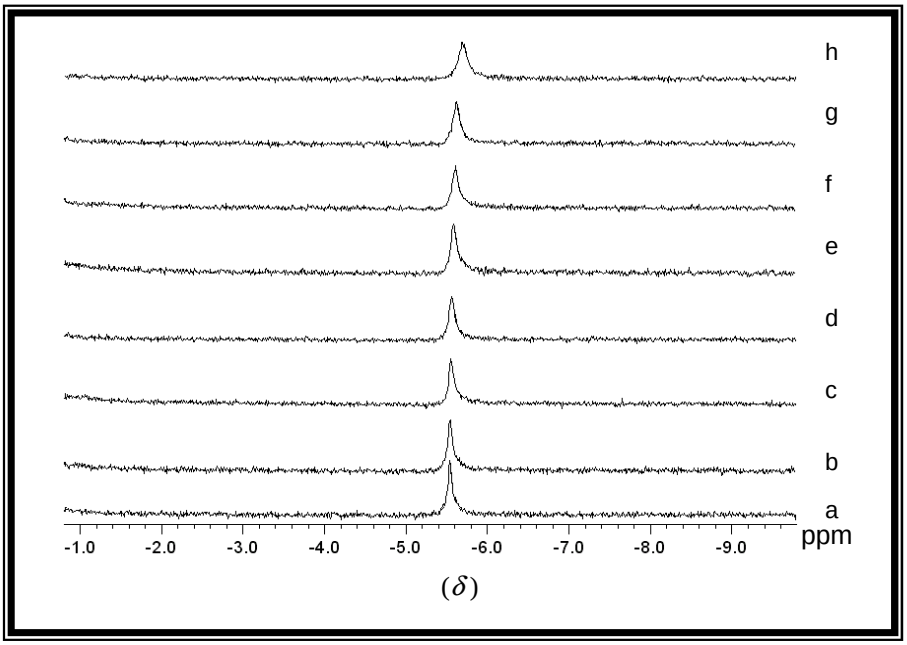

Figure 3.28 Overlay plot of the ^{31}P NMR spectra of PPh_3 with different amounts of β-cyclodextrin (β-CD) added in DMSO. [PPh_3] = 44.5 mM, scans were taken at 25 °C and 0 - 10 equivalents of β-cyclodextrin were added sequentially, [β-cyclodextrin] = 0 - 445 mM. a, b, c, d, e, f, g, h, = 0.1, 0.5, 1.5, 2.0, 3.0, 4.0, 5.0, 10.0 equivalents of β-cyclodextrin added respectively.

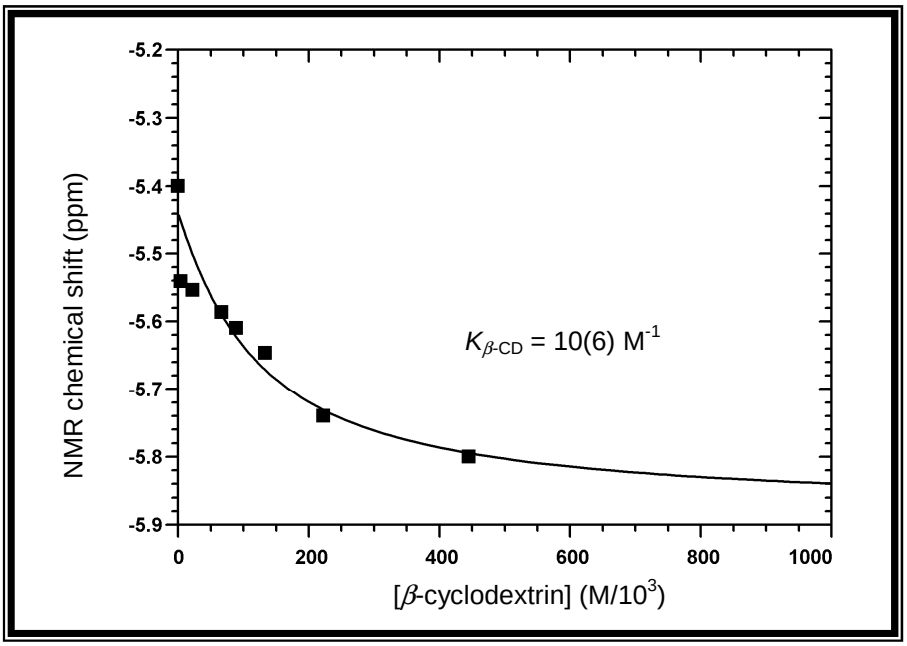

Figure 3.29 A graph showing the fit of data of the ^{31}P NMR chemical shift change (Fig. 3.28) to Eq. 3.4, when β-cyclodextrin concentration is varied in a solution of PPh_3 in DMSO. [PPh_3] = 44.5 mM, [β-cyclodextrin] = 0 - 445 mM and T = 25 °C. Solid line represents fit of data to Eq. 3.4.

3.6.6 ^{31}P NMR study of [Au(dppe)$_2$]Cl inclusion into β-cyclodextrin

The determination of the equilibrium constant when β-cyclodextrin is added to the [Au(dppe)$_2$]Cl complex is discussed. Fig. 3.30 indicates the ^{31}P NMR chemical shift change when various amounts of β-cyclodextrin are added to the complex while fit of data to Eq. 3.4 in order to calculate the equilibrium constant using Eq. 3.4 is given in Fig. 3.31.

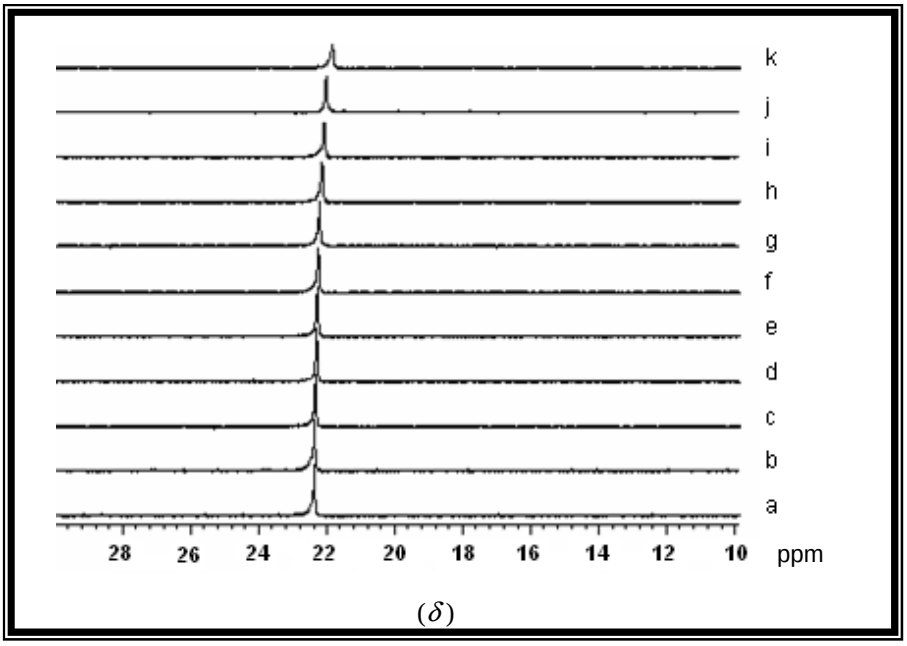

Figure 3.30 Overlay plot of the ^{31}P NMR spectra of $[Au(dppe)_2]Cl$ with different amounts of β-cyclodextrin (β-CD) added in DMSO. [Au] = 54.4 mM, scans were taken at 25 °C and 0 - 10 equivalents of β-cyclodextrin were added respectively. [β-cyclodextrin] = 0 - 544 mM. a, b, c, d, e, f, g, h, i, j, k = 0.0, 0.1, 0.5, 1.0, 1.2, 1.5, 2.0, 3.0, 4.0, 5.0, 10.0 equivalents of β-cyclodextrin added respectively.

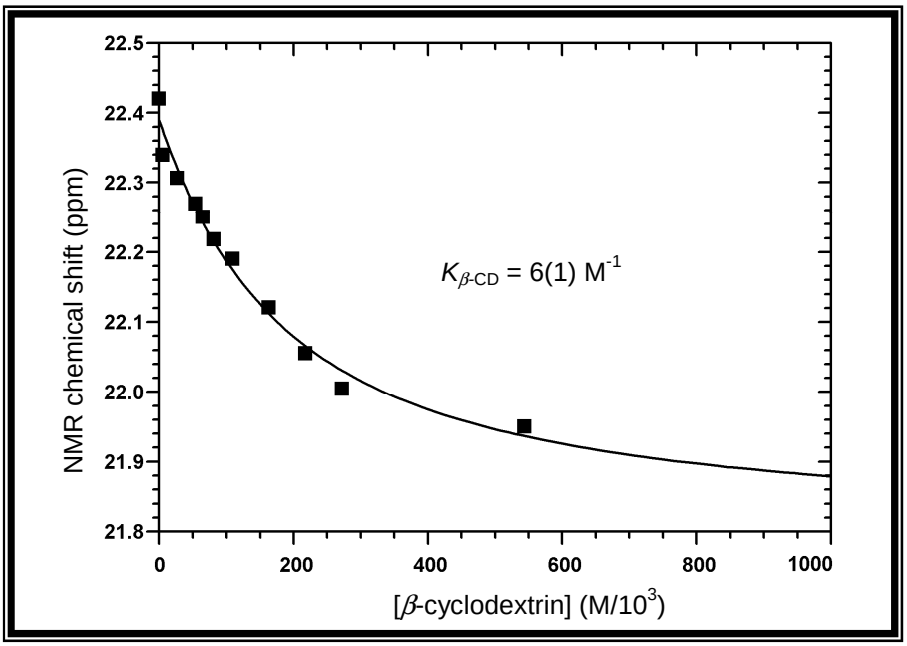

Figure 3.31 A graph showing the fit of data of the ^{31}P NMR chemical shift change (Fig. 3.30) to Eq. 3.4, when β-cyclodextrin concentration is varied in a solution of $[Au(dppe)_2]Cl$ in DMSO. [Au] = 54.4 mM, [β-cyclodextrin] = 0 - 544 mM and T = 25 °C. Solid line represents fit of data to Eq. 3.4.

The equilibrium constants calculated from fit of data when tertiary phosphine and PTA compounds and complexes thereof are included into β-cyclodextrin (§ 3.6.3 - 3.6.6) are presented in Table 3.6. The ^{31}P NMR experiments of the $[Au(dppe)_2]Cl$ and PPh_3 complexes with addition of equivalents of β-cyclodextrin were done to investigate if there will be a change in the chemical shift of the observed peak. The aim of these experiments was also to investigate the possible increase in solubility of these complexes when the β-cyclodextrin is added. Indeed there was a small shift in the peak observed as the β-cyclodextrin concentration is increased. The graphs showing the shift of the peak are illustrated by Figs. 3.28 and 3.30. Although the peak shift is not large enough, even when 10 equivalents of the β-cyclodextrin were added, this small shift might indicate some inclusion of the complexes to the β-cyclodextrin. Noted also, was a slight increase in solubility of the complexes.

Table 3.6 Summarised table of the equilibrium constants for the inclusion of various complexes and compounds into β-cyclodextrin at 25 °C, calculated from the fit of data.

Complex + β-cyclodextrin	K_D (M^{-1})[a]
$[Au(dppe)_2]Cl$	6(1)
PPh_3	10(6)
(PTAMe)I	23(4)
[Au(PTAMe)Cl]I	23(5)

[a] Obtained from Eq. 3.4 as derived in the Appendix, § A.6.3.

3.7 CONCLUSIONS

The synthesis and characterisation of gold(I) complexes with the water-soluble 1,3,5-triaza-7-phosphatricyclo[3.3.1.1^{3,7}] decane (PTA) ligand was successfully investigated. Though the PTA ligand and its methylated analogue are indeed water-soluble, the solubility and stability of the gold(I) complexes synthesised with the PTA ligand in aqueous media was still limited hence further determinations of these gold(I) complexes with ligands are done in DMSO. As mentioned in Chapter 1, the gold complex 2,3,4,6-tetra-*O*-acetyl-1-thio-β-D-glucopyranosato(triethylphosphine) gold(I) (auranofin) is an experimental chrysotherapeutic agent shown to be clinically effective in the treatment of rheumatoid arthritis when administered orally. In the interest of this current study auranofin and its analogue complexes were synthesised with the motive of manipulating the phosphine moiety in the original auranofin compound and using

these complexes for preliminary biological tests and assays against cell lines. Hence, a range of ligands including the water-soluble PTA ligand and its methylated analogue $(PTAMe)^+$, tertiary phosphine ligands such as triethylarsine and triphenylphospine were utilised for the synthesis of the various auranofin complexes by substituting the triethylphosphine group in the original auranofin and the use of these complexes in biological testing is discussed in Chapter 5.

The study of the substitution reactions of the chloride from the [Au(PTA)Cl] complex by SCN^-, thiourea and methyl thiourea was successfully achieved, also yielding equilibrium constants for these systems. These types of ligands were employed since they are S-donor ligands and it is anticipated that the ligands will induce solubility and stability of complexes thereof in biological environment if the complexes were to be used in biological testing. Since the solubility of these PTA gold complexes in aqueous media is limited, substitution reactions of the complexes with various S-donor ligands were done in DMSO. These equilibrium constant determinations were studied by ^{31}P NMR spectroscopy by monitoring the chemical shift change of the observed peak as stoichiometric amounts of the ligand are added to the [Au(PTA)Cl] solution in DMSO. The equilibrium constants obtained when reacting the [Au(PTA)Cl] complex with SCN^-, thiourea and methyl thiourea were 0.070(6), 4.191(1), 6.734(3) respectively. The equilibrium constant for SCN^- substitution into [Au(PTA)Cl] is small as compared to the constants obtained when the chloride is substituted from [Au(PTA)Cl] by thiourea and methyl thiourea.

As discussed in the introduction, § 3.1.2, cyclodextrins are of interest for chemists since they are chemically stable and are also water-soluble. They display 'host-guest' chemistry by virtue of hydrogen bonding of guests into their cavities. In this study such phenomenon was displayed by the inclusion of PTA into the β-cyclodextrin and this was investigated by X-ray crystallography. The glucose residues of the PTA-β-cyclodextrin compound are in a $^4C_1$ chair conformations and only dextrorotatory enantiomers were observed. The PTA ligand is included inside the cavity of the β-cyclodextrin unit and the packing of the molecule in the unit cell is of a herring-bone motif. The inclusion of auranofin into β-cyclodextrin was also attempted by X-ray crystallography. However, only auranofin crystallised out without inclusion into the β-cyclodextrin molecule. The data collection for the auranofin structure in this study was done at 100 K and since the structure of auranofin has been reported in literature, it was worthwhile to compare the two structures as the data collection for the one in

literature was done at ambient temperatures. The investigations done with auranofin at low temperatures clearly indicated a phase change and a new polymorph at 100 K which was evident in the approximate 1-4° changes in selected torsion and bond angles.

The determinations for the equilibrium constants when simple ligands such as PTA, its methylated analogue and PPh_3 and various gold(I) complexes ($[Au(dppe)_2]Cl$, [Au(PTAMe)Cl]I) are included into the β-cyclodextrin were determined by NMR spectroscopy. The equilibrium constants for the PTA inclusion into β-cyclodextrin as determined by using ^{1}H and ^{31}P NMR spectroscopy are approximately 2×10^{2} and 8×10^{2} M^{-1} respectively. It was observed that PTA compounds have higher inclusion constants as compared to the $[Au(dppe)_2]Cl$ and PPh_3 with phenyl groups. Also, the solubility of the phenyl compounds was not improved that much as compared to the PTA compounds which may be due to steric hindrance and orientation of the phenyl groups being too large to be incorporated into the β-cyclodextrin. This phenomenon was also seen in the unsuccessful incorporation of auranofin due to its orientation of the ethyl groups into β-cyclodextrin. The inclusion behaviour of the various guests molecules ranging from simple ligands and molecules to gold(I) complexes into β-cyclodextrin as studied by NMR spectroscopy in calculating the equilibrium constants illustrates the 'host-guest' chemistry portrayed by cyclodextrins.

[1] J.A. Cowan, 'Inorganic Biochemistry: An Introduction', VCH, Weinheim, 1993, 277.

[2] R.V. Parish, *Interdisc. Sci. Rev.,* 1992, **17**, 221.

[3] S.R. Fricker, in Medical Uses of Gold: Past, Present and Future, *Gold Bull.,* 1996, **29**, 53.

[4] A.E. Finkelstein, D.T. Walz, U. Batista, M. Mixraji, F. Roisman, A. Misher, *Ann. Rheum. Dis.,* 1976, **35**, 251.

[5] F.E. Berglof, K. Berglof, D.T. Walz, *J. Rheum.,* 1978, **5**, 68.

[6] D.T. Walz, M.J. DiMartino, L.W. Chakrin, B.M. Sutton, A. Misher, *J. Pharm. Exp. Ther.,* 1976, **197**, 142.

[7] D.T. Hill, B.M. Sutton, *Cryst. Struct. Commun.,* 1980, **9**, 679.

[8] J.W. Ellis, K.N. Harrison, P.A.T. Hoye, A.G. Orpen, P.G. Pringle, M.B. Smith, *Inorg. Chem.,* 1992, **31**, 3026.

[9] P.A.T. Hoye, P.G. Pringle, M.B. Smith, K. Worboys, *J. Chem. Soc., Dalton Trans.,* 1993, 269.

[10] V.S. Reddy, D.E. Berning, K.V. Katti, C.L. Barnes, W.A. Volkert, A.R. Ketring, *Inorg. Chem.,* 1996, **35**, 1753.

[11] D.J. Darensbourg, T.J. Decuir, N.W. Stafford, J.B. Robertson, J.D. Draper, J.H. Reibenspies, *Inorg. Chem.,* 1997, **36**, 4218.

[12] D. Daigle, A.B. Pepperman, S.L. Vail, *J. Heterocycl. Chem.,* 1974, **14**, 1217.

[13] J.R. De Lerno, L.M. Trefonas, M.Y. Darensbourg, R.J. Majeste, *Inorg. Chem.,* 1976, **15**, 816.

[14] D.J. Darensbourg, F. Joo, M. Kannisto, A. Katho, J.H. Reibenspies, *Organometallics,* 1992, **11**, 1990.

[15] E.C. Alyea, K.J. Fischer, S. Johnson, *Can. J. Chem.,* 1989, **67**, 1319.

[16] S. Otto, A. Roodt, *Inorg. Chem. Commun.,* 2001, **4**, 49.

[17] D.J. Darensbourg, F. Joó, M. Kannisto, A. Kathó, J.H. Reibenspies, D.J. Daigle, *Inorg. Chem.,* 1994, **33**, 200.

[18] S. Otto, A. Roodt, W. Purcell, *Inorg. Chem. Commun.,* 1998, **1**, 415.

[19] O.M. Ni Dhubhghaill, P.J. Sadler, R. Kuroda, *J. Chem. Soc., Dalton Trans.,* 1990, 2913.

[20] D.W. Grifiths, M.L. Bender, *Adv. Cat.,* 1973, **23**, 209.

[21] P.R. Sundarajan, V.S.R. Rao, *Carbohydr. Res.,* 1970, **13**, 351.

[22] V.G. Murphy, B. Zaslow, A.D. French, *Biopolymers,* 1975, **14**, 1487.

[23] M.L. Bender, M. Komiyama, 'Cyclodextrin Chemistry', Spinger Verlag; New York, 1978.

[24] D. French, A.O. Pulley, J.A. Effenberger, M.A. Rougvie, M. Abdullah, *Arch. Biochem Biophys.,* 1965, **111**, 153.

[25] J. Szejtli, 'Cyclodextrins and their Inclusion Complexes', Akadémiai Kiadó, Budapest, 1982.

[26] W. Saenger, *Angew. Chem. Int. Ed. Engl.,* 1980, **19**, 344.

[27] S. Li, W.C. Purdy, *Chem. Rev.,* 1992, **92**, 1457.

[28] G. Wenz, *Angew. Chem. Int. Ed. Engl.,* 1994, **33**, 803.

[29] J. Szejtli, 'Cyclodextrin Technology': in Topics in Inclusion Science (Ed.: J.E.D. Davies), Kluwer, Dordrecht, p. 26, 1988.

[30] H. Vakaliu, M. Miskolci-Torok, J. Szejtli, M Jarai, G. Seres (Chinoin), *Chem. Abstr.,* 1979, **91**, 91 923.

[31] Y. Takahashi, T. Ogawa, *Carbohydr. Res.,* 1987, **164**, 277.

[32] J. Szejtli, 'Cyclodextrin Technology', Kluwer, Boston, 1988.

[33] M. Paleologou, S. Li, W.C. Purdy, *J. Chromatogr. Sci.,* 1990, **28**, 311.

[34] A.P. Croft, R.A. Bartsch, *Tetrahedron,* 1983, **39**, 1417.

[35] A. Janshoff, C. Steinem, A. Michalke, C. Henke, H. Galla, *Sensors and Actuators,* 2000, **B 70**, 243.

[36] D. Hreczuk-Hirst, D. Chicco, L. German, R. Duncan, *Int. J. Pharm.,* 2001, **230**, 57.

[37] T. Cserháti, E. Forgács, *Eur. J. Pharm. Biopharm.,* 1998, **46**, 153.

[38] O.S. Tee, *Carbohydr. Res.,* 1989, **192**, 181.

[39] D.F. Shriver and M.A. Drezdzon, 'The Manipulation of Air-sensitive Compounds', Wiley-Interscience, New York, 1986.

[40] D.J. Daigle, T.J. Decuir, J.B. Robertson, D.J. Darensbourg, *Inorg. Synth.,* 1998, **32**, 40.

[41] R. Uson, A. Laguna, M. Laguna, D.A. Briggs, H.H. Murray, J.P. Fackler Jr., *Inorg. Synth.,* 1989, **26**, 85.

[42] Z. Assefa, B.G. McBurnett, R.J. Staples, J.P. Fackler Jr., B. Assmann, K. Angermaier, H. Schmidbaur, *Inorg. Chem.,* 1995, **34**, 75.

[43] A.A. Isab, M. Fettouhi, S. Ahmad, L. Ouahab, *Polyhedron,* 2003, **22**, 1349.

[44] F.G. Mann, A.F. Wells, D. Purdie, *J. Chem. Soc.,* 1937, 1828.

[45] M.I. Bruce, B.K. Nicholson, O. Bin Shawkataly, J.R. Shapley, T. Henley, *Inorg Synth.,* 1989, **26**, 324.

[46] R.A. Bell, C.J.L. Lock, C. Scholten, J.F. Valliant, *Inorg. Chim. Acta,* 1998, **274**, 137.

[47] Bruker SADABS (Version 2004/1) and SMART-NT (Version 5.050). Bruker AXS Inc., Madison, Wisconsin, USA, 1998.

[48] G.M. Sheldrick, SHELXS-97, Program for Crystal Structure Determination, University of Göttingen, Germany, 1997.

[49] G.M. Sheldrick, SHELXL-97, Program for Crystal Structure Refinement, University of Göttingen, Germany, 1997.

[50] (a) K. Brandenburg, M. Berndt, DIAMOND Version 2.1e, Program for Molecular Graphics, Crystal Impact, Bonn, Germany, 1997-2001.
(b) K. Brandenburg, DIAMOND, Release 3.0c, Crystal Impact GbR, Postfach 1251, D-53002 Bonn, Germany, 2005.

[51] W. Saenger, T. Steiner, *Acta Cryst.,* 1998, C**54**, 798.

[52] B.M. Sutton, E. McGusty, D.T. Walz, M.J. DiMartino, *J. Med. Chem.,* 1976, **15**, 251.

[53] Scientist for Windows, Least-squares Parameter Estimation, Version 4.00.950, MicroMath, 1990.

4 CRYSTALLOGRAPHIC STUDY OF FERROCENYL P-DONOR GOLD(I) COMPLEXES

4.1 INTRODUCTION

Ferrocene (Fig. 4.1) has played a major role in organometallic chemistry since its first preparation in the early 1950's[1,2], while the employment of ferrocenyl phosphines as ligands in coordination chemistry is well known[3]. The ability of these ligands to transfer the ferrocenyl qualities to the resultant complexes without disturbing the inherent characteristics of the latter has widened the scope of the metal complexes in the design of catalysts, drugs and materials. Hence, this has led to the preparation of several ferrocene-containing coordination compounds.

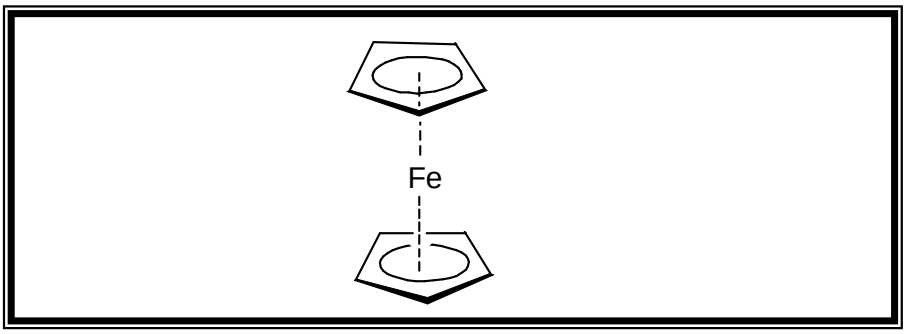

Figure 4.1 Structure of the ferrocene group.

The versatile nature of the 1,1'-bis(diphenylphosphino)ferrocene (dppf) as a complexed-ligand has attracted considerable attention because of its possible relevance to the catalytic applications of its complexes[4]. This metalloligand holds a unique ability to modify its steric bite by ring twisting and tilting in order to adapt to different geometric requirements of the metal centres to which it is attached. Thus, in its complexes the ligand is known to increase the stabilisation to form chelates[5,6,7] as well as the various bridging modes such as the open[8,9], half-closed[10] and closed[11] bridging systems. In the hope of relating various coordination modes of the dppf ligand to its structural conformations, characterisation by X-ray crystallography is required and utilised. In most X-ray characterised complexes containing the dppf ligand, the bis(diphenylphosphino)ferrocene acts as a bidentate chelating ligand. In its free state,

the dppf molecule is centrosymmetric with the inversion centre at the Fe atom[12]. This ideal conformation can be described as antiperiplanar when the C_p rings are parallel and staggered with a torsion angle of 180°. This *anti* arrangement of the PPh_2 moieties is understood based on its lowest conformational energy. Bond lengths and angles associated with the phosphorus atoms are reminiscent of those observed in the free triphenylphosphine[13]. Few examples of metal complexes exist though in which the geometry of the free ligand is preserved[14,3].

There has been interest and activity in asymmetric synthesis catalysed by transition metal complexes with chiral ligands. Among various types of asymmetric reactions, reaction with a chiral catalyst would be a better choice provided that the catalytic asymmetric reactions proceed with high stereoselectivity, producing the desired enantiomeric isomer in high yield[15]. Many of the transition metal complexes used for catalytic reactions contain tertiary phosphines as ligands, so that it is convenient to use optically active phosphine ligands to make the metal complexes function as chiral catalysts. Thus the most valuable point for obtaining high efficiency in the transition metal catalysed asymmetric reactions is the design and preparation of a chiral phosphine ligand that will bring about high enantioselectivity as well as high catalytic activity in a given reaction.

In this study, sterically modified dppf ligands are employed to synthesise gold(I) complexes thereof. Coordination of much smaller groups such as SCN^-, $-N(CH_3)_2$ and acetate groups to the gold(I) complexes and at the periphery of the dppf ligand is introduced in order to induce increased solubility within the complexes in polar solvents. Another aim was to examine if the modified dppf ligand will produce isostructural gold(I) complexes and hence comparing coordination modes of the modified dppf complexes to some known PPh_3 complexes of gold(I). The synthesis of gold(I) complexes with modified dppf is compared when different stoichiometric amounts of dppf ligand:gold, such as 1:1 and 1:2, are used.

4.2 EXPERIMENTAL

All common laboratory reagents and chemicals used in the preparations were of reagent grade and distilled water was used in all experiments. The following chemicals were commercially available: $HAuCl_4 \cdot 3H_2O$ (Next Chimica); Tetrahydrothiophene (Merck); Ferrocene (Fluka); KSCN (SaarChem). These reagents were used without further purification. Some of the starting ligands like the *N*,*N*-dimethyl-1-[1',2-bis(diphenylphosphino)ferrocenyl]ethylamine, 1-[1',2-bis(diphenylphosphino)ferrocenyl] ethylacetate were obtained from the Lund University Organic Chemistry Department.

The characterisation of the complexes was done with ^{1}H and ^{31}P NMR (Varian-500 spectrometer operating at 500 and 202.31 MHz, respectively). The ^{1}H and ^{31}P NMR spectra were recorded at 25 °C in $CDCl_3$. The ^{1}H NMR spectra were referenced relative to the residual $CDCl_3$ peak (7.25 ppm) while the ^{31}P NMR spectra were referenced relative to 85% H_3PO_4 as an external standard at 0.0 ppm. Infrared spectra were recorded as KBr disks between 4000 - 400 cm^{-1} using an Avatar 360 FT-IR spectrometer.

4.3 SYNTHESIS OF COMPOUNDS AND COMPLEXES

4.3.1 Synthesis of reactants and ligands

4.3.1.1 [Au(THT)Cl]

The synthesis of this complex was done using the following procedure[16]: Tetrachloroauric acid trihydrate, $HAuCl_4 \cdot 3H_2O$ (1.97 g, 5.0 mmol) was dissolved in an ice-cooled solution of absolute ethanol:water (25 mL : 5 mL). Tetrahydrothiophene (1 mL, 11.3 mmol) was then added dropwise to the solution over approximately a period of 10 min with stirring. A yellow $[Au(THT)Cl_3]$ precipitate appeared and this was subsequently reduced to the white [Au(THT)Cl] solid by continued addition of tetrahydrothiophene. After 20 min stirring at room temperature, the solid was filtered, washed with ethanol (2 x 10 mL) and dried. The product was transferred to a storage flask and further dried in vacuum, (Yield = 1.45 g, 90%). The material was then stored in the fridge as it slowly decomposes at room temperature when dry.

^{1}H NMR ($CDCl_3$): δ 2.181 (d, 4H), 3.402 (d, 4H) ppm.

4.3.1.2 (*S*)-*N*,*N*-dimethyl-1-[(*R*)-1',2-bis(diphenylphosphino)ferrocenyl] ethylamine

This complexed-ligand was obtained from the Lund University Organic Chemistry Department and was prepared from *N*,*N*-dimethyl-1-ferrocenylethylamine, *N*,*N*,*N*',*N*'-tetramethylethylenediamine (TMEDA) and chlorodiphenylphosphine[17].

^{1}H NMR ($CDCl_3$): δ 1.14 (d, 3H, CHCH_3), 1.73 (s, 6H, NCH_3), 3.51 - 4.34 (m, 8H), 7.15 - 7.50 (m, 20H, PC_6H_5) ppm.

^{31}P{^{1}H} NMR ($CDCl_3$): δ -16.61 (s), -22.64 (s) ppm.

4.3.1.3 (*R*)-1-[(*S*)-1',2-bis(diphenylphosphino)ferrocenyl] ethylacetate

The complexed-ligand was also obtained from the Lund University Organic Chemistry Department and was prepared by addition of acetic anhydride to the *N*,*N*-dimethyl-1-[1',2-bis(diphenylphosphino)ferrocenyl]ethylamine compound[17].

^{1}H NMR ($CDCl_3$): δ 1.14 (s, 3H, COCH_3), 1.47 (d, 3H, CHCH_3), 3.60 - 4.49 (m, 7H, $C_5H_4FeC_5H_3$), 6.18 (m, 1H, C*H*CH_3), 7.11 - 7.44 (m, 20H, C_6H_5) ppm.

^{31}P{^{1}H} NMR ($CDCl_3$): δ -16.98 (s), -24.64 (s) ppm.

4.3.1.4 Diphenylferrocenylphosphine

Diphenylferrocenylphosphine was synthesised according to a modified version of the published procedure[18].

Anhydrous aluminium chloride (1.2 g, 9.1 mmol) was added to a solution containing ferrocene (1.7 g, 9.1 mmol) in dry *n*-heptane (*ca.* 60 mL) under constant stirring. The anhydrous aluminium chloride was sublimed until a fine white powder was formed, free of any colouration. A solution of PPh_2Cl (1.0 g, 0.85 mL, 4.6 mmol) in *n*-heptane was added, followed by *ca.* 24 hours of reflux under a positive nitrogen atmosphere. After cooling, the *n*-heptane was decanted and the remaining solids were extracted with hot *n*-heptane (2 x 40 mL) and the fractions were combined, evaporated and unreacted ferrocene recovered from this solution. The remaining solids were carefully treated with hot water (5 x 50 mL) and the aqueous washings were discarded. The solids were then extracted with chloroform until the chloroform layer was nearly colourless. The chloroform fractions were combined, dried over anhydrous magnesium sulphate and evaporated to dryness. The product was purified by column chromatography

(hexane:benzene, 9:1) and recrystallised from benzene to give orange crystals (Yield: 1 g, 60%).

^{1}H NMR ($CDCl_3$): δ 4.05 (s, 5H); 4.09 (q, 2H); 4.35 (t, 2H); 7.35 (m, 10H) ppm.

^{31}P{H} NMR ($CDCl_3$): δ -16.18 ppm.

4.3.2 Synthesis of bis(diphenylphosphino) ferrocene Au(I) complexes

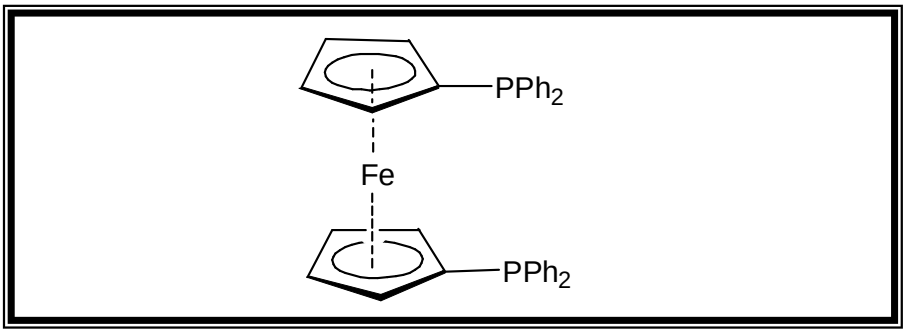

Figure 4.2 Illustration of the 1,1'-bis(diphenylphosphino)ferrocene complexed-ligand.

The synthesis of complexes described in § 4.3.2.1 - 4.3.2.3 was done according to the following procedures[19].

4.3.2.1 [(AuCl)$_2$(μ-dppf)]

A solution of [Au(THT)Cl] (128 mg, 0.4 mmol) in dichloromethane (40 mL) was treated with dppf (110 mg, 0.2 mmol) and the mixture was stirred for 30 minutes. The solvent was concentrated to approximately 10 mL and addition of diethyl ether (30 mL) gave the desired product (184 mg, 90%).

^{1}H NMR ($CDCl_3$): δ 4.27 (m, 4H), 4.71 (m, 4H), 7.47 (m, 20H) ppm.

^{31}P{^{1}H} NMR ($CDCl_3$): δ 28.65 (s) ppm.

The characterisation of the complex is identical to literature[19].

4.3.2.2 [(AuSCN)$_2$(μ-dppf)]

A solution of [(AuCl)$_2$(μ-dppf)] (102 mg, 0.1 mmol) in a mixture of dichloromethane (7.5 mL) and acetone (5 mL) was treated with solid KSCN (19 mg, 0.2 mmol) and the mixture was stirred for 1 hour. The solution was filtered through Celite and the solvent evaporated to 3 mL. The slow addition of diethyl ether (30 mL) gave the desired

product (88 mg, 83%). The compound was recrystallised by slow evaporation of an acetone solution of the prepared complex. The orange crystals were obtained as plates. The compound crystallises in a monoclinic space group *C*2/c with Z = 8. The crystal structure for the compound is discussed in § 4.4.5.

^{1}H NMR ($CDCl_3$): δ 4.37 (m, 4H), 4.71 (m, 4H), 7.47 (m, 20H) ppm.

^{31}P{^{1}H} NMR ($CDCl_3$): δ 32.52 (s) ppm.

The characterisation of the complex is identical to literature[19].

4.3.2.3 [AuCl(μ-dppf)]

To a stirred solution of [Au(THT)Cl] (64 mg, 0.2 mmol) in dichloromethane (20 mL), dppf (110 mg, 0.2 mmol) was added as a solid. The mixture was stirred for 30 minutes and the solution was evaporated to 10 mL. The slow addition of diethyl ether with stirring gave the product as a yellow fine powder (121 mg, 77%). Recrystallisation of the compound was attempted but decomposed in solution. The structure of the compound was anticipated in literature as a three coordinated gold(I) complex[20].

^{1}H NMR ($CDCl_3$): δ 4.27 (m, 4H), 4.71 (m, 4H), 7.47 (m, 20H) ppm.

^{31}P{^{1}H} NMR ($CDCl_3$): δ 28.65 (s, broad) ppm.

4.3.3 Synthesis of gold(I) complexes containing modified bis(diphenylphosphino) ferrocenyl ligands

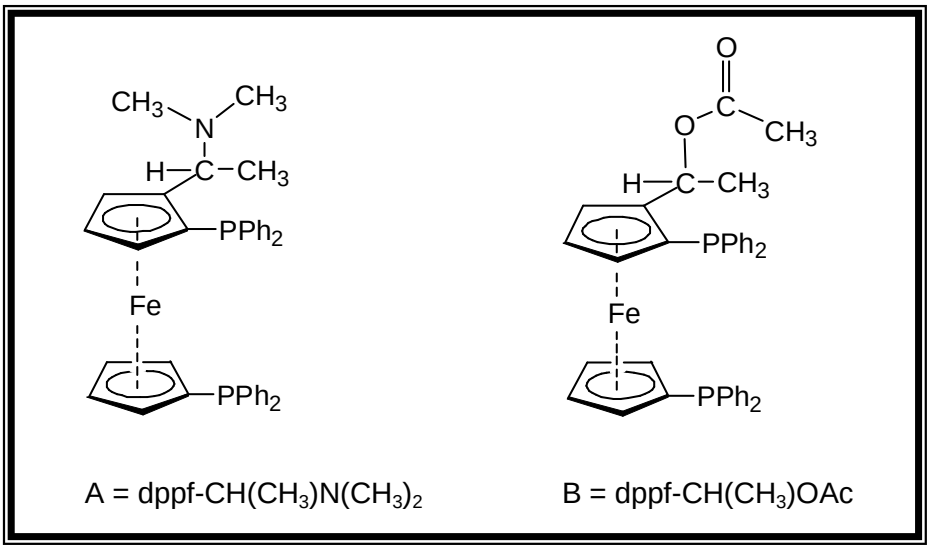

Figure 4.3 Illustration of the (*S*)-*N*,*N*-dimethyl-1-[(*R*)-1',2-bis(diphenylphosphino) ferrocenyl] ethylamine (A) and (*R*)-1-[(*S*)-1',2-bis(diphenylphosphino)ferrocenyl] ethylacetate (B) ligands.

The synthesis of complexes described in § 4.3.3.1 - 4.3.3.6 was done according to the following procedures[19].

4.3.3.1 $[(AuCl)_2(\mu\text{-dppf-CH(CH}_3\text{)N(CH}_3\text{)}_2)]$[21]

A solution of [Au(THT)Cl] (96 mg, 0.3 mmol) in dichloromethane (30 mL) was treated with the racemic mixture of dppf-$CH(CH_3)N(CH_3)_2$ (94 mg, 0.15 mmol) and the mixture was stirred for 30 minutes. The solution was concentrated to approximately 10 mL and addition of diethyl ether (25 mL) gave the desired product (150 mg, 92%). The compound was recrystallised in a dichloromethane/ether solution mixture at 298 K and orange crystals suitable for X-ray studies were isolated. The compound crystallises as a racemate in the monoclinic space group $P2_1/n$. The crystal structure of the compound is discussed in § 4.4.1.

^{1}H NMR ($CDCl_3$): δ 0.81 (d, 3H, CHCH_3), 1.55 (s, 6H, NCH_3), 3.74 - 4.91 (m, 8H), 7.34 - 7.74 (m, 20H, PC_6H_5) ppm.

^{31}P{^{1}H} NMR ($CDCl_3$): δ 26.96 (s), 28.68 (s) ppm.

IR (KBr): ν 692(s), 750(m), 1023(w), 1100(m), 1434(s), 1480(m) cm^{-1}.

4.3.3.2 $[(AuSCN)_2(\mu\text{-dppf-CH(CH}_3\text{)N(CH}_3\text{)}_2)]$[22]

A solution of $[(AuCl)_2(\mu$-dppf-$CH(CH_3)N(CH_3)_2)]$ (50 mg, 0.05 mmol) in a mixture of dichloromethane (4 mL) and acetone (3 mL) was treated with solid KSCN (10 mg, 0.1 mmol) and the mixture was stirred for 1 hour. The solution was filtered through Celite and evaporated to 3 mL. Addition of diethyl ether gave the desired product (30 mg, 58%). The orange and needle-like crystals suitable for X-ray studies were obtained when the compound was recrystallised at ambient temperatures by diffusion of ether in a dichloromethane solution. The compound crystallises in the triclinic space group $P\bar{1}$. The crystal structure of the compound is discussed in § 4.4.2.

^{1}H NMR ($CDCl_3$): δ 0.81 (d, 3H), 1.53 (s, 6H), 3.84 - 4.97 (m, 8H), 7.34 - 7.75 (m, 20H) ppm.

^{31}P{^{1}H} NMR ($CDCl_3$): δ 31.53 (s), 32.94 (s) ppm.

IR (KBr): ν (SCN) 2117(s) cm^{-1}.

4.3.3.3 [AuCl(μ-dppf-CH(CH_3)N(CH_3)$_2$)]

To a stirred solution of [Au(THT)Cl] (16 mg, 0.05 mmol) in dichloromethane (20 mL), dppf-CH(CH_3)N(CH_3)$_2$ (31 mg, 0.05 mmol) was added as a solid. The mixture was stirred for 30 minutes and the solution was evaporated to 3 mL. The slow addition of diethyl ether with stirring gave the product as a yellow fine powder (26 mg, 61%). Recrystallisation of the compound was attempted but decomposed in solution. The structure of the compound was anticipated as a three coordinated gold(I) complex similar to one in literature [20].

^{1}H NMR ($CDCl_3$): δ 0.90 (d, 3H), 1.55 (s, 6H), 3.60 - 4.57 (m, 8H), 7.27 - 7.63 (m, 20H) ppm.

^{31}P{^{1}H} NMR ($CDCl_3$): δ 15.74 (s, broad) ppm.

IR (KBr): *v* 468(m), 515(m), 695(s), 742(m), 1097(m), 1161(w), 1380(m), 1435(m) cm^{-1}.

4.3.3.4 [(AuCl)$_2$(μ-dppf-CH(CH_3)OAc)]

A solution of [Au(THT)Cl] (180 mg, 0.56 mmol) in dichloromethane (56 mL) was treated with the racemic mixture of dppf-CH(CH_3)OAc (180 mg, 0.28 mmol) and the mixture was stirred for 30 minutes. The solution was concentrated to approximately 15 mL and addition of diethyl ether (40 mL) gave the desired product (214 mg, 69%). Orange cuboidal crystals of the title compound were isolated when the compound was dissolved in a mixture of acetone/ether solution and left to evaporate slowly at room temperature. The compound crystallises as a racemate in the orthorhombic space group *P*bca with two molecules in an asymmetric unit. The crystal structure of the compound is discussed in § 4.4.3.

^{1}H NMR ($CDCl_3$): δ 1.08 (s, 3H, COCH_3), 1.53 (s, 3H, CHCH_3), 3.79 - 5.05 (m, 7H, $C_5H_4FeC_5H_3$), 6.38 (m, 1H, C*H*CH_3), 7.35 - 7.65 (m, 20H, C_6H_5) ppm.

^{31}P{^{1}H} NMR ($CDCl_3$): δ 23.15 (s), 28.41 (s) ppm.

IR (KBr): *v* 697(m), 748(m), 1099(m), 1230(s), 1367(w), 1436(s), 1736(s) cm^{-1}.

4.3.3.5 [(AuSCN)$_2$(μ-dppf-CH(CH_3)OAc)]

A solution of [(AuCl)$_2$(μ-dppf-CH(CH_3)OAc)] (102 mg, 0.1 mmol) in a mixture of dichloromethane (7.5 mL) and acetone was treated with solid KSCN (19.4 mg, 0.2 mmol) and the mixture was stirred for 1 hour. The solution was filtered through Celite and evaporated to 3 mL. Addition of diethyl ether (30 mL) gave the desired product (92

mg, 80%). Suitable crystals for X-ray studies were isolated when the compound was dissolved in a mixture of dichloromethane/ether solution and left to evaporate slowly at room temperature. The orange crystals were observed to have a needle-like morphology. The compound crystallises in the triclinic space group $P\bar{1}$ and the crystal structure of the compound is discussed in § 4.4.4.

^{1}H NMR ($CDCl_3$): δ 1.04 (s, 3H), 1.54 (s, 3H), 3.87 - 5.14 (m, 7H), 6.49 (m, 1H), 7.32 - 7.65 (m, 20H) ppm.

$^{31}P\{^{1}H\}$ NMR ($CDCl_3$): δ 27.17 (s), 32.58 (s) ppm.

IR (KBr): ν (SCN) 2119 cm^{-1}.

4.3.3.6 [AuCl(μ-dppf-CH(CH_3)OAc)]

To a stirred solution of [Au(THT)Cl] (32 mg, 0.1 mmol) in dichloromethane (10 mL), dppf-CH(CH_3)OAc (64 mg, 0.1 mmol) was added as a solid. The mixture was stirred for 30 minutes and the solution was evaporated to 5 mL. The slow addition of diethyl ether with stirring gave the product as a yellow fine powder (57 mg, 65%). Recrystallisation of the compound was attempted but decomposed in solution. The structure of the compound was anticipated as a three coordinated gold(I) complex similar to one in literature [20].

$^{31}P\{^{1}H\}$ NMR ($CDCl_3$): δ 28.14 (s, broad) ppm.

4.3.4 Synthesis of the diphenylferrocenylphosphine gold(I) complex

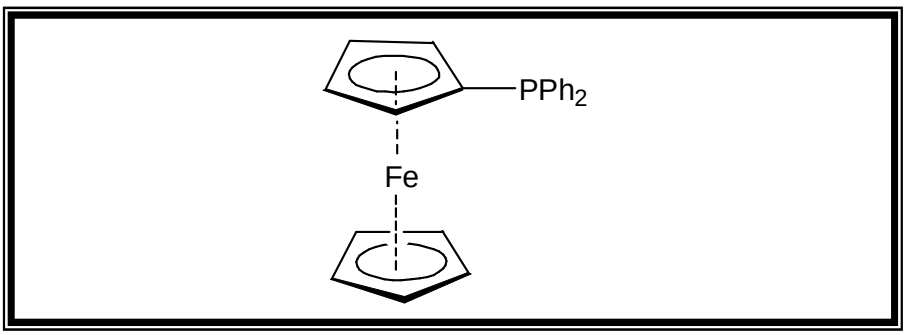

Figure 4.4 Illustration of the diphenylphosphino ferrocene complexed-ligand (PPh_2Fc, § 4.3.1.4).

4.3.4.1 [Au(PPh_2Fc)Cl]

To a stirred solution of [Au(THT)Cl] (87 mg, 0.27 mmol) in dichloromethane (20 mL), the PPh_2Fc ligand (100 mg, 0.27 mmol) was added as a solid. The mixture was stirred

for 45 min. The solution was concentrated to smaller volumes and addition of diethyl ether (25 mL) gave the desired product (97 mg, 60%). Recrystallisation of the compound was attempted and crystals obtained were not suitable for X-ray data collection.

^{1}H NMR ($CDCl_3$): δ 4.18 (s, 5H); 4.34 (s, 2H); 4.56 (s, 2H); 7.4 (m, 10H) ppm.

$^{31}P\{^{1}H\}$ NMR ($CDCl_3$): δ 28.42 (s) ppm.

4.4 X-RAY STRUCTURE DETERMINATIONS OF FERROCENE-TYPE DINUCLEAR GOLD(I) COMPLEXES

X-ray crystal structures for the following compounds: [$(AuSCN)_2$(μ-dppf)], [$(AuCl)_2$(μ-dppf-$CH(CH_3)N(CH_3)_2$)], [$(AuSCN)_2$(μ-dppf-$CH(CH_3)N(CH_3)_2$)], [$(AuCl)_2$(μ-dppf-$CH(CH_3)OAc$)] and [$(AuSCN)_2$(μ-dppf-$CH(CH_3)OAc$)] are discussed. The preparation and characterisation of these complexes were discussed previously in § 4.3.2.2, 4.3.3.1, 4.3.3.2, 4.3.3.4 and 4.3.3.5 respectively.

The crystals of the [$(AuCl)_2$(μ-dppf-$CH(CH_3)N(CH_3)_2$)], [$(AuSCN)_2$(μ-dppf-$CH(CH_3)N(CH_3)_2$)] and [$(AuSCN)_2$(μ-dppf-$CH(CH_3)OAc$)] complexes were mounted on a glass fibre and the X-ray intensity data were collected on a Bruker SMART CCD diffractometer at ambient temperature (293 K) while for the [$(AuCl)_2$(μ-dppf-$CH(CH_3)OAc$)] and [$(AuSCN)_2$(μ-dppf)] compounds, on a Bruker X8 Apex II 4K CCD area detector system at 100(2) K using an Oxford 700 series cryostream cooler. The diffractometer area detector systems were equipped with a graphite monochromator and Mo Kα fine-focus sealed tube (λ = 0.71073 Å). Individual frames were collected using the *phi* and/or *omega* scan technique and the first 50 frames were collected after completion to check for decay of which none was observed. The frames were integrated using a narrow-frame integration algorithm and reduced with the Bruker SAINT-Plus[23] and XPREP[23] software packages respectively. Data were corrected for absorption effects using the multi-scan technique SADABS[24].

All structures were solved by the heavy atom method and by means of conventional Patterson and Fourier methods and were refined through full matrix least-squares approximations using the SHELXS-97[25] and SHELXL-97[26] programs with F^2 being minimised. All non-hydrogen atoms were refined with anisotropic displacement parameters, while the hydrogen atoms were constrained to parent sites, using a riding

model. The positions of the hydrogen atoms were calculated as riding on the adjacent carbon atoms with bond distances: methylene C-H as 0.98 Å, methyl C-H = 0.96 Å and aromatic C-H = 0.93 Å.

The diagrams of the molecular structures obtained after refinement were drawn using DIAMOND software package[27].

Table 4.1 Crystallographic data and refinement parameters for $[(AuX)_2(\mu\text{-dppf-CH(CH}_3\text{)N(CH}_3\text{)}_2)]$, $[(AuX)_2(\mu\text{-dppf-CH(CH}_3\text{)OAc})]$ (X = Cl, SCN) and $[(AuSCN)_2(\mu\text{-dppf})]$ complexes.

Compound	$[(AuCl)_2(\mu$-dppf-RNR')$]$[a]	$[(AuSCN)_2(\mu$-dppf-RNR')$]$[a]	$[(AuCl)_2(\mu$-dppf-ROAc)$]$[a]	$[(AuSCN)_2(\mu$-dppf-ROAc)$]$[a]	$[(AuSCN)_2(\mu$-dppf)]
Empirical formula	$C_{38}H_{37}Au_2FeNP_2Cl_2$	$C_{40}H_{37}Au_2FeN_3P_2S_2$	$C_{38}H_{34}Au_2Cl_2FeO_2P_2$	$C_{40}H_{34}Au_2S_2N_2FeO_2P_2$	$C_{36}H_{28}Au_2FeN_2P_2S_2$
Formula weight	1090.31	1135.57	1105.28	1150.53	1064.45
Temperature (K)	293(2)	293(2)	100(2)	293(2)	100(2)
Wavelength (Å)	0.71073	0.71073	0.71073	0.71073	0.71073
Crystal system	Monoclinic	Triclinic	Orthorhombic	Triclinic	Monoclinic
Space group	$P\ 2_1/n$	$P\ \bar{1}$	P bca	$P\ \bar{1}$	$C\ 2/c$
a (Å) b (Å) c (Å)	17.136(3) 10.946(2) 20.658(4)	9.021(5) 13.397(5) 16.684(5)	16.3614(3) 21.6630(4) 40.2586(7)	8.7916(12) 13.3581(18) 17.190(2)	16.958(4) 19.079(4) 21.622(5)
α(°) β(°) γ(°)	90 108.39(3) 90	89.956(5) 82.946(5) 74.740(5)	90 90 90	86.292(3) 85.718(2) 75.494(3)	90 108.422(6) 90
Volume (Å^3)	3676.7(13)	1929.5(14)	14269.1(4)	1946.7(4)	6637(3)
Z	4	2	16	2	8
D_c (g.cm^{-3})	1.970	1.955	2.058	1.963	2.130
μ (mm^{-1})	8.610	8.180	8.879	8.112	9.503
F(000)	2080	1088	8416	1100	4032
Crystal size	0.03, 0.05, 0.17	0.08, 0.14, 0.37	0.12, 0.17, 0.31	0.12, 0.12, 0.42	0.07, 0.27, 0.30
θ range (°)	2.08 to 26.99	1.23 to 25.00	1.64 to 28.34	1.19 to 25.00	2.13 to 28.26
Limiting indices	$21 \le h \le 18$ $-13 \le k \le 13$ $-26 \le l \le 26$	$-10 \le h \le 10$ $-15 \le k \le 9$ $-18 \le l \le 19$	$-19 \le h \le 21$ $-28 \le k \le 24$ $-53 \le l \le 53$	$-10 \le h \le 10$ $-11 \le k \le 15$ $-20 \le l \le 20$	$-22 \le h \le 22$ $-25 \le k \le 24$ $-28 \le l \le 28$
Reflections collected / unique	30273 / 8020 [R_{int} = 0.0975]	10576 / 6743 [R_{int} = 0.1027]	58079 / 17721 [R_{int} = 0.0593]	10668 / 6810 [R_{int} = 0.1104]	39743 / 8199 [R_{int} = 0.0394]
Completeness to θ(°, %)	26.99, 100.0	25.00, 99.3	28.34, 99.6	25.00, 99.2	28.26, 99.8
T_{max} and T_{min}	0.772 and 0.600	0.519 and 0.260	0.343 and 0.180	0.376 and 0.322	0.507 and 0.073
Refinement method	Full-matrix least-squares on F^2	Full-matrix least-squares on F^2	Full-matrix least-squares on F^2	Full-matrix least-squares on F^2	Full-matrix least-squares on F^2
Data / restraints / parameters	8020 / 0 / 415	6743 / 0 / 421	17721 / 0 / 819	6810 / 0 / 462	8199 / 0 / 407
Goodness-of-fit on F^2	0.992	1.010	1.034	0.963	1.027
Final R indices [I>2σ(I)]	$R1$ = 0.0494, $wR2$ = 0.0887	$R1$ = 0.0576, $wR2$ = 0.1473	$R1$ = 0.0409, $wR2$ = 0.0813	$R1$ = 0.0436, $wR2$ = 0.0997	$R1$ = 0.0236, $wR2$ = 0.0495
R indices (all data)	$R1$ = 0.1202, $wR2$ = 0.1088	$R1$ = 0.0689, $wR2$ = 0.1578	$R1$ = 0.0652, $wR2$ = 0.0890	$R1$ = 0.0572, $wR2$ = 0.1059	$R1$ = 0.0320, $wR2$ = 0.0524
ρ_{max} and ρ_{min} (e.Å^{-3})	2.095 and -1.149	3.113 and -3.234	6.522 and -1.660	2.000 and -2.110	2.362 and -1.199

$R = [(\Sigma\Delta F)/(\Sigma\Delta F_0)]$

$wR = \Sigma[w(F_0^2 - F_c^2)^2]/\Sigma[w(F_0^2)^2]^{1/2}$

a) R = -CH(CH$_3$), R' = -(CH$_3$)$_2$

4.4.1 Crystal structure of $[(AuCl)_2(\mu\text{-dppf-CH(CH}_3\text{)N(CH}_3\text{)}_2)]$

The preparation and characterisation of the title compound was outlined earlier in § 4.3.3.1. The general crystal data and refinement parameters of the $[(AuCl)_2(\mu\text{-dppf-CH(CH}_3\text{)N(CH}_3\text{)}_2)]$ compound are presented in Table 4.1 while the supplementary material containing the complete lists of atomic coordinates, bond distances and angles, anisotropic displacement parameters as well as hydrogen coordinates is given in the Appendix, § B.1.

The molecular diagram of the compound is indicated in Fig. 4.5.

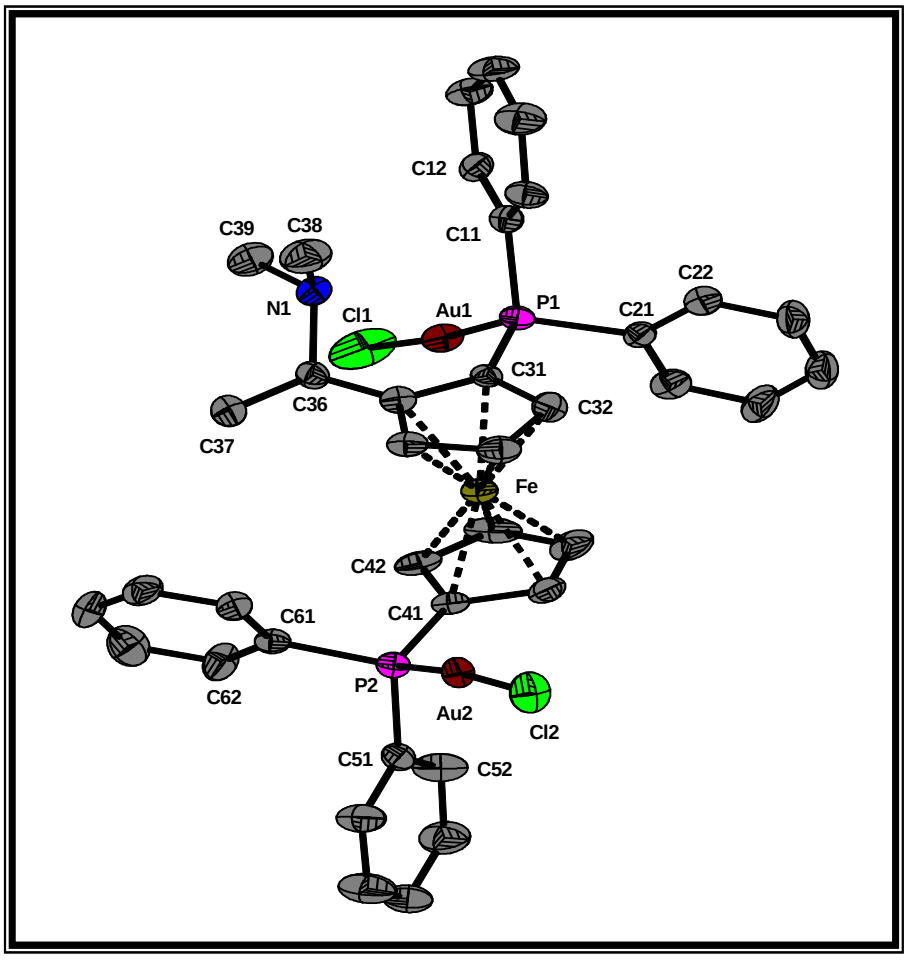

Figure 4.5 Molecular drawing of (*S*,*R*)-$[(AuCl)_2(\mu\text{-dppf-CH(CH}_3\text{)N(CH}_3\text{)}_2)]$, showing the numbering scheme and thermal displacement ellipsoids (30% probability). In the numbering scheme the first digit refers to the number of the ring and the second one to the number of the atom in the ring. Hydrogen atoms are omitted for clarity.

The structure of the [$(AuCl)_2$(μ-dppf-$CH(CH_3)N(CH_3)_2$)] complex displays a pseudo-linear two-coordinate geometry usually observed in gold(I) complexes. The bis(diphenylphosphino)ferrocenyl ligand links the gold metal centres in a bidentate fashion via the ferrocene group. The compound is a Au(I) complex comprising a dimethyl [bis(diphenylphosphino)ferrocenyl] ethylamine ligand bearing phosphorus and nitrogen coordination sites. As gold is a soft metal, it preferentially bonds to the P atom, the soft coordination site in the ferrocenyl ligand. Since there are two of these sites in the complex, gold bonds to each site, leading to a dinuclear gold system. The coordination mode of the bis(diphenylphosphine) moiety is of a trans open-bridged fashion, with the P(1)-Au(1)-Au(2)-P(2) torsion angle = 178.8(9)°. The angles between the approximate linear gold moieties and the corresponding Cp planes are 57.7(2) and 70.8(3)° for the P(1)-Cl(1)/Ring 3 and P(2)-Cl(2)/Ring 4 systems, respectively. The angle involving the two P atoms in the system (P-Fe-P) is 165.97(7)° and the cyclopentadienyl rings are partially eclipsed anticlinal relative to each other. The phenyl groups in the system are twisted approximately perpendicular to each other, with a $(C_{ar}\text{-}P\text{-}C_{ar})_{av}$ of 104.6(4)°. The average Fe-C bond distance is 2.047(8) Å and there are no Au…Au contacts observed within the molecule.

Table 4.2 Selected bond lengths and angles for [$(AuCl)_2$(μ-dppf-$CH(CH_3)N(CH_3)_2$)].

Bond lengths (Å)		Bond angles (°)	
Au(1)-P(1)	2.237(2)	P(1)-Au(1)-Cl(1)	175.41(10)
Au(2)-P(2)	2.224(2)	P(2)-Au(2)-Cl(2)	174.01(10)
Au(1)-Cl(1)	2.271(3)	C(11)-P(1)-Au(1)	110.3(3)
Au(2)-Cl(2)	2.278(2)	C(21)-P(1)-Au(1)	112.5(3)
P(1)-C(11)	1.825(9)	C(31)-P(1)-Au(1)	117.1(3)
P(1)-C(21)	1.839(9)	Cl(1)-Au(1)-Au(2)-Cl(2)	175.5(1)
P(1)-C(31)	1.810(9)	C(31)-Centr-Centr-C(41)[a]	-159.4(5)
P(2)-C(41)	1.781(9)		
P(2)-C(51)	1.826(9)		
P(2)-C(61)	1.828(9)		

[a] Centr = Centroid defined by C(31) - C(35) and C(41) - C(45).

Selected bond distances and angles of choice are listed in Table 4.2 and the supplementary material containing the complete lists of atomic coordinates, bond distances and angles, anisotropic displacement parameters as well as hydrogen coordinates is given in the Appendix, § B.1. The coordination around the gold atoms is pseudo-linear with P(1)-Au(1)-Cl(1) = 175.41(10)° and P(2)-Au(2)-Cl(2) = 174.01(10)°. The Au-P bond distances are 2.237(2) and 2.224(2) Å and the Au-Cl distances are 2.271(3) and 2.278(2) Å. The Au-P and Au-Cl bond distances are within the normal

range for (diphenylphosphino)ferrocenyl complexes found in the literature. The average P-C bond distance for the phenyl groups is 1.829(9) Å whereas the average P-C distance for the cyclopentadienyl rings is 1.795(9) Å. The latter P-C distances for the cyclopentadienyls are shorter and this may be due to the arrangement of the phenyl rings in order to minimise steric hindrance. The C(21)-P(1)-Au(1) and C(31)-P(1)-Au(1) bond angles are 112.5(3) and 117.1(3)° respectively as compared to C(31)-P(1)-Au(1) = 117.1(3)° suggesting that gold atom is orientated more closer to the phenyl rings than to the ferrocene. The Cl(1)-Au(1)-Au(2)-Cl(2) torsion angle of 175.5(1)° suggests that the gold moieties are linear relative to each other. Comparison of the parameters of this structure with other similar structures found in literature is made in § 4.5.

The partial packing of the molecules in the unit cell showing observed hydrogen bonding is illustrated in Fig. 4.6. It is clear that the Fe atom of the title compound in the asymmetric unit refined lies very close to the c-axis.

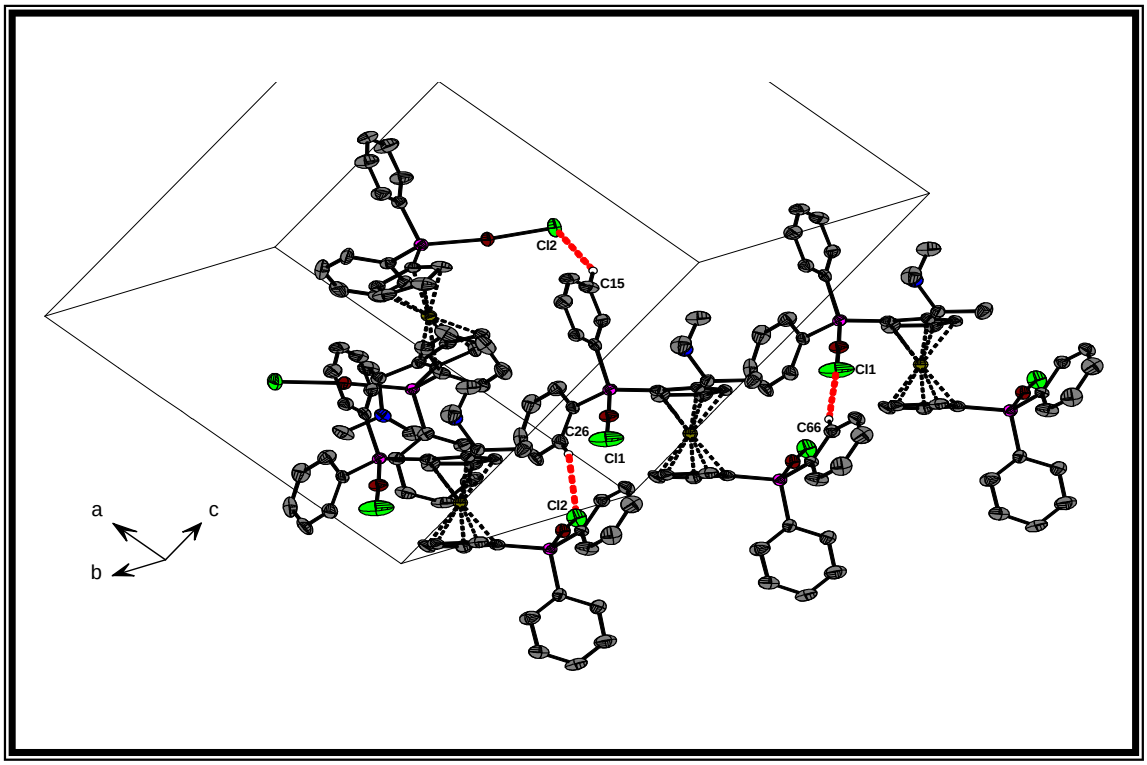

Figure 4.6 Partial packing diagram of $[(AuCl)_2(\mu\text{-dppf-CH}(CH_3)N(CH_3)_2)]$ showing hydrogen bonding. Hydrogen atoms except those involved in hydrogen bonding are omitted for clarity. Hydrogen bonding interactions are indicated by red dashed lines.

The molecule was also investigated for possible π-π interactions, but did not show any significant effects. However, weak intermolecular C-H...Cl hydrogen bonding of 2.529 Å, 143.0° is observed between C(66)-H(66)...Cl(1) atoms with the symmetry code (x,y-

1,z) and furthermore very weak hydrogen interactions for C(15)-H(15)...Cl(2) (-x+1/2,y+1/2,-z+1/2) and C(26)-H(26)...Cl(2) (x,y+1,z) of 2.834 Å, 151.9° and 2.847 Å, 158.7° respectively are observed.

4.4.2 Crystal structure of [(AuSCN)$_2$(μ-dppf-CH(CH$_3$)N(CH$_3$)$_2$)]

The preparation and characterisation of the title compound was outlined earlier in § 4.3.3.2. The general crystal data and refinement parameters of the [(AuSCN)$_2$(μ-dppf-CH(CH$_3$)N(CH$_3$)$_2$)] compound are presented in Table 4.1 while the supplementary material containing the complete lists of atomic coordinates, bond distances and angles, anisotropic displacement parameters as well as hydrogen coordinates is given in the Appendix, § B.2.

The coordination geometry around the gold is pseudo-linear as illustrated in Fig. 4.7, which is usually observed for gold(I) complexes and this linearity of the gold moieties show a slight deviation from the ideal 180°. Among the principal motivations for the structure determination was to establish whether, if any substitution of the chloride ions in the [(AuCl)$_2$(μ-dppf-CH(CH$_3$)N(CH$_3$)$_2$)] complex by the thiocyanate ligand occurs, the bonding mode of the ligand would be through the nitrogen or the sulphur donor atom. However, as expected for the soft Au(I) centre, coordination is *via* the sulphur atom of the SCN$^-$.

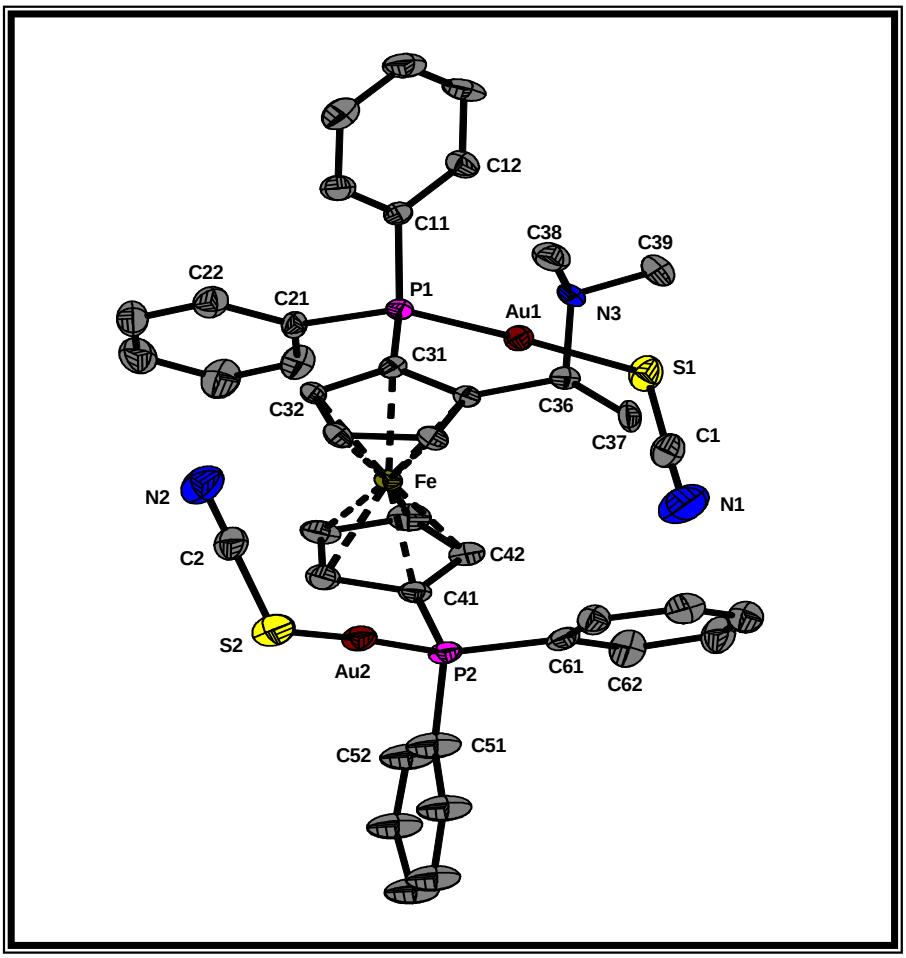

Figure 4.7 Molecular drawing of (*S*,*R*)-[(AuSCN)$_2$(μ-dppf-CH(CH$_3$)N(CH$_3$)$_2$)], showing the numbering scheme and thermal displacement ellipsoids (30% probability). In the numbering scheme the first digit refers to the number of the ring and the second one to the number of the atom in the ring. Hydrogen atoms are omitted for clarity.

The cyclopentadienyl rings do not deviate significantly from being planar and are partially eclipsed anticlinal relative to each other. The Cp planes are approximately parallel with the dihedral angle of 0.9(3)° between the two planes. The distances of the iron atom from the cyclopentadienyl rings planes are 1.652(1) and 1.646(1) Å. The dihedral angles between the planes of the phenyl rings defined by C1 and C2 atoms and C5 and C6 atoms are 58.07(34) and 86.79(45)° respectively.

Principal bond lengths and angles are given in Table 4.3 while the supplementary material containing the complete lists of atomic coordinates, bond distances and angles, anisotropic displacement parameters as well as hydrogen coordinates is given in the Appendix, § B.2. Both phenyl rings coordinated to Au(1) or Au(2) moieties are orthogonal relative to each other as defined by C(11)-P(1)-C(21) and C(51)-P(2)-C(61) bond angles of 107.1(4) and 106.7(6)° respectively.

Table 4.3 Selected bond lengths and angles for [$(AuSCN)_2$(μ-dppf-$CH(CH_3)N(CH_3)_2$)].

Bond lengths (Å)		Bond angles (°)	
Au(1)-P(1)	2.265(2)	P(1)-Au(1)-S(1)	175.61(9)
Au(2)-P(2)	2.260(3)	P(2)-Au(2)-S(2)	176.86(9)
Au(1)-S(1)	2.327(3)	N(1)-C(1)-S(1)	178.7(13)
Au(2)-S(2)	2.313(3)	N(2)-C(2)-S(2)	174.5(12)
S(1)-C(1)	1.678(15)	C(1)-S(1)-Au(1)	95.9(4)
S(2)-C(2)	1.673(12)	C(2)-S(2)-Au(2)	103.1(4)
N(1)-C(1)	1.158(18)	C(11)-P(1)-C(21)	107.1(4)
N(2)-C(2)	1.133(16)	C(61)-P(2)-C(51)	106.7(6)
P(1)-C(11)	1.813(9)	C(11)-P(1)-Au(1)	114.4(3)
P(1)-C(21)	1.831(9)	C(21)-P(1)-Au(1)	110.6(3)
P(1)-C(31)	1.799(9)	C(31)-P(1)-Au(1)	112.7(3)
P(2)-C(41)	1.769(10)	C(41)-P(2)-Au(2)	113.4(3)
P(2)-C(51)	1.816(12)	C(51)-P(2)-Au(2)	112.0(5)
P(2)-C(61)	1.803(10)	C(61)-P(2)-Au(2)	113.2(3)
		S(1)-Au(1)-Au(2)-S(2)	158.4(1)
		N(1)-S(1)-P(1)-C(31)	10.0(4)
		N(2)-S(2)-P(2)-C(41)	-24.8(4)

The average Au-P and Au-S bond distances are 2.263(3) and 2.320(3) Å respectively. The Au-P bond distances of the complex are slightly longer with a difference of 0.03 Å and the Au-S distances are approximately 0.1 Å longer than found in the chloro analogue, [$(AuCl)_2$(μ-dppf-$CH(CH_3)N(CH_3)_2$)]. This may be due to the difference of the *trans* influence of the SCN as compared to the Cl. The average P-C bond distance of the phenyl rings is 1.816(10) Å whereas the distances of the cyclopentadienyl rings average at 1.784(10) Å. The P-Au-S bond angles are approximately linear at 175.61(9) and 176.86(9)° and the average N-C-S angle = 176.6(13)°. The Au-S-C bond angles approximately form a 90° angle to the P-Au-S axis at 95.9(4) and 103.9(4)°. The phenyl rings are nearly orthogonal to each other with C-P-C angles = 107.1(4) and 106.7(6)°. The Fe-C distances lie in the range 2.023(9) - 2.060(9) Å. The S(1)-Au(1)-Au(2)-S(2) torsion angle of 158.4(1)° suggests that the gold moieties are not so linear relative to each other. The N(1)-S(1)-P(1)-C(31), N(2)-S(2)-P(2)-C(41) torsion angles of 10.0(4) and -24.8(4)° respectively indicate how the SCN is rotated relative to the ferrocene. Further comparison of the parameters of this structure with other similar structures found in literature is made in § 4.5.

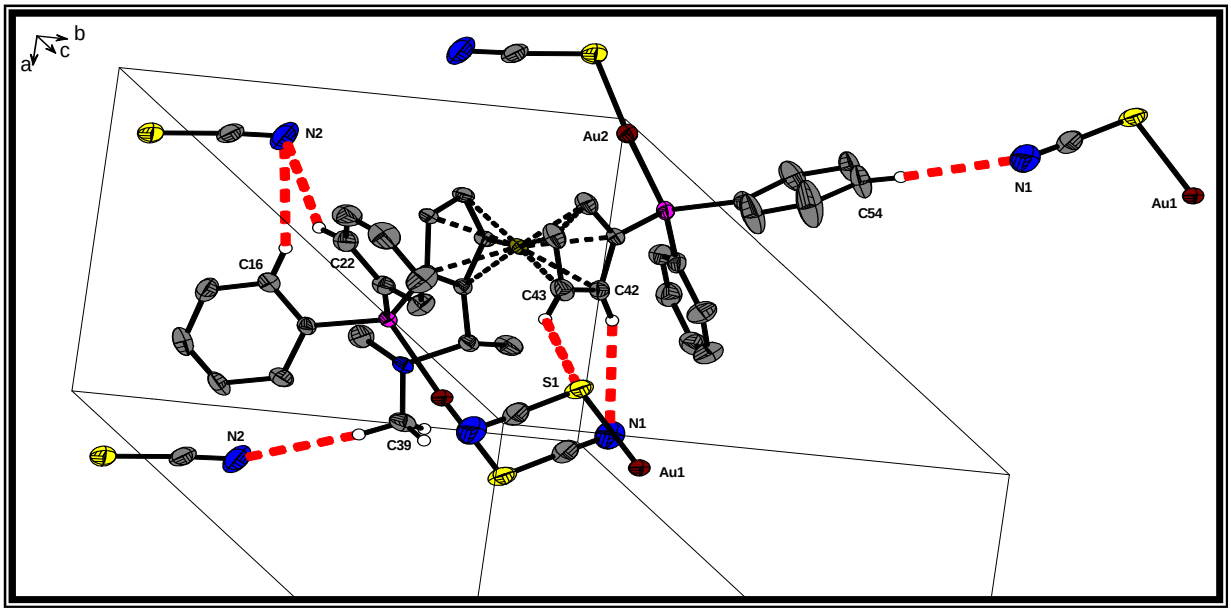

Figure 4.8 Partial packing diagram of [(AuSCN)$_2$(μ-dppf-CH(CH$_3$)N(CH$_3$)$_2$)] showing hydrogen bonds. Hydrogen atoms except those involved in hydrogen interactions are omitted for clarity. Hydrogen bonding interactions are indicated by red dashed lines between atom pairs.

The molecular partial packing diagram of the compound is shown in Fig. 4.8 showing hydrogen bond interactions. The molecule was investigated for π-π interactions but did not indicate any significant effects. A strong intermolecular hydrogen bonding is observed between the atom pair (C54, N1) (1-x,2-y,1-z) with the bond distance and angle of 3.501(18) Å and 160.0° respectively. There are no unusually short intermolecular contacts. Weak intra- and intermolecular hydrogen bonding is observed between the following atom pairs (C42, N1) (x,y,z); (C22, N2) (-x,-y+1,-z); (C16, N2) (-x,-y+1,-z); (C39, N2) (-x+1,-y+1,-z); (C43, S1) (-x+1,-y+1,-z+1) and (C54, N1) (-x,-y+2,-z+1) in the order of 2.858(1) Å, 146.2(4)°; 2.959(1) Å, 147.1(2)°; 2.829(1) Å, 157.1(4)°; 2.858(1) Å, 159.4(3)°; 2.977(1) Å, 137.8(2)° and 2.632(1) Å, 159.0(2)° respectively and as indicated in Fig. 4.8.

4.4.3 Crystal structure of [(AuCl)$_2$(μ-dppf-CH(CH$_3$)OAc)]

The preparation and characterisation of the title compound was outlined earlier in § 4.3.3.4. The general crystal data and refinement parameters of the [(AuCl)$_2$(μ-dppf-CH(CH$_3$)OAc)] complexes are listed in Table 4.1 while the supplementary material containing the complete lists of atomic coordinates, bond distances and angles, anisotropic displacement parameters as well as hydrogen coordinates is given in the

Appendix, § B.3. In Table 4.1, it is observed that in refinement of data for the [$(AuCl)_2$(μ-dppf-$CH(CH_3)OAc$)] compound, the minimum and maximum residual electron densities are located within 0.46 Å of the atom Au(22) and 0.68 Å of the atom C(261), indicating no physical meaning. There are two crystallographically independent molecules in the structure of the title compound [$(AuCl)_2$(μ-dppf-$CH(CH_3)OAc$)] as shown in Fig. 4.9.

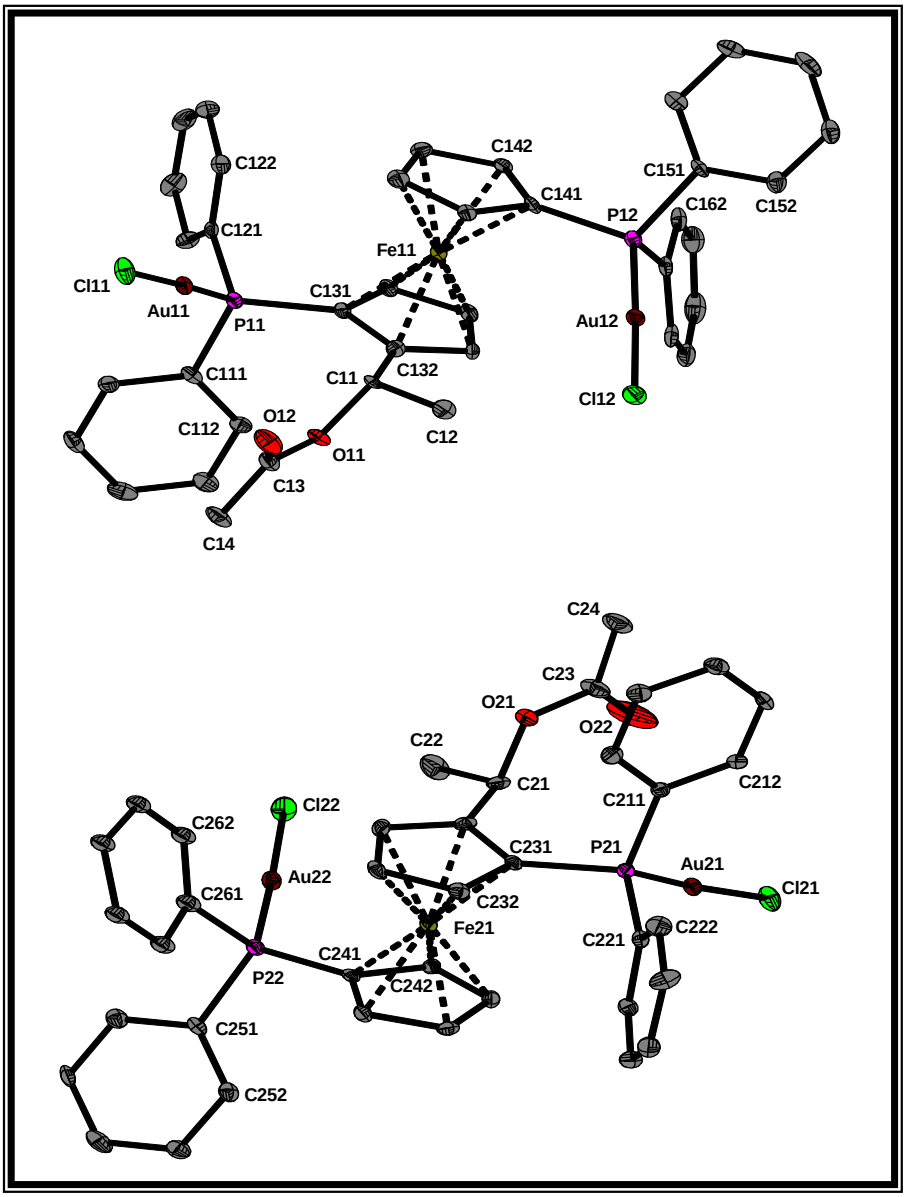

Figure 4.9 Molecular drawing of (*R*,*S*)-[$(AuCl)_2$(μ-dppf-$CH(CH_3)OAc$)], showing the numbering scheme of molecule 1 and 2 and thermal displacement ellipsoids (30% probability). In the numbering scheme the first digit refers to the number of the molecule, the second one to the number of the ring and the third digit to the number of the atom in the ring. Hydrogen atoms are omitted for clarity.

The two molecules in Fig. 4.9 occupy general positions within the cell and are approximately similar in structure. The geometry about each independent gold atom is linear, two-coordinate and with slight deviations from 180° at each gold atom.

The cyclopentadienyl rings are approximately eclipsed relatively to each other in both molecules, more in molecule 2 with C(234)-Centr-Centr-C(241) torsion angle = -9.3(4)° and C(144)-Centr-Centr-C(131) = 16.9(4)° for molecule 1. The Cp rings are also non-parallel with dihedral angles of 1.7(2) and 3.9(2)° for molecule 1 and 2 respectively. The phenyl rings on each set of the gold moieties are nearly perpendicular to each other with average C-P-C bond angle = 104.9(3)°.

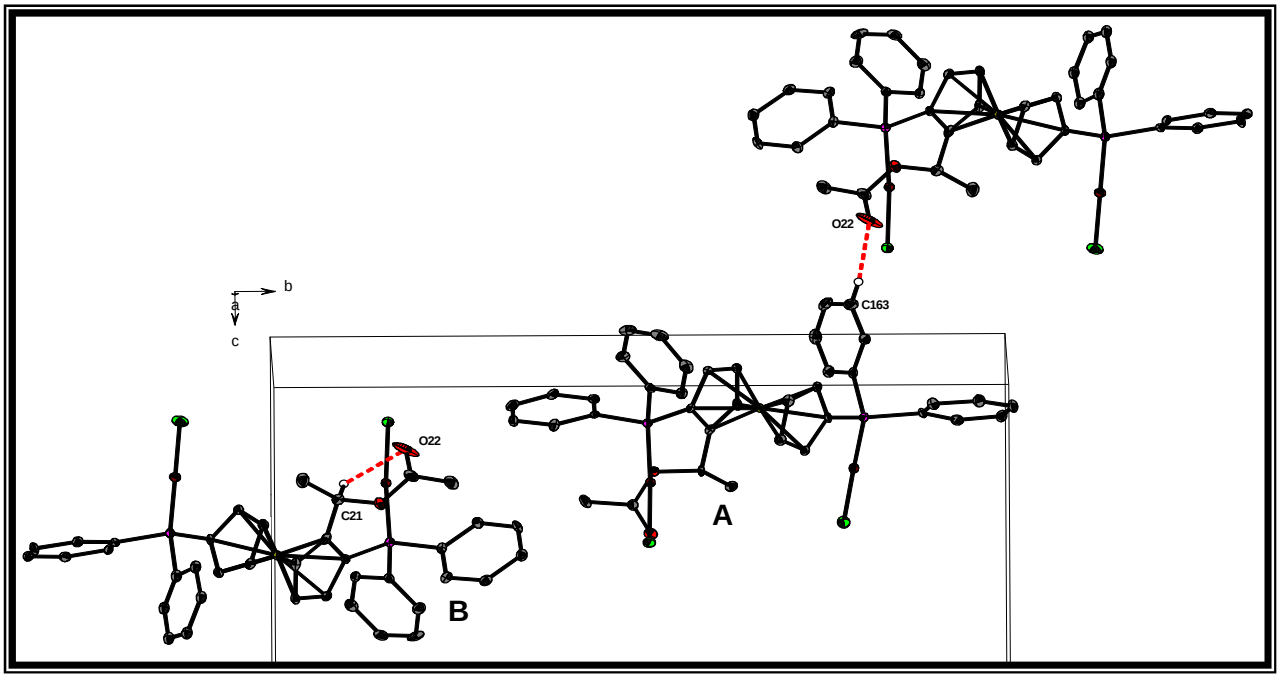

Figure 4.10 Partial packing diagram showing the packing of the [$(AuCl)_2$(μ-dppf-$CH(CH_3)OAc$)] compound along the a axis. Hydrogen atoms except those involved in hydrogen interactions are omitted for clarity. Hydrogen bonding interactions are indicated by red dashed lines between atom pairs.

The molecular partial packing diagram of the compound is given in Fig. 4.10 showing hydrogen bond interactions. A strong intramolecular hydrogen bonding is observed between the atom pair (C21, O22) with the bond distance and angle of 2.32 Å and 100° respectively and a strong intermolecular hydrogen bonding is observed between the atom pair (C163, O22) (-x,1-y,-z) with the bond distance and angle of 2.35 Å and 131° respectively. The torsion angles calculated for the structure are given in Table 4.4. The values for the Cl(n1)-Au(n1)-Au(n2)-Cl(n2) angle in molecule 1 and 2 are 47.97(6) and -43.97(7)° respectively while for the Au(n1)-Centr-Centr-Au(n2) dihedral angle the

values are -105.5(5) and 112.3(5)° for molecule 1 and 2 respectively. There are no major differences observed between the two molecules, except the difference is noted in the relative twist of the two molecules.

Table 4.4 Selected bond lengths and angles for molecule 1 of the [$(AuCl)_2$(μ-dppf-$CH(CH_3)OAc$)] compound, n = number of molecule.

Bond lengths (Å)			Bond angles (°)		
	Molecule 1	Molecule 2		Molecule 1	Molecule 2
Au(n1)-P(n1)	2.2312(16)	2.2943(16)	P(n1)-Au(n1)-Cl(n1)	176.66(6)	175.62(6)
Au(n2)-P(n2)	2.2217(17)	2.2324(17)	P(n2)-Au(n2)-Cl(n2)	177.34(7)	177.55(7)
Au(n1)-Cl(n1)	2.2872(16)	2.2330(16)	C(n11)-P(n1)-C(n21)	106.0(3)	108.0(3)
Au(n2)-Cl(n2)	2.2840(17)	2.2831(17)	C(n61)-P(n2)-C(n51)	104.0(3)	101.9(3)
P(n1)-C(n11)	1.817(6)	1.824(6)	C(n11)-P(n1)-Au(n1)	110.9(2)	109.3(2)
P(n1)-C(n21)	1.831(7)	1.817(7)	C(n21)-P(n1)-Au(n1)	112.9(2)	114.5(2)
P(n1)-C(n31)	1.802(6)	1.815(6)	C(n31)-P(n1)-Au(n1)	117.9(2)	118.5(2)
P(n2)-C(n41)	1.812(7)	1.792(6)	C(n41)-P(n2)-Au(n2)	112.3(2)	114.0(2)
P(n2)-C(n51)	1.824(6)	1.817(6)	C(n51)-P(n2)-Au(n2)	112.2(2)	113.9(2)
P(n2)-C(n61)	1.794(7)	1.965(8)	C(n61)-P(n2)-Au(n2)	115.4(2)	112.8(2)
			Cl(n1)-Au(n1)-Au(n2)-Cl(n2)	47.97(6)	-43.97(7)
			Au(n1)-Centr-Centr-Au(n2)	-105.5(5)	112.3(5)
			C(n31)-Centr-Centr-C(n41)[a]	161.1(4)	-153.7(4)

[a] Centr = Centroid defined by C(n31) - C(n35) and C(n41) - C(n45).

Selected bond lengths and angles of choice for molecule 1 and molecule 2 of the [$(AuCl)_2$(μ-dppf-$CH(CH_3)OAc$)] complex are given in Table 4.4. It is noted that for molecule 2, similar parameters are observed as in molecule 1 of the complex. Hence, the following discussion of parameters is for solely molecule 1. The Au-P bond distances are observed to be 2.2312(16) and 2.2217(17) Å whilst the Au-Cl bonds are = 2.2872(16) and 2.2840(17) Å and are longer than the Au-P distances. The P-C distances are within the normal range for the ferrocenyl complexes with average values of 1.817(7) Å for the phenyl and 1.807(7) Å for the cyclopentadienyl rings. The average for the Fe-C distances is 2.048(6) Å for both molecule 1 and 2. There is no short Fe…Au interaction, with the shortest such distance being 4.4276(9) Å and also there are no Au…Au interactions that are observed. The P-Au-Cl bond angles are 176.66(6) and 177.34(7)° and they nearly show an approximate linear geometry of the gold moieties. The C-C-C angles in the cyclopentadienyl rings (sp^2 hybridisation) are all normal and range from 107.0(5) to 109.3(6)°. The C-P-Au bond angles range from 110.9(2) to 117.9(2)°. Comparison of the parameters of this structure with other similar structures found in literature is made in § 4.5.

4.4.4 Crystal structure of [(AuSCN)$_2$(μ-dppf-CH(CH$_3$)OAc)]

The preparation and characterisation of the title compound was outlined earlier in § 4.3.3.5. The general crystal data and refinement parameters of the [(AuSCN)$_2$(μ-dppf-CH(CH$_3$)OAc)] complex are listed in Table 4.1 while the supplementary material containing the complete lists of atomic coordinates, bond distances and angles, anisotropic displacement parameters as well as hydrogen coordinates is given in the Appendix, § B.4.

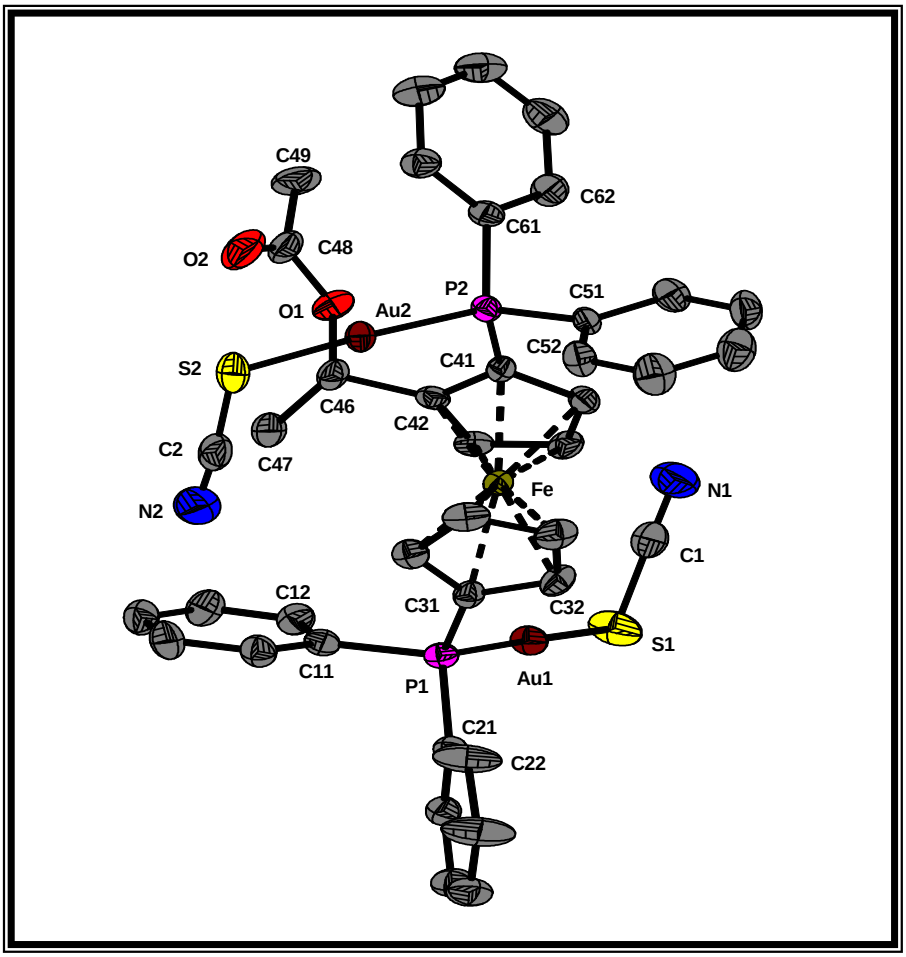

Figure 4.11 Molecular drawing of (*R*,*S*)-[(AuSCN)$_2$(μ-dppf-CH(CH$_3$)OAc)], showing the numbering scheme and thermal displacement ellipsoids (30% probability). In the numbering scheme the first digit refers to the number of the ring and the second one to the number of the atom in the ring. Hydrogen atoms are omitted for clarity.

Fig. 4.11 illustrates the molecular structure of the [(AuSCN)$_2$(μ-dppf-CH(CH$_3$)OAc)] complex. The dppf ligand coordinates both gold centres. The geometry about each gold moiety is linear and two-coordinate with slight deviation from 180° bond angles at each atom. The SCN$^-$ ligand is observed to be S-coordinated as gold is a soft metal

rather than through the nitrogen atom. The Cp rings are slightly non-parallel with an interplanar angle of 3.9(3)° and non-ideally eclipsed as indicated for example by the torsion angle C(43)-Centr-Centr-C(31) = 12.0(4)°. The bis(diphenylphosphino) ferrocenyl moiety adopts an *anti*-conformation with the torsion angle P(2)-Centr-Centr-P(1) = 158.4(5)°, thus minimising the steric interaction between the phenyl rings. The distances of the Fe atom from the Cp planes are -1.645(1) and 1.653(1) Å. The P-Au-S axis is rotated by 37.7(7)° out of the Cp plane, as defined by the torsion angle C(42)-C(41)-P(2)-Au(2). There are no Au…Au contacts between the gold centres in the molecule.

Principal bond lengths and angles are given in Table 4.5 and the supplementary material containing the complete lists of atomic coordinates, bond distances and angles, anisotropic displacement parameters as well as hydrogen coordinates is given in the Appendix, § B.4.

Table 4.5 Principal bond lengths and angles for [$(AuSCN)_2$(μ-dppf-$CH(CH_3)OAc$)].

Bond lengths (Å)		Bond angles (°)	
Au(1)-P(1)	2.2542(19)	P(1)-Au(1)-S(1)	177.51(9)
Au(2)-P(2)	2.2663(18)	P(2)-Au(2)-S(2)	176.72(8)
Au(1)-S(1)	2.313(2)	N(1)-C(1)-S(1)	175.3(10)
Au(2)-S(2)	2.317(2)	N(2)-C(2)-S(2)	175.5(10)
S(1)-C(1)	1.659(11)	C(1)-S(1)-Au(1)	101.9(3)
S(2)-C(2)	1.673(14)	C(2)-S(2)-Au(2)	96.0(3)
C(1)-N(1)	1.131(12)	C(11)-P(1)-C(21)	105.7(3)
C(2)-N(2)	1.150(15)	C(61)-P(2)-C(51)	108.2(3)
P(1)-C(11)	1.826(8)	C(11)-P(1)-Au(1)	112.6(3)
P(1)-C(21)	1.826(7)	C(21)-P(1)-Au(1)	113.0(2)
P(1)-C(31)	1.777(8)	C(31)-P(1)-Au(1)	113.5(2)
P(2)-C(41)	1.799(8)	C(41)-P(2)-Au(2)	112.3(2)
P(2)-C(51)	1.830(8)	C(51)-P(2)-Au(2)	110.8(3)
P(2)-C(61)	1.813(8)	C(61)-P(2)-Au(2)	113.2(3)
		S(1)-Au(1)-Au(2)-S(2)	156.8(1)
		N(1)-S(1)-P(1)-C(31)	-26.4(3)
		N(2)-S(2)-P(2)-C(41)	8.3(3)

The Au-P bond distances are 2.2542(19) and 2.2663(18) Å whereas the Au-S distances are 2.313(2) and 2.317(2) Å. These Au-P bond distances of the complex are slightly longer with a difference of 0.03 Å and the Au-S distances are approximately 0.1 Å longer than the ones for its chloro analogue, [$(AuCl)_2$(dppf-$CH(CH_3)OAc$)]. This may be due to the difference of the *trans* influence of the SCN as compared to the Cl. The P-C bond distances of the phenyl rings average at 1.823(7) Å whereas those of the

cyclopentadienyl rings average at 1.788(8) Å. The average C-C bond distances of the phenyl and cyclopentadienyl rings are 1.377(12) and 1.414(11) Å respectively. The P-Au-S bond angles are approximately linear at 177.51(9) and 176.72(8)°. The average for the N-C-S angles = 175.4(10)°. The Au-S-C bond angles approximately form a 90° angle to the P-Au-S axis, with such angles = 101.9(3) and 96.0(3)°. The phenyl rings are nearly orthogonal to each other with C-P-C angles = 105.7(3) and 108.2(3)°.

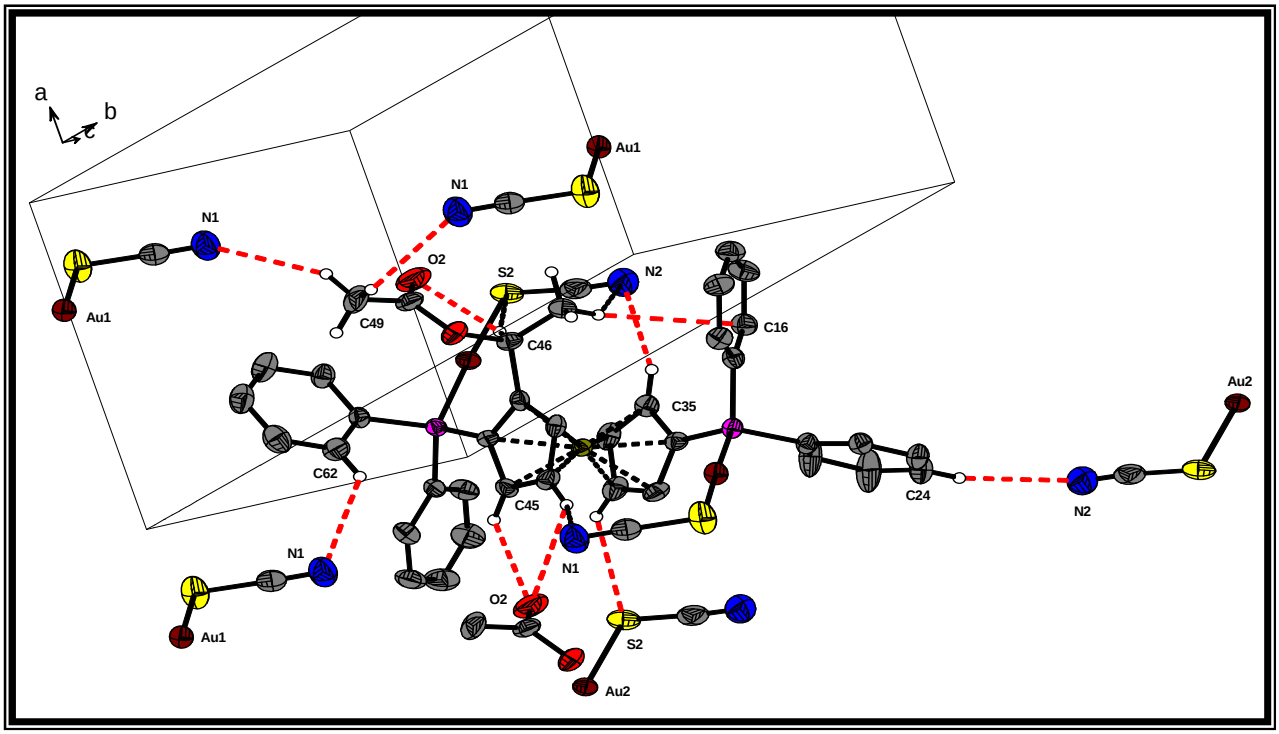

Figure 4.12 Molecular drawing of [$(AuSCN)_2$(μ-dppf-$CH(CH_3)OAc$)] showing the partial packing in the unit cell. Hydrogen atoms except those involved in hydrogen interactions are omitted for clarity. Hydrogen bonding interactions are indicated by red dashed lines between atom pairs.

The molecular packing diagram of the compound is shown in Fig. 4.12. The molecule was investigated for π-π interactions but did not indicate any significant effects. A strong intramolecular hydrogen bonding is observed between the atom pair (C46, O2) with the bond distance and angle of 2.675 Å and 101.63° respectively with weaker intramolecular hydrogen bonding interactions for (C44, N1) and (C35, N2) with 3.716 Å, 139.31° and 3.538 Å, 143.01° respectively. Several intermolecular hydrogen interactions are observed with a strong hydrogen bonding noted for thiocyanate nitrogen atom at (C62, N1) (-x-1,-y+1,-z); (C24, N2) (-x-1,-y+2,-z+1); (C49-H4A, N1) (-x,-y+1,-z) and (C49-H4B, N1) (x+1,y,z) with bond distances and angles of 3.461 Å, 130.19°; 3.565(14) Å, 160.9°; 3.667 Å, 151.83° and 3.744 Å, 138.50° respectively.

Further hydrogen bonding interactions are observed for the carboxylate moiety with an associated cyclopentadiene ring system (C44, O2) (x-1,y,z) and (C45, O2) (x-1,y,z) at 3.351 Å, 106.12° and 3.093 Å, 128.04° respectively. Hydrogen bonding is observed also for the thiocyanate sulphur at (C33, S2) (x-1,y,z) in the order of 3.651 Å, 140.99°. Possible bifurcated hydrogen bonding was observed for the C(46) and C(44) atoms and on further investigation the bifurcating bonding mode of the C(44) hydrogen atom could be excluded due to the non-planar conformation of the donor atoms. In contrast, C(46)-H(46) has a strong intramolecular hydrogen bond to O(2) with a weaker and long range intramolecular hydrogen bond to S(2) (3.887(5) Å, 165.1(4)°) atom of the thiocyanate moiety.

Interestingly enough, the two [$(AuSCN)_2$(μ-dppf-$CH(CH_3)N(CH_3)_2$)] and [$(AuSCN)_2$(μ-dppf-$CH(CH_3)OAc$)] structures are isomorphous. Thus, from unit cell parameters and fractional atomic coordinates, it can be concluded that the relative space occupied by the -$N(CH_3)_2$ and -OAc groups in the individual structures does not significantly affect the crystallographic packing of the molecules. Isomorphism in these complexes indicates a solid state energy minimum at this specific orientation and this will be exploited in future utilising computational chemistry methods.

The superimposed wire frames and a comparison of the packing of the [$(AuSCN)_2$(μ-dppf-$CH(CH_3)N(CH_3)_2$)] and [$(AuSCN)_2$(μ-dppf-$CH(CH_3)OAc$)] structures are illustrated in Figs. 4.13 and 4.14 respectively.

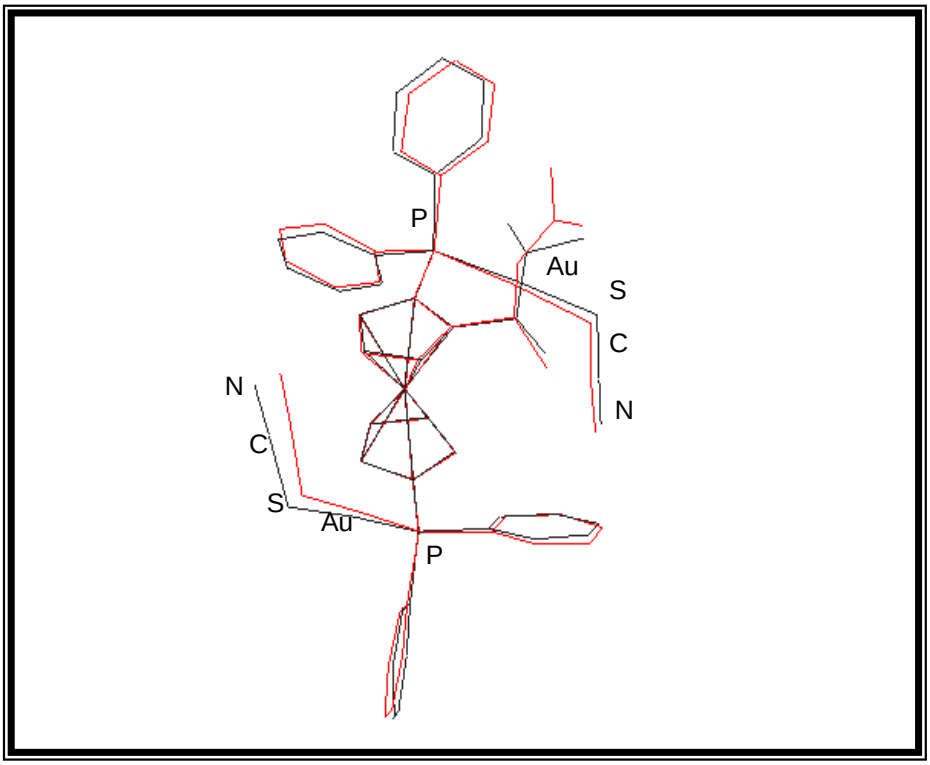

Figure 4.13 Superimposed wire frames of [$(AuSCN)_2$(μ-dppf-$CH(CH_3)N(CH_3)_2$)] (black) and [$(AuSCN)_2$(μ-dppf-$CH(CH_3)OAc$)] (red) structures. Hydrogens are omitted for clarity.

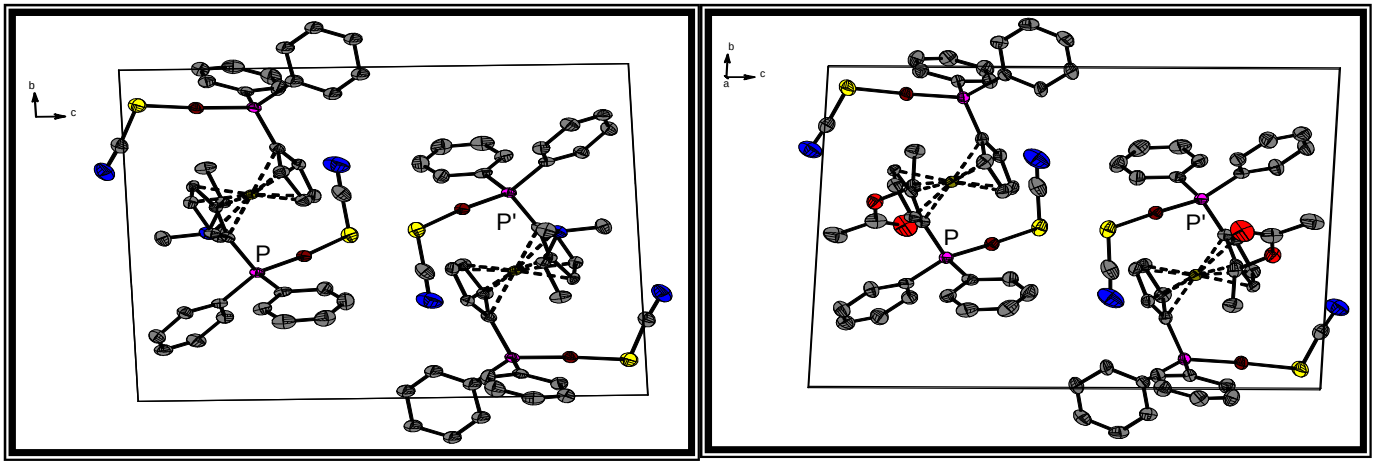

A **B**

Figure 4.14 Comparison of partial packing diagrams along the a axis for [$(AuSCN)_2$(μ-dppf-$CH(CH_3)N(CH_3)_2$)] (**A**, symmetry operator: P' (2-x,1-y,1-z)) and [$(AuSCN)_2$(μ-dppf-$CH(CH_3)OAc$)] (**B**, symmetry operators: P (1+x,y,z), P' (1-x,1-y,1-z)) structures.

Further comparison of the parameters of the [$(AuSCN)_2$(μ-dppf-$CH(CH_3)OAc$)] structure with other similar structures found in literature is made in § 4.5.

4.4.5 Crystal structure of [(AuSCN)$_2$(μ-dppf)]

The preparation and characterisation of the complex was discussed in § 4.3.2.2. The general crystal data and refinement parameters of the [(AuSCN)$_2$(μ-dppf)] compound are listed in Table 4.1 while the supplementary material containing the complete lists of atomic coordinates, bond distances and angles, anisotropic displacement parameters as well as hydrogen coordinates is given in the Appendix, § B.5.

The Fe atom of the ferrocene moiety lies on a special position which could be due to the centrosymmetry of the structure and upon refinement of the structure the Fe atom was loaded with 50% occupancy.

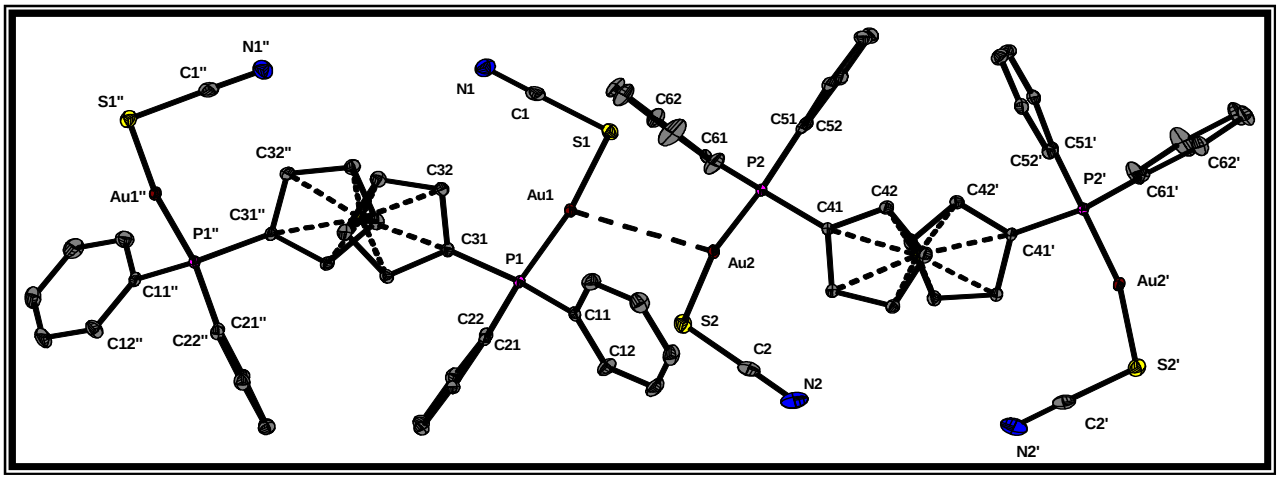

Figure 4.15 Molecular drawing of [(AuSCN)$_2$(μ-dppf)], showing the numbering scheme of the two molecules and thermal displacement ellipsoids (30% probability). In the numbering scheme the first digit refers to the number of the ring and the second one to the number of the atom in the ring. Symmetry operators: atom' (2-x,y,3/2-z) and atom'' (2-x,y,1/2-z). Hydrogen atoms are omitted for clarity.

Fig 4.15 illustrates a molecular drawing of the crystal structure of the [(AuSCN)$_2$(μ-dppf)] compound. There are two molecules in the structure of the [(AuSCN)$_2$(μ-dppf)] compound as shown in Fig. 4.15 above and are linked by short Au…Au contacts of 2.9798(7) Å. Again, as shown in the previous examples for the ferrocenyl gold(I) complexes with coordinated thiocyanate (§ 4.4.2 and 4.4.4), the SCN^- in [(AuSCN)$_2$(μ-dppf)] coordinated to the soft Au(I) metal *via* the softer S atom. Since the Fe atom of the ferrocene lies on a special position, it is observed that in the two molecules one half of the cyclopentadienyl ring is occupied by the same atoms as found on the other half.

The geometry about each independent gold atom is linear, two-coordinate and with slight deviations from 180° bond angles at each gold atom. The cyclopentadienyl rings are approximately eclipsed relatively to each other in both molecules, with C(43')-Centr-Centr-C(41) torsion angle = -19.6(2)° for molecule 2 and C(34)-Centr-Centr-C(31'') = -17.1(2)° for molecule 1. The Cp rings for molecule 1 (C3 and C3'' atoms) are non-parallel with a dihedral angle of 1.9(1)° but for molecule 2 (C4 and C4' atoms) are more parallel to each other as indicated by the dihedral angle of 0.02(17)°. The dihedral angles between the phenyl rings are 65.7(1)° for the planes defined by C1 and C2 atoms and 78.2(1)° for the planes defined by C5 and C6 atoms.

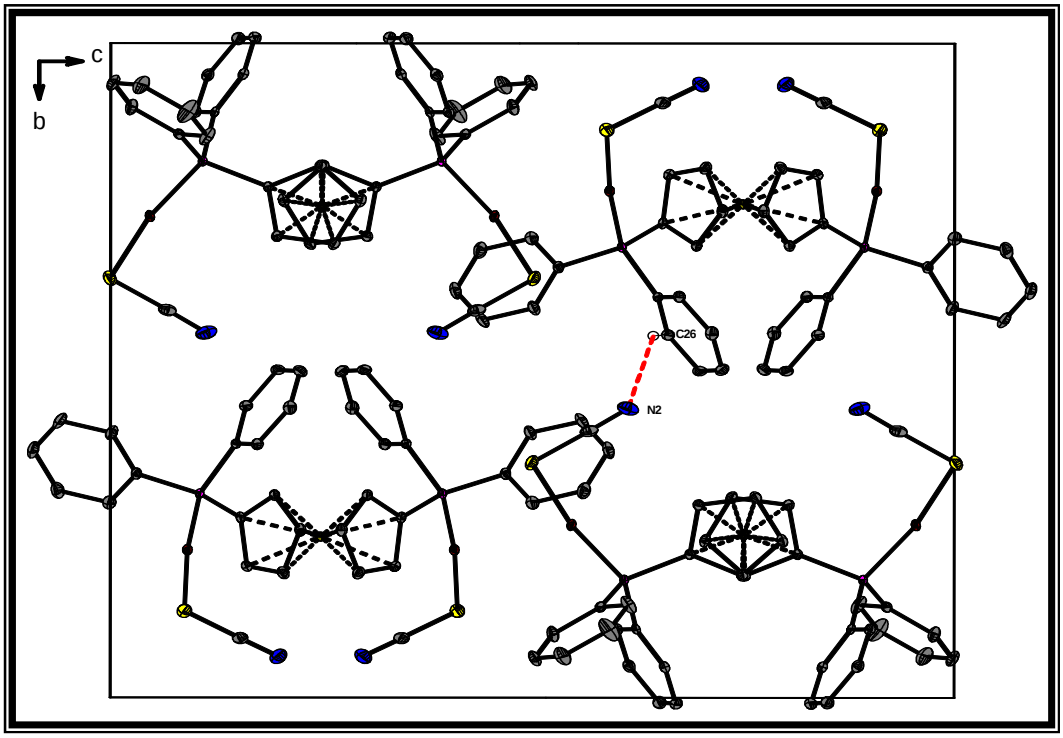

Figure 4.16 Illustration of the packing diagram of [(AuSCN)$_2$(μ-dppf)] along the a-axis. Hydrogen atoms except those involved in hydrogen interactions are omitted for clarity. The hydrogen bonding interactions are indicated by red dashed lines between atom pairs.

Fig 4.16 represents a packing diagram of the [(AuSCN)$_2$(μ-dppf)] complex clearly illustrating how the ferrocene moiety is arranged or folded within the unit cell. The molecule packs in a 'crab-creature' like interlocking motive with the coordinated SCN ligand representing the arms. A strong intermolecular hydrogen bonding is observed between the atom pair (C26, N2) (2-x,1-y,1-z) with the bond distance and angle of 2.546 Å and 125° respectively.

Table 4.6 Selected bond lengths and angles for the [(AuSCN)$_2$(μ-dppf)] compound.

Bond lengths (Å)		Bond angles (°)	
Au(1)…Au(2)	2.9798(7)	P(1)-Au(1)-S(1)	173.21(3)
Au(1)-P(1)	2.269(1)	P(2)-Au(2)-S(2)	170.13(3)
Au(2)-P(2)	2.261(1)	S(1)-C(1)-N(1)	178.6(4)
Au(1)-S(1)	2.322(1)	S(2)-C(2)-N(2)	177.9(4)
Au(2)-S(2)	2.328(1)	Au(1)-S(1)-C(1)	95.24(13)
S(1)-C(1)	1.693(4)	Au(2)-S(2)-C(2)	97.12(14)
S(2)-C(2)	1.684(4)	C(11)-P(1)-C(21)	107.50(17)
C(1)-N(1)	1.144(5)	C(51)-P(2)-C(61)	101.81(16)
C(2)-N(2)	1.155(6)	P(1)-Au(1)-Au(2)	94.69(2)
P(1)-C(11)	1.818(4)	P(2)-Au(2)-Au(1)	106.35(3)
P(1)-C(21)	1.813(4)	S(1)-Au(1)-Au(2)	91.89(3)
P(1)-C(31)	1.800(4)	S(2)-Au(2)-Au(1)	83.51(3)
P(2)-C(41)	1.790(4)	S(1)-Au(1)-Au(2)-S(2)	-18.5(3)
P(2)-C(51)	1.812(4)	N(1)-S(1)-P(1)-C(31)	-20.8(1)
P(2)-C(61)	1.815(4)	N(2)-S(2)-P(2)-C(41)	-10.9(1)

Selected bond lengths and angles for the [(AuSCN)$_2$(μ-dppf)] complex are given in Table 4.6. The Au-P bond distances are observed to be 2.269(1) and 2.261(1) Å whilst the Au-S bonds are = 2.322(1) and 2.328(1) Å and the latter are much longer than the Au-P distances. The average values for the S-C and C-N bond distances are 1.689(4) and 1.155(6) Å respectively. The P-C distances for the structure are within the normal range as noted for the ferrocenyl complexes with an average of 1.815(4) Å for the phenyl and 1.795(4) Å for the cyclopentadienyl rings which are slightly shorter than for the phenyl rings. The average Fe-C distances is 2.054(6) Å for both molecule 1 and 2. There is no short Fe…Au interaction, with the shortest such distance being 4.196(1) Å.

The P-Au-S bond angles are 173.21(3) and 170.13(3)° and they nearly show an approximate linear geometry of the gold moieties for the other digold ferrocenyl complexes. The Au-S-C bond angles are orthogonal at 95.24(13) and 97.12(14)°. The coordinated SCN ligand shows linearity with S-C-N angles of 178.6(4) and 177.9(4)°. The C-C-C angles in the cyclopentadienyl rings (sp^2 hybridisation) are all normal and range from 107.1(3) to 108.7(3)°. The C-P-Au bond angles range from 106.5(1) to 118.9(1)°.

Comparison of the parameters of this structure with other similar structures found in literature is made in § 4.5.

4.5 STRUCTURAL PARAMETER CORRELATIONS OF SIMILAR GOLD(I) AND OTHER METAL FERROCENYL COMPLEXES

Different individual structural aspects for the various complexes studied were discussed separately in § 4.4.1 - 4.4.5. Here in Table 4.7, the parameters are compared and correlated with those for similar gold ferrocenyl complexes found in literature.

Table 4.7 Comparative table of bond lengths (Å) and angles (°) of similar P-ferrocenyl complexes (X = halide, pseudo-halide or coordinating ligand).

Entry	Complex	M-P	M-X	P-M-X	Ref.
1	$[(AuCl)_2(\mu\text{-dppf})]$	2.226(1)	2.278(1)	177.56(8)	28
2	$[(AuCl)_2(\mu\text{-dppf})]\cdot CH_2Cl_2$	2.2262(13)	2.2815(13)	179.59(5)	29
3	$[(AuCl)_2(\mu\text{-dppf})]\cdot CH_3Cl$	2.239(3)	2.300(3)	176.0(1)	30
		2.222(3)	2.273(4)	175.5(1)	
4	$[(AuI)_2(\mu\text{-dppf})]\cdot 2CH_2Cl_2$	2.248(9)	2.545(3)	177.7(2)	29
		2.240(8)	2.561(2)	176.3(2)	
5	$[(AuSCN)_2(\mu\text{-dppf})]$	2.269(1)	2.322(1)	173.21(3)	This work[a]
		2.261(1)	2.328(1)	170.13(3)	
6	$[(AuCl)_2(\mu\text{-dppf-CH}(CH_3)N(CH_3)_2)]$	2.237(2)	2.271(3)	175.41(10)	21[b]
		2.224(2)	2.278(2)	174.01(10)	
7	$[(AuSCN)_2(\mu\text{-dppf-CH}(CH_3)N(CH_3)_2)]$	2.265(2)	2.327(3)	175.61(9)	22[c]
		2.260(3)	2.313(3)	176.86(9)	
8	$[(AuCl)_2(\mu\text{-dppf-CH}(CH_3)OAc)]$	2.2312(16)	2.2872(16)	176.66(6)	This work[d]
		2.2217(17)	2.2840(17)	177.34(7)	
9	$[(AuSCN)_2(\mu\text{-dppf-CH}(CH_3)OAc)]$	2.2663(18)	2.313(2)	177.51(9)	This work[e]
		2.2542(19)	2.317(2)	176.72(8)	
10	$[Au(PPh_2CH_2Fc)Cl]$[f]	2.236(18)	2.3014(18)	176.01(7)	31
11	$[Au(C_{27}H_{28}FeNP)Cl]\cdot 1.5C_6H_6$ [g]	2.24(1)	2.32(1)	176.5(5)	32
12	$[(AuCl)_3(dppf\text{-}L)_2]\cdot Et_2O$[h]	2.31(2)	2.52(3)	113(2)	33
		2.20(2)	2.28(2)	177(2)	
13	$[Au(PPhFc_2)Cl]$[f]	2.234(2)	2.289(2)	176.1(1)	34
14	$[(AuCl)_2(dppf)_3]$	2.345(3)	2.929(3)	100.5(1)	35
		2.391(3)		105.3(1)	
		2.405(3)		86.1(1)	

dppf = 1,1'-bis(diphenylphosphino)ferrocene; a) See § 4.4.5; b) § 4.4.1; c) § 4.4.2; d) § 4.4.3; e) § 4.4.4;

f) Fc = $(\eta^5\text{-}C_5H_5)Fe(\eta^5\text{-}C_5H_4)$; g) $C_{27}H_{28}FeNP$ = (α-dimethylamino ferrocenophanyl) diphenylphosphine;

h) L = $-CH(CH_3)N(CH_3)CH_2CH_2N(CH_3)_2$

In Table 4.7 above, selected geometrical parameters of the complexes investigated in this study are compared with those from other relevant gold ferrocenyl complexes found in literature. It is clear that for the ferrocenyl complexes with the chloro ligand *i.e.*, the complex with no solvent of crystallisation (1) and [$(AuCl)_2$(μ-dppf)] complexes with a coordinated solvent (entries 2 and 3), the [$Au(PPh_2CH_2Fc)Cl$] (10), [$(AuCl)_2$(μ-dppf-$CH(CH_3)N(CH_3)_2$)] (6) and [$(AuCl)_2$(μ-dppf-$CH(CH_3)OAc$)] (8) complexes, the M-P bond lengths are comparable to each other. These M-P bond lengths range from 2.221(1) to 2.239(3) Å and are approximately of normal length for the ferrocenyl complexes[36]. Also for [$Au(PPhFc_2)Cl$] (13) the M-P bond distance falls within this range and is 2.234(2) Å. However, for the [$(AuI)_2$(μ-dppf)]·$2CH_2Cl_2$ (4) complex, the Au-P bond distances are slightly longer at 2.24 Å and for the [$(AuSCN)_2$(μ-dppf-$CH(CH_3)N(CH_3)_2$)] (7) and [$(AuSCN)_2$(μ-dppf-$CH(CH_3)OAc$)] (9) complexes the distances vary from 2.260(3) to 2.266(1) Å. This may be due to the changes in the *trans* influence when the Cl atom in the gold chloro complexes is substituted with I or SCN.

The Au-Cl bond length of the chloro complexes with the dppf ligand *i.e.* [$(AuCl)_2$(μ-dppf)] (1), [$(AuCl)_2$(μ-dppf)]·CH_2Cl_2 (2), [$(AuCl)_2$(μ-dppf)]·CH_3Cl (3) and [$(AuCl)_2(dppf)_3$] (14) vary from 2.273(4) to 2.929(3) Å. The latter being an exception, as it can be noted that the Au-Cl bond distance in the [$(AuCl)_2(dppf)_3$] (14) complex is very long at 2.929(3) Å and this suggests a considerable Au-Cl character in the polymeric form of the structure. In this structure ([$(AuCl)_2(dppf)_3$], 14), the dppf ligand adopts both chelating and bridging binding modes with the Fe atom of the central bridging ligand lying at a centre of symmetry. When the coordinated ligands are varied in the dppf complexes, *i.e.* changing from Cl, SCN to I in the [$(AuCl)_2$(μ-dppf)] (1) and its coordinated solvent variations (2 and 3), [$(AuSCN)_2$(μ-dppf)] (5) and [$(AuI)_2$(μ-dppf)]·$2CH_2Cl_2$ (4) complexes, the Au-X bond distances increase respectively. These bond distances lengthen from approximately 2.2, 2.3 to 2.5 Å and this is due to the different *trans* influences of the Cl, SCN and I. The [$(AuI)_2$(μ-dppf)]·$2CH_2Cl_2$ complex (4) displays long Au-I bonds with the average at 2.553(3) Å typical of iodide gold complexes because of the large iodide radius.

There is not much change observed in the Au-Cl distances for the dinuclear chloro complexes with a modified dppf ligand ([$(AuCl)_2$(μ-dppf-$CH(CH_3)N(CH_3)_2$)] (6) and [$(AuCl)_2$(μ-dppf-$CH(CH_3)OAc$)] (8)) as such distances only vary from approximately 2.27 to 2.28 Å. Similarly, the Au-Cl distances for the mononuclear chloro complexes that also have modified dppf ligands, ([$Au(PPhFc_2)Cl$] (13), [$Au(PPh_2CH_2Fc)Cl$] (10)

and [Au($C_{27}H_{28}$FeNP)Cl]·1.5C_6H_6 (11)), do not vary that much from each other as the distances for these complexes are 2.289(2), 2.3014(18), and 2.32(1) Å respectively. However, the [$(AuCl)_3$(dppf-$L)_2$]·Et_2O (12) complex differs significantly by 0.2 Å with a distance of 2.52(3) Å.

The dppf ligand and its modified analogues as illustrated in Table 4.7 above act as bidentate ligands capable of bridging and/or chelation and can form complexes with ratios of metal atom to ligand of 1 or 2, behaving in a manner similar to that of dppe[37]. In complexes with entry numbers 1 - 9, the pure dppf or modified dppf ligands act as bridging ligands. In the [$(AuCl)_2$(dppf)$_3$] (14) the dppf ligands adopt both bridging and chelating binding modes with the Fe atom of the central bridging ligand lying at the centre of symmetry. Also noted for the dppf brigded complexes, the ligand is mostly in a *trans* orientation and adopts an *anti*-conformation thus minimising the steric interaction between the phenyl rings.

Comparing the three thiocyanate complexes, the [$(AuSCN)_2$(μ-dppf)] (5), [$(AuSCN)_2$(μ-dppf-CH(CH_3)N($CH_3)_2$)] (7) and [$(AuSCN)_2$(μ-dppf-CH(CH_3)OAc)] (9) the Au-S bond lengths are similar and vary only from 2.313(3) to 2.327(3) Å.

The P-M-X bond angles are similar in all the linear gold complexes listed and are approximately 180° which is usually observed for gold complexes. Exception is again also observed for the polymeric [$(AuCl)_2$(dppf)$_3$] (14) complex with much smaller P-M-X angles, *i.e.* of around 90-100°.

In conclusion, it can be stated that the functionalisation of ferrocene and the dppf ligand and the corresponding synthesis of gold(I) complexes was successfully achieved as manifested by the successful characterisation of gold ferrocenyl structures discussed above. In digold ferrocenyl complexes the ferrocene moiety acts as a bridge as it coordinates both the gold atoms in its complexes. In this study the dppf as a complexed-ligand was functionalised by substituting one of the hydrogen atoms in the cyclopentadienyl rings with ethylamine or ethyl acetate ligands and also by substituting the Cl ligand with SCN. Hence, by investigating a range of complexes (entries number 6, 7, 8, 9 and 5 in Table 4.7) results in different characteristics of the complexes. The functionalised complexes also displayed different solubilties with the ethylacetate complexes (entries number 8 and 9) more soluble than the ethylamine (entries number

8 and 9) complexes. The introduction of the SCN^- ligand also improved the solubility of the complexes as compared to the pure dppf complexes.

Gold-gold interaction was invoked unequivocally as illustrated in [$(AuCl)_2$(μ-dppf)] (1), [$(AuCl)_2$(μ-dppf)]·CH_3Cl (3) and [$(AuSCN)_2$(μ-dppf)] (5) complexes, (calculated as 6.3212(13), 3.083(1) and 2.9798(7) Å respectively) indicative of bonding interactions which contribute to the stabilisation of the product and moreover in (3) to form polymeric chains.

Table 4.8 Comparative table of bond lengths (Å) and angles (°) of similar transition metal ferrocenyl complexes (X = coordinated ligand).

Entry	Complex	M-P	M-X	P-M-X	Ref.
15	[$Ag(NO_3)$(μ-dppf)]$_2$	2.433(3)	2.476(8)	97.0(3)	38
		2.435(3)	2.873(7)	99.3(2)	
16	*cis*-[Rh(dppf-*P*,*P*')(nbd)][ClO_4]				39
17	[Ir(dppf-*P*,*P*')$_2$][BPh_4]	2.317(6)	-	-	40
		2.389(5)	-	-	
		2.337(5)	-	-	
		2.343(6)	-	-	
18	*cis*-[$PdCl_2$(dppf-*P*,*P*')]·CH_2Cl_2	2.278(1)	2.289(1)	89.96(4)[a]	41
		2.340(1)	2.358(1)	97.98(4)[b]	
19	*cis*-[$PdCl_2$(dppf-*P*,*P*')]·$CHCl_3$	2.283(1)	2.347(1)	87.8(1)[a]	42
		2.301(1)	2.348(1)	99.07(5)[b]	
20	*cis*-[$PtCl_2$(dppf-*P*,*P*')]·0.5 $(CH_3)_2CO$	2.252(4)	2.413(3)	83.0(1)	43
		2.260(4)	2.396(4)	91.4(1)	
21	[$Pt(H_2O)_2$(dppf)][$OTf]_2$	2.243(2)	2.122(4)	174.72(14)	44
		2.246(2)	2.103(5)	90.25(14)	
				86.54(13)	
				172.17(14)	
22	[$NiCl_2$(dppf-*P*,*P*')]	2.320(2)	2.211(2)	109.4(1)	12
		2.303(2)	2.235(2)	112.5(1)	
				107.7(1)	
				95.6(1)	
23	[$NiBr_2$(dppf-*P*,*P*')]	2.281(6)	2.344(4)	127.0(2)[a]	41
		2.299(6)	2.351(4)	102.5(2)[b]	

[a] X-M-X bond angle, [b] P-M-P bond angle

The M-P, M-X and P-M-X bond distances and angles for the ferrocenyl complexes of transition metal complexes other than gold are presented in Table 4.8.

The M-P bond distances of the chloro platinum and palladium complexes, *cis*-[$PtCl_2$(dppf-*P*,*P*')]·0.5 $(CH_3)_2CO$ (20), *cis*-[$PdCl_2$(dppf-*P*,*P*')]·CH_2Cl_2 (18) and *cis*-[$PdCl_2$(dppf-*P*,*P*')]·$CHCl_3$ (19), range from 2.252(4) - 2.283(1) Å. For the two palladium chloro complexes (*cis*-[$PdCl_2$(dppf-*P*,*P*')]·CH_2Cl_2 (18) and *cis*-[$PdCl_2$(dppf-*P*,*P*')]·$CHCl_3$ (19)), the pairs of Pd-P and Pd-Cl bond lengths in the chloroform solvate complex (19) differ by 0.018 and 0.001 Å compared with the corresponding differences of 0.012 and 0.018 Å in the dichloromethane solvate complex (18). The [$Ag(NO_3)$(μ-dppf)]$_2$ complex (15) records the longest M-P bond distance compared with the other complexes described in Table 4.8.

A change in the coordinating ligand in the platinum dppf complexes, *i.e. cis*-[$PtCl_2$(dppf-*P*,*P*')]·0.5 $(CH_3)_2CO$ (20) and [$Pt(H_2O)_2$(dppf)][OTf]$_2$ (21) brings about a decrease in the M-P distance by approximately 0.02 Å. However with the Ni dppf complexes ([$NiCl_2$(dppf-*P*,*P*')] (22) and [$NiBr_2$(dppf-*P*,*P*')] (23)), similar M-P distances are observed.

The M-X bond distances of the *cis*-[$PdCl_2$(dppf-*P*,*P*')]·CH_2Cl_2 (18), *cis*-[$PdCl_2$(dppf-*P*,*P*')]·$CHCl_3$ (19) and [$NiBr_2$(dppf-*P*,*P*')] (23) complexes range from approximately 2.29 to 2.36 Å. The M-X bond distances of the [$NiCl_2$(dppf-*P*,*P*')] (22) complex are 2.211(2) and 2.235(2) with shortest distances observed for the [$Pt(H_2O)_2$(dppf)][OTf]$_2$ (21) complex at 2.122(4) and 2.103(5) Å. The longest M-X bond distances for the complexes compared in Table 4.8 are observed for [$Ag(NO_3)$(μ-dppf)]$_2$ (15) and *cis*-[$PtCl_2$(dppf-*P*,*P*')]·0.5 $(CH_3)_2CO$ (20) complexes with distances of approximately 2.4 Å. For the [$Ag(NO_3)$(μ-dppf)]$_2$ (15) complex, stabilisation of the 14-electron P-Ag(1)-P fragment is achieved by the NO_3^- coordination in a semibridging and semichelating manner whereby one-atom bridging oxygens are weakly coordinated to the Ag atom hence the long Ag(1a)-O(1) of 2.873(7) Å.

The P-M-X bond angles for the compared structures in Table 4.8 range from 83.0(1)° as observed in the *cis*-[$PtCl_2$(dppf-*P*,*P*')]·0.5 $(CH_3)_2CO$ (20) complex to 112.5(1)° for the [$NiCl_2$(dppf-*P*,*P*')] complex (22). However a linear P-M-X angle is noted for the [$Pt(H_2O)_2$(dppf)][OTf]$_2$ complex (21) at 174.72(14)°.

In conclusion, it was shown by this crystallographic study that several factors, including a change in the ligands coordinated to the metal, account for the variations in the M-P and M-X bond distances observed in structure determinations. The careful characterisation of the complexes in this study was very important to aid in the elucidation of the complex stoichiometric mechanism. In general, only smaller ground state differences in bond lengths, angles and so forth for the gold ferrocenyl complexes studied were observed.

[1] M. Roseblum, 'Chemistry of the Iron Group Metallocenes', John Wiley, New York, 1965.

[2] G.E. Coates, M.L.H. Green, K. Wade, 'Organometallic Compounds', Vol. 2, Methuen, London, 1960.

[3] W.R. Cullen, J.D. Woollins, *Coord. Chem. Rev.,* 1981, **39**, 1.

[4] (a) P.W.N. Van Leeuwen, C.F. Roobeek, *J. Mol. Catal.,* 1985, **31**, 345.
(b) K. Tani, T. Yamagata, S. Akutagawa, H. Komobayashi, T. Tatomi, H. Takaya, A. Miyashita, R. Noyori, S. Otsuka, *J. Am. Chem. Soc.,* 1984, **106**, 5208.
(c) T. Hayashi, M. Konishi, K. Yolota, M. Kumada, *J. Organomet. Chem.,* 1985, **285**, 359.
(d) N. Miyaura, T. Ishiyama, H. Sasaki, M. Ishikawa, M. Sato, A. Suzuki, *J. Am. Chem. Soc.,* 1989, **111**, 314.

[5] S. Onaka, *Bull. Chem. Soc. Jpn.,* 1986, **59**, 2359.

[6] C.E. Housecroft, S.M. Owen, P.R. Raithby, B.A.M. Shaykh, *Organometallics,* 1990, **9**, 1617.

[7] V. Scarcia, A. Furlani, B. Longato, B. Corain, G. Pilloni, *Inorg. Chim. Acta,* 1988, **153**, 67.

[8] S. Onaka, A. Mizuno, S. Takagi, *Chem. Lett.,* 1989, 2037.

[9] T.S.A. Hor, L.-T. Phang, L.-K. Liu, Y.-S. Wen, *J. Organomet. Chem.,* 1990, **397**, 29.

[10] P. Kalck, C. Randrianalimanana, M. Ridmy, A. Thorez, *New J. Chem.,* 1988, **12**, 679.

[11] S.T. Chacon, W.R. Cullen, M.I. Bruce, O. bin Shawkataly, F.W.B. Einstein, R.H. Jones, A.C. Willis, *Can. J. Chem.,* 1990, **68**, 2001.

[12] U. Casellato, D. Ajó, G. Valle, B. Corain, B. Longato, R. Graziani, *J. Crystallogr. Spectrosc. Res.,* 1988, **18**, 583.

[13] J.J. Daly, *J. Chem. Soc.,* 1964, 3799.

[14] A. Togni, T. Hayashi, 'Ferrocenes: Homogeneous Catalysis, Organic Synthesis, Materials Science', VCH, New York, 1995.

[15] (a) H. Brunner, *Synthesis,* 1988, 645.
(b) G. Consiglio, R.M. Waymouth, *Chem. Rev.,* 1989, **89**, 257.
(c) I. Ojima, N. Clos, C. Bastos, *Tetrahedron,* 1989, **45**, 6901.

[16] R. Uson, A. Laguna, M. Laguna, D.A. Briggs, H.H. Murray, J.P. Fackler Jr., *Inorg. Synth.*, 1989, **26**, 85.

[17] T. Hayashi, T. Mise, M. Fukushima, M. Kagotani, N. Nagashima, Y. Hamada, A. Matsumoto, S. Kawakami, M. Konishi, K. Yamamoto, M. Kumada, *Bull. Chem. Soc. Jpn.,* 1980, **53**, 1138.

[18] G.P. Sollot, H. Edgar Jr., *J. Org. Chem.,* 1962, **27**, 4034.

[19] M.C. Gimeno, A. Laguna, C. Sarroca, *Inorg. Chem.*, 1993, **32**, 5926.

[20] A. Houlton, R.M.G. Roberts, J. Silver, *J. Organomet. Chem.,* 1991, **418**, 269.

[21] Z.A. Sam, Å. Oskarsson, S.K.C. Elmroth, A. Roodt, *Acta Cryst.,* 2005, E**61**, m2090.

[22] Z.A. Sam, S.K.C. Elmroth, A. Roodt, A.J. Muller, *Acta Cryst.,* 2006, E**62**, m1699.

[23] Bruker SAINT-Plus Version 6.02 (including XPREP), Bruker AXS Inc., Area-Detector Software, Madison, WI, USA, 1999.

[24] Bruker SADABS (Version 2004/1) and SMART-NT (Version 5.050). Bruker AXS Inc., Madison, Wisconsin, USA, 1998.

[25] G.M. Sheldrick, SHELXS-97, Program for Crystal Structure Determination, University of Göttengen, Germany, 1997.

[26] G.M. Sheldrick, SHELXL-97, Program for Crystal Structure Refinement, University of Göttengen, Germany, 1997.

[27] (a) K. Brandenburg, DIAMOND, Release 3.0c, Crystal Impact GbR, Postfach 1251, D-53002 Bonn, Germany, 2005.
(b) K. Brandenburg, M. Berndt, DIAMOND, Release 2.1e, Crystal Impact GbR, Postfach 1251, D-53002 Bonn, Germany, 2001.

[28] O. Crespo, M.C. Gimeno, P.G. Jones, A. Laguna, *Acta Cryst.,* 2001, C**56**, 1433.

[29] F. Canales, M.C. Gimeno, P.G. Jones, A. Laguna, C. Sarroca, *Inorg. Chem.,* 1997, **36**, 5206.

[30] D.T. Hill, G.R. Girard, F.L. McCabe, R.K. Johnson, P.D. Stupik, J.H. Zhang, W.M. Reiff, D.S. Eggelston, *Inorg. Chem.,* 1989, **28**, 3529.

[31] E.M. Barranco, O. Crespo, M.C. Gimeno, A. Laguna, *Inorg. Chem.,* 2000, **39**, 680.

[32] M. Viotte, B. Gautheron, R.G. Parish, R.G. Pritchard, *Acta Cryst.,* 1996, C**52**, 1891.

[33] A. Togni, S.D. Pastor, G. Rihs, *J. Organomet. Chem.,* 1990, **381**, C21.

[34] P.G. Jones, C.F. Erdbrügger, R. Hohbein, E. Schwarzmann, *Acta Cryst.,* 1988, C**44**, 1302.

[35] A. Houlton, D.M.P. Mingos, D.M. Murphy, D.J. Williams, *Acta Cryst.,* 1995, C**51**, 30.

[36] (a) P.G. Jones, *Acta Crystallogr.,* 1980, **1336**, 2775.
(b) P.G. Jones, *Gold Bull.,* 1981, **14**, 102.

[37] A.W. Rudie, D.W. Lichtenberg, M.L. Katcher, A. Davison, *Inorg. Chem.,* 1978, **17**, 2859.

[38] T.S.A. Hor, S.P. Neo, C.S. Tan, T.C.W. Mak, K.W.P. Leung, R.-J. Wang, *Inorg. Chem.,* 1992, **31**, 4510.

[39] W.R. Cullen, T.-J. Kim, F.W.B. Einstein, T. Jones, *Organometallics,* 1985, **4**, 346.

[40] U. Casellato, B. Corain, R. Graziani, B. Longato, G. Pilloni, *Inorg. Chem.,* 1990, **29**, 1193.

[41] I.R. Butler, W.R. Cullen, T.-J. Kim, S.J. Rettig, J. Trotter, *Organometallics,* 1985, **4**, 972.

[42] T. Hayashi, M. Konishi, Y. Kobori, M. Kumada, T. Higuchi, K. Hirotsu, *J. Am. Chem. Soc.,* 1984, **106**, 158.

[43] D.A. Clemente, G. Pilloni, B. Corain, B. Longato, M. Tiripicchio-Camellini, *Inorg. Chim. Acta,* 1986, **115**, L9.

[44] P.J. Stang, B. Olenyuk, J. Fan, A.M. Arif, *Organometallics,* 1996, **15**, 904.

5 BIOCHEMICAL ACTIVITY OF AURANOFIN ANALOGUES

5.1 INTRODUCTION

The biochemistry of gold has evolved primarily in response to the prolonged use of gold compounds in treating rheumatoid arthritis and in response to efforts to develop complexes with anti-tumour activity. As stated before in the previous theory chapters, the modern use of gold complexes traces its beginnings to the experimental work of Robert Koch, a physician who discovered the bacteriostatic effects of the $[Au(CN)_2]^-$ compound[1,2]. The first report on the anti-arthritic activity of gold complexes was made in the late 1920's[1,2] but despite the medical impetus, it was only in the early 1970's that extensive research, driven partly by the emerging field of bioinorganic chemistry, led to extensive studies of the inorganic and biochemical properties of the relevant gold compounds[3,4,5]. Since that time, interest in potential anti-tumour agents[6,7] based on gold has contributed to the research in its biochemistry. Subsequently, gold compounds have also been investigated for their anti-tumour activity and more recently for their anti-HIV activity.

Gold(I) thiolates have been the principal compounds used in the treatment of rheumatoid arthritis with gold-based drugs. The gold(I) thiolates, being water-soluble owing to the presence of solubilising groups and/or charge are, administered parenterally.

The design and testing of gold complexes for anti-tumour activity over the past several decades have been based on three rationales:

- analogies between square planar complexes of Pt(II) and Au(III), both of which are d^8 ions.
- analogy to the immunomodulatory effects of gold(I) antiarthritic agents.
- complexation of gold(I) and gold(III) with known anti-tumour agents to form new compounds with enhanced activity.

As mentioned earlier, the use of metal complexes in the pharmaceutical field shows great potential. The cytostatic activity could be the direct result of the interaction of metal complexes with DNA, thus interfering with DNA replication, the inhibition or activation enzymes directly or indirectly related to DNA replication. These complexes might also indicate a decrease in metabolic activity of tumour cells due to inhibition of respiratory enzymes. Gold-based compounds have been used for decades in the treatment of rheumatoid arthritis. One of the most promising fields of these gold-based compounds is their affect as anti-tumour agents. Unlike cisplatin that mainly target the DNA, their cytotoxicity is mediated by their ability to alter mitochondrial function and inhibit protein synthesis.

The gold(I) phosphine derivatives which are among several gold compounds investigated have shown great potential as anticancer agents. It has been speculated that the anti-tumour properties of gold (I) phosphine complexes *in vivo* are closely related to their cytotoxic effects on tumour cells *in vitro*. The precise mechanical action of gold(I) phosphine induced cytotoxicity is vague although it is thought that the mitochondria may play the key role.

Auranofin is a lipophilic two-coordinate complex, which has been widely used in the treatment of rheumatoid arthritis. This orally active agent has remarkable immuno-suppressive and anti-inflammatory properties. Auranofin has shown to be highly cytotoxic to tumour cells. In this chapter 2,3,4,6-tetra-*O*-acetyl-1-thio-β-D-glucopyranosato(triethylphosphine) gold(I) (auranofin); 2,3,4,6-tetra-*O*-acetyl-1-thio-β-D-glucopyranosato(1,3,5-triaza-7-phosphatricyclo[3.3.1.1^{3,7}]decane) gold(I) (PTA-auranofin); 2,3,4,6-tetra-*O*-acetyl-1-thio-β-D-glucopyranosato(1-methyl-1,3,5-triaza-7-phosphatricyclo[3.3.1.1^{3,7}]decanium-*P*) gold(I) (PTAMe-auranofin) and 2,3,4,6-tetra-*O*-acetyl-1-thio-β-D-glucopyranosato(triethylarsine) gold(I) (arsine-auranofin) compounds are tested for biological activity, if any, against cancer cell lines. Also, a chemiluminescence assay is done with the compounds at various concentrations to determine the effect they have on the chemiluminescence of isolated blood neutrophils.

Thus, the preliminary evaluation of selected gold(I) complexes synthesised in this study, is described in this chapter based on the above-mentioned rationale.

5.2 BIOLOGICAL STUDIES OF AURANOFIN AND ANALOGUES

5.2.1 Cell Assays

In the early 1980's, auranofin was found to be effective at increasing the lifespan of mice inoculated with P388 lymphocytic leukemia. At optimal dose, auranofin produced an increase in the life span of mice of 59% compared with 117% with cisplatin. According to several studies, auranofin showed activity against P388 leukemia when the drug was injected intraperitoneally. Although auranofin demonstrated definite activity, its anti-tumour effects were limited compared to conventional chemotherapeutic agents against murine tumour models *in vivo*. Under culture conditions, auranofin inhibited the ability of tumour cells to grow, and no changes were observed in the cell cycle. Three derivatives of auranofin namely PTA-auranofin, arsine-auranofin and PTAMe-auranofin (see § 5.1) with varying degrees of lipophilicity have been employed in the biochemical activity studies. These derivatives have different chemical properties than auranofin, which could possibly influence the distribution and entry of the derivatives into the cells. Thus the aim of this current biochemical study was to determine whether the derivatives of auranofin possess similar anti-tumour activity than the original drug.

The IC_{50} is a parameter used in pharmacological research and is commonly used as a measure of the concentration of inhibitor that affords 50% inhibition of the biologic activity[8]. The IC_{50} value is then defined as the half maximal inhibitory concentration which represents the concentration of an inhibitor that is required for 50% inhibition of its target (*i.e*. an enzyme, cell or microorganism)[9]. The IC_{50} value increases as the enzyme concentration increases and furthermore depending on the type of inhibition, other factors may influence the IC_{50} value.

5.2.2 Chemiluminescence Assays

Neutrophil chemiluminescence is used as a measure of reactive oxidant generation by resting or stimulated neutrophils. Polymorphonuclear neutrophils destroy microbial organisms by producing reactive oxygen species[10]. Together with photoemitters such as a lucigenin and luminol, different reactive oxidants can be measured including

superoxide (O_2^-) or oxidants of the MPO/halide/H_2O_2 system such as HOCl. In addition, this test can be performed in whole blood or in isolated neutrophils. The chemiluminescence assay experiment is based on the ability of neutrophils to emit flashes of light during phagocytosis. Phagocytosis is one of the main defences against bacterial infection and neutrophils are aided in taking up bacteria by antibody mechanism. The most crucial factor of phagocytosis is that once the organism is attached to the cell membrane, it is enclosed or engulfed in a pouch of the cell membrane and the phagoctic vesicle with its enclosed bacterium is free to sink into the endoplasm of the neutrophil.

5.3 EXPERIMENTAL

5.3.1 General

The preparation and characterisation of the complexes namely 2,3,4,6-tetra-*O*-acetyl-1-thio-β-D-glucopyranosato(triethylphosphine) gold(I) (auranofin); 2,3,4,6-tetra-*O*-acetyl-1-thio-β-D-glucopyranosato(1,3,5-triaza-7-phosphatricyclo[3.3.1.1^{3,7}]decane) gold(I) (PTA-auranofin); 2,3,4,6-tetra-*O*-acetyl-1-thio-β-D-glucopyranosato(1-methyl-1,3,5-triaza-7-phosphatricyclo[3.3.1.1^{3,7}]decanium-*P*) gold(I) (PTAMe-auranofin) and 2,3,4,6-tetra-*O*-acetyl-1-thio-β-D-glucopyranosato(triethylarsine) gold(I) (arsine-auranofin) which are used in cell assay and neutrophil chemiluminescence experiments as described in sections to follow were discussed in Chapter 3 under § 3.3.4.

The experiments done with auranofin and its analogue complexes as mentioned above, for the cell assays were done at the University of Pretoria, South Africa. The experimental procedures and the details including how the cell lines were assayed could not be made available for the purposes of this thesis.

The experimental procedure for the utilisation of the auranofin complexes mentioned above for the chemiluminescence assays is also discussed below. The experiments and experimental procedures used for the chemiluminescence assays were as well as for the cell assays mentioned above, protocols prepared at the Department of Pharmacology, University of Pretoria, South Africa. All common laboratory reagents and chemicals used in the preparations were of reagent grade and distilled water was used in all experiments. The following chemicals were commercially available: Heparin (Sigma Diagnostics); Histopaque-1077 (Sigma Diagnostics); NH_4Cl (Merck); Phosphate

buffered saline (Buffer) (Becton Dickinson); Hanks Balanced Salt Solution (Highveld Biological); Lucigenin (Sigma Diagnostics); Luminol (Sigma Diagnostics); 5-amino 2,3-dihydro-1,4-pthalazine-dione (Luminol) (Sigma Diagnostics); N-formyl-L-methionyl-L-leucyl-L-phenylalanine (Stimulant) (Sigma Diagnostics); Phorbol myristate acetate (Stimulant) (Sigma Diagnostics); Cal (Calcium ionophore) and opsonised zymosan. The blood specimen used for the isolation of neutrophils was obtained from the hospital. The chemiluminescence experiments were done on a Wallac chemiluminometer calibrated and thermostated at 37 °C.

The protocol procedures used for the chemiluminescence assays included protocols for the isolation of neutrophils from blood and for the actual neutrophil chemiluminescence experiments and these can be briefly summarised as follows in § 5.3.3.

5.3.2 Cell line Tests

The chemotherapeutic activity of auranofin and its three derivatives was evaluated using the following cell lines:

- human colon cancer (CoLo 320 DM)
- human adenocarcinoma cells of the cervix (HeLa)
- human leukemia cells (Jurkat)
- human ovarian cancer (A2780)
- human ovarian cancer (cisplastin resistant) (A2870 *cis*)

The following primary cultures were used to determine the cytotoxicity against normal cells.

- Lymphocytes (unstimulated and stimulated)
- Primary chicken fibroblasts

The cell assay experiments with auranofin and its analogue complexes involved addition of these four auranofin derivatives to samples of cell lines mentioned above according to the in-house protocol of the Pharmacology Department at the University of Pretoria, South Africa. The experimental procedures and the details including how the cell lines were assayed could not be made available for the purposes of this thesis.

5.3.3 Isolation of neutrophils and sample preparation for chemiluminescence studies

5.3.3.1 Isolation of neutrophils

Heparin (90 mg, 0.15 mmol) was mixed with distilled water (30 mL) and the solution was filtered and sterilised. This solution was then stored at temperatures of *ca*. 5 °C. Ammonium chloride (8.3 g, 0.16 mol), $NaHCO_3$ (1 g, 12 mmol) and EDTA (74 mg, 0.25 mmol) were dissolved in distilled water (2 l) and the solution was also stored in the fridge. The leucocyte counting fluid was prepared by mixing 0.1 mL of a 0.1% (100 mg/100 mL) gentian violet solution and glacial acetic acid (2 mL) with distilled water (100 mL) and the solution was also stored at 5 °C.

A sample of blood was collected and mixed with heparin (0.1 mL of the prepared heparin solution was used per millilitre of blood) in a blood collection bottle. This blood solution was carefully layered onto a histopaque solution (15 mL) which was already in a Ficoll plastic tube and the tube was filled to the top. The sample was centrifuged at room temperature for 25 minutes and after centrifugation the blood separated into various layers of red blood cells which settled at the bottom of the tube followed by a layer of neutrophils, histopaque solution layer, monocytes and lymphocytes layer and the top layer containing the plasma and platelets. The top layer was removed and discarded and the granulocyte layer was carefully separated into a clean 50 mL tube. The granulocytes were lysed by filling the tube to the top with ice cold 0.84% NH_4Cl. The solution was mixed well, allowed to stand in ice for 10 minutes and centrifuged for 10 minutes. The supernatant fluid was discarded and the pellet still containing some red blood cells was again repeatedly treated with NH_4Cl, discarding the supernatant fluid in each step, and the resultant white pellet abundantly containing neutrophils then treated with the phosphate buffered saline solution to wash off any remaining ammonium chloride. The solution was centrifuged for 10 minutes and the resultant supernatant fluid discarded and the pellet was vortexed and the cells were eventually counted under a microscope, standardised and suspended in a cold Hanks balanced salt solution of which the salt solution volume used is dependant on the amount of cells in the pellet.

5.3.3.2 Preparation of different samples for chemiluminescence experiments

The following reagents were used for the preparation of the different samples for the chemiluminescence experiment: Hanks balanced salt solution; A stimulant which contained N-formyl-L-methionyl-L-leucyl-L-phenylalanine, Phorbol myristate acetate (PMA), Calcium ionophore solution (a final concentration of 1μM was used in the cell suspension), Opsonised zymosan and a luminol (5-amino 2,3-dihydro-1,4-pthalazine-dione)-lucigenin solution; isolated and purified cells from blood and the several samples of auranofin complexes at three different concentrations (*i.e*. 0.3, 3.1 and 12.5 μM) for each of the four auranofin (auranofin, PTA-auranofin, PTAMe-auranofin and arsine-auranofin) complexes.

The opsonised zymosan solution was prepared by mixing zymosan (500 mg) with a 1M NaOH solution (10 mL) and the solution was put into a beaker of recently boiled water. After a few minutes the solution was mixed with plasma (500 mL) collected from the neutrophil purification procedure that had been spun down several times to remove platelets and debris. The solution was incubated in 37 °C water bath for 30 minutes while mixed frequently. The plasma was removed by centrifugation and washing twice in. The opsonised zymosan was diluted in the phosphate buffered saline solution so as to give a concentration of 10 mg/mL and the use of 100 μL into 1 mL of reaction volumes will give a final concentration of 1 mg/mL.

Before the chemiluminescence experiment was started, the cells were pre-incubated together with the chemiluminescent agent for at least 30 minutes. Equal volumes of the cell suspension (±1 x 10^7 cells/mL) and lucigenin were mixed and incubated on wet ice for a minimum of 30 minutes. The controls were also aliquoted for the same time interval as the experimental samples. Each experimental run for the chemiluminescence assay when each auranofin complex was used contained six separate cuvettes for the three different auranofin concentrations and three controls (*i.e*. a blank solution, a resting control and a positive control).

The experimental procedure indicated that the samples added to the six different chemiluminometer cuvettes were prepared as follows for each of the experimental runs:

Cuvette 1 contained the blank with luminol-lucigen and the Hanks solutions.
Cuvette 2 contained the resting control with luminol-lucigen solution, Hanks solution and the cells but no stimulant nor the auranofin solution.
Cuvette 3 contained the positive control with the luminol-lucigen solution, Hanks solution, the cells and the stimulant but no auranofin solution.
The last three cuvettes, (cuvettes 4-6), each contained a different auranofin concentration (either 0.3, 3.1 or 12.5 μM) with the luminol-lucigen solution, Hanks solution, the cells and the stimulant. Thus the different additions of the solutions to the different chemiluminometer cuvettes for the experiment can be tabulated as follows.

Table 5.1 The different amounts of solutions added to the several chemiluminescence cuvettes in order to make up samples for the experiment.

Solution added	Samples			
	Blank (cuvette 1)	Resting control (cuvette 2)	Positive control (cuvette 3)	Auranofin samples (three different concentrations, cuvettes 4 - 6)
Hanks balanced salt solution (mL)	0.9	0.8	0.7	0.6
Luminol (μL)	100	-	-	-
Lucigenin / Cell suspension luminol (μL)	-	200	200	200
Auranofin analogue (μL)	-	-	-	100
Stimulant (μL)	-	-	100	100

The values obtained for the blank sample from the chemiluminescence experiment were subtracted from the value of each subsequent tube. The resting samples were included in order to give an indication of the degree of stimulation of the neutrophils and the positive controls for comparison purposes when the effects of the pharmacological agents on chemiluminescence are assessed.

5.4 RESULTS AND DISCUSSION

5.4.1 Cell line Tests

The IC_{50} values for the different auranofin complexes are presented in Table 5.2.

Table 5.2 IC_{50} values (μg/mL) of auranofin and its analogues towards selected cell lines.

	1[a]	2[b]	3[c]	4	5	6	7	8
	Lymph A	Lymph B	Fibro	Colo	HeLa	Jurkat	A2780	A2870 *cis*
Auranofin, I	0.713	1.234	0.873	0.371	0.172	0.747	0.012	0.551
PTA-auranofin, II	6.428	3.334	2.729	1.122	8.463	2.474	0.018	2.388
Arsine-auranofin, III	0.383	1.996	3.383	0.502	1.070	0.299	0.0076	1.219
PTAMe-auranofin, IV	4.078	5.018	1.003	0.614	4.993	5.995	0.010	1.986

[a] Lymph A = Lymphocytes (stimulated)
[b] Lymph B = Lymphocytes (unstimulated)
[c] Fibro = Chicken fibroblasts

The results of the effectiveness of auranofin and its derivatives against selected cell lines as outlined in Table 5.2 can be summarised as follows:

- All the results presented in Table 5.2 show a dose-dependant response (columns1-8).
- Auranofin and arsine-auranofin show the most activity against all the cell lines and primary cultures (see rows I and III *vs* II and IV).
- Auranofin and arsine-auranofin seem to be closely related to each other whereas PTA-auranofin and PTAMe-auranofin show more correlation to each other (see rows I and III *vs* II and IV).
- A2780 human ovarian cancer cell lines are the cell lines which are most sensitive to all derivatives (see column 7).
- The arsine-auranofin compound seems to be the most promising derivative especially against A2780 human ovarian cancer cell lines showing an IC_{50} of only about 0.0076.

5.4.2 Chemiluminescence Assays

The chemiluminescence of neutrophils in the presence of varying concentrations of auranofin and its three derivatives (PTA-auranofin, PTAMe-auranofin and arsine-auranofin) is compared and discussed in this section. For each of the auranofin derivatives three concentrations (0.3, 3.1 and 12.5 μM) are employed and compared to the controls. Chemilumiescence assay experiments can vary from experiment to experiment and hence the experiments are done in duplicate to show the general trends observed and to check for reproducibility of the results and the graphs obtained are presented in Figs 5.1 - 5.4.

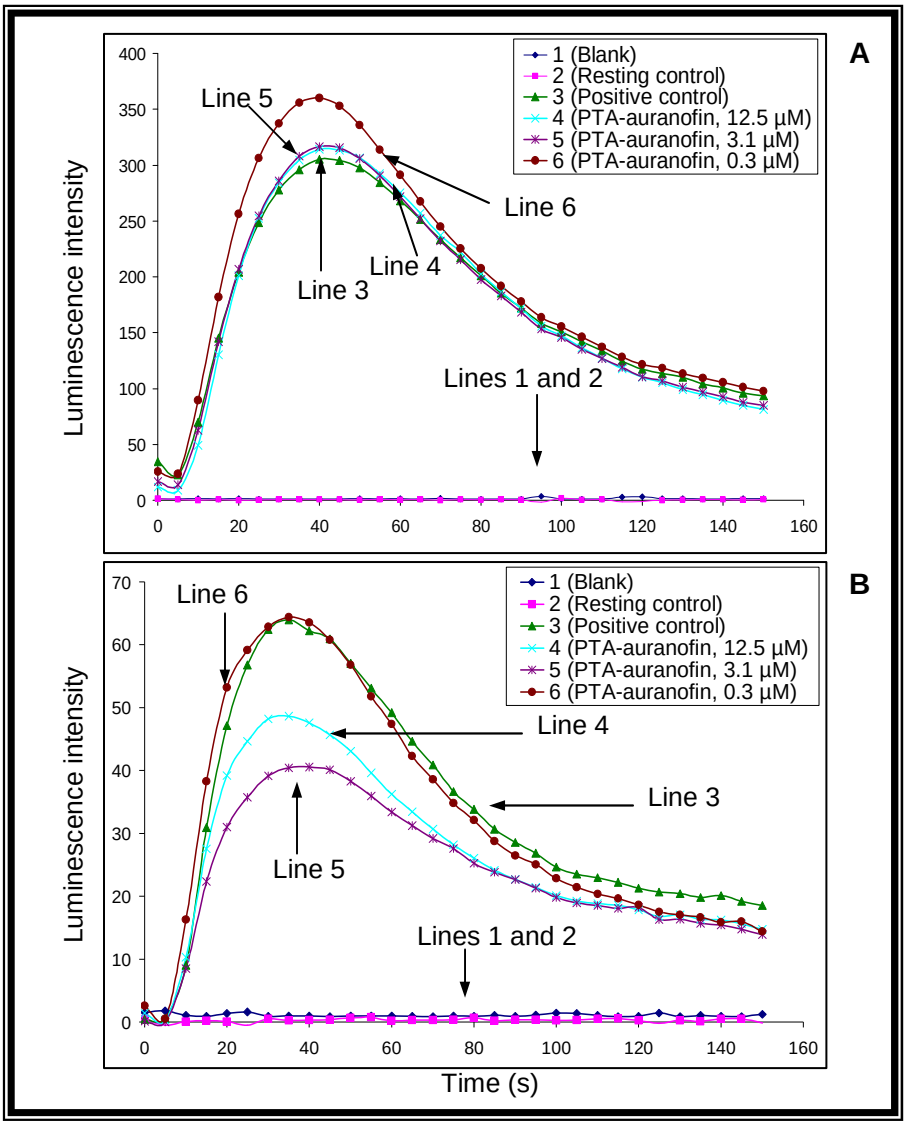

Figure 5.1 The graphs showing the luminol-dependent chemiluminescence *vs* time response of neutrophils when treated with three different concentrations (0.3, 3.1 and 12.5 μM) of PTA-auranofin. Graph B = duplicate experiment. The three concentrations namely 12.5, 3.1 and 0.3 μM are represented by lines 4, 5, and 6 respectively. Lines 3 = positive control. The blank and resting control lines (lines 1 and 2) are overlapping each other on the time axis.

Fig. 5.1 indicates the chemiluminescence intensity of the various concentrations of PTA-auranofin with time over a period of approximately 3 minutes. The lower the concentration of the PTA-auranofin complex, the higher is the luminescence intensity. This indicates that at high concentrations the complex act as an inhibitor to the neutrophils. In this experiment, it is noted that the 3.1 and 12.5 μM concentrations have approximately the same intensity.

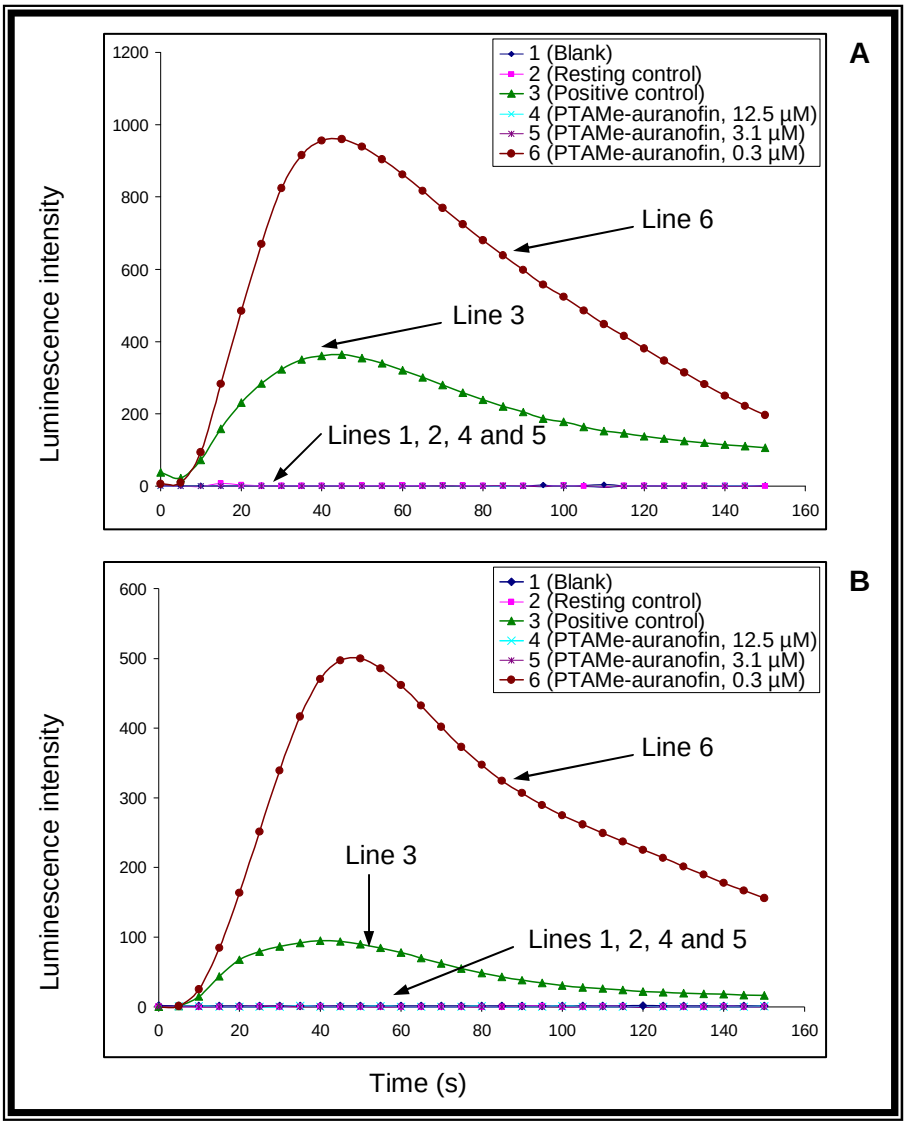

Figure 5.2 The graphs showing the luminol-dependent chemiluminescence *vs* time response of neutrophils when treated with three different concentrations (0.3, 3.1 and 12.5 μM) of PTAMe-auranofin. Graph B = duplicate experiment. Lines 3 and 6 = positive control and 0.3 μM PTAMe-auranofin respectively. The blank, resting control, 3.1 and 12.5 μM PTAMe-auranofin lines are overlapping each other on the time axis.

Fig. 5.2 indicates the chemiluminescence intensity of the various concentrations of the PTAMe-auranofin complex with time over a period of approximately 3 minutes. At 0.3

μM concentration of the complex, the graph shows the highest intensity which indicates that at this concentration the complex acts as a stimulant to the neutrophils. There is no luminescence intensity shown when 3.1 and 12.5 μM concentrations of the PTAMe-auranofin are investigated resulting in the inhibition of the neutrophils. Within neutrophils, the heme protein myeloperoxidase (MPO) mediates the production of hypochlorous acid (HOCl), a potent microbial compound[11]. Early in the phagocytic process, neutrophils undergo a respiratory burst, generating oxygen free radicals which after their production and release decay naturally and emit light[12]. Thus, chemiluminescence enhanced by the presence of luminol (5-amino 2,3-dihydro-1,4-pthalazine-dione) may be used as a measure of phagocytic activity.

The figures showing the chemiluminescence intensity when different concentrations of each of the PTA-auranofin or PTAMe-auranofin complex is used, are illustrated in Figs. 5.1 and 5.2 respectively. It can therefore be noted that when PTA-auranofin is investigated the peak chemiluminescence was reached within 30 s whereas for the PTAMe-auranofin the highest peak of the chemiluminescence activity was reached within 50 s. Also PTAMe-auranofin showed a longer decline in luminescence as compared with PTA-auranofin which indicated a sharper decline. Fig 5.1 also illustrates that all three concentrations show peak chemilumescence with 0.3 μM showing the highest peak activity. This indicates that at 0.3 μM concentration PTA-auranofin acts as a stimulant to the neutrophils as the line corresponds with the one for the positive control which has an added stimulant.

In Fig. 5.2 where PTAMe-auranofin at different concentrations is investigated for neutrophil activity, it is observed that concentrations 3.1 and 12.5 μM do not show any activity suggesting that at these concentrations PTAMe-auranofin acts as an inhibitor to the neutrophils.

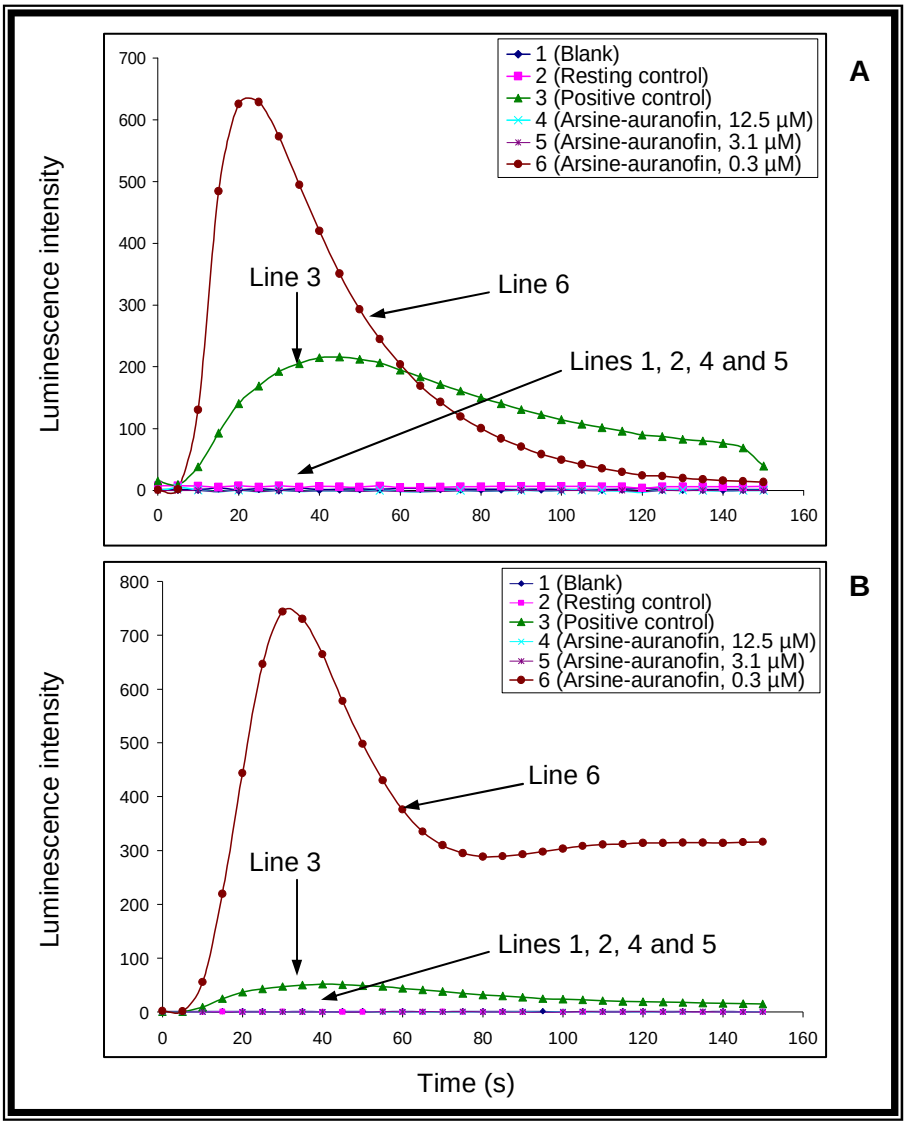

Figure 5.3 The graphs showing the luminol-dependent chemiluminescence *vs* time response of neutrophils when treated with three different concentrations (0.3, 3.1 and 12.5 μM) of arsine-auranofin. Graph B = duplicate experiment. Lines 3 and 6 = positive control and 0.3 μM arsine-auranofin respectively. The blank, resting control, 3.1 and 12.5 μM arsine-auranofin lines are overlapping each other on the time axis.

The chemiluminescence activity of the neutrophils with different concentrations of the arsine-auranofin is presented in Fig. 5.3 above. The graph indicates that the low concentration (0.3 μM) of the complex acts as a stimulant while high concentrations (3.1 and 12.5 μM) act as inhibitors hence no luminescence activity is observed. The result obtained is comparable to the one observed for the PTAMe-auranofin, Fig 5.2.

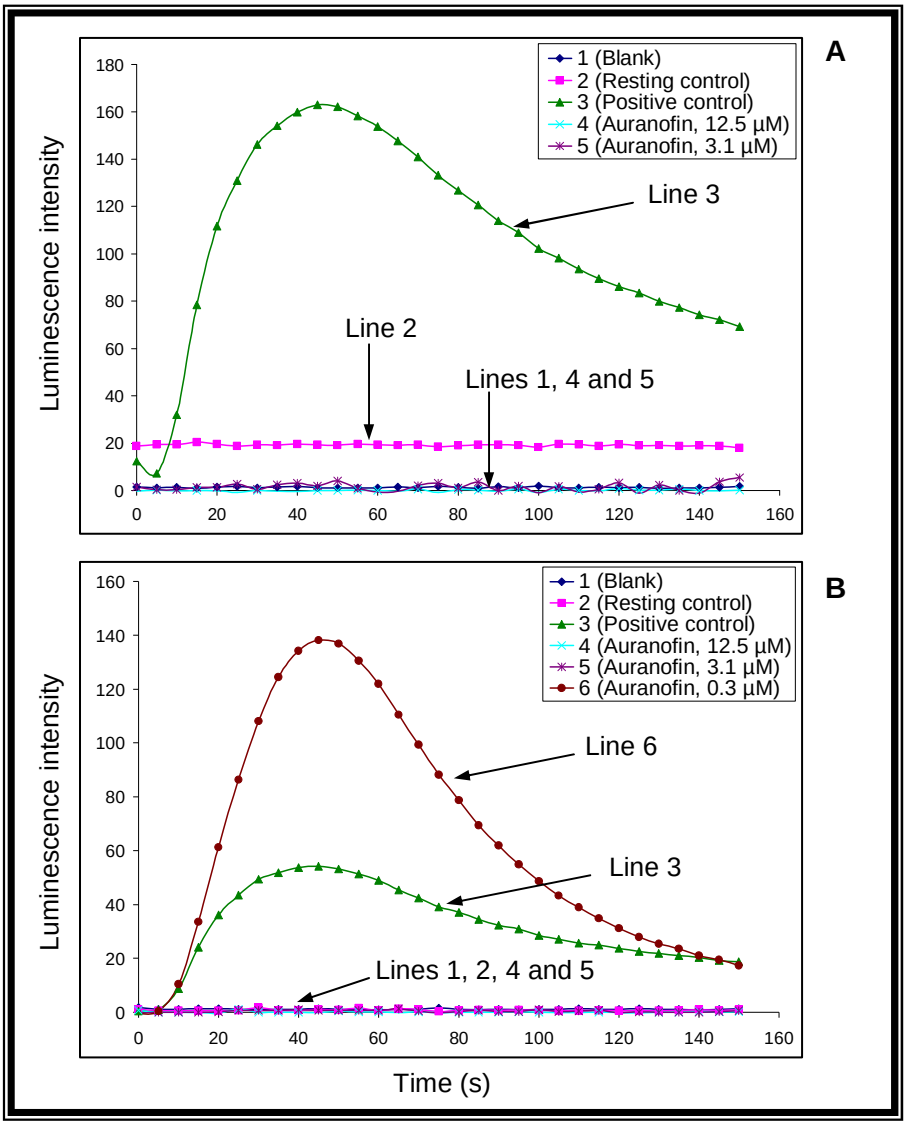

Figure 5.4 The graphs showing the luminol-dependent chemiluminescence *vs* time response of neutrophils when treated with three different concentrations (0.3, 3.1 and 12.5 μM) of auranofin. Graph A reported experimental error and discrepancy hence lines 6 is not shown, lines 2 and 3 = resting and positive controls respectively. In this graph the blank, 3.1 and 12.5 μM auranofin lines are overlapping each other on the time axis. Graph B = duplicate experiment where lines 3 and 6 = positive control and 0.3 μM auranofin respectively. The blank, resting control, 3.1 and 12.5 μM auranofin lines are overlapping each other on the time axis.

Figure 5.4 shows a comparison of neutrophil chemiluminescence in the presence of varying concentrations of auranofin. The concentrations of auranofin which were used for the determination were 0.3, 3.1 and 12.5 μM. From this experiment, it was noted that for the 0.3 μM auranofin sample the line indicating the chemiluminescence intensity had too much noise as compared with other auranofin samples at different concentrations hence it was not plotted in the figure. As can be seen on the figure,

there was no intensity observed for when 3.1 and 12.5 μM auranofin concentrations are used. This indicates that at these auranofin concentrations the auranofin compound acts as an inhibitor to neutrophil chemilumescence activity.

Figs 5.3 and 5.4 illustrate graphs showing the effects of auranofin and arsine-auranofin at different concentrations on chemiluminescence intensity from stimulated neutrophils respectively. The graphs for auranofin and arsine-auranofin are observed to be similar to each other. On both graphs, at 0.3 μM concentration the highest chemiluminesence peak is observed compared to other higher concentrations, indicating that the complexes at this concentration act as stimulants to the neutrophils. The arsine-auranofin at 0.3 μM concentration shows the highest peak intensity when compared with auranofin at the same concentration. At 3.1 and 12.5 μM concentrations no chemiluminescence activity is observed for both complexes indicating inhibition of the neutrophils. At a concentration of 0.3 μM, auranofin shows a longer decline after the high peak chemiluminescence intensity is reached whereas for the arsine auranofin a sharper decline is observed for the same concentration.

5.5 CONCLUSION

5.5.1 Cell line Studies

The activity of auranofin and its derivatives namely PTA-auranofin, PTAMe-auranofin and arsine-auranofin against selected cell lines for anti-cancer or anti-tumour activity was investigated. From the results above, the following can be noted:

- From the cell line assay experiments it is noted that toxicity of the compounds to the cells showed a dose-dependant response.
- More prominent was the activity observed for auranofin and arsine-auranofin derivatives as compared to the PTA analogues, which had less activity.
- The arsine derivative of auranofin *i.e*. the 2,3,4,6-tetra-*O*-acetyl-1-thio-β-D-glucopyranosato(triethylarsine) gold(I) complex was the most promising derivative against A2780 human ovarian cancer cell lines but was observed to have higher toxicity to other cells.

5.5.2 Chemiluminescence Studies

Also discussed in this chapter is a preliminary chemiluminescence experiment to determine the effect of the complexes on isolated neutrophils. For the preliminary chemiluminescence experiments it can be concluded that for all auranofin derivatives at low concentrations the compounds act as stimulants to the neutrophil chemiluminescence activity and at higher concentrations the compounds act as inhibitors to neutrophil chemiluminescence activity.

However, for the chemiluminescence experiments the results can be affected by a number of factors such as the type of machinery used and the number of neutrophils in the blood specimen used to mention but a few. Hence the chemiluminescence assay system is subject to a variety of factors that need to be carefully controlled in the application of this test. It can then be concluded that more research coupled by complimentary experiments to the study of neutrophil chemiluminescence needs to be explored further in future.

[1] G.J. Higby, *Gold Bull.,* 1982, **15**, 130.

[2] W.F. Kean, C.J.L. Lock, H. Howard-Lock, *Inflammopharmacology,* 1991, **1**, 103.

[3] P.J. Sadler, *Struct. Bonding,* 1976, **29**, 171.

[4] C.F. Shaw III, *Inorg. Persp. Biol. Med.,* 1979, **2**, 278.

[5] D.H. Brown, W.E. Smith, *Chem. Soc. Rev.,* 1980, **9**, 217.

[6] P.J. Sadler, M. Nasr, V.L. Narayanan, In 'Platinum Coordination Complexes in Cancer Chemotherapy', edited by M.P. Hacker, E.B. Douple, I.H. Krakoff; Martinus Nijhoff, Boston, 1984, pp 290-304.

[7] C.F. Shaw III, In 'Metal Compounds in Cancer Therapy', edited by S.P. Fricker; Chapman and Hall, London, 1994, p. 46-64.

[8] R. Munoz, Y. Arias, J.M. Ferreras, M.A. Rojo, M.J. Gayoso, M. Nocito, J. Benitez, P. Jimenez, C. Bernabeu, T. Girbes, *Cancer Lett.,* 2007, **256**, 73.

[9] http://www.en.wikipedia.org/wiki/IC50.

[10] C.M. Casimir, C.G. Teahan, In 'Immunopharmacology of neutrophils', edited by P.G. Hellewell, T.J. Williams; Academic Press, London, 1994, 27.

[11] J.E. Harrison, J. Schultz, *J. Biol. Chem.,* 1976, **251**, 1371.

[12] B.M. Babior, R.S. Kipnes, J.T. Curnutte, *J. Clin. Investig.,* 1973, **52**, 741.

6 SUBSTITUTION REACTIONS OF GOLD(I) TERTIARY PHOSPHINE COMPLEXES

6.1 INTRODUCTION

Research on gold complexes has been ongoing because of their importance in several applications such as in medicine, glass and ceramics industry and in the field of nanoparticles[1]. Although kinetic studies of nucleophilic displacement of ligands from square planar complexes of d^8 transition metal ions have in the past been limited mainly to those of platinum(II)[2], sufficient information about the behaviour of corresponding gold(III) complexes has emerged for it to be possible to attempt to make a preliminary general comparison of the kinetic behaviour of Pt(II) and Au(III) substrates. Previous kinetic studies of reduction of gold(III) complexes by various one-electron reducing nucleophiles Y, such as iodide, thiocyanate, thiosulphate, thiourea and alkyl sulphides provide evidence for a common intermolecular reaction mechanism in many of these systems[3,4]. Research about the *cis* and *trans* effects in square-planar gold(III) complexes have been the subject of a review[5]. Reactions between gold(III) complexes and efficient nucleophiles such as iodide has been widely investigated[6,7,8,9]. Extensive mechanistic studies of ligand substitution reactions in solution have long been reported for four- and six-coordinated transition metal complexes[10,11]. Very few studies can however be found in the chemical literature concerning ligand substitution of linear two-coordinate systems such as that of gold(I) complexes. The interest in the investigation of substitution kinetics of linear gold(I) complexes stems from an attempt to correlate kinetic data and perhaps mechanistic pathways imposed on other widely studied transition metals such as Pt(II).

As mentioned in earlier chapters of this thesis the platinum(II) complex, *cis*-$[Pt(NH_3)_2Cl_2]$ (cisplatin) is widely used as a chemotherapeutic agent for the treatment of a variety of cancers[12]. It is generally believed that DNA is the cellular target for the drug[13] and X-ray and NMR studies of short oligonucleotide-Pt complexes establish that the N-7 sites of the purine rings of DNA are involved in coordination to platinum[14,15]. Platinum(II) has a remarkable affinity for sulphur donors and there are substantial thiol

concentrations in the cell due to cysteine, glutathione (GSH) and various cytosolic proteins. A significant portion of the administered drugs binds to biological thiols, among which cysteine and glutathione are the most reactive towards platinum(II).

It is of general knowledge that gold also has much affinity to sulphur donor ligands and hence with the interesting build up of research as briefly mentioned above, the reaction kinetics of linear gold(I) complexes with such ligands was attempted. Substitution investigations of the reactions of the tertiary phosphine gold(I) complexes used in the research as synthesised and discussed in Chapters 3 and 4 with ligands such as L-cysteine, SCN^- and dimethyl thiourea are attempted and discussed in this chapter.

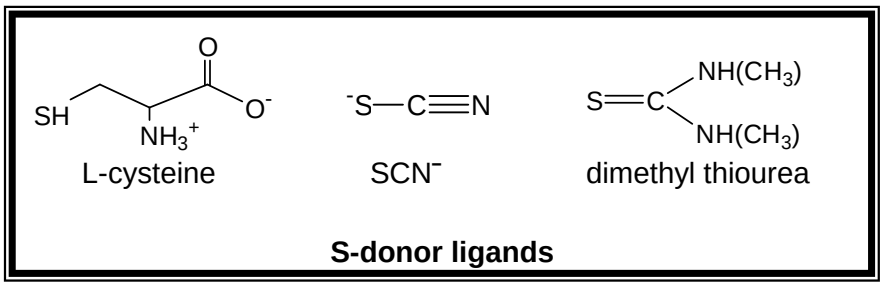

6.2 EXPERIMENTAL

The preparation, spectroscopic and crystallographic characterisation of the gold(I) ferrocenyl complexes used in the investigations were described in Chapter 4, § 4.3.3.1, 4.3.3.4 and 4.3.4.1 and of the linear $[Au(PPh_3)Cl]$ complex in Chapter 3, § 3.3.3.3. All common laboratory reagents and chemicals used in the preparations were of reagent grade and distilled water was used in all experiments.

6.2.1 Equilibrium studies

UV-Vis investigations for the initial preliminary evaluation of stability or decomposition reactions of the complexes with ligands were performed using a Cary 50 Conc spectrophotometer. The apparatus was equipped with constant temperature water baths regulated within 0.1 °C. The experiments for substitution reactions were conducted with gold ferrocenyl complexes such as ($[(AuCl)_2(\mu\text{-dppf-CH}(CH_3)N(CH_3)_2)]$, $[(AuCl)_2(\mu\text{-dppf-CH}(CH_3)OAc)]$, $[(AuSCN)_2(\mu\text{-dppf-CH}(CH_3)OAc)]$), $[Au(PPh_2Fc)Cl]$ and linear $[Au(PPh_3)Cl]$ and these complexes were reacted with ligands such as L-cysteine, thiourea and SCN^-. These thiol ligands were used in order to investigate substitution reactions that would mimic reactions in biological environments. The solutions of the

complexes were prepared in 1% DMSO:H_2O, DMSO or ethanol as described in the captions of the respective figures and different concentrations of the ligands were added to these solutions. The investigations were done at 25 °C.

The equilibrium constant determination experiments as investigated by use of ^{31}P NMR by monitoring the chemical shift of the peaks observed were all conducted using freshly prepared gold complexes and ligand solutions, in DMSO solvent and at 25 °C. For equilibrium constant determinations the gold solutions were mixed with different concentrations of the various halide/pseudo-halide solutions and the final concentrations for Au(I) and halide are indicated in the respective figure captions. Data analysis was conducted by means of Microsoft Excel 97 and the chemical shifts of the peaks observed were plotted against halide concentrations in order to obtain equilibrium constants using the least-squares program Scientist[16]. The phosphorus-31 NMR spectra for the gold complexes dissolved in DMSO were recorded on a 300 MHz Bruker spectrometer operating at 121.497 MHz for ^{31}P. The ^{31}P chemical shifts are reported as calibrated at 0 ppm relative to 85% H_3PO_4 as an internal standard in a capillary. Experiments were done with the various mono and dinuclear gold complexes with different SCN^- concentrations. The equilibrium constants (K_L) obtained from reacting mononuclear R-Au-Cl (R = P-donor ligand) complexes with the various ligands (L = SCN^-) were determined using the following equation which also represents the equilibrium reaction process:

$$[\text{Au-Cl}] + \text{L} \underset{}{\overset{K_L}{\rightleftharpoons}} [\text{Au-L}] + \text{Cl}^- \qquad (6.1)$$

The equation used in fitting the data and obtaining the plots of the observed chemical shift (δ_{obs}) versus ligand concentration, [L], is presented as Eq. 6.2. This model allows for the calculation of the uncoordinated ligand concentration at equilibrium using an additional quadratic function with δ_R as the chemical shift observed for the reactants, δ_P as the chemical shift for the products and $[L]_f$ as the final ligand concentration. The derivation of the equation is given in the Appendix, § A.6.1.

$$\delta_{obs} = \frac{\delta_R[Cl^-] + \delta_P K_L[L]_f}{[Cl^-] + K_L[L]_f} \qquad (6.2)$$

Similarly, the equilibrium constants (K_L) obtained from reacting dinuclear ferrocenyl gold(I) complexes with ligand SCN^- were determined using the following equation which also represents the equilibrium reaction process:

$$[\text{Au}_2\text{-Cl}_2] + 2\text{L} \underset{}{\overset{K_L}{\rightleftharpoons}} [\text{Au}_2\text{-L}_2] + 2\text{Cl}^- \qquad (6.3)$$

The equation used in fitting the data and obtaining the plots of the chemical shift versus ligand concentration is presented as Eq. 6.4 and this model allows for the calculation of the uncoordinated ligand concentration at equilibrium using an additional cubic function with parameters δ_R, δ_P and $[L]_f$ as described above. The derivation of the equation is given in the Appendix, § A.6.2.

$$\delta_{obs} = \frac{\delta_R[Cl^-]^2 + \delta_P K_L[L]_f^2}{[Cl^-]^2 + K_L[L]_f^2} \qquad (6.4)$$

6.2.2 Kinetic studies

The fast reaction kinetic experiments of the chloride substitution from $[Au(PPh_3)Cl]$ with different ligands were done at 2 °C on an Applied Photophysics instrument attached to a J&M diode array detection unit of which the apparatus was equipped with a constant temperature bath which regulates temperature within ± 0.1 °C and also at -5 °C on a High-Tech Scientific Kinet Asyst stopped-flow system equipped with a cryogenic temperature unit[17]. The experiments were all conducted using freshly prepared $[Au(PPh_3)Cl]$ complex and ligand (L = SCN^- and dimethyl thiourea) solutions, in methanol as a solvent. The final $[Au(PPh_3)Cl]$ and halide concentrations for each of the reactions investigated and the selected wavelengths are indicated in the respective figure captions in § 6.3.7. Data analysis was conducted by means of Microsoft Excel 97 and observed reaction rates were obtained from the absorbance versus time traces using the least-squares program Scientist[16]. The equation for the determination of the rate constants of chloride substitution reactions with ligands such as SCN^- from linear, mononuclear Au-Cl systems can be represented as follows.

$$[Au\text{-}Cl] + L \underset{k_{-1}}{\overset{k_1}{\rightleftharpoons}} [Au\text{-}L] + Cl^- \qquad (6.5)$$

The k_{obs} values were calculated from plots of absorbance versus time graphs for each of the ligand concentration used (*i.e*. for when 0 - 150 mM ligand added) using the following first-order equation with parameters A_{obs}, A_1, A_0 and T as the overall observed absorbance, initial absorbance at the start of the reaction, final absorbance and temperature respectively.

$$A_{obs} = A_1 - (A_1 - A_0)*\exp((-k_{obs})*T) \qquad (6.6)$$

The rate equation for the chloride substitution process defined in Eq. 6.5 is given in Eq. 6.7,

$$R = k_1[L][Au\text{-}Cl] - k_{-1}[Au\text{-}L][Cl^-] \quad (6.7)$$

which reduces under [L], [Cl^-] >> [Au] pseudo first-order conditions to Eq. 6.8 (see also more complete discussions in § 6.3.6). The calculated k_{obs} values obtained were then plotted against the different ligand concentrations using Eq. 6.8 to obtain the forward reaction rate constant (k_1) and the reverse reaction rate constant (k_{-1}).

$$k_{obs} = k_1[L] + k_{-1} \quad (6.8)$$

6.3 RESULTS AND DISCUSSION

6.3.1 Substitution of chloride from tertiary phosphine dinuclear gold(I) complexes by various entering ligands

In this section, different experiments and results are described which have been performed in an attempt to evaluate the dynamics and equilibrium characteristics of these dinuclear [$(AuCl)_2$(μ-dppf-$CH(CH_3)N(CH_3)_2$)] and [$(AuCl)_2$(μ-dppf-$CH(CH_3)OAc$)] complexes. Therefore, stability experiments as well as preliminary substitution experiments on the chloride substitution from [$(AuCl)_2$(μ-dppf-$CH(CH_3)OAc$)] by different ligands like L-cysteine were done. The [$(AuCl)_2$(μ-dppf-$CH(CH_3)OAc$)] complex was primarily selected for the substitution experiments since it had better solubility properties than [$(AuCl)_2$(μ-dppf-$CH(CH_3)N(CH_3)_2$)].

6.3.1.1 Stability of the [$(AuCl)_2$(μ-dppf-$CH(CH_3)OAc$)] complex

The stability of the [$(AuCl)_2$(μ-dppf-$CH(CH_3)OAc$)] complex in 1% DMSO:H_2O solution was investigated for decomposition over a time period and none was observed, see Fig. 6.1.

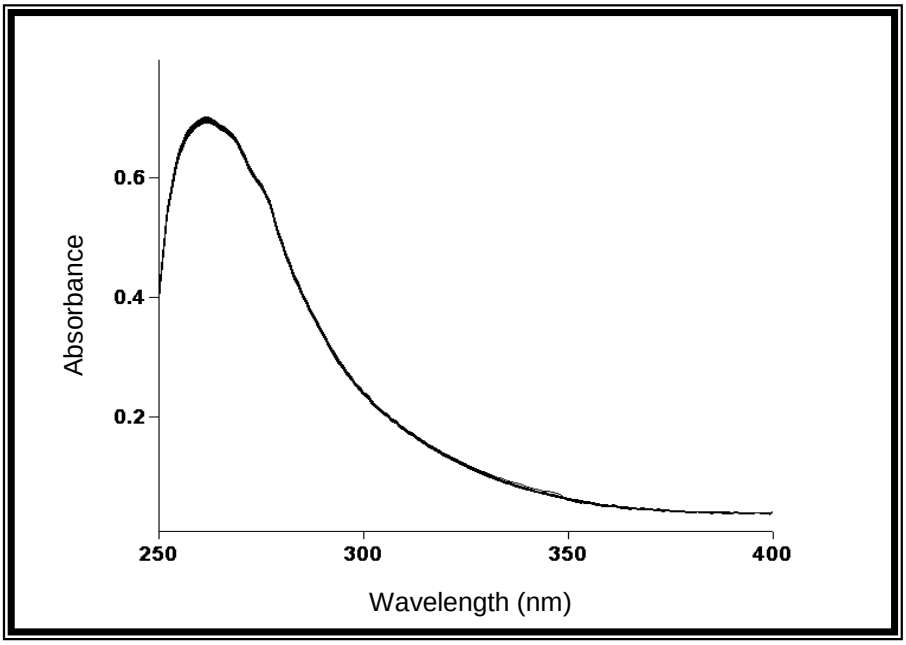

Figure 6.1 UV-Vis overlay of spectra of the [$(AuCl)_2$(μ-dppf-$CH(CH_3)OAc$)] complex in 1% DMSO:H_2O. [Au] = 0.01 mM. Scans were taken over 2 h and at 25 °C.

6.3.1.2 Reaction of [$(AuCl)_2$(μ-dppf-$CH(CH_3)OAc$)] with L-cysteine

The 0.01 mM solution of the [$(AuCl)_2$(μ-dppf-$CH(CH_3)OAc$)] complex was reacted with equimolar solutions of L-cysteine in 1% DMSO:H_2O as presented in Fig. 6.2 below. The absorbance readings were taken over time and at different wavelengths.

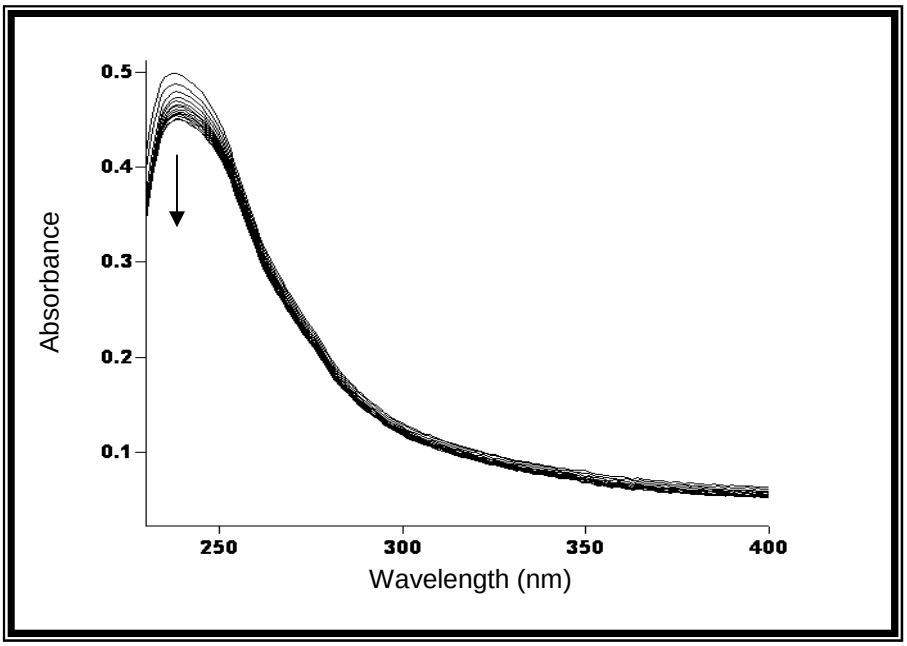

Figure 6.2 UV-Vis overlay of spectra of [$(AuCl)_2$(μ-dppf-$CH(CH_3)OAc$)] with L-cysteine in 1% DMSO:H_2O. [Au] and [L-cysteine] were both 0.01 mM. Scans were taken over a period of approximately 2 h and at 25 °C.

Upon conclusion of the experiment, selected data points at wavelength of 237 nm were plotted against time and the graph is presented in Fig. 6.3, showing a deviation from first-order behaviour.

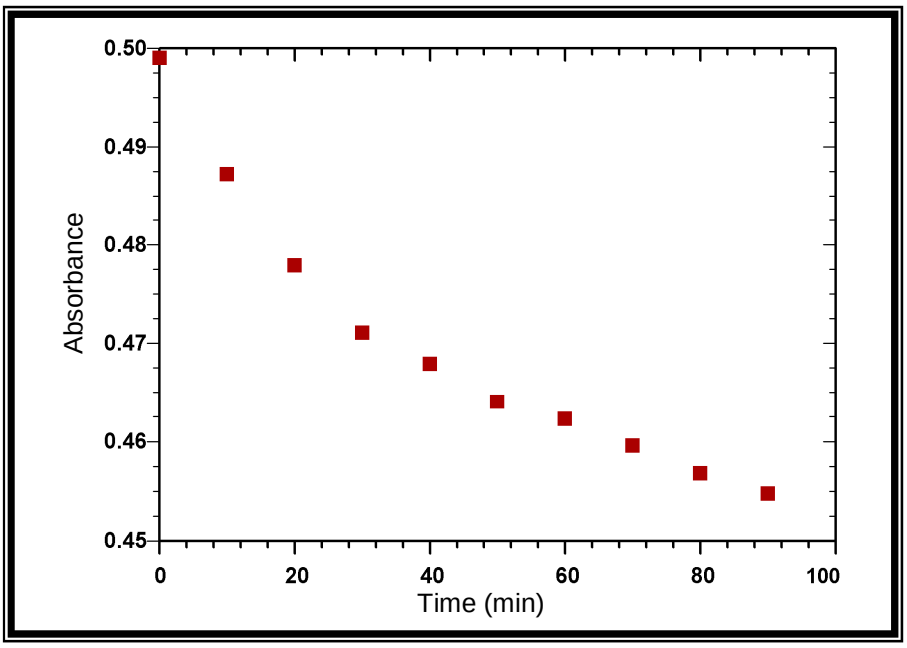

Figure 6.3 Scientist plot of absorbance changes over time when $[(AuCl)_2(\mu\text{-dppf-}CH(CH_3)OAc)]$ is reacted with equimolar amounts of L-cysteine in 1% DMSO:H_2O solution at 25 °C. [Au] and [L-cysteine] = 0.01 mM. λ = 237 nm.

Fig. 6.2 illustrates the reaction of the $[(AuCl)_2(\mu\text{-dppf-}CH(CH_3)OAc)]$ complex with the ligand L-cysteine. It can be assumed that bond formation between the gold(I) complex and L-cysteine is *via* the S-group of the amino acid as gold has a high affinity for S-donor ligands and is anticipated from previous research studies of Pt(II) complexes[18,19,20]. The substitution reaction of $[(AuCl)_2(\mu\text{-dppf-}CH(CH_3)OAc)]$ complex with L-cysteine indicated a decrease in absorbance change as illustrated in Figs. 6.2 and 6.3. The information obtained when data points of absorbance were plotted against time as shown in Fig. 6.3 above showed a slow reaction. However, other preliminary tests (see Chapter 3 and structural studies in Chapter 4) indicated substitution reactions for gold(I) complexes were anticipated to be very fast reactions. The slow reaction observed was therefore assumed to be either a hydrolysis or a decomposition reaction. It is clear from Fig. 6.3 that the reaction is not simple first order. However, due to solubility problems of the ligand as well as the complex in common media, the reactions could not be investigated in further details *i.e*. with a larger range of concentrations. Therefore, a preliminary reaction of the $[(AuCl)_2(\mu\text{-dppf-}CH(CH_3)OAc)]$ complex with other simpler ligands like SCN^- was attempted which is presented in the following section.

6.3.1.3 Substitution of chloride from [$(AuCl)_2$(μ-dppf-$CH(CH_3)OAc$)] with SCN^-

Fig. 6.4 illustrates the reaction of [$(AuCl)_2$(μ-dppf-$CH(CH_3)OAc$)] complex with SCN^- as ligand at equimolar concentrations.

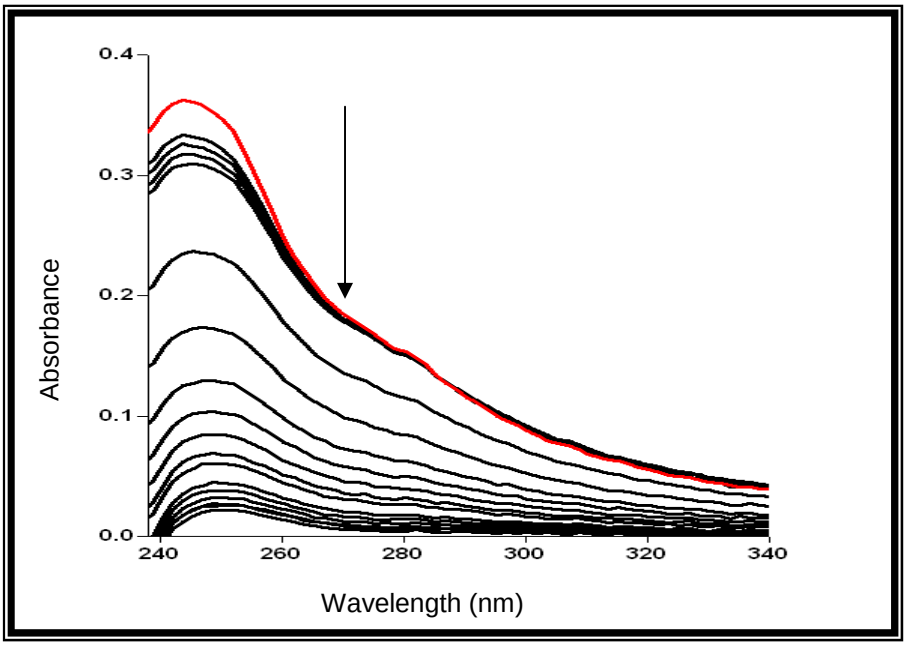

Figure 6.4 UV-Vis overlay of spectra of [$(AuCl)_2$(μ-dppf-$CH(CH_3)OAc$)] with SCN^- at 25 °C in 1% DMSO:H_2O solution. Scans were taken over a period of 36 hours at 2 h intervals. [Au] and [SCN^-] = 0.01 mM.

An absorbance decrease was observed as the [$(AuCl)_2$(μ-dppf-$CH(CH_3)OAc$)] complex was reacted SCN^-. From this experiment the [$(AuCl)_2$(μ-dppf-$CH(CH_3)OAc$)] complex slowly reacted with SCN^- and data was selected at wavelength 248 nm and a plot of the absorbance change versus time is shown in Fig. 6.5.

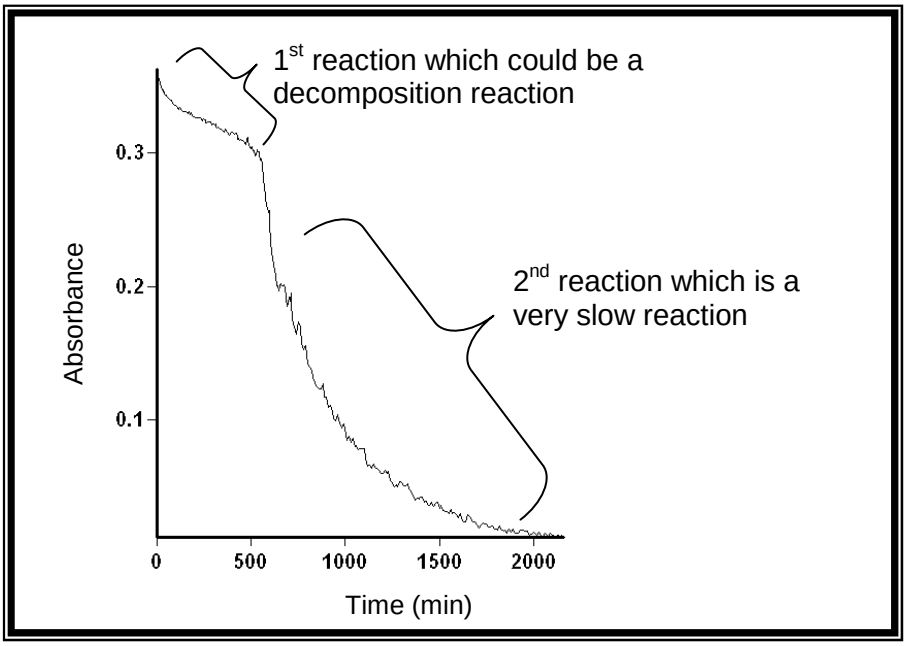

Figure 6.5 Absorbance changes over time when $[(AuCl)_2(\mu\text{-dppf-CH}(CH_3)OAc)]$ is reacted with equimolar amounts of SCN^- in 1% DMSO:H_2O solution at T = 25 °C. [Au] and $[SCN^-]$ = 0.01 mM. λ = 248 nm.

It was noted in Fig. 6.5 that there are two reactions observed for the reaction of $[(AuCl)_2(\mu\text{-dppf-CH}(CH_3)OAc)]$ with SCN^-. The first reaction which could be a decomposition reaction is observed within approximately 400 minutes (though there was no reduction to metallic gold observed), followed by the slow second reaction. The data for the second reaction at 248 nm was fitted on a Scientist curve as illustrated in Fig. 6.6. However, again as it is the case with L = L-cysteine, the reactions were very slow and it was concluded from preliminary tests that more rapid reactions which represent chloride substitution are not observed.

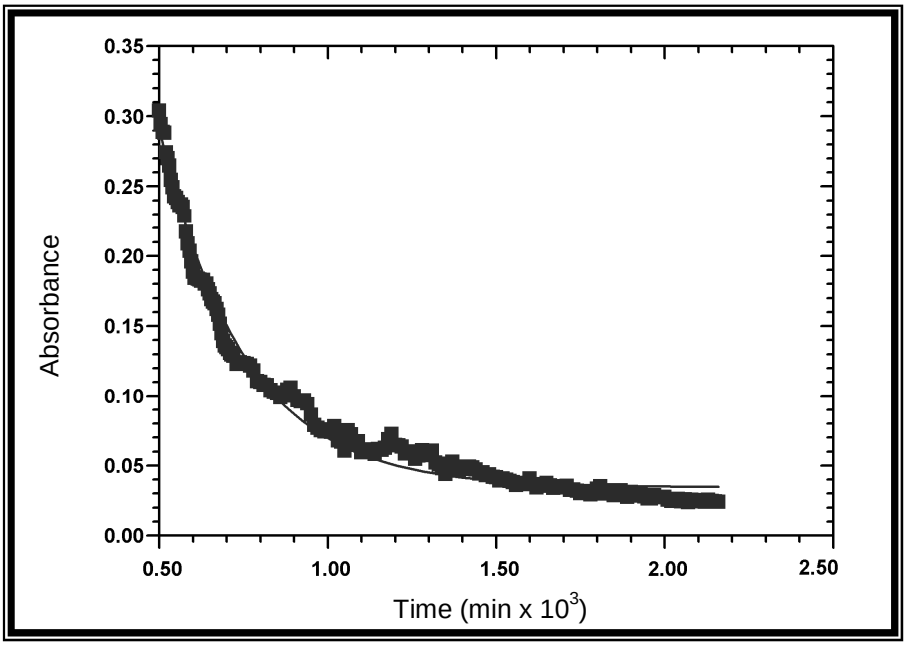

Figure 6.6 Absorbance changes over time for the second reaction when $[(AuCl)_2(\mu$-dppf-$CH(CH_3)OAc)]$ is reacted with equimolar amounts of SCN^- in 1% DMSO:H_2O solution at T = 25 °C. [Au] and $[SCN^-]$ = 0.01 mM. λ = 248 nm.

It is clearly observed that with these Au-dppf systems, the substitution reactions as monitored by UV-Vis mechanisms portray a complex behaviour as the complexes are dinuclear systems. Again, very slow reactions were observed suggesting that it is not the expected rapid chloride substitution. Further characterisation and determinations of the dinuclear ferrocenyl complexes with ligands were explored by other methods such as ^{31}P NMR.

6.3.2 Stability evaluations of the gold(I) phosphine complexes by ^{31}P NMR

The stabilities of the tertiary phosphine gold(I) complexes namely $[(AuCl)_2(\mu$-dppf-$CH(CH_3)N(CH_3)_2)]$, $[(AuCl)_2(\mu$-dppf-$CH(CH_3)OAc)]$ and $[Au(PPh_2Fc)Cl]$ were next evaluated and are discussed. The preparation and characterisation of these complexes were discussed previously in Chapter 4 in § 4.3.3.1, 4.3.3.4 and 4.3.4.1 respectively. The stabilities of the complexes when dissolved in DMSO as a solvent were evaluated by ^{31}P NMR by monitoring a change in the chemical shift over a period 5 hours. The stacked plots from ^{31}P NMR spectra for the stability check for each of the complexes are presented below in § 6.3.2.1 - 6.3.2.3.

6.3.2.1 Stability of the [$(AuCl)_2$(μ-dppf-$CH(CH_3)N(CH_3)_2$)] complex as monitored by ^{31}P NMR

The stability of the [$(AuCl)_2$(μ-dppf-$CH(CH_3)N(CH_3)_2$)] complex in DMSO was investigated by observing a ^{31}P NMR chemical shift change over a time period and the stacked plot of spectra is presented in Fig. 6.7. It is clear that again, as in the case of the UV-Vis experiments described above, these complexes were quite stable over extended periods of time.

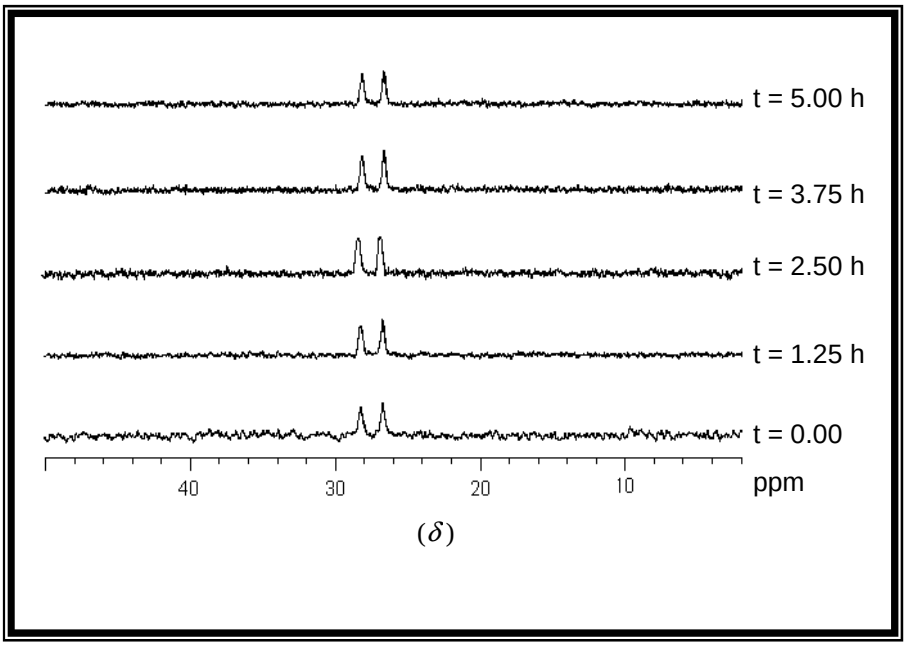

Figure 6.7 Overlay plot of ^{31}P NMR spectra of [$(AuCl)_2$(μ-dppf-$CH(CH_3)N(CH_3)_2$)] in DMSO. [Au] = 20 mM. Scans were taken at 25 °C and at 15 minute intervals for a period of 5 hours. At t = 0, $^1J_{P1\text{-}P2}$ = 626 Hz, with the shift of the substituted *P*Ph_2 resonating downfield.

6.3.2.2 Stability of the [$(AuCl)_2$(μ-dppf-$CH(CH_3)$OAc)] complex as monitored by ^{31}P NMR

The stability of the [$(AuCl)_2$(μ-dppf-$CH(CH_3)$OAc)] complex in DMSO was investigated by observing a ^{31}P NMR chemical shift change over a time period and the stacked plot of spectra is presented in Fig. 6.8. The [$(AuCl)_2$(μ-dppf-$CH(CH_3)$OAc)] complex was stable over a 5 hour period.

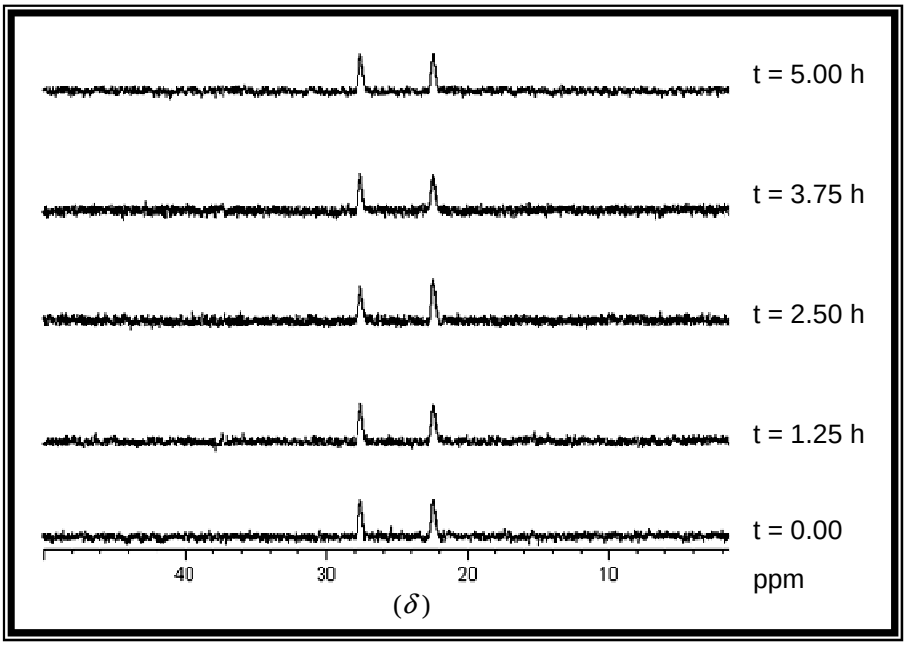

Figure 6.8 Overlay plot of ^{31}P NMR spectra of [$(AuCl)_2$(μ-dppf-$CH(CH_3)OAc$)] in DMSO. [Au] = 10 mM. Scans were taken at 25 °C and at 15 minute intervals for a period of 5 hours.

6.3.2.3 Stability of the [$Au(PPh_2Fc)Cl$] complex as monitored by ^{31}P NMR

The stability of the [$Au(PPh_2Fc)Cl$] complex in DMSO was investigated by observing a ^{31}P NMR chemical shift change over a time period and the stacked plot of spectra is presented in Fig. 6.9. Similarly to the above, the mononuclear [$Au(PPh_2Fc)Cl$] complex was also stable over a 5 hour period.

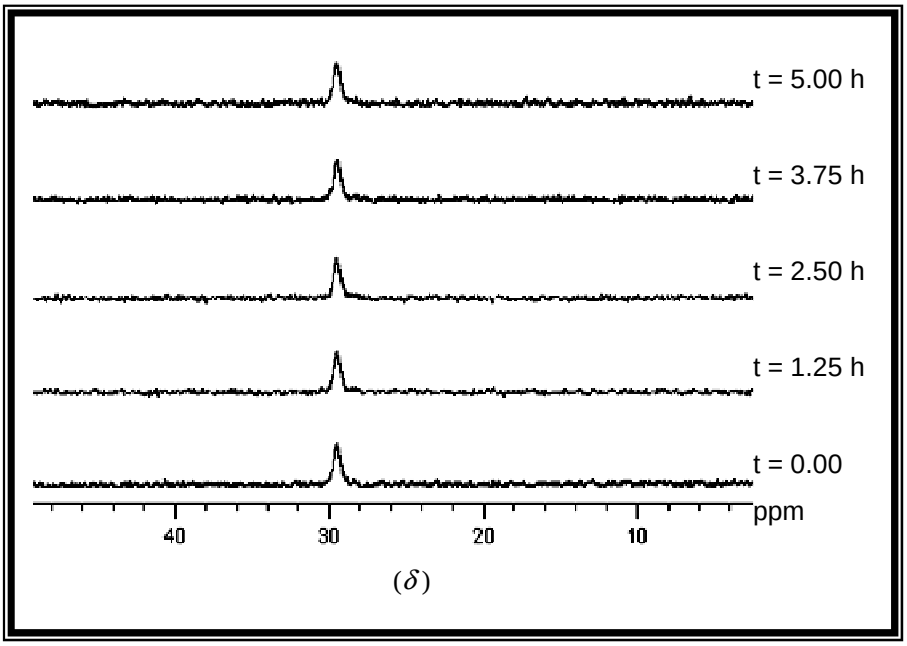

Figure 6.9 Overlay plot of ^{31}P NMR spectra of [Au(PPh_2Fc)Cl] in DMSO. [Au] = 23 mM. Scans were taken at 25 °C and at 15 minute intervals for a period of 5 hours.

In summary, Figs. 6.7 - 6.9 as presented above illustrate the stability of the gold ferrocenyl complexes as monitored by ^{31}P NMR. The graphs showed little or no change in the observed chemical shift of the peaks indicating stability in the medium for the specified time.

6.3.3 ^{31}P NMR equilibrium studies of the chloride substitution from tertiary phosphine gold complexes by SCN^-

The determination of the equilibrium constant when the tertiary phosphine gold complexes such as [$(AuCl)_2$(μ-dppf-$CH(CH_3)OAc$)], [$(AuCl)_2$(μ-dppf-$CH(CH_3)N(CH_3)_2$)], [Au(PPh_2Fc)Cl] and [Au(PPh_3)Cl] were reacted with SCN^- as a ligand is discussed in § 6.3.3.2 - 6.3.3.5. In these reactions the ^{31}P NMR chemical shift change was monitored while stoichiometric amounts of the ligand were added. The equation used in the determinations of equilibrium constants with the mononuclear [Au(PPh_2Fc)Cl] and [Au(PPh_3)Cl] complexes is given as Eq. 6.2 while for the dinuclear [$(AuCl)_2$(μ-dppf-$CH(CH_3)OAc$)] and [$(AuCl)_2$(μ-dppf-$CH(CH_3)N(CH_3)_2$)] complexes is given as Eq. 6.4.

6.3.3.1 Stability of the [(AuCl)$_2$(μ-dppf-CH(CH$_3$)OAc)] complex with excess SCN$^-$ as monitored by ^{31}P NMR

The stability of the [(AuCl)$_2$(μ-dppf-CH(CH$_3$)OAc)] complex when excess SCN$^-$ ligand was added to the complex in DMSO was investigated by observing a ^{31}P NMR chemical shift change over a time period and the stacked plot of spectra is presented in Fig. 6.10.

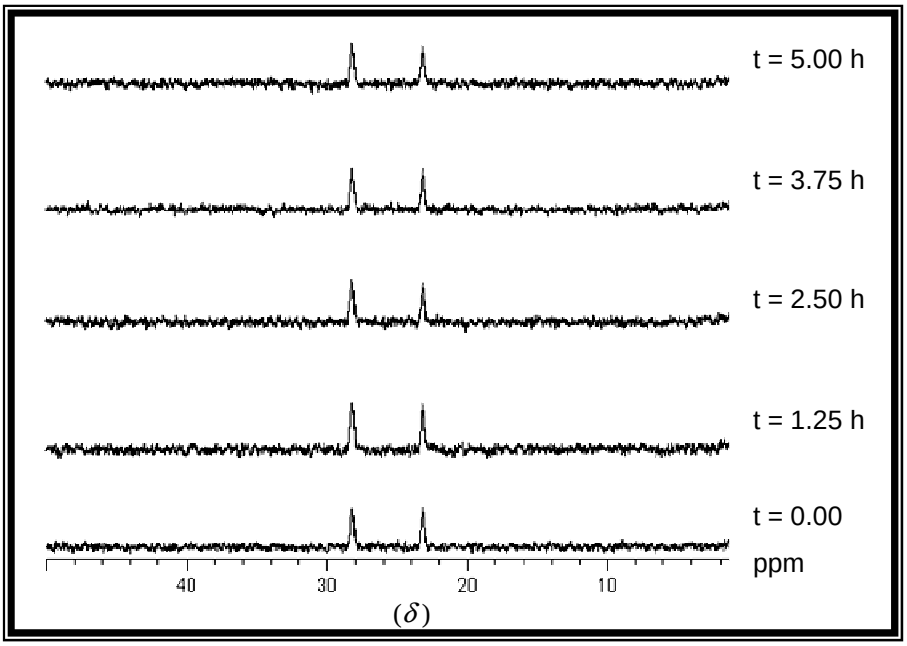

Figure 6.10 Overlay plot of ^{31}P NMR spectra of [(AuCl)$_2$(μ-dppf-CH(CH$_3$)OAc)] with 20 equivalents of SCN$^-$ in DMSO. [Au] and [SCN$^-$] = 15 and 301 mM respectively. Scans were taken at 25 °C and at 15 minute intervals for a period of 5 hours. At t = 0, $^1J_{P1\text{-}P2}$ = 611 Hz.

Figure 6.10 above illustrates the stability of the [(AuCl)$_2$(μ-dppf-CH(CH$_3$)OAc)] complex by observing a change in the ^{31}P NMR chemical shift when an excess of the SCN$^-$ ligand was added to the complex. Comparing the spectrum at t = 0 of Fig 6.10 and the spectrum at t = 0 of Fig 6.8, it is noted that a slight change in the chemical shift of the peaks was observed. Thus, there was an observed reaction when the [(AuCl)$_2$(μ-dppf-CH(CH$_3$)OAc)] complex was reacted with an excess of the ligand. Hence, the determination of equilibrium constants by ^{31}P NMR when [(AuCl)$_2$(μ-dppf-CH(CH$_3$)OAc)] and other related gold(I) tertiary phosphine complexes were reacted with SCN$^-$ is presented in the following sections, § 6.3.3.2 - 6.3.3.5.

6.3.3.2 Study of equilibrium of chloride substitution by SCN^- from $[(AuCl)_2(\mu\text{-dppf-CH}(CH_3)OAc)]$

The determination of the equilibrium constant when the $[(AuCl)_2(\mu\text{-dppf-CH}(CH_3)OAc)]$ complex was reacted with SCN^- is discussed. Fig. 6.11 indicates the ^{31}P NMR chemical shift change when stoichiometric amounts of the ligand were added while fit of data in order to calculate the equilibrium constant using Eq. 6.4 is given in Fig. 6.12. The results for the calculated equilibrium constant are summarised in Table 6.1, § 6.3.4.

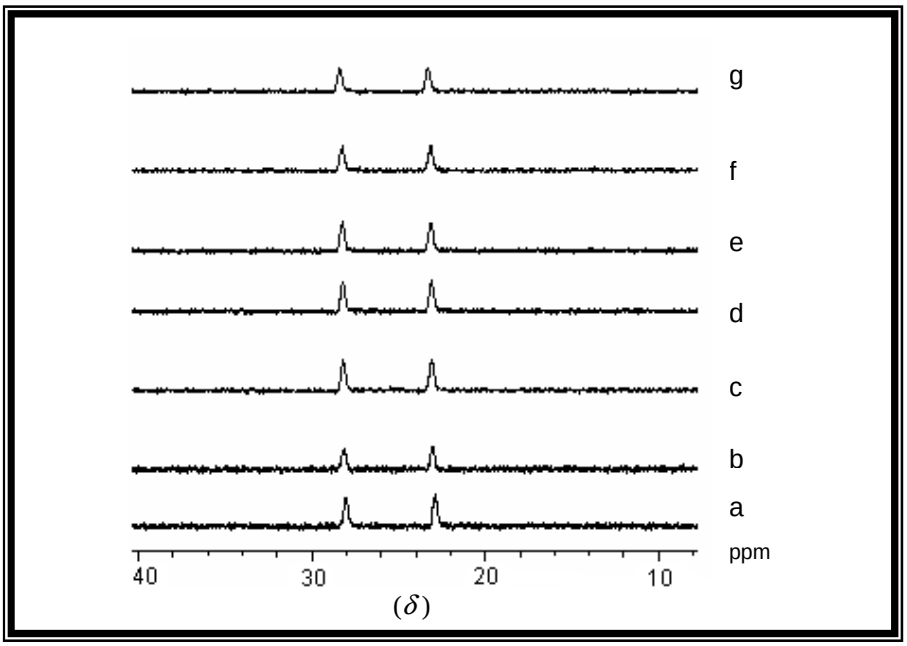

Figure 6.11 Overlay plot of the ^{31}P NMR spectra of $[(AuCl)_2(\mu\text{-dppf-CH}(CH_3)OAc)]$ with different equivalents of SCN^- added in DMSO. [Au] = 14.5 mM and $[SCN^-]$ = 0 - 105.7 mM. Scans were taken at 15 minute intervals at 25 °C and a, b, c, d, e, f and g = 0.0, 0.1, 0.5, 1.0, 1.2, 1.5 and 5.0 equivalents of added SCN^- respectively.

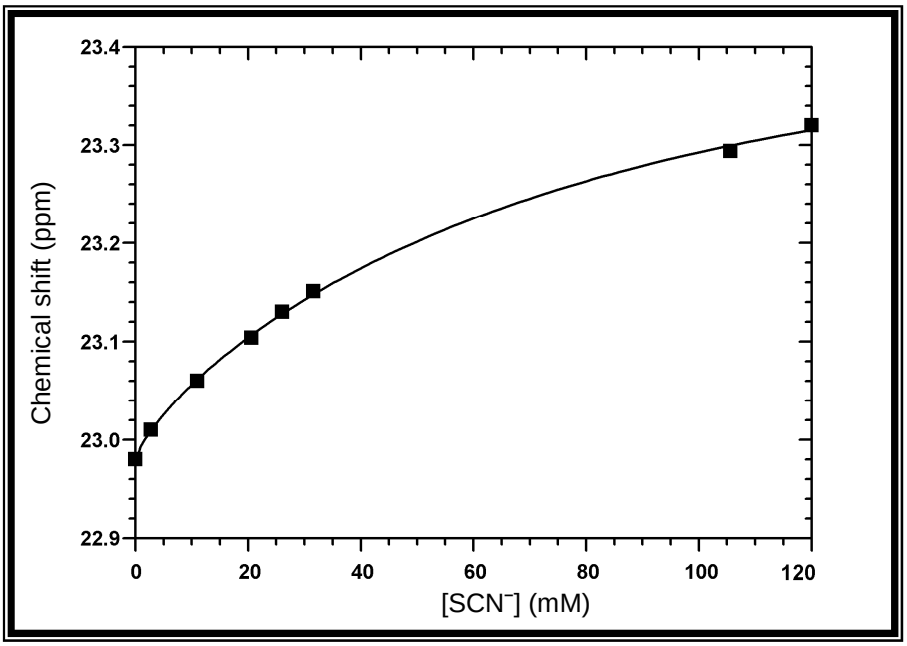

Figure 6.12 A graph showing the fit of data of the ^{31}P NMR chemical shift change (Fig. 6.11) to Eq. 6.4, when SCN^- concentration is varied in a solution of $[(AuCl)_2(\mu\text{-dppf-}CH(CH_3)OAc)]$ in DMSO. [Au] = 14.5 mM, $[SCN^-]$ = 0 - 105.7 mM and T = 25 °C. Solid line represents fit of data to Eq. 6.4.

6.3.3.3 Study of equilibrium of chloride substitution by SCN^- from $[(AuCl)_2(\mu\text{-dppf-}CH(CH_3)N(CH_3)_2)]$

The determination of the equilibrium constant when the $[(AuCl)_2(\mu\text{-dppf-}CH(CH_3)N(CH_3)_2)]$ complex was reacted with SCN^- is discussed. Fig. 6.13 indicates the ^{31}P NMR chemical shift change when stoichiometric amounts of the ligand were added while fit of data in order to calculate the equilibrium constant using Eq. 6.4 is given in Fig. 6.14. The results for the calculated equilibrium constant are summarised in Table 6.1, § 6.3.4.

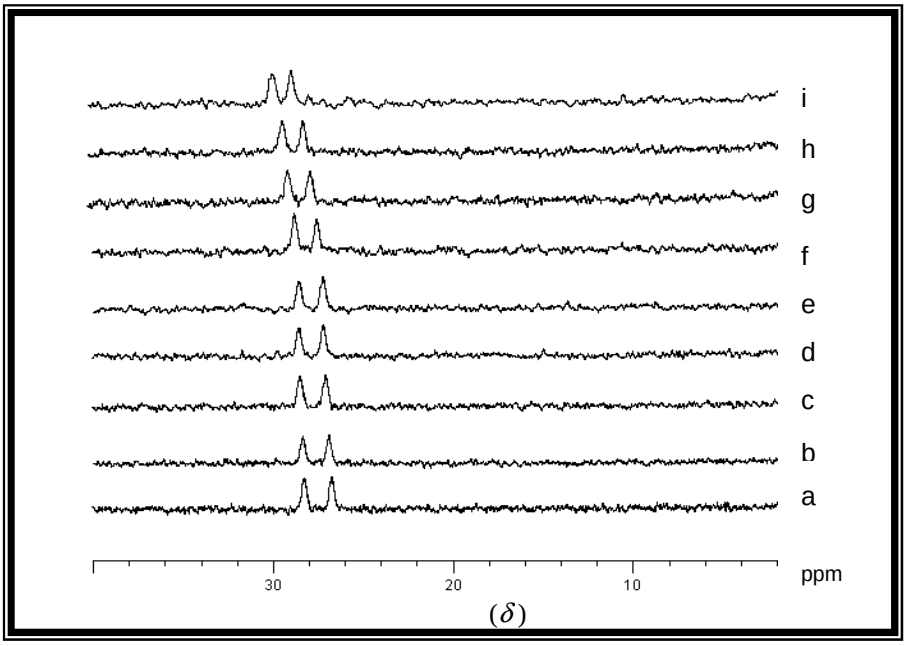

Figure 6.13 Overlay plot of the ^{31}P NMR spectra of [$(AuCl)_2$(μ-dppf-$CH(CH_3)N(CH_3)_2$)] with different equivalents of SCN^- added in DMSO. [Au] = 20 mM and [SCN^-] = 0 - 401 mM. Scans were taken at 15 minute intervals at 25 °C and a, b, c, d, e, f, g, h and i = 0.0, 0.5, 1.0, 1.5, 2.0, 4.0, 5.0, 10.0 and 20.0 equivalents of added SCN^- respectively.

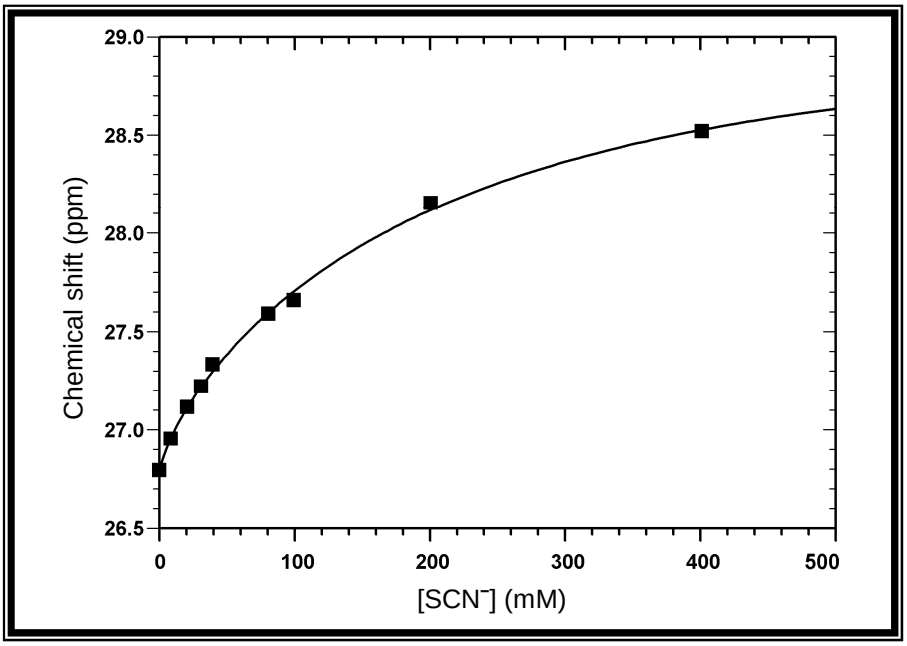

Figure 6.14 A graph showing the fit of data of the ^{31}P NMR chemical shift change (Fig. 6.13) to Eq. 6.4, when SCN^- concentration is varied in a solution of [$(AuCl)_2$(μ-dppf-$CH(CH_3)N(CH_3)_2$)] in DMSO. [Au] = 20 mM, [SCN^-] = 0 - 401 mM and T = 25 °C. Solid line represents fit of data to Eq. 6.4.

6.3.3.4 Study of equilibrium of chloride substitution by SCN^- from $[Au(PPh_2Fc)Cl]$

The determination of the equilibrium constant when the $[Au(PPh_2Fc)Cl]$ complex was reacted with SCN^- is discussed. Fig. 6.15 indicates the ^{31}P NMR chemical shift change when various amounts of the ligand were added while fit of data in order to calculate the equilibrium constant using Eq. 6.2 is given in Fig. 6.16. The results for the calculated equilibrium constant are summarised in Table 6.1, § 6.3.4.

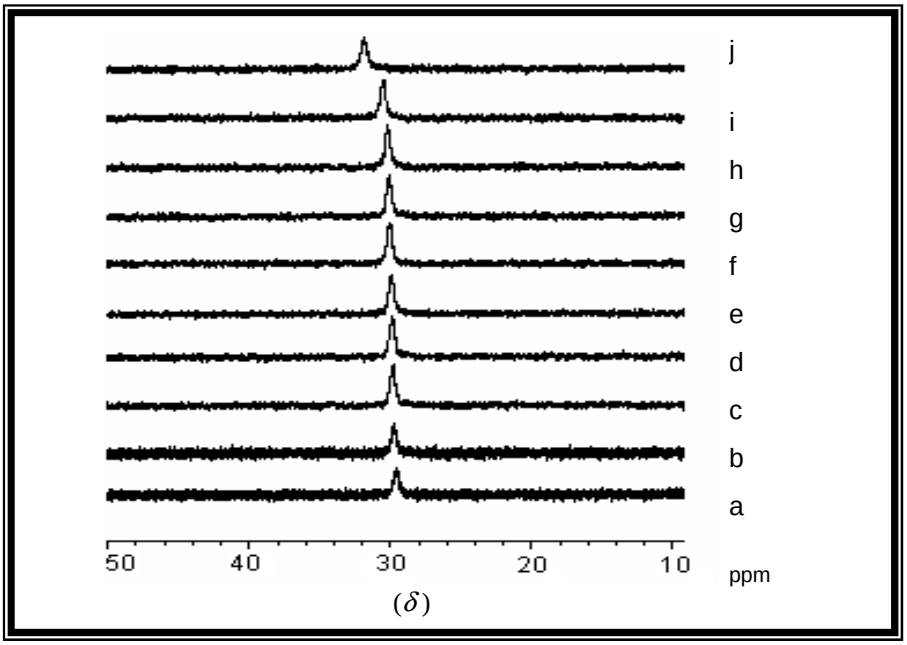

Figure 6.15 Overlay plot of the ^{31}P NMR spectra of $[Au(PPh_2Fc)Cl]$ with different equivalents of SCN^- added in DMSO. [Au] = 45 mM and $[SCN^-]$ = 0 - 898.7 mM. Scans were taken at 15 minute intervals at 25 °C and a, b, c, d, e, f, g, h, i and j = 0.0, 0.5, 1.0, 1.5, 2.0, 3.0, 4.0, 5.0, 10.0 and 20.0 equivalents of added SCN^- respectively.

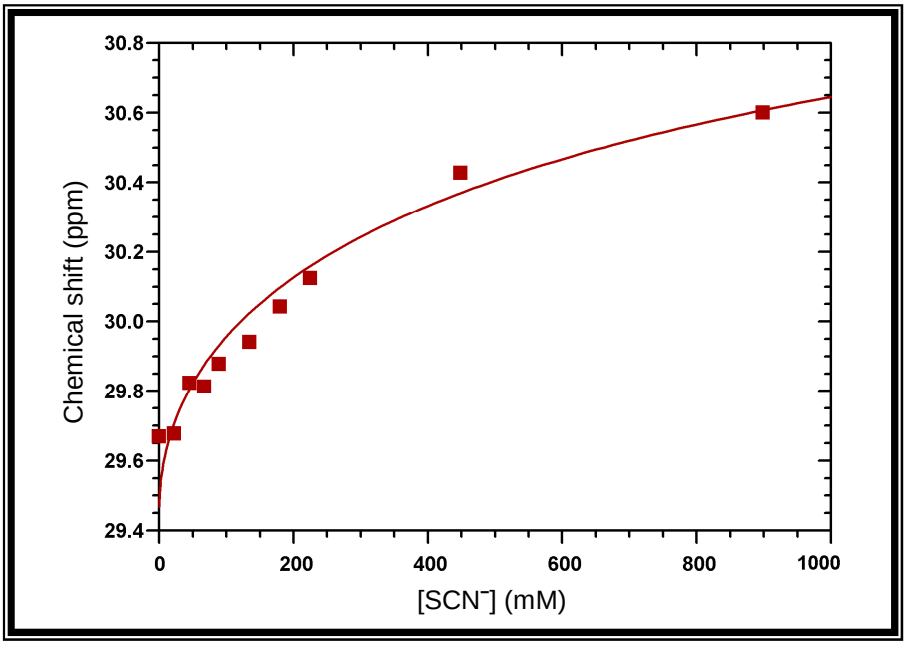

Figure 6.16 A graph showing the fit of data of the ^{31}P NMR chemical shift change (Fig. 6.15) to Eq. 6.2, when SCN^- concentration is varied in a solution of $[Au(PPh_2Fc)Cl]$ in DMSO. [Au] = 45 mM, $[SCN^-]$ = 0 - 898.7 mM and T = 25 °C. Solid line represents fit of data to Eq. 6.2.

6.3.3.5 Study of equilibrium of chloride substitution by SCN^- from $[Au(PPh_3)Cl]$

The determination of the equilibrium constant when the $[Au(PPh_3)Cl]$ complex was reacted with SCN^- is discussed. Fig. 6.17 indicates the ^{31}P NMR chemical shift change when various amounts of the ligand were added while fit of data in order to calculate the equilibrium constant is given in Fig. 6.18. The results for the calculated equilibrium constant are summarised in Table 6.1, § 6.3.4.

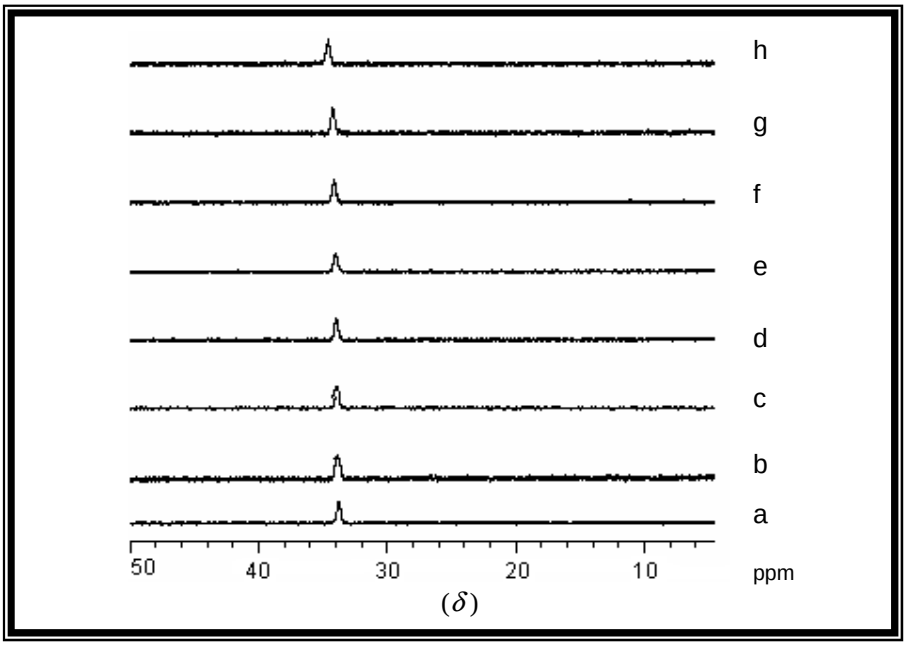

Figure 6.17 Overlay plot of the ^{31}P NMR spectra of [[Au(PPh_3)Cl] with different equivalents of SCN^- added in DMSO. [Au] = 50 mM and [SCN^-] = 0 - 498 mM. Scans were taken at 15 minute intervals at 25 °C and a, b, c, d, e, f, g and h = 0.0, 0.5, 1.0, 1.5, 2.0, 4.0, 5.0 and 10.0 equivalents of added SCN^- respectively.

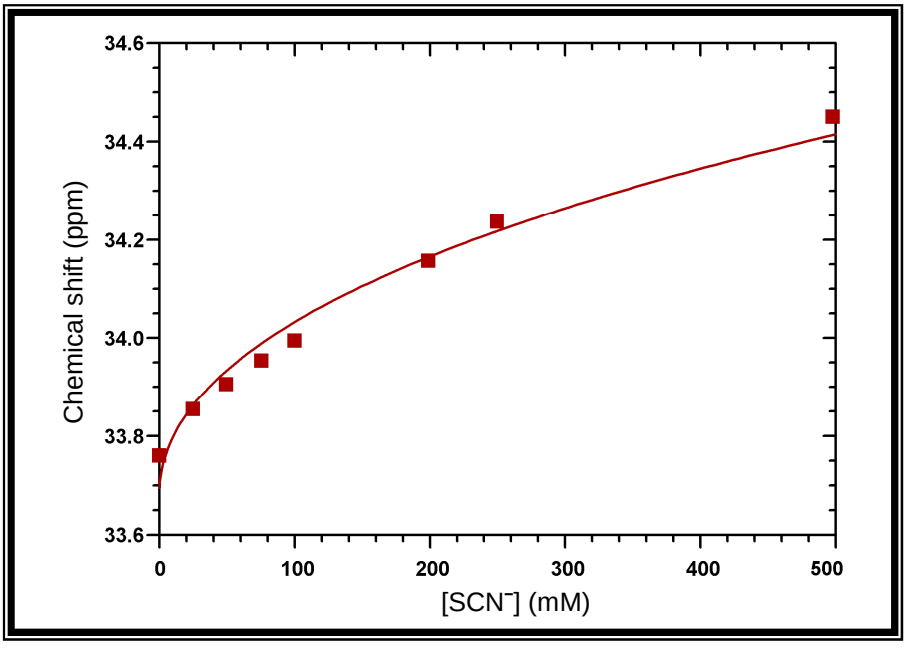

Figure 6.18 A graph showing the fit of data of the ^{31}P NMR chemical shift change (Fig. 6.17) to Eq. 6.2 when SCN^- concentration is varied in a solution of [Au(PPh_3)Cl] in DMSO. [Au] = 50 mM, [SCN^-] = 0 - 498 mM and T = 25 °C. Solid line represents fit of data to Eq. 6.2.

6.3.4 Summary of equilibrium constant determinations

The equilibrium constants obtained from the reactions (§ 6.3.3.2 - 6.3.3.5) of the various tertiary phosphine gold(I) complexes with SCN^- as monitored by ^{31}P NMR are summarised Table 6.1. The ^{31}P NMR experiments of the tertiary phosphine gold(I) complexes with addition of equivalents of SCN^- were done to investigate if there will be a change in the chemical shift of the observed peak and to calculate the equilibrium constants for the reactions of the various complexes with SCN^-. Indeed, when the complexes were reacted with SCN^- ligand, a change in the ^{31}P NMR chemical shift was observed. In Table 6.1 it is noted that the equilibrium constants for the $[(AuCl)_2(\mu\text{-dppf-}CH(CH_3)OAc)]$ and $[(AuCl)_2(\mu\text{-dppf-}CH(CH_3)N(CH_3)_2)]$ are comparable to each other at approximately 0.02 and 0.03 respectively and with the smallest value for the $[Au(PPh_3)Cl]$ complex at 0.0050(2). The equilibrium constants for the ferrocenyl gold complexes are much larger than for the $[Au(PPh_3)Cl]$ complex due to the ability of the ferrocene moiety donating electrons to the metal centre.

Table 6.1 Equilibrium constant values for the reactions of tertiary phosphine gold(I) complexes + L (L = SCN^-) as monitored by ^{31}P NMR at 25 °C, calculated from the fit of data represented by Figs. 6.12, 6.14, 6.16 and 6.18.

Complex	K_L	δ_R (ppm)	δ_P (ppm)	$^1J_{\delta P\text{-}\delta R}$ (Hz)
$[Au(PPh_3)Cl]$	0.0050(2)[a]	33.69	37.31	440
$[Au(PPh_2Fc)Cl]$	0.0361(1)[a]	29.48	31.50	245
$[(AuCl)_2(\mu\text{-dppf-}CH(CH_3)OAc)]$	0.016(8)[b]	22.98	23.32	41
$[(AuCl)_2(\mu\text{-dppf-}CH(CH_3)N(CH_3)_2)]$	0.031(12)[b]	26.79	28.63	224

[a] Obtained from Eq. 6.2 as derived in the Appendix, § A.6.1.
[b] Obtained from Eq. 6.4 as derived in the Appendix, § A.6.2.

6.3.5 Kinetic investigations of S-donor ligand substitutions on mononuclear gold(I) phosphine complexes

It was noted from the results of the substitution behaviour of the ferrocenyl gold complexes with various ligands as presented in sections above, that the reactions proceeded by complex mechanisms. The substitution reaction determinations of the ferrocenyl gold complexes resulted in longer reaction times. Also noted, was that because the complexes are dinuclear species, perhaps several reactions are taking place including hydrolysis and the stepwise substitution of the two chloride moieties at the gold centres of the $[(AuCl)_2(\mu\text{-dppf-}CH(CH_3)OAc)]$ complex, for example. Following

the argument, simpler gold complexes such as [Au(PPh_2Fc)Cl] and [Au(PPh_3)Cl] were utilised in the substitution reactions with ligands and determinations with [Au(PPh_3)Cl] are outlined in the following sections.

6.3.5.1 Stability of the [Au(PPh_3)Cl] complex

The stability of a simpler tertiary phosphine gold(I) complex such as [Au(PPh_3)Cl] was evaluated and is discussed in this section. This stability study of the complex when dissolved in DMSO as a solvent was evaluated by UV-Vis for a period of 7 hours by monitoring if there would be a change in the absorbance observed and the spectrum of such experiment is presented below in Fig. 6.19.

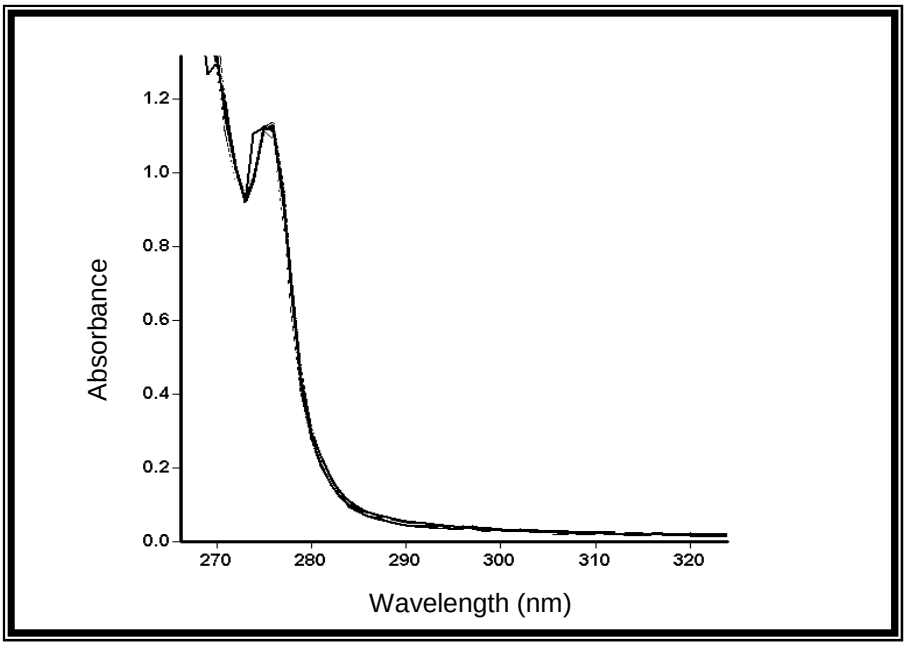

Figure 6.19 UV-Vis overlay of spectra of the [Au(PPh_3)Cl] complex in DMSO solution and at 25 °C. Scans were taken over a 7 hour period. [Au] = 0.5 mM.

6.3.5.2 Fast reaction kinetics of chloride substitution with SCN^- from the [Au(PPh_3)Cl] complex

Fig 6.20 illustrates a graph representing the substitution reaction of the chloride in the [Au(PPh_3)Cl] complex with SCN^- as ligand. As the first aliquot of the SCN^- ligand was added to the solution of the [Au(PPh_3)Cl] complex, a significant change in absorbance was observed and this change indicated a very fast substitution reaction of the chloride from the [Au(PPh_3)Cl] complex by the SCN^- ligand. Hence stopped-flow techniques

were used to further follow the reaction more accurately which is presented in the following section (§ 6.3.7).

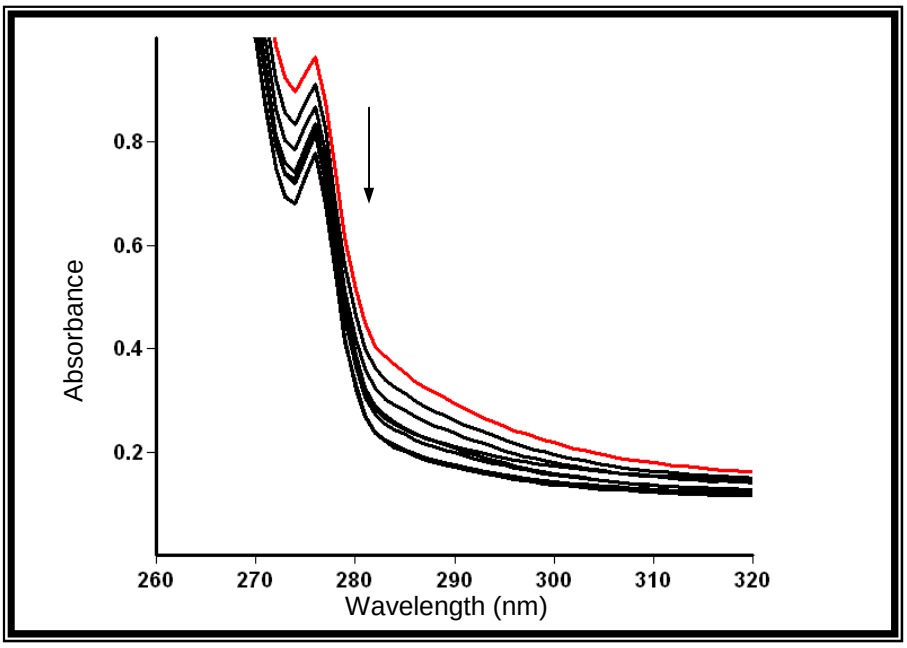

Figure 6.20 UV-Vis spectra of [Au(PPh_3)Cl] when an amount of SCN^- is added to the complex in ethanol solution at 25 °C. Scans were taken at approximately 5 minute intervals. [Au] = 0.3 mM and [SCN^-] = 115.3 mM.

As was illustrated above, chloride substitution reactions by SCN^- particularly, from a range of dinuclear gold(I) complexes were observed. However, the substitution reactions of the dinuclear gold complexes kinetically involve a two-step process, which are expected to be quite complicated to analyse. It was therefore decided to only further evaluate the more simple chloride substitution with the mononuclear gold(I) complexes, *i.e.*, [Au(PX)Cl] (with X = Ph_3 or Ph_2Fc). Preliminary investigations however, indicated that the [Au(PPh_2Fc)Cl] also did not show simple kinetics (assumed to be linked to possible redox reactions of the Fe(II) centre). Furthermore, the presence of the ferrocene moiety prevented accurate measurements at low wavelengths, overshadowing changes induced at the Au(I) centre. Thus, only kinetics of the reactions of the [Au(PPh_3)Cl] complex with SCN^- and thiourea analogues are further described.

6.3.6 Reaction scheme and rate law of mononuclear Au(I)-P complexes of the type [Au(PPh$_3$)Cl]

Studies on the substitution reactions of linear gold(I) complexes are of importance in understanding the kinetics involved in these reactions. Substitution reactivity of mononuclear and linear Au(I) systems were investigated by means of UV-Vis spectrophotometry and stopped-flow techniques. Since substitution reactions of linear gold(I) systems are fast reactions, the reaction rates were monitored with stopped-flow techniques as presented in § 6.3.7 and under pseudo first-order conditions with excess ligand concentrations.

Since substitution studies of gold(I) systems with ligands are not well understood and hence not documented, it has been anticipated that, in general, the substitution reactions occur *via* a dissociative mechanism and the rate laws for the reactions are more complicated when different equilibria are present.

A schematic representation of such a more general square planar substitution reaction is given in Scheme 6.1.

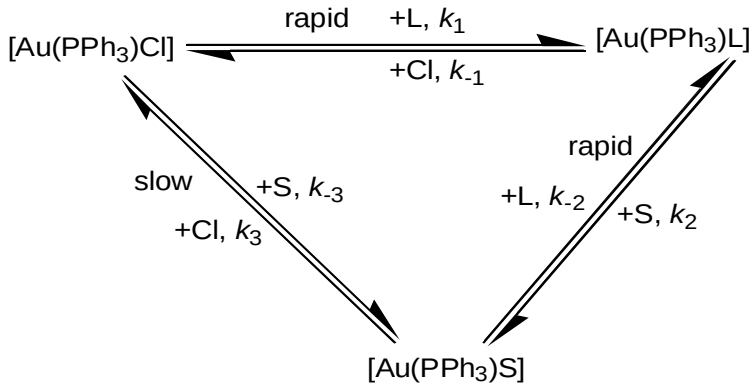

Scheme 6.1 Anticipated representation of the two parallel pathways in gold(I) substitution reaction. S = solvent of which its concentration is included in the rate constants k_3 and k_2.

The equation for chloride substitution in linear Au-Cl systems with ligands such as SCN^- can be represented by the following equation

$$[\text{Au-Cl}] + \text{L} \underset{k_{-1}}{\overset{k_1}{\rightleftharpoons}} [\text{Au-L}] + \text{Cl}^- \qquad (6.9)$$

Although it may be anticipated that the overall reaction consists of many steps to produce the Au-SCN product, for example, the observable reaction studied by stopped-flow techniques indicated formation of the final reaction products, as characterised from X-ray studies in Chapter 4.

Substitution reactions of Cl^- for SCN^- in Au-Cl (Eq. 6.9) generally follow a two-term rate law and this rate law for the second-order reversible kinetics as shown in Eq. 6.10 can be illustrated as:

$$R = k_1[SCN^-][Au\text{-}Cl] - k_{-1}[Au\text{-}SCN][Cl^-] \quad (6.10)$$

Under pseudo first-order conditions, ($[SCN^-]$, $[Cl^-]$ >> [Au]), the rate law for the substitution reactions can be simplified by doing the rate determinations at very high $[SCN^-]$ concentrations resulting in the following equation,

$$k_{obs} = k_1[SCN^-] + k_{-1} \quad (6.11)$$

with k_{obs} as the observed reaction rate constant. The values of k_1 and k_{-1} can thus be obtained from a graph of k_{obs} *vs*. $[SCN^-]$ as discussed in the following section.

6.3.7 Substitution reactions of tertiary phosphine gold(I) complexes with ligands

In this section the results of the substitution investigations, when reactions of linear $[Au(PPh_3)Cl]$ complex with ligands such as SCN^- and dimethyl thiourea were studied with the stopped-flow spectrophotometer for fast-reaction kinetics, are presented. The $[Au(PPh_3)Cl]$ complex was chosen for the investigations because it was observed that the employment of ferrocenyl complexes with the thio ligands yielded results with complex mechanisms, (as presented in § 6.3.1), since the complexes used are dinuclear complexes. Therefore it was necessary to employ simpler gold complexes like the linear $[Au(PPh_3)Cl]$ complex and the results are presented below.

6.3.7.1 Rate constant determinations when chloride is substituted from [Au(PPh$_3$)Cl] with SCN$^-$

The rate constant determination by stopped-flow methods when the [Au(PPh$_3$)Cl] complex in methanol was reacted with SCN$^-$ ligand is discussed in this section. Fig. 6.21 indicates an example of the absorbance change with time when a solution of the ligand at a certain concentration was reacted with the complex while fit of the k_{obs} values for the different ligand concentrations in order to calculate the overall reaction rates is given in Fig. 6.22.

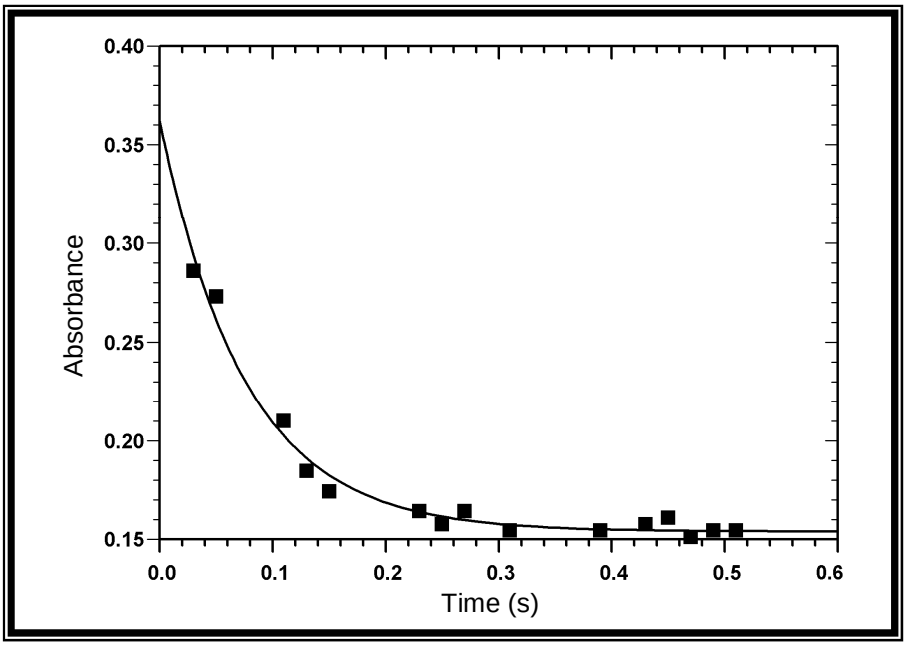

Figure 6.21 A typical example of the graph showing fit of data of absorbance change with time when [Au(PPh$_3$)Cl] was reacted with SCN$^-$ in ethanol. [Au] = 0.2 mM, [SCN$^-$] = 75 mM, T = -5 °C, and λ = 360 nm.

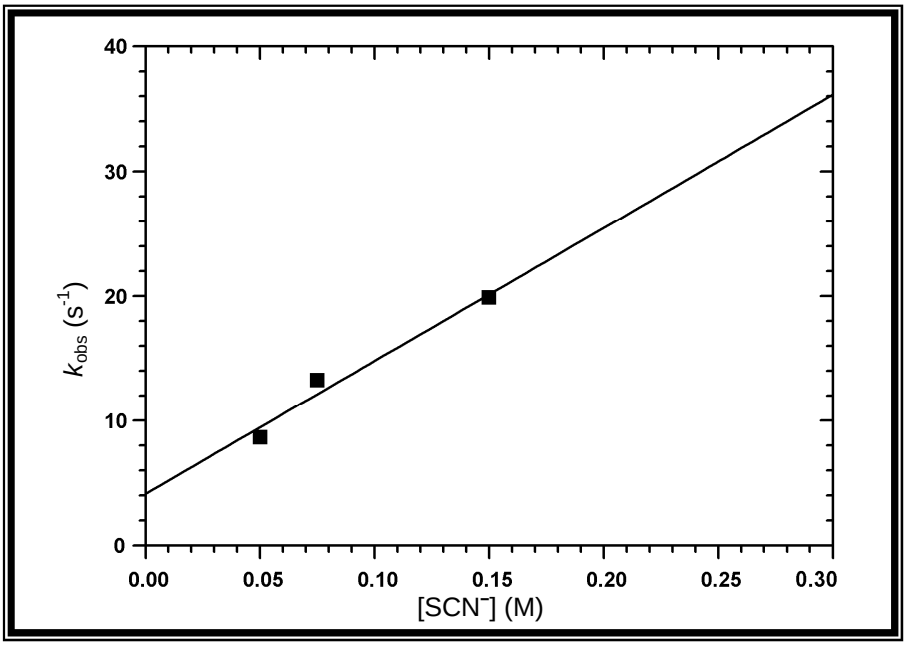

Figure 6.22 A graph showing the various k_{obs} values obtained from fit of data when the different concentrations of SCN^- were varied in a solution of [Au(PPh_3)Cl] in ethanol. [Au] = 0.2 mM, [SCN^-] = 0 - 150 mM, T = -5 °C and λ = 360 nm. Solid line represents fit of data to Eq. 6.10.

The k_{obs} values were calculated from plots of absorbance versus time graphs for each of the SCN^- concentration used (*i.e*. for when 0 - 150 mM ligand added) and a typical example of such graph is presented in Fig. 6.21. The k_{obs} values obtained were then plotted against the different SCN^- concentrations to obtain the overall rate constant (Fig. 6.22). The points were fitted to the following equation:

$$A_{obs} = A_1 - (A_1 - A_0)*\exp((-k_{obs})*T) \qquad (6.12)$$

The overall rate constant obtained from the graph indicating the reaction of the [Au(PPh_3)Cl] complex with SCN^- was obtained as k_1 = 13(1) $M^{-1}s^{-1}$ representing the forward consistent reaction. However, the results were found to be not accurately repeatable to obtain average k_{obs} values and the concentration range accessible for SCN^- was not large enough. There were typically greater than 30% variations in k_{obs} values observed, hence another ligand such as dimethyl thiourea was used for the reaction with [Au(PPh_3)Cl].

6.3.7.2 Rate constant determinations when chloride is substituted from [Au(PPh$_3$)Cl] with dimethyl thiourea

The determination of the rate constant by stopped-flow methods when the [Au(PPh$_3$)Cl] complex was reacted with dimethyl thiourea in methanol is discussed. Preliminary work for this kind of ligand showed a larger K_L value and more consistent kinetic traces (compare for example Fig. 6.21 *vs*. 6.23). Fig. 6.23 indicates the absorbance change with time when a solution of the ligand at a certain concentration was reacted with the complex while fit of the k_{obs} values for the different ligand concentrations in order to calculate the overall reaction rates is given in Fig. 6.24. The experiments on the stopped-flow were done using different wavelength and a satisfactory one which gave repeatable results for the determinations of the rate constant for the substitution reaction was hence chosen.

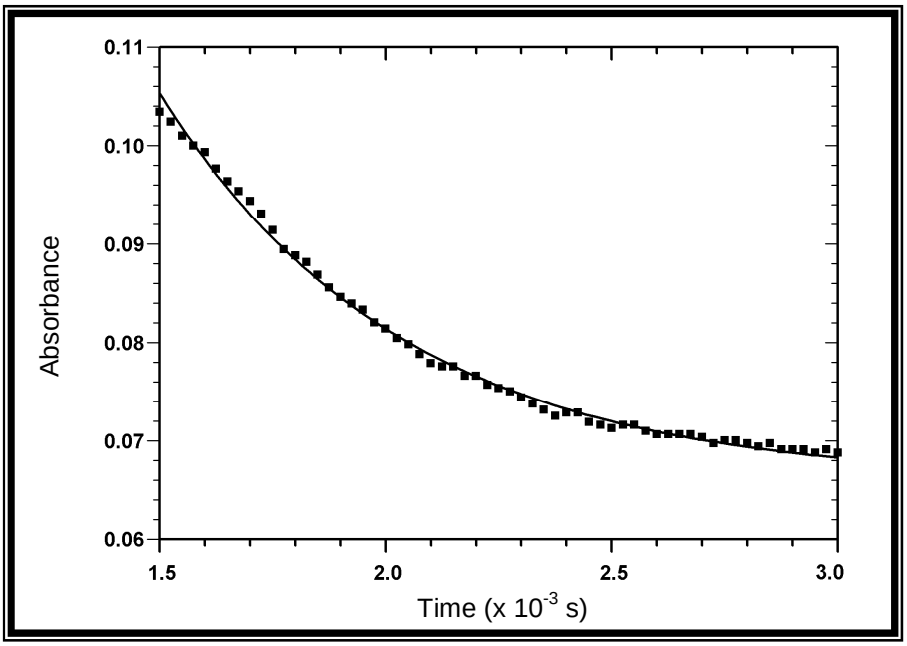

Figure 6.23 A typical example of the graph showing fit of data of absorbance change with time when [Au(PPh$_3$)Cl] was reacted with dimethyl thiourea in ethanol. [Au] = 0.4 mM, [Me$_2$Tu] = 500 mM, T = 2.3 °C and λ = 320 nm.

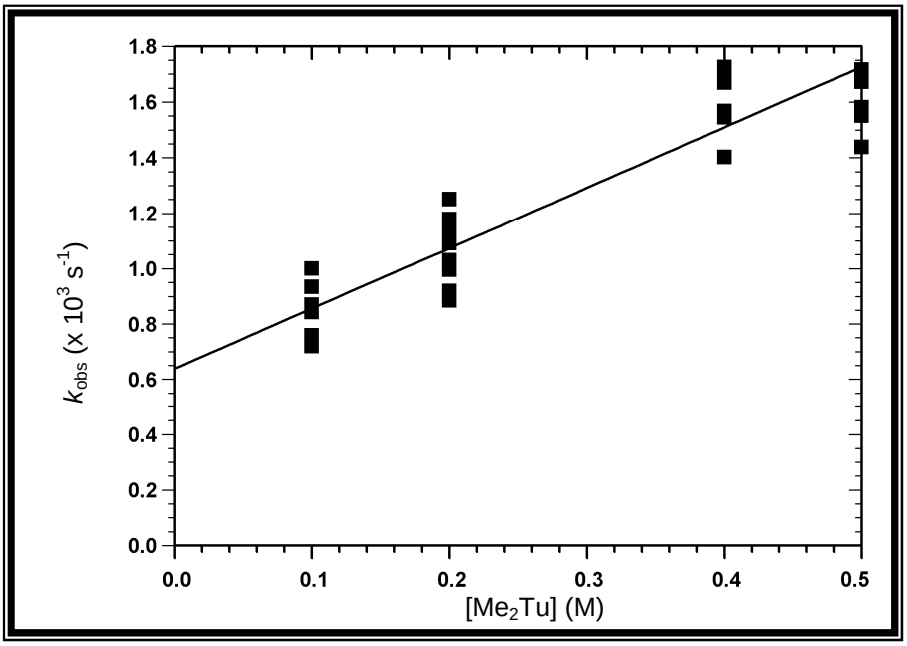

Figure 6.24 A graph showing the various k_{obs} values obtained from fit of data of the different concentrations of dimethyl thiourea were varied in a solution of [Au(PPh_3)Cl] in ethanol. [Au] = 0.4 mM, [Me_2Tu] = 0 - 500 mM, T = 2.3 °C and λ = 360 nm. Solid line represents fit of data to Eq. 6.8.

The k_{obs} values were calculated from plots of absorbance versus time graphs for each of the dimethyl thiourea concentration used (*i.e*. for when 0 - 500 mM ligand added) and a typical example of such graph is presented in Fig. 6.23. The k_{obs} values obtained were then plotted against the different dimethyl thiourea concentrations to obtain the overall rate constant (Fig. 6.24). The plot of the first-order rate constants fitted to data measured under pseudo first-order conditions versus different ligand concentrations yielded a straight line with a positive slope and a non-zero intercept. It was again clear that the spread in the independent k_{obs} values at each concentration was again *ca*. 20-30%, prohibiting accurate measurements and a complete study. However, the preliminary study confirmed the very rapid kinetics.

The overall rate constant obtained from the graph indicating the reaction of the [Au(PPh_3)Cl] complex with dimethyl thiourea was obtained as k_1 = 2.17(1) x 10^3 $M^{-1}s^{-1}$ representing the forward reaction and with an intercept of 6.38(5) x 10^2 s^{-1} representing the reverse reaction rate k_{-1}. Based on equilibrium results presented in Chapter 3 (§ 3.5.2.3) for the substitution with methyl thiourea of the chloride in a linear gold(I) complex, the equilibrium constant was calculated to be approximately 6.7(3). Considering the results obtained in Fig. 6.24 and if the intercept and slope calculated

from the graph represent the forward and reverse reaction respectively, then the equilibrium constant (K_L for Me_2Tu = 3.3 ± 0.3) can be calculated from these kinetic results. It was observed that techniques used for the thermodynamic determination of the equilibrium constant (as discussed in Chapter 3) represent similar observation for the kinetic equilibrium constant. It was therefore concluded that the intercept observed in Fig. 6.24 is the reverse reaction and not the solvent pathway and the slope represented the rate constant of the direct substitution of the Cl^-.

Based on the above it is concluded that chloride substitution reactions on linear gold(I) systems are extremely fast reactions with limitations encountered with equipment to accurately monitor these fast reactions. The limitations included very low temperature investigations needed and the dual solubility of complexes and ligands in various conducible media. The Au(I) centre is therefore clearly extremely reactive to substitution which may be due to linearity of the complexes since the P atom in complexes is *trans* to the chloride. Hence, the phosphine in gold(I) complexes therefore labilises the chloride significantly because of the *trans* effect of the P atom to the chloride.

6.4 CONCLUSIONS

Exploring substitution reactions of gold(I) tertiary phosphine complexes with ligands, as presented in this chapter and with the aim of extending the limited research of gold(I) reaction kinetics available in literature, the following brief conclusions can be drawn:

- A complex substitution behaviour as studied by UV-Vis in [$(AuCl)_2$(μ-dppf-$CH(CH_3)N(CH_3)_2$)] and [$(AuCl)_2$(μ-dppf-$CH(CH_3)OAc$)] complexes when reacted with ligands such as L-cysteine existed as these gold(I) complexes are dinuclear species. These substitution reactions were observed to be slow in spite of anticipations that gold(I) substitutions are fast reactions. These slow reactions were then concluded to be either due to hydrolysis or are decomposition reactions. Although the solubility of the [$(AuCl)_2$(μ-dppf-$CH(CH_3)OAc$)] complex was higher than its amino [$(AuCl)_2$(μ-dppf-$CH(CH_3)N(CH_3)_2$)] counterpart because of the acetate as the spectator group in the ligand, using this [$(AuCl)_2$(μ-dppf-$CH(CH_3)OAc$)] complex and changing the entering ligand from L-cysteine to SCN^- in order to follow substitution reactions, had little effect as the reactions were still slow and hence not conclusive.

- The stability of the mononuclear and dinuclear ferrocenyl gold(I) complexes in DMSO was investigated by ^{31}P NMR by monitoring a change of the chemical shift of the observed peak over a period of time. There was little or no change in the chemical shift for the various spectra of the complexes and it was concluded that the complexes were stable in the media hence determinations of the equilibrium constants when the chloride is substituted from both the mononuclear and dinuclear ferrocenyl gold(I) complexes with SCN^- was feasible and investigated.

- The equilibrium constant determinations for the substitution of the chloride with SCN^- from the various mononuclear and dinuclear tertiary phosphine gold(I) complexes as monitored by ^{31}P NMR was done with success. These equilibrium determination experiments done by using ^{31}P NMR included primarily monitoring a change in the chemical shift of the observed peak when stoichiometric equivalents of the SCN^- ligand were added to the various complexes. The equilibrium constant values obtained were calculated by fit of data to the various equations when the respective mononuclear and dinuclear ferrocenyl gold(I) complexes were employed as presented earlier. It was observed that the calculated value for the equilibrium constant obtained for chloride substitutions from the $[Au(PPh_3)Cl]$ complex was much smaller at approximately 0.0050(2) as compared to the ferrocenyl gold(I) complexes which were approximately an order of magnitude larger than for the former. This may be due to the ability of the ferrocene moiety in the $[Au(PPh_2Fc)Cl]$ system donating electrons to the metal centre. The calculated values of the equilibrium constants when the $[(AuCl)_2(\mu\text{-dppf-}CH(CH_3)OAc)]$ and $[(AuCl)_2(\mu\text{-dppf-}CH(CH_3)N(CH_3)_2)]$ complexes were used for the substitution reactions varied from 0.02-0.04 respectively which were approximately of similar magnitude to the mononuclear $[Au(PPh_2Fc)Cl]$ system. Hence, ^{31}P NMR investigations were more successful for the purpose of this study in the investigations of the chloride substitution reactions from mononuclear and dinuclear tertiary phosphine gold(I) complexes than as with UV-Vis methods.

- Fast reaction kinetic studies at low temperatures when the chloride was substituted from the simple mononuclear and linear $[Au(PPh_3)Cl]$ complex with S-donor ligands such as SCN^- and dimethyl thiourea were investigated using stopped-flow techniques. The thiourea analogue was chosen by reason of its

easier solubility in polar solvents than SCN^-. The experiments done for the rate constant determinations when the chloride was substituted from the $[Au(PPh_3)Cl]$ complex with the chosen ligands had limitations such as the reproducibility of the results, encountered less solubility of the ligand as much higher concentrations of both complex and ligand were needed as well as perhaps machinery that can operate at very low temperatures in order to calculate accurate rate constants and for the results to be repeatable. It can then be concluded that chloride substitution reactions on linear gold(I) systems are extremely fast reactions which would be better followed with high concentrations of the complex and ligand and at very low temperatures.

- In general, it can be mentioned that little research if at all on substitution reactions of gold(I) systems has been documented in literature. Though to a lesser extent, it is only the Au(III) systems that are isoelectronic with Pt(II) systems that have received attention for investigations. These investigations with Au(III) systems included ligand exchange studies and in fact the two-term rate law which is now widely and commonly used for square-planar substitution reactions was first recognised[21] for the exchange of $^{36}Cl^-$ with $AuCl_4^-$. The *cis* and *trans* effects in square-planar gold(III) complexes have been the subject of review[22]. The reactions[23] in which the four ammonia ligands in $[Au(NH_3)_4]^{3+}$ are replaced successively with Br^- and the rates of reaction[24] of the chloro species in $Au(dien)X^{2+}$ and $Au(dien\text{-}H)X^+$ with a variety of different reagents have also been investigated. Alexander and Holper[25] have reported the effect of solvent composition (aqueous MeOH) on the kinetics of the replacement of Cl^- by Br^- in $[Au(Et_4dien\text{-}H)Cl]^+$. Some of the investigations done with Au(III) systems also include the reaction[26] of $[Au(A)Cl_3]$ (A = amine) with Y^- which is determined as a function of the changes in the amine A and in the nucleophile Y^-.

[1] M.C. Gimeno, A. Laguna, 'Comprehensive Coordination Chemistry II'; J.A. McCleverty, T.J. Meyer, Eds.: Elsevier, New York, 2003.

[2] C.H. Langford, H.B. Gray, 'Ligand Substitution Processes', W.A. Benjamin Inc., New York, 1965.

[3] L.H. Skibsted, *Adv. Inorg. Bioinorg. Mech.,* 1986, **4**, 137.

[4] J. Berglund, L.I. Elding, *Inorg. Chem.,* 1995, **34**, 513.

[5] B.I. Peshchevitskii, G.I. Shamovskaya, *Koord. Chim.,* 1980, **6**, 1657.

[6] R. Romeo, *Comments Inorg. Chem.,* 1990, **11**, 21.

[7] L.I. Elding, A.-B. Gröning, Ö. Gröning, *J. Chem. Soc., Dalton Trans.,* 1981, 1093.

[8] E.V. Makotchenko, B.I. Peschchevitskii, R.I. Novoselov, *Izb. Sib. Otd. Akad. Nauk SSSR, Ser. Khim. Nauk,* 1981, **9**, 47, 52, 56; 1978, **14**, 44.

[9] G. Annibale, L. Canovese, L. Cattalini, G. Natile, *J. Chem. Soc., Dalton Trans.,* 1980, 1070.

[10] F. Basolo, R.G. Pearson, 'Mechanisms of Inorganic Reactions', Wiley, New York, 1967.

[11] H.B. Gray, C.H. Langford, *Chem. Eng. News,* 1968, 68.

[12] B. Rosenberg, L. Van Camp, J.R. Trosko, V.A. Mansours, *Nature,* 1969, **222**, 385.

[13] S.L. Bruin, P.M. Pil, J.M. Essigmann, D.E. Houseman, S.J. Lippard, *Proc. Nat. Acad. Sci. U.S.A.,* 1992, **89**, 2307 and references therein.

[14] S.E. Sherman, D. Gibson, A.H.J. Wang, S.J. Lippard, *J. Am. Chem. Soc.,* 1988, **110**, 7368; *Science,* 1985, **230**, 412.

[15] G. Admiraal, J.L. Van der Veer, R.A.G. de Graaff, J.H.J. den Hartog, J. Reedijk, *J. Am. Chem. Soc.,* 1987, **109**, 592.

[16] Scientist for Windows, Least-squares Parameter Estimation, Version 4.00.950, MicroMath, 1990.

[17] J. Cousins, L. Herbet, Kinet Asyst for Windows, Version 4.10 Build 2222, 2002.

[18] S.J. Lippard, J.M. Berg, 'Principles of Bioinorganic Chemistry', University Science Books, CA, 1994.

[19] R.N. Bose, S.K. Ghosh, S. Moghaddas, *J. Inorg. Biochem.,* 1997, **65**, 199.

[20] R.W. Hay, D.S. Porter, *Transition Met. Chem.,* 1999, **24**, 186.

[21] R.L. Rich, H. Taube, *J. Phys. Chem.,* 1954, **58**, 1, 6.

[22] B.I. Peshchevitskii, G.I. Shamovskaya, *Koord. Khim.,* 1980, **6**, 1657.

[23] L.H. Skibsted, *Acta Chem. Scand.,* 1979, **A33**, 113.

[24] (a) W.H. Baddley, F. Basolo, H.B. Gray, C. Nolting, A.J. Poë, *Inorg. Chem.,* 1963, **2**, 921.

(b) W.H. Baddley, F. Basolo, *ibid.,* 1964, **3**, 1087.

[25] R.D. Alexander, P.N. Holper, *Transition Met. Chem.,* 1980, **5**, 108.

[26] L. Cattalini, M.L. Tobe, *Inorg. Chem.,* 1966, **5**, 1145, 1674.

7 EVALUATION OF STUDY

7.1 INTRODUCTION

The evaluation and results of this study are briefly discussed (§ 7.2) in terms of the aims presented in Chapter 1 while some future aspects of the research are outlined in § 7.3.

This project commenced by conducting a thorough literature review to gather applicable theoretical information and overall understanding of relevant metal systems and thus formulating practical work. This literature review highlighted that the history of metal-containing anti-tumour agents began with the detection of anti-tumour properties for the inorganic compound, *cis*-diamminedichloro platinum(II) (cisplatin, *cis*-$[Pt(NH_3)_2Cl_2]$). It is noted that much research with regard to the coordination chemistry and biological activity of metal complexes is necessary to understand the *in vivo* behaviour thereof. This has prompted research on the implications of other transition metal systems such as gold compounds. Gold has an intriguing chemistry dominated by relativistic effects which play an important role in the physical and chemical properties of the metal. It is therefore, interesting to consider studying the metal properties based on the coordination chemistry, substitution and biological activity, if any, of which the breakthrough in literature for gold was with the biological activity of 2,3,4,6-tetra-*O*-acetyl-1-thio-β-D-glucopyranosato(triethylphosphine) gold(I) (auranofin) compound against cancer cell strains and rheumatoid arthritis.

7.2 SCIENTIFIC RELEVANCE

As presented above as introduction to metal compounds being employed for biological motives and also noted in literature with the important discovery in the area of water-soluble phosphine ligands such as that of 1,3,5-triaza-7-phosphatricyclo[3.3.1.$1^{3,7}$] decane (PTA), the synthesis of gold(I) complexes with these systems was envisaged.

The synthesis and characterisation of gold(I) complexes with PTA and related ligands such as PTAMe was completed with success.

The study of the equilibrium for the substitution of the chloride from the [Au(PTA)Cl] complex with S-donor ligands such as SCN^-, thiourea and methyl thiourea was successfully investigated. The general equilibrium reaction for the process is given as Eq. 7.1.

$$[Au(PTA)Cl] + L \underset{}{\overset{K_L}{\rightleftharpoons}} [Au(PTA)L] + Cl^- \qquad (7.1)$$

The equilibrium process for these PTA gold(I) complexes and S-donor ligands was investigated by ^{31}P NMR spectroscopy. For these reactions the ^{31}P NMR chemical shift change was monitored while stoichiometric amounts of the ligand are added to the solution of the [Au(PTA)Cl] complex. It was noted from the results presented in Chapter 3 that the equilibrium constants for the thiourea and methyl thiourea are comparable to each other while a smaller value for the thiocyanate ligand was obtained.

The 'host-guest' chemistry displayed by the β-cyclodextrin (β-CD) with guests such as PTA was investigated in this study by X-ray crystallography and spectroscopy. The PTA-β-CD·$8H_2O$ structure shows that the PTA ligand is situated inside the cavity of the β-cyclodextrin. The utilisation of cyclodextrins in the interest of this research was for possible stability and increased solubility of the compounds and related gold(I) complexes when used in for example, biological systems. Such an attempt was made with the inclusion of auranofin to the β-cyclodextrin but however, only auranofin crystallised out. The data collection for the auranofin structure was done at 100 K and although the structure is already known in literature, interesting properties in parameters for the low-temperature studied structure clearly indicated a phase change and hence a new polymorph at 100 K. Further study of the interactions of β-cyclodextrin with ligands and gold(I) complexes was done with NMR spectroscopy to determine the equilibrium constants when these complexes are included into the β-cyclodextrin. The equilibrium constants (K_D) obtained from including various guest ligands (G) such as PTA and gold(I) complexes into β-cyclodextrin (β-CD) were determined using the following equation which also represents the equilibrium reaction process:

$$G + \beta\text{-CD} \underset{}{\overset{K_D}{\rightleftharpoons}} G\text{-}\beta\text{-CD} \qquad (7.2)$$

It was observed that the results obtained from substitution behaviour of PTA with β-cyclodextrin are comparable with the resultant structure of the PTA-β-cyclodextrin

inclusion compound. Also, it was noted that PTA compounds have higher inclusion constants as compared to the $[Au(dppe)_2]Cl$ and PPh_3 systems with phenyl groups.

The study of the coordination chemistry of gold(I) complexes with ferrocenyl phosphines was done with X-ray crystallography. The ligands employed included the 1,1'-bis(diphenylphosphino)ferrocene (dppf) and its modified analogues such as the *N*,*N*-dimethyl-1-[1',2-bis(diphenylphosphino)ferrocenyl]ethylamine and 1-[1',2-bis(diphenylphosphino)ferrocenyl] ethylacetate. The characterisation of the chloro gold complexes with the former dppf ligand by X-ray crystallography is widely reported in literature with the synthesis and NMR characterisation only included for comparison. Therefore, the focus of this study was based using the latter (ethylamine and ethylacetate) dppf analogues while the dppf thiocyanato gold(I) complex was also characterised in this study. The synthesis and characterisation of the gold(I) complexes with these ferrocenyl ligands was successfully done. The structures of the $[(AuCl)_2(\mu$-dppf-$CH(CH_3)N(CH_3)_2)]$, $[(AuSCN)_2(\mu$-dppf-$CH(CH_3)N(CH_3)_2)]$, $[(AuCl)_2(\mu$-dppf-$CH(CH_3)OAc)]$, $[(AuSCN)_2(\mu$-dppf-$CH(CH_3)OAc)]$ and $[(AuSCN)_2(\mu$-dppf)] compounds were reported in Chapter 4. The structures are generally dinuclear complexes with linearity around the gold(I) centre. Interestingly enough, the two $[(AuSCN)_2(\mu$-dppf-$CH(CH_3)N(CH_3)_2)]$ and $[(AuSCN)_2(\mu$-dppf-$CH(CH_3)OAc)]$ structures were found to be isomorphous while the structure of the $[(AuSCN)_2(\mu$-dppf)] compound indicated short Au…Au contacts of which none were observed for other structures.

As mentioned in § 7.1 above, literature shows that auranofin was found to have biological activity against cancer cell strains. In this project, auranofin and its derivative compounds (PTA-auranofin, PTAMe-auranofin and arsine-auranofin), (see Chapter 5), were prepared and tested for biological activity against cancer cell lines. A chemiluminescence assay was also done with the compounds at various concentrations to determine the effect they have on the chemiluminescence of isolated blood neutrophils. Auranofin and arsine-auranofin seemed to give results closely related to each other in activity against cell lines with arsine-auranofin having higher toxicity to other cells whereas PTA-auranofin and PTAMe-auranofin showed more correlation to each other and had less activity. The preliminary chemiluminescence assays showed that for all auranofin derivatives, at low concentrations, the compounds act as stimulants to the neutrophil chemiluminescence activity and at higher concentrations the compounds act as inhibitors to neutrophil activity.

The substitution reactions of chloride from gold(I) tertiary phosphine complexes with different entering ligands were also investigated in this work using UV-Vis and ^{31}P NMR spectroscopy (see Chapter 6). UV-Vis investigations included substitutions using synthesised dinuclear ferrocenyl complexes as presented in Chapter 4 (for example [$(AuCl)_2$(μ-dppf-$CH(CH_3)OAc$)]) with entering ligands such as SCN^- and L-cysteine. However, these systems showed complex solution behaviour, with very slow reactions observed in contrast to known gold substitutions being fast. Therefore, investigations with gold(I) tertiary phosphine complexes were continued by other methods such as using ^{31}P NMR spectroscopy. Thus, the equilibrium constant determinations for the substitution of the chloride with SCN^- from the various mononuclear and dinuclear tertiary phosphine gold(I) complexes were successfully done by ^{31}P NMR. The general equilibrium reactions for the processes using mono and dinuclear complexes are given as Eq. 7.3 and 7.4 respectively.

$$[\text{Au-Cl}] + \text{L} \underset{}{\overset{K_L}{\rightleftharpoons}} [\text{Au-L}] + \text{Cl}^- \tag{7.3}$$

$$[\text{Au}_2\text{-Cl}_2] + 2\text{L} \overset{K_L}{\rightleftharpoons} [\text{Au}_2\text{-L}_2] + 2\text{Cl}^- \tag{7.4}$$

The mononuclear complexes ([$Au(PPh_2Fc)Cl$] and [$Au(PPh_3)Cl$]) and dinuclear complexes ([$(AuCl)_2$(μ-dppf-$CH(CH_3)OAc$)] and [$(AuCl)_2$(μ-dppf-$CH(CH_3)N(CH_3)_2$)]) were used for the investigation of the anation reactions, when the chloride is substituted with SCN^-. The equilibrium constants obtained for the ferrocenyl gold(I) complexes were comparable to each other and are much larger than for the [$Au(PPh_3)Cl$] complex. Furthermore, very fast reaction kinetics (Chapter 6, § 6.3.7) for the chloride substitution with ligands such as SCN^- and dimethylthiourea from the mononuclear [$Au(PPh_3)Cl$] complex was observed and preliminary investigated with stopped-flow techniques. Though the fast substitution reaction prevailed, more so for the dimethyl thiourea, restrictions such as accuracy, solubility of the complexes and ligands in higher concentrations were still encountered with these gold(I) complexes and limited a complete and detailed investigation. Thus, it was concluded that chloride substitution reactions on linear gold(I) systems are extremely fast which could, perhaps, be better followed at very low temperatures.

In general, it is therefore concluded that this study, with the aims and perspectives as presented in Chapter 1, was successfully completed and yielded interesting results on the gold(I) systems studied.

7.3 FUTURE ASPECTS

The concept of micro-encapsulation (*i.e*. including some 'guest' compound into the cavity of the 'host' cyclodextrin) is interesting to evaluate and the overall research with cyclodextrins has led to a number of attractive pharmaceutical uses for cyclodextrins as they can be models for non-covalent and hydrogen bonding, for example. Though the motive for the use of cyclodextrins in this study was based on increasing solubility and stability properties of the compounds and related gold(I) complexes, there still lies the challenge of including larger molecules into the cyclodextrins. Recent interest is in the use of chemically modified cyclodextrins and with larger cavities. There is a vast range of modifications for cyclodextrins which include acylated and alkylated motifs or attachment of various functional groups to render them, and inclusion compounds thereof, more soluble to various media.

The X-ray crystallographic study of coordination chemistry of gold(I) ferrocenyl phosphine complexes can be optimised by using modified dppf analogues that coordinate selected spectator ligands which will give the complexes other interesting applications such as increased solubility as well as electronic and steric properties.

Chrysotherapy, the use of gold compounds in medicine, refers to the fact that gold compounds are used clinically in the alleviation of the symptoms associated with several diseases. The challenges to identifying an effective gold agent still exist which include the synthesis of applicable compounds with lesser side effects, finding biological test systems that are suitable and understanding the mechanism of action for these gold compounds.

Since the rate of the substitution of the chloride in gold(I) complexes such as $[Au(PPh_3)Cl]$ with various ligands was too fast to be accurately monitored with stopped-flow techniques and a more complex substitution mechanism was observed with dinuclear gold(I) systems, the investigations should be extended by changing the phosphine moiety of the complexes and using entering ligands with properties so as to increase solubility and stability in aqueous media. The systems should then be investigated with higher concentrations and at very low temperatures also using NMR spectroscopy.

APPENDIX

A SUPPLEMENTARY DATA FOR CHAPTER 3 AND CHAPTER 6

A.1 Crystal data of PTA-β-Cyclodextrin.

Table A.1.1 Atomic coordinates (x 10^4) and equivalent isotropic displacement parameters (Å^2 x 10^3) for PTA-β-Cyclodextrin. U(eq) is defined as one third of the trace of the orthogonalized Uij tensor.

	x	y	z	U(eq)
C(1)	5184(2)	4387(3)	7385(1)	19(1)
C(11)	9135(2)	3023(3)	8867(1)	11(1)
C(12)	9105(2)	2767(3)	8176(1)	11(1)
C(13)	10036(2)	3201(3)	8094(1)	12(1)
C(14)	10175(2)	4662(3)	8250(1)	11(1)
C(15)	9369(2)	4473(3)	9043(1)	11(1)
C(16)	9531(2)	4727(3)	9758(1)	14(1)
C(2)	7033(2)	5152(3)	7825(1)	15(1)
C(21)	6183(2)	1720(3)	9174(1)	12(1)
C(22)	6690(2)	892(3)	8803(1)	12(1)
C(23)	7693(2)	676(3)	9213(1)	13(1)
C(24)	8160(2)	1990(3)	9455(1)	13(1)
C(25)	6697(2)	3003(3)	9391(1)	12(1)
C(26)	6292(2)	3874(3)	9805(1)	16(1)
C(3)	5961(2)	5885(3)	6611(1)	18(1)
C(31)	3056(2)	3061(3)	7981(1)	11(1)
C(32)	3410(2)	1775(3)	7794(1)	13(1)
C(33)	3790(2)	881(3)	8376(1)	13(1)
C(34)	4486(2)	1623(3)	8928(1)	12(1)
C(35)	3782(2)	3697(3)	8555(1)	11(1)
C(36)	3423(2)	4885(3)	8818(1)	14(1)
C(4)	5787(2)	6085(3)	8195(1)	17(1)
C(41)	2037(2)	6384(3)	6251(1)	10(1)
C(42)	2127(2)	4959(3)	6077(1)	12(1)
C(43)	1620(2)	4080(3)	6428(1)	11(1)
C(44)	1936(2)	4349(3)	7159(1)	12(1)
C(45)	2403(2)	6533(3)	6988(1)	11(1)
C(46)	2317(2)	7910(3)	7217(1)	15(1)
C(5)	6452(2)	7362(3)	7525(1)	16(1)
C(51)	3837(2)	9310(3)	5343(1)	11(1)
C(52)	3244(2)	8231(3)	4915(1)	11(1)
C(53)	2234(2)	8253(3)	4927(1)	12(1)
C(54)	2212(2)	8331(3)	5626(1)	11(1)
C(55)	3718(2)	9300(3)	6018(1)	12(1)
C(56)	4203(2)	10381(3)	6470(1)	13(1)

C(6)	4863(2)	6693(3)	7138(2)	18(1)
C(61)	7222(2)	9079(3)	5896(1)	10(1)
C(62)	6655(2)	8339(3)	5294(1)	12(1)
C(63)	5919(2)	9220(3)	4850(1)	13(1)
C(64)	5347(2)	9921(3)	5228(1)	11(1)
C(65)	6575(2)	9721(3)	6231(1)	12(1)
C(66)	7086(2)	10538(3)	6816(1)	13(1)
C(71)	9629(2)	6377(3)	7420(1)	12(1)
C(72)	9162(2)	5991(3)	6715(1)	14(1)
C(73)	9256(2)	7127(3)	6286(1)	16(1)
C(74)	8815(2)	8359(3)	6459(1)	14(1)
C(75)	9223(2)	7672(3)	7573(1)	13(1)
C(76)	9741(2)	8239(3)	8234(1)	13(1)
P(1)	6233(1)	4340(1)	7096(1)	17(1)
N(1)	5006(2)	5670(2)	7636(1)	16(1)
N(2)	6662(2)	6358(2)	8042(1)	16(1)
N(3)	5693(2)	7005(2)	6943(1)	16(1)
O(1)	300(2)	144(2)	4989(1)	20(1)
O(10)	8219(1)	2729(2)	8911(1)	11(1)
O(12)	8947(1)	1398(2)	8032(1)	15(1)
O(13)	10045(1)	2981(2)	7450(1)	16(1)
O(15)	10206(1)	4875(2)	8902(1)	13(1)
O(16)	9549(2)	6085(2)	9914(1)	16(1)
O(2)	102(1)	1478(2)	6063(1)	19(1)
O(20)	5266(1)	1955(2)	8732(1)	12(1)
O(22)	6229(2)	-352(2)	8632(1)	17(1)
O(23)	8227(1)	-20(2)	8875(1)	17(1)
O(25)	7641(1)	2707(2)	9784(1)	12(1)
O(26)	6320(2)	3216(2)	10389(1)	22(1)
O(3)	1378(2)	865(2)	9112(1)	24(1)
O(30)	2863(1)	3907(2)	7428(1)	11(1)
O(32)	2677(1)	1093(2)	7325(1)	14(1)
O(33)	4254(1)	-238(2)	8222(1)	16(1)
O(35)	4060(1)	2764(2)	9080(1)	13(1)
O(36)	2556(1)	4654(2)	8944(1)	17(1)
O(4)	2663(2)	2662(2)	9829(1)	23(1)
O(40)	2582(1)	7134(2)	5935(1)	12(1)
O(42)	1733(1)	4813(2)	5392(1)	14(1)
O(43)	1772(1)	2742(2)	6297(1)	14(1)
O(45)	1858(1)	5705(2)	7274(1)	11(1)
O(46)	2837(2)	8078(2)	7879(1)	22(1)
O(5)	5421(2)	-1712(4)	9530(1)	47(1)
O(50)	4794(1)	8984(2)	5407(1)	12(1)
O(52)	3234(1)	8373(2)	4257(1)	15(1)
O(53)	1730(1)	7129(2)	4615(1)	14(1)
O(55)	2735(1)	9406(2)	5953(1)	12(1)
O(56)	3896(2)	11671(2)	6245(1)	17(1)
O(6)	8026(2)	-2618(2)	9107(1)	17(1)
O(60)	7834(1)	8159(2)	6320(1)	12(1)
O(62)	7236(1)	7870(2)	4933(1)	14(1)
O(63)	5280(1)	8523(2)	4335(1)	17(1)
O(65)	5947(1)	10591(2)	5770(1)	12(1)
O(66)	7788(1)	11370(2)	6719(1)	16(1)

O(7)	10827(2)	623(2)	7331(1)	17(1)
O(70)	9427(1)	5371(2)	7822(1)	12(1)
O(72)	9574(1)	4878(2)	6520(1)	17(1)
O(73)	8835(2)	6840(2)	5619(1)	22(1)
O(75)	9238(1)	8677(2)	7112(1)	15(1)
O(76)	10640(1)	8732(2)	8246(1)	16(1)
O(8)	12056(2)	7186(2)	8780(1)	17(1)

Table A.1.2 Bond lengths (Å) and angles (°) for PTA-β-Cyclodextrin.

C(1)-N(1)	1.468(4)	C(21)-C(22)	1.520(4)
C(1)-P(1)	1.867(3)	C(21)-H(21)	0.9800
C(1)-H(1A)	0.9700	C(22)-O(22)	1.434(3)
C(1)-H(1B)	0.9700	C(22)-C(23)	1.512(4)
C(11)-O(10)	1.438(3)	C(22)-H(22)	0.9800
C(11)-C(12)	1.507(4)	C(23)-O(23)	1.428(3)
C(11)-C(15)	1.536(4)	C(23)-C(24)	1.525(4)
C(11)-H(11)	0.9800	C(23)-H(23)	0.9800
C(12)-O(12)	1.430(3)	C(24)-O(25)	1.410(3)
C(12)-C(13)	1.527(4)	C(24)-O(10)	1.423(3)
C(12)-H(12)	0.9800	C(24)-H(24)	0.9800
C(13)-O(13)	1.416(3)	C(25)-O(25)	1.444(3)
C(13)-C(14)	1.524(4)	C(25)-C(26)	1.514(4)
C(13)-H(13)	0.9800	C(25)-H(25)	0.9800
C(14)-O(15)	1.414(3)	C(26)-O(26)	1.419(4)
C(14)-O(70)	1.415(3)	C(26)-H(26A)	0.9700
C(14)-H(14)	0.9800	C(26)-H(26B)	0.9700
C(15)-O(15)	1.441(3)	C(3)-N(3)	1.467(4)
C(15)-C(16)	1.514(4)	C(3)-P(1)	1.863(3)
C(15)-H(15)	0.9800	C(3)-H(3A)	0.9700
C(16)-O(16)	1.420(3)	C(3)-H(3B)	0.9700
C(16)-H(16A)	0.9700	C(31)-O(30)	1.430(3)
C(16)-H(16B)	0.9700	C(31)-C(32)	1.513(4)
C(2)-N(2)	1.482(4)	C(31)-C(35)	1.522(4)
C(2)-P(1)	1.859(3)	C(31)-H(31)	0.9800
C(2)-H(2A)	0.9700	C(32)-O(32)	1.427(3)
C(2)-H(2B)	0.9700	C(32)-C(33)	1.517(4)
C(21)-O(20)	1.435(3)	C(32)-H(32)	0.9800
C(21)-C(25)	1.515(4)	C(33)-O(33)	1.427(3)
C(33)-C(34)	1.525(4)	C(5)-N(2)	1.475(4)
C(33)-H(33)	0.9800	C(5)-H(5A)	0.9700
C(34)-O(20)	1.405(3)	C(5)-H(5B)	0.9700
C(34)-O(35)	1.411(3)	C(51)-O(50)	1.440(3)
C(34)-H(34)	0.9800	C(51)-C(55)	1.529(4)
C(35)-O(35)	1.441(3)	C(51)-C(52)	1.533(4)
C(35)-C(36)	1.505(4)	C(51)-H(51)	0.9800
C(35)-H(35)	0.9800	C(52)-O(52)	1.429(3)
C(36)-O(36)	1.429(3)	C(52)-C(53)	1.526(4)
C(36)-H(36A)	0.9700	C(52)-H(52)	0.9800
C(36)-H(36B)	0.9700	C(53)-O(53)	1.422(3)
C(4)-N(1)	1.465(4)	C(53)-C(54)	1.526(4)
C(4)-N(2)	1.477(4)	C(53)-H(53)	0.9800
C(4)-H(4A)	0.9700	C(54)-O(55)	1.403(3)

C(4)-H(4B)	0.9700	C(54)-O(40)	1.418(3)
C(41)-O(40)	1.438(3)	C(54)-H(54)	0.9800
C(41)-C(42)	1.513(4)	C(55)-O(55)	1.443(3)
C(41)-C(45)	1.528(4)	C(55)-C(56)	1.503(4)
C(41)-H(41)	0.9800	C(55)-H(55)	0.9800
C(42)-O(42)	1.427(3)	C(56)-O(56)	1.426(3)
C(42)-C(43)	1.520(4)	C(56)-H(56A)	0.9700
C(42)-H(42)	0.9800	C(56)-H(56B)	0.9700
C(43)-O(43)	1.422(3)	C(6)-N(1)	1.465(4)
C(43)-C(44)	1.532(4)	C(6)-N(3)	1.469(4)
C(43)-H(43)	0.9800	C(6)-H(6A)	0.9700
C(44)-O(30)	1.407(3)	C(6)-H(6B)	0.9700
C(44)-O(45)	1.412(3)	C(61)-O(60)	1.431(3)
C(44)-H(44)	0.9800	C(61)-C(62)	1.519(4)
C(45)-O(45)	1.440(3)	C(61)-C(65)	1.527(4)
C(45)-C(46)	1.504(4)	C(61)-H(61)	0.9800
C(45)-H(45)	0.9800	C(62)-O(62)	1.422(3)
C(46)-O(46)	1.417(3)	C(62)-C(63)	1.516(4)
C(46)-H(46A)	0.9700	C(62)-H(62)	0.9800
C(46)-H(46B)	0.9700	C(63)-O(63)	1.417(3)
C(5)-N(3)	1.462(4)	C(63)-C(64)	1.533(4)
C(63)-H(63)	0.9800	O(16)-H(16C)	0.79(4)
C(64)-O(50)	1.394(3)	O(2)-H(2D)	0.61(4)
C(64)-O(65)	1.415(3)	O(2)-H(2E)	0.90(4)
C(64)-H(64)	0.9800	O(22)-H(22C)	0.80(4)
C(65)-O(65)	1.446(3)	O(23)-H(23C)	0.78(4)
C(65)-C(66)	1.513(4)	O(26)-H(26C)	0.76(4)
C(65)-H(65)	0.9800	O(3)-H(3D)	0.86(4)
C(66)-O(66)	1.417(3)	O(3)-H(3E)	0.83(4)
C(66)-H(66A)	0.9700	O(32)-H(32C)	0.84(4)
C(66)-H(66B)	0.9700	O(33)-H(33C)	0.87(4)
C(71)-O(70)	1.435(3)	O(36)-H(36C)	0.82(4)
C(71)-C(72)	1.524(4)	O(4)-H(4D)	0.88(4)
C(71)-C(75)	1.529(4)	O(4)-H(4E)	0.95(4)
C(71)-H(71)	0.9800	O(42)-H(42C)	0.71(4)
C(72)-O(72)	1.415(3)	O(43)-H(43C)	0.79(4)
C(72)-C(73)	1.516(4)	O(46)-H(46C)	0.82(4)
C(72)-H(72)	0.9800	O(5)-H(5D)	0.91(4)
C(73)-O(73)	1.417(4)	O(5)-H(5E)	0.80(4)
C(73)-C(74)	1.517(4)	O(52)-H(52C)	0.60(4)
C(73)-H(73)	0.9800	O(53)-H(53C)	0.90(4)
C(74)-O(75)	1.399(3)	O(56)-H(56C)	0.78(4)
C(74)-O(60)	1.424(3)	O(6)-H(6D)	0.92(4)
C(74)-H(74)	0.9800	O(6)-H(6E)	0.83(4)
C(75)-O(75)	1.434(3)	O(62)-H(62C)	0.83(4)
C(75)-C(76)	1.517(4)	O(63)-H(63C)	0.71(4)
C(75)-H(75)	0.9800	O(66)-H(66C)	0.76(4)
C(76)-O(76)	1.431(3)	O(7)-H(7D)	0.87(4)
C(76)-H(76A)	0.9700	O(7)-H(7E)	0.91(4)
C(76)-H(76B)	0.9700	O(72)-H(72C)	0.81(4)
O(1)-H(1D)	0.84(4)	O(73)-H(73C)	0.74(4)
O(1)-H(1E)	0.81(4)	O(76)-H(76C)	0.77(4)
O(12)-H(12C)	0.74(4)	O(8)-H(8D)	0.90(4)

O(13)-H(13C)	0.87(4)	O(8)-H(8E)	0.80(4)
N(1)-C(1)-P(1)	114.5(2)	P(1)-C(1)-H(1A)	108.6
N(1)-C(1)-H(1A)	108.6	N(1)-C(1)-H(1B)	108.6
P(1)-C(1)-H(1B)	108.6	O(16)-C(16)-C(15)	113.2(2)
H(1A)-C(1)-H(1B)	107.6	O(16)-C(16)-H(16A)	108.9
O(10)-C(11)-C(12)	107.1(2)	C(15)-C(16)-H(16A)	108.9
O(10)-C(11)-C(15)	109.5(2)	O(16)-C(16)-H(16B)	108.9
C(12)-C(11)-C(15)	110.3(2)	C(15)-C(16)-H(16B)	108.9
O(10)-C(11)-H(11)	110.0	H(16A)-C(16)-H(16B)	107.7
C(12)-C(11)-H(11)	110.0	N(2)-C(2)-P(1)	115.42(19)
C(15)-C(11)-H(11)	110.0	N(2)-C(2)-H(2A)	108.4
O(12)-C(12)-C(11)	109.7(2)	P(1)-C(2)-H(2A)	108.4
O(12)-C(12)-C(13)	110.6(2)	N(2)-C(2)-H(2B)	108.4
C(11)-C(12)-C(13)	108.5(2)	P(1)-C(2)-H(2B)	108.4
O(12)-C(12)-H(12)	109.3	H(2A)-C(2)-H(2B)	107.5
C(11)-C(12)-H(12)	109.3	O(20)-C(21)-C(25)	110.9(2)
C(13)-C(12)-H(12)	109.3	O(20)-C(21)-C(22)	105.8(2)
O(13)-C(13)-C(14)	109.3(2)	C(25)-C(21)-C(22)	110.5(2)
O(13)-C(13)-C(12)	110.8(2)	O(20)-C(21)-H(21)	109.9
C(14)-C(13)-C(12)	108.8(2)	C(25)-C(21)-H(21)	109.9
O(13)-C(13)-H(13)	109.3	C(22)-C(21)-H(21)	109.9
C(14)-C(13)-H(13)	109.3	O(22)-C(22)-C(23)	109.7(2)
C(12)-C(13)-H(13)	109.3	O(22)-C(22)-C(21)	110.2(2)
O(15)-C(14)-O(70)	110.6(2)	C(23)-C(22)-C(21)	109.9(2)
O(15)-C(14)-C(13)	109.4(2)	O(22)-C(22)-H(22)	109.0
O(70)-C(14)-C(13)	108.9(2)	C(23)-C(22)-H(22)	109.0
O(15)-C(14)-H(14)	109.3	C(21)-C(22)-H(22)	109.0
O(70)-C(14)-H(14)	109.3	O(23)-C(23)-C(22)	112.7(2)
C(13)-C(14)-H(14)	109.3	O(23)-C(23)-C(24)	109.8(2)
O(15)-C(15)-C(16)	107.0(2)	C(22)-C(23)-C(24)	110.1(2)
O(15)-C(15)-C(11)	111.6(2)	O(23)-C(23)-H(23)	108.0
C(16)-C(15)-C(11)	111.8(2)	C(22)-C(23)-H(23)	108.0
O(15)-C(15)-H(15)	108.8	C(24)-C(23)-H(23)	108.0
C(16)-C(15)-H(15)	108.8	O(25)-C(24)-O(10)	109.3(2)
C(11)-C(15)-H(15)	108.8	O(25)-C(24)-C(23)	111.1(2)
O(10)-C(24)-C(23)	108.5(2)	C(23)-C(24)-H(24)	109.3
O(25)-C(24)-H(24)	109.3	O(25)-C(25)-C(26)	105.9(2)
O(10)-C(24)-H(24)	109.3	O(25)-C(25)-C(21)	108.5(2)
C(26)-C(25)-C(21)	115.3(2)	O(20)-C(34)-C(33)	108.4(2)
O(25)-C(25)-H(25)	109.0	O(35)-C(34)-C(33)	109.8(2)
C(26)-C(25)-H(25)	109.0	O(20)-C(34)-H(34)	109.3
C(21)-C(25)-H(25)	109.0	O(35)-C(34)-H(34)	109.3
O(26)-C(26)-C(25)	110.2(2)	C(33)-C(34)-H(34)	109.3
O(26)-C(26)-H(26A)	109.6	O(35)-C(35)-C(36)	106.2(2)
C(25)-C(26)-H(26A)	109.6	O(35)-C(35)-C(31)	109.0(2)
O(26)-C(26)-H(26B)	109.6	C(36)-C(35)-C(31)	113.6(2)
C(25)-C(26)-H(26B)	109.6	O(35)-C(35)-H(35)	109.3
H(26A)-C(26)-H(26B)	108.1	C(36)-C(35)-H(35)	109.3
N(3)-C(3)-P(1)	115.16(19)	C(31)-C(35)-H(35)	109.3
N(3)-C(3)-H(3A)	108.5	O(36)-C(36)-C(35)	113.2(2)
P(1)-C(3)-H(3A)	108.5	O(36)-C(36)-H(36A)	108.9
N(3)-C(3)-H(3B)	108.5	C(35)-C(36)-H(36A)	108.9

P(1)-C(3)-H(3B)	108.5	O(36)-C(36)-H(36B)	108.9
H(3A)-C(3)-H(3B)	107.5	C(35)-C(36)-H(36B)	108.9
O(30)-C(31)-C(32)	107.0(2)	H(36A)-C(36)-H(36B)	107.7
O(30)-C(31)-C(35)	109.8(2)	N(1)-C(4)-N(2)	114.2(2)
C(32)-C(31)-C(35)	111.3(2)	N(1)-C(4)-H(4A)	108.7
O(30)-C(31)-H(31)	109.6	N(2)-C(4)-H(4A)	108.7
C(32)-C(31)-H(31)	109.6	N(1)-C(4)-H(4B)	108.7
C(35)-C(31)-H(31)	109.6	N(2)-C(4)-H(4B)	108.7
O(32)-C(32)-C(31)	110.7(2)	H(4A)-C(4)-H(4B)	107.6
O(32)-C(32)-C(33)	108.1(2)	O(40)-C(41)-C(42)	106.4(2)
C(31)-C(32)-C(33)	111.6(2)	O(40)-C(41)-C(45)	111.7(2)
O(32)-C(32)-H(32)	108.8	C(42)-C(41)-C(45)	108.9(2)
C(31)-C(32)-H(32)	108.8	O(40)-C(41)-H(41)	109.9
C(33)-C(32)-H(32)	108.8	C(42)-C(41)-H(41)	109.9
O(33)-C(33)-C(32)	111.7(2)	C(45)-C(41)-H(41)	109.9
O(33)-C(33)-C(34)	108.1(2)	O(42)-C(42)-C(41)	108.6(2)
C(32)-C(33)-C(34)	110.4(2)	O(42)-C(42)-C(43)	110.3(2)
O(33)-C(33)-H(33)	108.9	C(41)-C(42)-C(43)	110.0(2)
C(32)-C(33)-H(33)	108.9	O(42)-C(42)-H(42)	109.3
C(34)-C(33)-H(33)	108.9	C(41)-C(42)-H(42)	109.3
O(20)-C(34)-O(35)	110.7(2)	C(43)-C(42)-H(42)	109.3
O(43)-C(43)-C(42)	109.1(2)	C(52)-C(51)-H(51)	110.6
O(43)-C(43)-C(44)	111.0(2)	O(52)-C(52)-C(53)	108.1(2)
C(42)-C(43)-C(44)	111.6(2)	O(52)-C(52)-C(51)	110.9(2)
O(43)-C(43)-H(43)	108.4	C(53)-C(52)-C(51)	112.0(2)
C(42)-C(43)-H(43)	108.4	O(52)-C(52)-H(52)	108.6
C(44)-C(43)-H(43)	108.4	C(53)-C(52)-H(52)	108.6
O(30)-C(44)-O(45)	111.4(2)	C(51)-C(52)-H(52)	108.6
O(30)-C(44)-C(43)	108.9(2)	O(53)-C(53)-C(52)	111.5(2)
O(45)-C(44)-C(43)	109.9(2)	O(53)-C(53)-C(54)	110.1(2)
O(30)-C(44)-H(44)	108.9	C(52)-C(53)-C(54)	110.0(2)
O(45)-C(44)-H(44)	108.9	O(53)-C(53)-H(53)	108.4
C(43)-C(44)-H(44)	108.9	C(52)-C(53)-H(53)	108.4
O(45)-C(45)-C(46)	106.6(2)	C(54)-C(53)-H(53)	108.4
O(45)-C(45)-C(41)	108.8(2)	O(55)-C(54)-O(40)	110.7(2)
C(46)-C(45)-C(41)	113.4(2)	O(55)-C(54)-C(53)	111.2(2)
O(45)-C(45)-H(45)	109.3	O(40)-C(54)-C(53)	107.4(2)
C(46)-C(45)-H(45)	109.3	O(55)-C(54)-H(54)	109.2
C(41)-C(45)-H(45)	109.3	O(40)-C(54)-H(54)	109.2
O(46)-C(46)-C(45)	111.7(2)	C(53)-C(54)-H(54)	109.2
O(46)-C(46)-H(46A)	109.3	O(55)-C(55)-C(56)	106.7(2)
C(45)-C(46)-H(46A)	109.3	O(55)-C(55)-C(51)	108.8(2)
O(46)-C(46)-H(46B)	109.3	C(56)-C(55)-C(51)	116.3(2)
C(45)-C(46)-H(46B)	109.3	O(55)-C(55)-H(55)	108.3
H(46A)-C(46)-H(46B)	107.9	C(56)-C(55)-H(55)	108.3
N(3)-C(5)-N(2)	114.3(2)	C(51)-C(55)-H(55)	108.3
N(3)-C(5)-H(5A)	108.7	O(56)-C(56)-C(55)	114.1(2)
N(2)-C(5)-H(5A)	108.7	O(56)-C(56)-H(56A)	108.7
N(3)-C(5)-H(5B)	108.7	C(55)-C(56)-H(56A)	108.7
N(2)-C(5)-H(5B)	108.7	O(56)-C(56)-H(56B)	108.7
H(5A)-C(5)-H(5B)	107.6	C(55)-C(56)-H(56B)	108.7
O(50)-C(51)-C(55)	108.2(2)	H(56A)-C(56)-H(56B)	107.6
O(50)-C(51)-C(52)	105.7(2)	N(1)-C(6)-N(3)	114.8(2)

C(55)-C(51)-C(52)	110.9(2)	N(1)-C(6)-H(6A)	108.6
O(50)-C(51)-H(51)	110.6	N(3)-C(6)-H(6A)	108.6
C(55)-C(51)-H(51)	110.6	N(1)-C(6)-H(6B)	108.6
N(3)-C(6)-H(6B)	108.6	O(66)-C(66)-H(66B)	108.7
H(6A)-C(6)-H(6B)	107.5	C(65)-C(66)-H(66B)	108.7
O(60)-C(61)-C(62)	107.9(2)	H(66A)-C(66)-H(66B)	107.6
O(60)-C(61)-C(65)	110.6(2)	O(70)-C(71)-C(72)	107.9(2)
C(62)-C(61)-C(65)	110.4(2)	O(70)-C(71)-C(75)	108.0(2)
O(60)-C(61)-H(61)	109.3	C(72)-C(71)-C(75)	110.3(2)
C(62)-C(61)-H(61)	109.3	O(70)-C(71)-H(71)	110.2
C(65)-C(61)-H(61)	109.3	C(72)-C(71)-H(71)	110.2
O(62)-C(62)-C(63)	107.4(2)	C(75)-C(71)-H(71)	110.2
O(62)-C(62)-C(61)	111.2(2)	O(72)-C(72)-C(73)	107.2(2)
C(63)-C(62)-C(61)	111.0(2)	O(72)-C(72)-C(71)	113.4(2)
O(62)-C(62)-H(62)	109.0	C(73)-C(72)-C(71)	108.5(2)
C(63)-C(62)-H(62)	109.0	O(72)-C(72)-H(72)	109.2
C(61)-C(62)-H(62)	109.0	C(73)-C(72)-H(72)	109.2
O(63)-C(63)-C(62)	112.9(2)	C(71)-C(72)-H(72)	109.2
O(63)-C(63)-C(64)	107.3(2)	O(73)-C(73)-C(72)	111.8(2)
C(62)-C(63)-C(64)	110.8(2)	O(73)-C(73)-C(74)	109.3(2)
O(63)-C(63)-H(63)	108.6	C(72)-C(73)-C(74)	110.4(2)
C(62)-C(63)-H(63)	108.6	O(73)-C(73)-H(73)	108.4
C(64)-C(63)-H(63)	108.6	C(72)-C(73)-H(73)	108.4
O(50)-C(64)-O(65)	112.4(2)	C(74)-C(73)-H(73)	108.4
O(50)-C(64)-C(63)	108.0(2)	O(75)-C(74)-O(60)	111.4(2)
O(65)-C(64)-C(63)	110.3(2)	O(75)-C(74)-C(73)	110.1(2)
O(50)-C(64)-H(64)	108.7	O(60)-C(74)-C(73)	109.4(2)
O(65)-C(64)-H(64)	108.7	O(75)-C(74)-H(74)	108.6
C(63)-C(64)-H(64)	108.7	O(60)-C(74)-H(74)	108.6
O(65)-C(65)-C(66)	107.3(2)	C(73)-C(74)-H(74)	108.6
O(65)-C(65)-C(61)	107.9(2)	O(75)-C(75)-C(76)	105.8(2)
C(66)-C(65)-C(61)	113.6(2)	O(75)-C(75)-C(71)	111.8(2)
O(65)-C(65)-H(65)	109.3	C(76)-C(75)-C(71)	114.1(2)
C(66)-C(65)-H(65)	109.3	O(75)-C(75)-H(75)	108.3
C(61)-C(65)-H(65)	109.3	C(76)-C(75)-H(75)	108.3
O(66)-C(66)-C(65)	114.4(2)	C(71)-C(75)-H(75)	108.3
O(66)-C(66)-H(66A)	108.7	O(76)-C(76)-C(75)	111.0(2)
C(65)-C(66)-H(66A)	108.7	O(76)-C(76)-H(76A)	109.4
C(75)-C(76)-H(76A)	109.4	C(32)-O(32)-H(32C)	106(3)
O(76)-C(76)-H(76B)	109.4	C(33)-O(33)-H(33C)	105(3)
C(75)-C(76)-H(76B)	109.4	C(34)-O(35)-C(35)	113.6(2)
H(76A)-C(76)-H(76B)	108.0	C(36)-O(36)-H(36C)	109(3)
C(2)-P(1)-C(3)	94.42(13)	H(4D)-O(4)-H(4E)	111(4)
C(2)-P(1)-C(1)	95.42(13)	C(54)-O(40)-C(41)	118.8(2)
C(3)-P(1)-C(1)	96.05(14)	C(42)-O(42)-H(42C)	97(3)
C(4)-N(1)-C(6)	107.6(2)	C(43)-O(43)-H(43C)	112(3)
C(4)-N(1)-C(1)	111.8(2)	C(44)-O(45)-C(45)	113.96(19)
C(6)-N(1)-C(1)	111.2(2)	C(46)-O(46)-H(46C)	113(3)
C(5)-N(2)-C(4)	107.6(2)	H(5D)-O(5)-H(5E)	102(4)
C(5)-N(2)-C(2)	110.2(2)	C(64)-O(50)-C(51)	118.5(2)
C(4)-N(2)-C(2)	111.2(2)	C(52)-O(52)-H(52C)	107(4)
C(5)-N(3)-C(3)	110.9(2)	C(53)-O(53)-H(53C)	102(2)
C(5)-N(3)-C(6)	108.1(2)	C(54)-O(55)-C(55)	112.9(2)

C(3)-N(3)-C(6)	110.9(2)	C(56)-O(56)-H(56C)	107(3)
H(1D)-O(1)-H(1E)	103(4)	H(6D)-O(6)-H(6E)	109(4)
C(24)-O(10)-C(11)	118.0(2)	C(74)-O(60)-C(61)	117.5(2)
C(12)-O(12)-H(12C)	103(3)	C(62)-O(62)-H(62C)	107(3)
C(13)-O(13)-H(13C)	100(3)	C(63)-O(63)-H(63C)	110(3)
C(14)-O(15)-C(15)	113.9(2)	C(64)-O(65)-C(65)	113.1(2)
C(16)-O(16)-H(16C)	107(3)	C(66)-O(66)-H(66C)	109(3)
H(2D)-O(2)-H(2E)	122(5)	H(7D)-O(7)-H(7E)	107(3)
C(34)-O(20)-C(21)	118.4(2)	C(14)-O(70)-C(71)	119.2(2)
C(22)-O(22)-H(22C)	109(3)	C(72)-O(72)-H(72C)	114(3)
C(23)-O(23)-H(23C)	108(3)	C(73)-O(73)-H(73C)	112(3)
C(24)-O(25)-C(25)	114.0(2)	C(74)-O(75)-C(75)	116.1(2)
C(26)-O(26)-H(26C)	111(3)	C(76)-O(76)-H(76C)	111(3)
H(3D)-O(3)-H(3E)	100(4)	H(8D)-O(8)-H(8E)	100(4)
C(44)-O(30)-C(31)	117.3(2)		

Table A.1.3 Anisotropic displacement parameters ($Å^2$ x 10^3) for PTA-β-Cyclodextrin. The anisotropic displacement factor exponent takes the form: $-2\pi^2[h^2a^{*2}U11 + ... + 2hka^*b^*U12]$.

	U11	U22	U33	U23	U13	U12
C(1)	16(1)	19(2)	21(2)	3(1)	6(1)	-1(1)
C(11)	7(1)	12(2)	15(1)	1(1)	4(1)	0(1)
C(12)	11(1)	9(1)	14(1)	0(1)	3(1)	0(1)
C(13)	14(1)	12(1)	11(1)	1(1)	6(1)	3(1)
C(14)	10(1)	13(2)	12(1)	3(1)	5(1)	-1(1)
C(15)	7(1)	11(1)	13(1)	2(1)	2(1)	0(1)
C(16)	16(1)	15(2)	13(1)	-1(1)	6(1)	-2(1)
C(2)	12(1)	16(2)	18(2)	5(1)	6(1)	2(1)
C(21)	11(1)	12(2)	12(1)	3(1)	4(1)	3(1)
C(22)	14(1)	8(1)	14(1)	0(1)	6(1)	-1(1)
C(23)	14(1)	13(2)	16(1)	2(1)	10(1)	3(1)
C(24)	10(1)	16(2)	14(1)	3(1)	6(1)	1(1)
C(25)	10(1)	13(2)	14(1)	3(1)	6(1)	1(1)
C(26)	13(1)	17(2)	16(2)	-4(1)	4(1)	1(1)
C(3)	21(2)	21(2)	13(1)	3(1)	7(1)	-4(1)
C(31)	10(1)	13(2)	13(1)	3(1)	6(1)	-1(1)
C(32)	12(1)	15(2)	12(1)	-1(1)	4(1)	-2(1)
C(33)	12(1)	11(1)	18(1)	0(1)	6(1)	1(1)
C(34)	11(1)	14(2)	12(1)	1(1)	5(1)	-1(1)
C(35)	11(1)	12(1)	11(1)	1(1)	4(1)	1(1)
C(36)	14(1)	15(2)	14(1)	-1(1)	4(1)	-1(1)
C(4)	18(2)	18(2)	19(2)	1(1)	9(1)	3(1)
C(41)	8(1)	12(1)	14(1)	0(1)	8(1)	-2(1)
C(42)	11(1)	14(1)	12(1)	-1(1)	5(1)	0(1)
C(43)	11(1)	9(1)	12(1)	-1(1)	4(1)	-1(1)
C(44)	10(1)	11(1)	14(1)	2(1)	4(1)	-2(1)
C(45)	12(1)	12(1)	12(1)	2(1)	6(1)	-1(1)
C(46)	19(1)	13(2)	14(1)	0(1)	7(1)	-2(1)
C(5)	13(1)	16(2)	20(2)	1(1)	5(1)	-2(1)
C(51)	7(1)	11(1)	14(1)	3(1)	5(1)	1(1)
C(52)	10(1)	13(1)	11(1)	2(1)	5(1)	2(1)
C(53)	10(1)	9(1)	16(1)	0(1)	3(1)	2(1)

C(54)	9(1)	11(1)	15(1)	2(1)	4(1)	1(1)
C(55)	11(1)	11(1)	13(1)	2(1)	3(1)	2(1)
C(56)	14(1)	15(2)	12(1)	1(1)	6(1)	2(1)
C(6)	15(2)	18(2)	22(2)	4(1)	6(1)	2(1)
C(61)	8(1)	10(1)	13(1)	1(1)	4(1)	-1(1)
C(62)	10(1)	12(1)	16(1)	-1(1)	8(1)	-1(1)
C(63)	13(1)	16(2)	11(1)	1(1)	6(1)	1(1)
C(64)	9(1)	13(1)	14(1)	-1(1)	5(1)	0(1)
C(65)	12(1)	11(1)	14(1)	2(1)	6(1)	0(1)
C(66)	12(1)	14(2)	14(1)	2(1)	5(1)	1(1)
C(71)	9(1)	12(1)	16(1)	3(1)	7(1)	1(1)
C(72)	11(1)	16(2)	14(1)	0(1)	6(1)	2(1)
C(73)	12(1)	19(2)	19(2)	4(1)	6(1)	3(1)
C(74)	9(1)	17(2)	17(1)	4(1)	4(1)	-1(1)
C(75)	9(1)	12(1)	18(1)	1(1)	6(1)	1(1)
C(76)	13(1)	12(1)	16(1)	0(1)	7(1)	1(1)
P(1)	20(1)	16(1)	18(1)	-2(1)	10(1)	0(1)
N(1)	16(1)	16(1)	21(1)	4(1)	10(1)	1(1)
N(2)	15(1)	14(1)	18(1)	-1(1)	4(1)	0(1)
N(3)	11(1)	19(1)	17(1)	2(1)	5(1)	-1(1)
O(1)	17(1)	28(1)	17(1)	-3(1)	6(1)	-4(1)
O(10)	9(1)	14(1)	11(1)	4(1)	5(1)	0(1)
O(12)	20(1)	13(1)	12(1)	-2(1)	8(1)	-4(1)
O(13)	19(1)	14(1)	18(1)	2(1)	13(1)	4(1)
O(15)	11(1)	16(1)	12(1)	-1(1)	5(1)	-3(1)
O(16)	17(1)	14(1)	15(1)	-2(1)	2(1)	0(1)
O(2)	10(1)	25(1)	20(1)	0(1)	3(1)	0(1)
O(20)	10(1)	14(1)	14(1)	1(1)	5(1)	1(1)
O(22)	13(1)	13(1)	25(1)	-6(1)	7(1)	-2(1)
O(23)	17(1)	14(1)	25(1)	1(1)	14(1)	3(1)
O(25)	9(1)	16(1)	12(1)	0(1)	4(1)	1(1)
O(26)	17(1)	37(1)	16(1)	3(1)	10(1)	7(1)
O(3)	30(1)	22(1)	23(1)	-6(1)	14(1)	-6(1)
O(30)	11(1)	11(1)	13(1)	0(1)	6(1)	-1(1)
O(32)	13(1)	12(1)	15(1)	-1(1)	2(1)	0(1)
O(33)	12(1)	10(1)	25(1)	-2(1)	5(1)	0(1)
O(35)	13(1)	13(1)	13(1)	0(1)	6(1)	2(1)
O(36)	17(1)	17(1)	22(1)	2(1)	12(1)	4(1)
O(4)	26(1)	25(1)	22(1)	-3(1)	13(1)	-5(1)
O(40)	11(1)	12(1)	14(1)	4(1)	7(1)	0(1)
O(42)	16(1)	12(1)	12(1)	-1(1)	4(1)	1(1)
O(43)	15(1)	12(1)	15(1)	-2(1)	5(1)	-3(1)
O(45)	11(1)	10(1)	13(1)	-1(1)	7(1)	-2(1)
O(46)	30(1)	22(1)	14(1)	-4(1)	10(1)	-13(1)
O(5)	19(1)	96(3)	30(1)	31(2)	12(1)	15(2)
O(50)	8(1)	13(1)	16(1)	4(1)	6(1)	-1(1)
O(52)	13(1)	22(1)	12(1)	1(1)	7(1)	-1(1)
O(53)	11(1)	15(1)	14(1)	-1(1)	2(1)	-2(1)
O(55)	9(1)	11(1)	17(1)	-2(1)	7(1)	0(1)
O(56)	16(1)	14(1)	19(1)	2(1)	5(1)	-3(1)
O(6)	20(1)	13(1)	16(1)	-2(1)	3(1)	-1(1)
O(60)	8(1)	14(1)	14(1)	5(1)	2(1)	1(1)
O(62)	11(1)	19(1)	12(1)	-1(1)	5(1)	4(1)

O(63)	12(1)	23(1)	15(1)	-8(1)	4(1)	3(1)
O(65)	9(1)	13(1)	12(1)	1(1)	2(1)	0(1)
O(66)	17(1)	14(1)	17(1)	2(1)	3(1)	-4(1)
O(7)	15(1)	17(1)	21(1)	3(1)	10(1)	1(1)
O(70)	9(1)	12(1)	16(1)	2(1)	6(1)	0(1)
O(72)	22(1)	18(1)	15(1)	1(1)	9(1)	6(1)
O(73)	23(1)	33(1)	14(1)	4(1)	10(1)	15(1)
O(75)	14(1)	13(1)	17(1)	3(1)	1(1)	-2(1)
O(76)	11(1)	14(1)	20(1)	0(1)	3(1)	-1(1)
O(8)	17(1)	18(1)	16(1)	-1(1)	3(1)	2(1)

Table A.1.4 Hydrogen coordinates (x 10^4) and isotropic displacement parameters ($Å^2$ x 10^3) for PTA-β-Cyclodextrin.

	x	y	z	U(eq)
H(1A)	4639	4139	7029	22
H(1B)	5263	3736	7725	22
H(11)	9602	2454	9162	13
H(12)	8596	3279	7882	14
H(13)	10546	2702	8394	14
H(14)	10766	4951	8192	14
H(15)	8846	5019	8791	13
H(16A)	9039	4301	9888	17
H(16B)	10122	4332	10004	17
H(2A)	7188	4524	8180	18
H(2B)	7609	5374	7735	18
H(21)	6134	1230	9552	14
H(22)	6683	1359	8406	14
H(23)	7689	152	9592	16
H(24)	8792	1832	9749	15
H(25)	6717	3498	9008	14
H(26A)	6648	4684	9906	19
H(26B)	5650	4096	9567	19
H(3A)	6505	6131	6486	21
H(3B)	5455	5708	6217	21
H(31)	2479	2904	8091	13
H(32)	3912	1963	7605	15
H(33)	3269	580	8523	16
H(34)	4687	1055	9312	15
H(35)	4329	3947	8426	13
H(36A)	3887	5158	9217	17
H(36B)	3340	5600	8509	17
H(4A)	5908	5402	8523	21
H(4B)	5604	6872	8378	21
H(41)	1380	6657	6091	12
H(42)	2790	4716	6206	14
H(43)	948	4262	6256	13
H(44)	1532	3858	7357	14
H(45)	3060	6259	7143	14
H(46A)	2541	8527	6956	18
H(46B)	1664	8104	7157	18
H(5A)	6289	8177	7697	20
H(5B)	7013	7523	7404	20

H(51)	3675	10175	5139	13
H(52)	3518	7374	5075	13
H(53)	1928	9040	4696	14
H(54)	1562	8424	5626	14
H(55)	3946	8454	6224	14
H(56A)	4103	10247	6887	16
H(56B)	4871	10319	6536	16
H(6A)	4656	7489	7300	22
H(6B)	4366	6414	6758	22
H(61)	7595	9761	5771	12
H(62)	6346	7589	5426	14
H(63)	6234	9886	4665	15
H(64)	4935	10566	4942	14
H(65)	6209	9038	6362	14
H(66A)	6633	11076	6938	16
H(66B)	7372	9951	7176	16
H(71)	10307	6458	7507	14
H(72)	8498	5815	6647	16
H(73)	9923	7297	6360	20
H(74)	8914	9087	6191	17
H(75)	8572	7519	7555	15
H(76A)	9375	8946	8335	16
H(76B)	9819	7562	8562	16
H(1D)	-250(30)	-130(40)	4800(20)	37(2)
H(1E)	250(30)	510(40)	5310(20)	37(2)
H(12C)	8740(30)	1390(40)	7674(19)	37(2)
H(13C)	10270(30)	2180(40)	7486(19)	37(2)
H(16C)	9160(30)	6430(40)	9627(19)	37(2)
H(2D)	-290(30)	1720(40)	5960(20)	37(2)
H(2E)	300(30)	1090(40)	6450(20)	37(2)
H(22C)	5680(30)	-220(40)	8450(19)	37(2)
H(23C)	8340(30)	470(40)	8627(19)	37(2)
H(26C)	5830(30)	3150(40)	10417(19)	37(2)
H(3D)	1110(30)	220(40)	8868(19)	37(2)
H(3E)	1030(30)	930(40)	9342(19)	37(2)
H(32C)	2410(30)	1660(40)	7040(20)	37(2)
H(33C)	3830(30)	-850(40)	8124(18)	37(2)
H(36C)	2640(30)	4110(40)	9234(19)	37(2)
H(4D)	2360(30)	2050(40)	9560(20)	37(2)
H(4E)	2520(30)	2630(40)	10226(19)	37(2)
H(42C)	1940(30)	4190(40)	5370(20)	37(2)
H(43C)	1300(30)	2360(40)	6145(19)	37(2)
H(46C)	2610(30)	7680(40)	8126(19)	37(2)
H(5D)	5670(30)	-1270(40)	9256(19)	37(2)
H(5E)	5850(30)	-2170(40)	9720(20)	37(2)
H(52C)	3620(30)	8270(40)	4250(20)	37(2)
H(53C)	1890(30)	6530(40)	4934(19)	37(2)
H(56C)	3350(30)	11650(40)	6116(19)	37(2)
H(6D)	8100(30)	-1740(40)	9033(18)	37(2)
H(6E)	7640(30)	-2940(40)	8780(20)	37(2)
H(62C)	7700(30)	7540(40)	5197(19)	37(2)
H(63C)	5530(30)	8080(40)	4200(20)	37(2)
H(66C)	7550(30)	11910(40)	6480(20)	37(2)

H(7D)	11420(30)	580(40)	7379(18)	37(2)
H(7E)	10690(30)	-20(40)	7579(19)	37(2)
H(72C)	9680(30)	4280(40)	6781(19)	37(2)
H(73C)	9070(30)	6290(40)	5510(20)	37(2)
H(76C)	11020(30)	8220(40)	8393(19)	37(2)
H(8D)	12090(30)	6320(40)	8870(18)	37(2)
H(8E)	12450(30)	7460(40)	9090(20)	37(2)

A.2 Crystal data of 2,3,4,6-tetra-*O*-acetyl-1-thio-β-D-glucopyranosato(triethylphosphine)gold(I) (auranofin).

Table A.2.1 Atomic coordinates (x 10^4) and equivalent isotropic displacement parameters (Å^2 x 10^3) for auranofin. U(eq) is defined as one third of the trace of the orthogonalized Uij tensor.

	x	y	z	U(eq)
Au	6829(1)	1292(1)	4259(1)	11(1)
S	6436(2)	-1103(2)	3468(1)	14(1)
P	7372(2)	3448(2)	5179(1)	13(1)
C(1)	7207(7)	2958(8)	6247(4)	17(1)
C(10)	2770(6)	-314(7)	1045(4)	12(1)
C(11)	3385(6)	1079(9)	1680(4)	13(2)
C(12)	5712(8)	-4709(9)	2201(5)	19(2)
C(13)	6936(8)	-5735(9)	2148(5)	29(2)
C(14)	3539(6)	-3776(13)	-40(4)	14(1)
C(15)	2923(7)	-5460(8)	-205(5)	18(2)
C(16)	976(8)	75(9)	-279(5)	24(2)
C(17)	547(8)	1096(12)	-1061(4)	27(2)
C(18)	2279(6)	2174(8)	1860(4)	14(1)
C(19)	285(7)	1762(8)	2365(5)	21(2)
C(2)	7931(6)	1366(14)	6633(4)	22(1)
C(20)	-802(7)	544(9)	2430(5)	23(2)
C(3)	9170(7)	4093(8)	5343(4)	17(1)
C(4)	9508(8)	4487(10)	4501(5)	32(2)
C(5)	6336(7)	5300(8)	4854(4)	17(2)
C(6)	6728(7)	6746(7)	5467(5)	22(2)
C(7)	5333(6)	-530(7)	2415(4)	11(1)
C(8)	4693(6)	-2059(7)	1906(4)	10(1)
C(9)	3867(6)	-1580(7)	1007(4)	13(1)
O(1)	4173(4)	426(5)	2496(3)	12(1)
O(2)	5765(4)	-3199(5)	1846(3)	14(1)
O(3)	4810(6)	-5159(6)	2491(4)	32(1)
O(4)	3152(4)	-3060(6)	617(3)	14(1)
O(5)	4293(5)	-3137(5)	-403(3)	24(1)
O(6)	2252(4)	462(5)	215(3)	14(1)
O(7)	281(6)	-1015(8)	-103(4)	41(2)
O(8)	1252(4)	1073(6)	2063(3)	19(1)
O(9)	294(6)	3197(7)	2566(4)	35(1)

Table A.2.2 Bond lengths (Å) and angles (°) for auranofin.

Au-S	2.3021(16)	C(18)-H(18A)	0.9700
P-Au	2.2642(16)	C(18)-H(18B)	0.9700
P-C(1)	1.823(7)	C(19)-O(8)	1.325(8)
P-C(3)	1.824(7)	C(2)-C(1)	1.529(12)
P-C(5)	1.822(7)	C(2)-H(2A)	0.9600
C(1)-H(1A)	0.9700	C(2)-H(2B)	0.9600
C(1)-H(1B)	0.9700	C(2)-H(2C)	0.9600
C(10)-O(6)	1.439(7)	C(20)-C(19)	1.499(9)
C(10)-C(9)	1.520(8)	C(20)-H(20A)	0.9600
C(10)-C(11)	1.536(9)	C(20)-H(20B)	0.9600
C(10)-H(10)	0.9800	C(20)-H(20C)	0.9600
C(11)-O(1)	1.435(7)	C(3)-C(4)	1.524(10)
C(11)-H(11)	0.9800	C(3)-H(3A)	0.9700
C(12)-O(3)	1.187(9)	C(3)-H(3B)	0.9700
C(12)-O(2)	1.363(9)	C(4)-H(4A)	0.9600
C(13)-C(12)	1.506(10)	C(4)-H(4B)	0.9600
C(13)-H(13A)	0.9600	C(4)-H(4C)	0.9600
C(13)-H(13B)	0.9600	C(5)-C(6)	1.516(9)
C(13)-H(13C)	0.9600	C(5)-H(5A)	0.9700
C(14)-O(5)	1.198(8)	C(5)-H(5B)	0.9700
C(14)-O(4)	1.359(8)	C(6)-H(6A)	0.9600
C(14)-C(15)	1.495(12)	C(6)-H(6B)	0.9600
C(15)-H(15A)	0.9600	C(6)-H(6C)	0.9600
C(15)-H(15B)	0.9600	C(7)-O(1)	1.436(7)
C(15)-H(15C)	0.9600	C(7)-C(8)	1.529(8)
C(16)-O(7)	1.209(9)	C(7)-S	1.810(6)
C(16)-O(6)	1.342(8)	C(7)-H(7)	0.9800
C(16)-C(17)	1.471(10)	C(8)-O(2)	1.443(7)
C(17)-H(17A)	0.9600	C(8)-H(8)	0.9800
C(17)-H(17B)	0.9600	C(9)-C(8)	1.507(10)
C(17)-H(17C)	0.9600	C(9)-H(9)	0.9800
C(18)-O(8)	1.470(7)	O(4)-C(9)	1.451(7)
C(18)-C(11)	1.513(9)	O(9)-C(19)	1.210(8)
O(8)-C(18)-C(11)	106.4(5)	C(12)-C(13)-H(13C)	109.5
O(8)-C(18)-H(18A)	110.5	H(13A)-C(13)-H(13C)	109.5
C(11)-C(18)-H(18A)	110.5	H(13B)-C(13)-H(13C)	109.5
O(8)-C(18)-H(18B)	110.5	C(16)-O(6)-C(10)	119.1(5)
C(11)-C(18)-H(18B)	110.5	C(2)-C(1)-P	114.3(5)
H(18A)-C(18)-H(18B)	108.6	C(2)-C(1)-H(1A)	108.7
O(6)-C(10)-C(9)	109.6(5)	P-C(1)-H(1A)	108.7
O(6)-C(10)-C(11)	105.7(5)	C(2)-C(1)-H(1B)	108.7
C(9)-C(10)-C(11)	111.5(5)	P-C(1)-H(1B)	108.7
O(6)-C(10)-H(10)	110.0	H(1A)-C(1)-H(1B)	107.6
C(9)-C(10)-H(10)	110.0	C(16)-C(17)-H(17A)	109.5
C(11)-C(10)-H(10)	110.0	C(16)-C(17)-H(17B)	109.5
O(1)-C(11)-C(18)	106.6(5)	H(17A)-C(17)-H(17B)	109.5
O(1)-C(11)-C(10)	110.8(5)	C(16)-C(17)-H(17C)	109.5
C(18)-C(11)-C(10)	112.5(5)	H(17A)-C(17)-H(17C)	109.5
O(1)-C(11)-H(11)	108.9	H(17B)-C(17)-H(17C)	109.5
C(18)-C(11)-H(11)	108.9	O(2)-C(8)-C(9)	108.7(5)

C(10)-C(11)-H(11)	108.9	H(13A)-C(13)-H(13B)	109.5
O(5)-C(14)-O(4)	123.6(8)	O(2)-C(8)-C(7)	110.5(5)
O(5)-C(14)-C(15)	126.6(7)	C(9)-C(8)-C(7)	110.0(5)
O(4)-C(14)-C(15)	109.8(6)	O(2)-C(8)-H(8)	109.2
C(14)-O(4)-C(9)	118.7(6)	C(9)-C(8)-H(8)	109.2
O(4)-C(9)-C(8)	105.9(5)	C(7)-C(8)-H(8)	109.2
O(4)-C(9)-C(10)	107.7(5)	O(3)-C(12)-O(2)	124.6(6)
C(8)-C(9)-C(10)	110.1(5)	O(3)-C(12)-C(13)	125.1(7)
O(4)-C(9)-H(9)	111.0	O(2)-C(12)-C(13)	110.3(7)
C(8)-C(9)-H(9)	111.0	C(12)-O(2)-C(8)	115.7(5)
C(10)-C(9)-H(9)	111.0	C(5)-P-C(1)	104.9(3)
O(1)-C(7)-C(8)	105.1(4)	C(5)-P-C(3)	105.4(3)
O(1)-C(7)-S	110.5(4)	C(1)-P-C(3)	105.9(3)
C(8)-C(7)-S	110.5(4)	C(5)-P-Au	116.0(2)
O(1)-C(7)-H(7)	110.2	C(1)-P-Au	112.5(2)
C(8)-C(7)-H(7)	110.2	C(3)-P-Au	111.4(2)
S-C(7)-H(7)	110.2	C(4)-C(3)-P	112.9(5)
C(6)-C(5)-P	115.5(4)	C(4)-C(3)-H(3A)	109.0
C(6)-C(5)-H(5A)	108.4	P-C(3)-H(3A)	109.0
P-C(5)-H(5A)	108.4	C(4)-C(3)-H(3B)	109.0
C(6)-C(5)-H(5B)	108.4	P-C(3)-H(3B)	109.0
P-C(5)-H(5B)	108.4	H(3A)-C(3)-H(3B)	107.8
H(5A)-C(5)-H(5B)	107.5	C(5)-C(6)-H(6A)	109.5
C(1)-C(2)-H(2A)	109.5	C(5)-C(6)-H(6B)	109.5
C(1)-C(2)-H(2B)	109.5	H(6A)-C(6)-H(6B)	109.5
H(2A)-C(2)-H(2B)	109.5	C(5)-C(6)-H(6C)	109.5
C(1)-C(2)-H(2C)	109.5	H(6A)-C(6)-H(6C)	109.5
H(2A)-C(2)-H(2C)	109.5	H(6B)-C(6)-H(6C)	109.5
H(2B)-C(2)-H(2C)	109.5	C(3)-C(4)-H(4A)	109.5
O(7)-C(16)-O(6)	123.3(7)	C(3)-C(4)-H(4B)	109.5
O(7)-C(16)-C(17)	124.5(7)	H(4A)-C(4)-H(4B)	109.5
O(6)-C(16)-C(17)	112.3(6)	C(3)-C(4)-H(4C)	109.5
C(19)-C(20)-H(20A)	109.5	H(4A)-C(4)-H(4C)	109.5
C(19)-C(20)-H(20B)	109.5	H(4B)-C(4)-H(4C)	109.5
H(20A)-C(20)-H(20B)	109.5	C(14)-C(15)-H(15A)	109.5
C(19)-C(20)-H(20C)	109.5	C(14)-C(15)-H(15B)	109.5
H(20A)-C(20)-H(20C)	109.5	H(15A)-C(15)-H(15B)	109.5
H(20B)-C(20)-H(20C)	109.5	C(14)-C(15)-H(15C)	109.5
C(11)-O(1)-C(7)	111.6(5)	H(15A)-C(15)-H(15C)	109.5
O(9)-C(19)-O(8)	123.7(7)	H(15B)-C(15)-H(15C)	109.5
O(9)-C(19)-C(20)	124.7(7)	P-Au-S	172.69(6)
O(8)-C(19)-C(20)	111.6(6)	C(19)-O(8)-C(18)	117.1(5)
C(12)-C(13)-H(13A)	109.5	C(7)-S-Au	105.6(2)
C(12)-C(13)-H(13B)	109.5		

Table A.2.3 Anisotropic displacement parameters ($Å^2$ x 10^3) for auranofin. The anisotropic displacement factor exponent takes the form:
$-2\pi^2[h^2a^{*2}U11 + ... + 2hka^*b^*U12]$.

	U11	U22	U33	U23	U13	U12
Au	13(1)	11(1)	10(1)	-1(1)	3(1)	0(1)
S	18(1)	11(1)	12(1)	-1(1)	1(1)	1(1)
P	15(1)	12(1)	12(1)	-1(1)	4(1)	1(1)

C(1)	18(3)	18(3)	14(4)	0(3)	5(3)	1(3)
C(10)	12(3)	16(3)	9(3)	2(3)	4(3)	1(2)
C(11)	12(3)	14(5)	10(3)	4(3)	-2(2)	3(2)
C(12)	24(4)	13(4)	18(4)	-4(3)	1(3)	2(3)
C(13)	28(4)	25(4)	34(5)	0(3)	5(3)	14(3)
C(14)	19(3)	13(3)	8(3)	-1(4)	-2(2)	1(4)
C(15)	24(4)	15(3)	16(4)	-6(3)	4(3)	-2(3)
C(16)	23(4)	24(4)	21(4)	-2(3)	2(3)	-4(3)
C(17)	32(4)	22(6)	17(3)	-6(3)	-10(3)	7(3)
C(18)	18(3)	11(3)	15(4)	3(3)	10(3)	4(2)
C(19)	21(3)	17(5)	25(4)	5(3)	6(3)	4(2)
C(2)	27(3)	22(3)	17(3)	0(6)	8(2)	3(5)
C(20)	17(4)	32(4)	23(4)	2(3)	12(3)	1(3)
C(3)	18(3)	19(3)	16(4)	-6(3)	6(3)	-3(3)
C(4)	28(4)	40(5)	33(5)	-6(4)	16(4)	-13(3)
C(5)	18(3)	17(4)	17(4)	2(3)	6(3)	0(3)
C(6)	26(3)	15(5)	23(4)	-2(3)	8(3)	5(2)
C(7)	10(3)	13(3)	9(3)	1(2)	2(3)	0(2)
C(8)	11(3)	11(3)	10(3)	-5(3)	6(3)	1(2)
C(9)	12(3)	10(3)	17(4)	-7(3)	6(3)	-2(2)
O(1)	17(2)	13(2)	7(2)	0(2)	6(2)	2(2)
O(2)	15(2)	10(3)	18(2)	-3(2)	8(2)	4(2)
O(3)	27(3)	17(3)	55(4)	12(3)	17(3)	1(2)
O(4)	18(2)	13(2)	12(2)	-8(2)	5(2)	-4(2)
O(5)	39(3)	20(3)	22(3)	-5(2)	21(2)	-7(2)
O(6)	15(2)	15(2)	8(2)	2(2)	-1(2)	-1(2)
O(7)	29(4)	47(4)	39(4)	16(3)	-2(3)	-9(3)
O(8)	21(2)	13(3)	30(3)	3(2)	17(2)	3(2)
O(9)	37(3)	24(3)	49(4)	0(3)	22(3)	5(2)

Table A.2.4 Hydrogen coordinates (x 10^4) and isotropic displacement parameters ($Å^2$ x 10^3) for auranofin.

	x	y	z	U(eq)
H(10)	2006	-845	1210	14
H(11)	4000	1749	1440	15
H(1A)	7591	3859	6635	20
H(1B)	6228	2874	6213	20
H(13A)	6900	-6783	2414	44
H(13B)	7782	-5182	2442	44
H(13C)	6905	-5893	1554	44
H(15A)	2964	-5835	-761	27
H(15B)	1972	-5427	-192	27
H(15C)	3437	-6200	232	27
H(17A)	1257	1892	-1055	41
H(17B)	-305	1653	-1077	41
H(17C)	407	410	-1562	41
H(18A)	2681	2898	2342	16
H(18B)	1845	2840	1358	16
H(2A)	7802	1194	7194	33
H(2B)	8906	1445	6683	33
H(2C)	7539	459	6264	33
H(20A)	-1157	834	2904	34

H(20B)	-399	-535	2524	34
H(20C)	-1546	551	1905	34
H(3A)	9347	5059	5710	21
H(3B)	9783	3225	5640	21
H(4A)	10463	4816	4624	48
H(4B)	8921	5365	4211	48
H(4C)	9353	3529	4140	48
H(5A)	6411	5638	4293	21
H(5B)	5369	5029	4789	21
H(6A)	6127	7658	5244	32
H(6B)	7674	7054	5524	32
H(6C)	6632	6441	6022	32
H(7)	5868	89	2096	13
H(8)	4076	-2595	2199	12
H(9)	4477	-1164	675	15

A.3 Supplementary material for equilibrium constant determinations reported in Chapter 3.

A.3.1 Chemical shift values plotted against ligand concentration used in the determination of the equilibrium constant for the reaction of [Au(PTA)Cl] with L (SCN^-, thiourea or methyl thiourea) in DMSO at 25 °C. [Au] = 51.3, 42.7 and 51.3 mM for SCN^-, thiourea or and methyl thiourea respectively.

[SCN^-] (mM)	Chemical shift (ppm)	[Thiourea] (mM)	Chemical shift (ppm)	[Methyl thiourea] (mM)	Chemical shift (ppm)
0.00	-51.236	0.00	-51.110	0.00	-51.208
5.13	-51.171	4.38	-50.199	4.44	-50.590
25.67	-51.106	21.90	-49.800	26.62	-49.958
51.33	-51.073	43.79	-49.474	51.03	-49.576
61.60	-51.050	50.36	-49.325	62.12	-49.144
77.00	-51.027	63.50	-49.195	77.65	-49.051
102.67	-51.003	85.39	-49.019	102.05	-48.949
128.34	-50.980	129.18	-48.879	153.08	-48.837
154.00	-50.920	170.78	-48.782	206.32	-48.721
205.34	-50.878	214.57	-48.730	257.35	-48.703
256.67	-50.822	426.96	-48.725	512.48	-48.517
513.35	-50.707	500.00	-48.681	600.00	-48.671

A.3.2 Chemical shift values plotted against ligand concentration used in the determination of the equilibrium constant for the reaction of PTA with β-cyclodextrin by ^1H and ^{31}P NMR in D_2O at 25 °C. [PTA] = 30 mM.

^1H NMR				^{31}P NMR	
doublet(d) region		doublet of doublets(dd) region			
[β-cyclodextrin] (mM)	Chemical shift (ppm)	β-cyclodextrin (mM)	Chemical shift (ppm)	β-cyclodextrin (mM)	Chemical shift (ppm)
0.00	3.803	0.00	4.354	0.00	-97.731
16.20	3.821	16.20	4.372	16.20	-98.702
32.30	3.838	32.30	4.413	32.30	-99.358

47.00	3.843	47.00	4.394	63.10	-99.576
63.10	3.846	63.10	4.396		
95.40	3.848	95.40	4.397		

A.3.3 Chemical shift values plotted against ligand concentration used in the determination of the equilibrium constant for the reaction of [PTAMe]I and [Au(PTAMe)Cl]I with β-cyclodextrin by ^{31}P NMR in DMSO at 25 °C. [[PTAMe]I] = 54.8 mM and [[Au(PTAMe)Cl]I] = 16.6 mM.

[PTAMe]I		[Au(PTAMe)Cl]	
[β-cyclodextrin] (mM)	Chemical shift (ppm)	[β-cyclodextrin] (mM)	Chemical shift (ppm)
0.00	-85.600	0.00	-30.000
5.46	-85.629	1.62	-29.980
27.49	-85.750	8.37	-29.901
54.80	-85.855	16.59	-29.799
65.73	-85.864	19.70	-29.752
82.29	-85.883	24.96	-29.706
109.60	-85.915	33.19	-29.622
164.40	-85.966	49.93	-29.483
219.38	-86.008	66.52	-29.430
274.18	-86.050	83.11	-29.410
548.37	-86.100	100.00	-29.339
600.00	-86.086	500.00	-29.099
1000.00	-86.101		

A.3.4 Chemical shift values plotted against ligand concentration used in the determination of the equilibrium constant for the reaction of PPh_3 and $[Au(dppe)_2]Cl$ with β-cyclodextrin by ^{31}P NMR in DMSO at 25 °C. [PPh_3] = 44.5 mM and [$[Au(dppe)_2]Cl$] = 54.4 mM.

PPh_3		$[Au(dppe)_2]Cl$	
[β-cyclodextrin] (mM)	Chemical shift (ppm)	[β-cyclodextrin] (mM)	Chemical shift (ppm)
0.00	-5.400	0.00	22.420
4.40	-5.541	5.46	22.339
22.20	-5.554	27.14	22.306
66.70	-5.587	54.45	22.269
89.00	-5.610	65.37	22.250
133.50	-5.647	81.59	22.218
222.50	-5.740	108.90	22.190
445.00	-5.800	163.17	22.120
1000.00	-5.840	217.62	22.055
		272.07	22.004
		544.14	21.950
		1000.00	21.879

A.4 Supplementary material for equilibrium constant determinations reported in Chapter 6.

Table A.4.1 Chemical shift values plotted against the SCN^- concentrations used in the determination of the equilibrium constants for the reactions of $[(AuCl)_2(\mu\text{-dppf-}CH(CH_3)OAc)]$ (**1**), $[(AuCl)_2(\mu\text{-dppf-}CH(CH_3)N(CH_3)_2)]$ (**2**), $[Au(PPh_2Fc)Cl]$ (**3**) and $[Au(PPh_3)Cl]$ (**4**) respectively with SCN^- in DMSO at 25 °C. [Au] = 14.5, 20.0, 45.0 and 50.0 mM for **1**, **2**, **3** and **4** respectively.

1		**2**		**3**		**4**	
SCN^- (mM)	Chemical shift (ppm)	SCN^- (mM)	Chemical shift (ppm)	SCN^- (mM)	Chemical shift (ppm)	SCN^- (mM)	Chemical shift (ppm)
0.00	22.900	0.00	26.793	0.00	29.668	0.00	33.760
2.74	23.010	8.58	26.953	21.95	29.676	24.70	33.854
10.98	23.070	20.58	27.114	45.28	29.822	49.39	33.905
20.58	23.104	30.87	27.222	67.23	29.812	75.46	33.954
26.07	23.130	39.45	27.334	89.18	29.877	100.16	33.994
31.56	23.151	80.61	27.590	134.46	29.940	198.94	34.157
105.65	23.294	99.47	27.658	179.74	30.042	249.71	34.237
120.00	23.328	200.66	28.153	225.01	30.123	498.04	34.450
		401.32	28.520	448.65	30.427	500.00	34.415
		500.00	28.569	898.68	30.600		
				1000.00	30.645		

A.5 Supplementary material for rate constant determinations reported in Chapter 6.

Table A.5.1 k_{obs} values plotted against ligand concentration (SCN^-, Me_2Tu) used in the determination k_{obs} for the reactions of $[Au(PPh_3)Cl]$ with SCN^- and Me_2Tu by stopped-flow in ethanol at -5 and 2.3 °C respectively; [Au] = 0.2 and 0.4 mM respectively.

SCN^- (M)	k_{obs} (s^{-1}), λ = 360 nm	Me_2Tu (M)	k_{obs} (s^{-1}), λ = 320 nm
0.000	4.13	0.0	638
0.030	7.33	0.1	933
0.050	9.47		841
0.075	12.14		869
0.150	20.14		758
			999
			751
			719
		0.2	995
			1091
			919
			1029
			884
			1132
			1250
			1178

		0.4	1724
			1672
			1402
			1668
			1544
			1566
			1811
		0.5	1812
			1716
			1581
			1550
			1438
			1672

A.6 Derivation of equations used in the equilibrium constant determinations for Chapters 3 and 6

A.6.1 Equation used when mononuclear gold(I) complexes are reacted with various ligands

The occurring equilibrium process can be illustrated by the following equation:

$$[(PTA)AuCl] + L \underset{}{\overset{K_L}{\rightleftharpoons}} [(PTA)AuL] + Cl^- \quad (1)$$

(L = SCN^-, Thiourea, Methiourea)

The equation used in fitting data and getting the plots of the chemical shift versus ligand concentration is represented by the following Micromath Scientist Model.

MicroMath Scientist Model File:

Independent Variable: L; Dependent Variable: A_{obs}; Parameters: A_R, A_P, K_L, Au

L_f (final ligand concentration) = L/1000

$A = K_L - 1$, $B = (K_L * Au) - (K_L * L_f) + (2 * L_f)$, $C = (-L_f)^2$

$X = (-B + (B^2 - 4*A*C)^{0.5})/(2*A)$

Conditions: $0<X<1$, $-1e6 < B < 1e6$

$$A_{obs} = (A_R*(L_f - X) + K_L*X*A_P)/((L_f - X) + K_L*X) \quad (2)$$

A_R = absorbance observed for the reactants and A_P = for the products

Derivation of A, B and C:

Eq. 1 can be written in a shortened version as follows:

$$AuCl + L \underset{}{\overset{K_L}{\rightleftharpoons}} AuL + Cl^- \quad (3)$$

Equilibrium reaction:	Au	L_f	0	0
At equilibrium:	Au-y	L_f-y	y	y

Let $y = L_f - x$

From Eq. (3),

The equilibrium constant (K_L) is defined as

$$K_L = \frac{[AuL]\,[Cl^-]}{[AuCl]\,[L]}$$

Substitution by y in the equilibrium constant equation gives

$$K_L = \frac{(L_f - x)\,(L_f - x)}{(Au - L_f + x)\,(x)}$$

$$= \frac{(L_f - x)^2}{(Au*x - L_f*x + x^2)}$$

$$= \frac{(L_f^2 - 2L_f*x + x^2)}{(Au*x - L_f*x + x^2)}$$

$$\therefore K_L*Au*x - K_L*L_f*x + K_L*x^2 = L_f^2 - 2L_f*x + x^2$$

$$\therefore (K_L - 1)x^2 + (K_L*Au - K_L*L_f + 2L_f)x - L_f^2 = 0$$

$$\therefore A = (K_L - 1),\ B = (K_L*Au - K_L*L_f + 2L_f),\ C = -L_f^2$$

<u>Derivation of the equilibrium constant equation K_L:</u>

From Eq. (3)

The equilibrium constant (K_L) can be written as

$$K_L = \frac{[AuL]\,[Cl^-]}{[AuCl]\,[L]} \qquad (4)$$

At any given time, the total Au concentration is given by

$$[Au]_T = [AuCl] + [AuL]_f \qquad (5)$$

From (4)

$$[AuCl] = \frac{[AuL]\,[Cl^-]}{K_L[L]_f} \qquad (6)$$

Also

$$[AuL] = \frac{K_L[AuCl][L]_f}{[Cl^-]} \qquad (7)$$

Substitution of (7) into (5) and after multiplication by $[Cl^-]/[Cl^-]$ gives

$$[AuCl] = \frac{[Au]_T\,[L]_f}{[Cl^-] + K_L[L]_f} \qquad (8)$$

Also substitution of (6) into (5) and after multiplication by $K_L[L_f]/K_L[L_f]$ gives

$$[AuL] = \frac{[Au]_T\,[L]_f\,K_L}{[Cl^-] + K_L[L]_f} \quad (9)$$

The total absorbance observed at equilibrium is

$$A_{obs} = A_{AuCl} + A_{AuL}$$

$$= \varepsilon_{AuCl}\,[AuCl] + \varepsilon_{AuL}\,[AuL]$$

$$= \varepsilon_{AuCl}\,\frac{[Au]_T[Cl^-]}{[Cl^-] + K_L[L]_f} + \varepsilon_{AuL}\,\frac{[Au]_T\,K_L[L]_f}{[Cl^-] + K_L[L]_f} \quad \text{(from Eq. 8 and 9)} \quad (10)$$

Since $A = \varepsilon cl$ then absorbance observed for the reactants (A_R) and absorbance for the products (A_P) is given by

$A_R = \varepsilon_{AuCl}\,[AuCl]$ and $A_P = \varepsilon_{AuL}\,[AuL]$ respectively.

Therefore from Eq. (10)

$$A_{obs} = \frac{A_R[Cl^-] + A_P K_L[L]_f}{[Cl^-] + K_L[L]_f} \quad (11)$$

A.6.2 Equation used when dinuclear gold(I) complexes are reacted with various ligands

The occurring equilibrium process can be illustrated by the following equation:

$$[(AuCl)_2(dppf\text{-}CH(CH_3)N(CH_3)_2)] + 2L \underset{(L = SCN^-)}{\overset{K_L}{\rightleftharpoons}} [(AuL)_2(dppf\text{-}CH(CH_3)N(CH_3)_2)] + 2Cl^- \quad (12)$$

The equation used in fitting data and getting the plots of the chemical shift versus ligand concentration is represented by the following Micromath Scientist Model.

MicroMath Scientist Model File:

Independent Variable: L; Dependent Variable: A_{obs}; Parameters: A_R, A_P, K_L, Au, X

$L = L_i/1000$

$AA = (L\text{-}L_f)/2$

K_L =(AA* (X+2*AA)^2)/((Abs(Au-AA)) *(L- 2*AA)^2)

$$A_{obs} = (A_R*(X+2*AA)^2 + A_P*K_L*L_f^2)/((X+2*AA)^2 + K_L* L_f^2) \quad (13)$$

Conditions: $0<L_f<1$

A_R = absorbance observed for the reactants, A_P = for the products and Abs = Absolute

Derivation of Eq. 13:

Eq. 12 can be written in a shortened version as follows:

$$[Au_2\text{-}Cl_2] + 2L \underset{}{\overset{K_L}{\rightleftharpoons}} [Au_2\text{-}L_2] + 2Cl^- \quad (14)$$

Equilibrium reaction:	Au	L	0	c
At equilibrium:	Au-y	L-2y	y	c+2y

Let $L_f = L - 2y$

with L_f = [free entering ligand]

$\therefore y = (L-L_f)/2$

$\therefore$ At equilibrium: $Au-((L-L_f)/2)$ $L-2((L-L_f)/2)$ $(L-L_f)/2$ $c+2(L-L_f)/2)$

From Eq. (14),

The equilibrium constant (K_L) is defined as

$$K_L = \frac{[AuL]\,[Cl^-]^2}{[AuCl]\,[L]^2}$$

Substitution by parameters at equilibrium in the equilibrium constant equation gives

$$K_L = \frac{((L-L_f)/2)\,(c+2(L-L_f)/2))^2}{(Au-((L-L_f)/2))\,(L-2((L-L_f)/2))^2}$$

$$\text{Let } AA = \frac{L - L_f}{2}$$

Then,

$$K_L = \frac{(AA)\,(c+2(AA))^2}{(Au-(AA))\,(L-2(AA))^2}$$

and

$$A_{obs} = \frac{A_R\,(c+2(AA))^2 + A_P K_L [L_f]^2}{(c+2(AA))^2 + K_L [L_f]^2}$$

APPENDIX

Derivation of the equilibrium constant equation K_L:

From Eq. (14)

The equilibrium constant (K_L) can be written as

$$K_L = \frac{[AuL]\,[Cl^-]^2}{[AuCl]\,[L]^2} \tag{15}$$

At any given time, the total Au concentration is given by

$$[Au]_T = [AuCl] + [AuL]_f \tag{16}$$

From (15)

$$[AuCl] = \frac{[AuL]\,[Cl^-]^2}{K_L[L]_f^2} \tag{17}$$

Also

$$[AuL] = \frac{K_L[AuCl][L]_f^2}{[Cl^-]^2} \tag{18}$$

Substitution of (18) into (16) and after multiplication by $[Cl^-]^2/[Cl^-]^2$ gives

$$[AuCl] = \frac{[Au]_T\,[L]_f^2}{[Cl^-]^2 + K_L[L]_f^2} \tag{19}$$

Also substitution of (17) into (16) and after multiplication by $K_L[L]_f^2/K_L[L]_f^2$ gives

$$[AuL] = \frac{[Au]_T\,[L]_f^2\,K_L}{[Cl^-]^2 + K_L[L]_f^2} \tag{20}$$

The total absorbance observed at equilibrium is

$$\begin{aligned} A_{obs} &= A_{AuCl} + A_{AuL} \\ &= \varepsilon_{AuCl}\,[AuCl] + \varepsilon_{AuL}\,[AuL] \\ &= \varepsilon_{AuCl}\,\frac{[Au]_T[Cl^-]^2}{[Cl^-]^2 + K_L[L]_f^2} + \varepsilon_{AuL}\,\frac{[Au]_T\,K_L[L]_f^2}{[Cl^-]^2 + K_L[L]_f^2} \quad \text{(from Eq. 19 and 20)} \end{aligned} \tag{21}$$

Since $A = \varepsilon cl$ then absorbance observed for the reactants (A_R) and absorbance for the products (A_P) is given by

$A_R = \varepsilon_{AuCl}\,[AuCl]$ and $A_P = \varepsilon_{AuL}\,[AuL]$ respectively.

Therefore from Eq. (21)

$$A_{obs} = \frac{A_R[Cl^-]^2 + A_P K_L[L]_f^2}{[Cl^-]^2 + K_L[L]_f^2} \tag{22}$$

A.6.3 Equation used when guest ligands and gold(I) complexes are included into β-cyclodextrin

The equilibrium constants (K_D) obtained from including various guest ligands (G) such as PTA and gold(I) complexes into β-cyclodextrin (β-CD) was determined using the following equation which also represents the equilibrium reaction process:

$$\text{Guest} + \beta\text{-cyclodextrin} \underset{}{\overset{K_D}{\rightleftharpoons}} \text{Guest:}\beta\text{-cyclodextrin} \qquad (23)$$

The equation used in fitting data and getting the plots of the chemical shift versus ligand concentration is represented by the following Micromath Scientist Model.

MicroMath Scientist Model File:

Independent Variable: L; Dependent Variable: A_{obs}; Parameters: A_R, A_P, K_D, Au

L_f (final ligand concentration) = L/1000

$A = K_D$, $B = (K_D*Au)-(K_D*L_f + 1)$, $C = -L_f$

$X = (-B + (B^2-4*A*C)^{0.5})/(2*A)$

Conditions: 0<X<1, -1e6 < B <1e6

$$A_{obs} = (A_R + K_D*X*A_P)/(1 + K_D*X) \qquad (24)$$

A_R = absorbance observed for the reactants and A_P = for the products

Derivation of A, B and C:

Eq. 23 can be written in a shortened version as follows:

$$G + \beta\text{-CD} \underset{}{\overset{K_D}{\rightleftharpoons}} G\text{-}\beta\text{-CD} \qquad (25)$$

Equilibrium reaction:	Au	L_f	0
At equilibrium:	Au-y	L_f-y	y

Let $y = L_f-x$

From Eq. (25),

The equilibrium constant (K_D) is defined as

$$K_D = \frac{[G\text{-}\beta\text{-CD}]}{[G]\,[\beta\text{-CD}]}$$

Substitution by y in the equilibrium constant equation gives

$$K_D = \frac{(L_f - x)}{(Au - L_f + x)(x)}$$

$$= \frac{(L_f - x)}{(Au*x - L_f*x + x^2)}$$

$\therefore K_D*Au*x - K_D*L_f*x + K_D*x^2 = L_f - x$

$\therefore (K_D)x^2 + (K_D*Au - K_D*L_f + 1)x - L_f = 0$

$\therefore A = (K_D),\ B = (K_D*Au - K_D*L_f + 1),\ C = -L_f$

Derivation of the equilibrium constant equation K_D:

From Eq. (25)

The equilibrium constant (K_D) can be written as

$$K_D = \frac{[G\text{-}\beta\text{-CD}]}{[G]\,[\beta\text{-CD}]} \qquad (26)$$

At any given time, the total guest (G) concentration is given by

$$[G]_T = [G] + [G\text{-}\beta\text{-CD}] \qquad (27)$$

From (27)

$$[G] = \frac{[G\text{-}\beta\text{-CD}]}{[\beta\text{-CD}]\,K_D} \qquad (28)$$

Also

$$[G\text{-}\beta\text{-CD}] = K_D[G][\beta\text{-CD}] \qquad (29)$$

Substitution of (29) into (27) gives

$$[G] = \frac{[G]_T}{1 + K_D[\beta\text{-CD}]} \qquad (30)$$

Also substitution of (28) into (27) and after multiplication by $K_D[\beta\text{-CD}]/K_D[\beta\text{-CD}]$ gives

$$[G\text{-}\beta\text{-CD}] = \frac{[G]_T\,[\beta\text{-CD}]\,K_D}{1 + K_D[\beta\text{-CD}]} \qquad (31)$$

The total absorbance observed at equilibrium is

$A_{obs} = A_G + A_{G\text{-}\beta\text{-CD}}$

$$= \varepsilon_G [G] + \varepsilon_{G\text{-}\beta\text{-}CD} [G\text{-}\beta\text{-}CD]$$

$$= \varepsilon_G \frac{[G]_T}{1 + K_D[\beta\text{-}CD]} + \varepsilon_{G\text{-}\beta\text{-}CD} \frac{[G]_T K_D[\beta\text{-}CD]}{1 + K_D[\beta\text{-}CD]} \quad \text{(from Eq. 30 and 31)} \qquad (32)$$

Since $A = \varepsilon cl$ then absorbance observed for the reactants (A_R) and absorbance for the products (A_P) is given by

$A_R = \varepsilon_G [G]$ and $A_P = \varepsilon_{G\text{-}\beta\text{-}CD} [G\text{-}\beta\text{-}CD]$ respectively.

Therefore from Eq. (32)

$$A_{obs} = \frac{A_R + A_P K_D[\beta\text{-}CD]}{1 + K_D[\beta\text{-}CD]} \qquad (33)$$

B SUPPLEMENTARY CRYSTALLOGRAPHIC DATA FOR CHAPTER 4

B.1 Crystal data of [$(AuCl)_2$(μ-dppf-$CH(CH_3)N(CH_3)_2$)].

Table B.1.1 Atomic coordinates (x 10^4) and equivalent isotropic displacement parameters ($Å^2$ x 10^3) for [$(AuCl)_2$(μ-dppf-$CH(CH_3)N(CH_3)_2$)]. U(eq) is defined as one third of the trace of the orthogonalized Uij tensor.

	x	y	z	U(eq)
Au(1)	701(1)	3594(1)	2853(1)	48(1)
Au(2)	-1200(1)	-3512(1)	1274(1)	40(1)
Fe	26(1)	-15(1)	2002(1)	38(1)
P(1)	1526(1)	2098(2)	2720(1)	36(1)
P(2)	-1747(1)	-1795(2)	1512(1)	35(1)
N(1)	1206(5)	1108(7)	4088(4)	49(2)
Cl(1)	-61(2)	5148(3)	3069(2)	111(1)
Cl(2)	-747(2)	-5271(2)	923(2)	65(1)
C(11)	2501(5)	2132(8)	3413(4)	39(2)
C(12)	2700(6)	3173(8)	3815(4)	45(2)
C(13)	3437(7)	3250(9)	4331(5)	63(3)
C(14)	3975(7)	2291(11)	4439(5)	71(3)
C(15)	3782(7)	1256(10)	4069(6)	70(4)
C(16)	3039(6)	1164(8)	3554(5)	49(3)
C(21)	1802(6)	2267(8)	1933(4)	39(2)
C(22)	2515(6)	1742(9)	1860(5)	54(3)
C(23)	2662(7)	1836(10)	1245(6)	64(3)
C(24)	2117(8)	2452(10)	703(6)	67(3)
C(25)	1412(8)	2972(10)	768(5)	69(3)
C(26)	1274(6)	2912(8)	1383(5)	51(3)
C(31)	1130(5)	554(7)	2656(4)	33(2)
C(32)	1253(6)	-367(8)	2201(5)	47(2)
C(33)	837(6)	-1451(8)	2299(5)	52(3)
C(34)	477(6)	-1192(7)	2810(5)	41(2)
C(35)	640(5)	38(7)	3031(4)	37(2)
C(36)	416(5)	694(8)	3590(4)	40(2)
C(37)	-124(6)	-80(10)	3886(5)	69(3)
C(38)	1743(7)	133(11)	4451(6)	84(4)
C(39)	1085(7)	2036(10)	4549(6)	79(4)
C(41)	-1160(5)	-468(7)	1476(4)	38(2)
C(42)	-1124(6)	710(8)	1799(5)	51(3)
C(43)	-647(6)	1473(9)	1531(6)	66(4)
C(44)	-355(7)	839(10)	1070(5)	65(3)
C(45)	-661(6)	-373(9)	1029(5)	50(3)
C(51)	-2739(5)	-1520(8)	864(5)	40(2)

C(52)	-2901(6)	-496(9)	471(6)	68(3)
C(53)	-3637(7)	-371(11)	-20(6)	79(4)
C(54)	-4242(6)	-1201(11)	-134(6)	71(3)
C(55)	-4071(7)	-2247(12)	249(7)	89(4)
C(56)	-3334(6)	-2410(10)	751(5)	67(3)
C(61)	-1986(5)	-1766(7)	2315(4)	37(2)
C(62)	-2569(6)	-997(10)	2389(5)	62(3)
C(63)	-2771(7)	-987(11)	2990(7)	75(4)
C(64)	-2380(7)	-1775(11)	3512(6)	70(3)
C(65)	-1803(7)	-2561(9)	3421(5)	58(3)
C(66)	-1602(6)	-2572(8)	2826(5)	44(2)

Table B.1.2 Bond lengths (Å) and angles (°) for [$(AuCl)_2$(μ-dppf-$CH(CH_3)N(CH_3)_2$)].

Au(1)-P(1)	2.237(2)	C(32)-C(33)	1.431(12)
Au(2)-P(2)	2.224(2)	C(33)-C(34)	1.411(13)
Au(1)-Cl(1)	2.271(3)	C(34)-C(35)	1.421(11)
Au(2)-Cl(2)	2.278(2)	C(35)-C(36)	1.508(12)
P(1)-C(11)	1.825(9)	C(36)-C(37)	1.518(12)
P(1)-C(21)	1.839(9)	C(41)-C(42)	1.444(12)
P(1)-C(31)	1.810(9)	C(41)-C(45)	1.447(13)
P(2)-C(41)	1.781(9)	C(42)-C(43)	1.399(14)
P(2)-C(51)	1.826(9)	C(43)-C(44)	1.392(15)
P(2)-C(61)	1.828(9)	C(44)-C(45)	1.419(13)
N(1)-C(36)	1.489(11)	C(51)-C(52)	1.359(12)
N(1)-C(38)	1.454(12)	C(51)-C(56)	1.377(12)
N(1)-C(39)	1.451(12)	C(52)-C(53)	1.353(14)
Fe-C(31)	2.045(8)	C(53)-C(54)	1.342(14)
Fe-C(32)	2.047(9)	C(54)-C(55)	1.369(15)
Fe-C(33)	2.059(9)	C(55)-C(56)	1.370(14)
Fe-C(34)	2.057(8)	C(61)-C(62)	1.353(12)
Fe-C(35)	2.054(8)	C(61)-C(66)	1.374(11)
Fe-C(41)	2.041(8)	C(62)-C(63)	1.388(14)
Fe-C(42)	2.042(9)	C(63)-C(64)	1.379(15)
Fe-C(45)	2.022(9)	C(64)-C(65)	1.367(14)
Fe-C(43)	2.055(9)	C(65)-C(66)	1.378(13)
Fe-C(44)	2.052(9)	C(12)-H(12)	0.9300
C(11)-C(12)	1.388(11)	C(13)-H(13)	0.9300
C(11)-C(16)	1.374(12)	C(14)-H(14)	0.9300
C(12)-C(13)	1.375(13)	C(15)-H(15)	0.9300
C(13)-C(14)	1.367(14)	C(16)-H(16)	0.9300
C(14)-C(15)	1.348(14)	C(22)-H(22)	0.9300
C(15)-C(16)	1.382(13)	C(23)-H(23)	0.9300
C(21)-C(22)	1.401(12)	C(24)-H(24)	0.9300
C(21)-C(26)	1.400(12)	C(25)-H(25)	0.9300
C(22)-C(23)	1.375(13)	C(26)-H(26)	0.9300
C(23)-C(24)	1.386(15)	C(32)-H(32)	0.9300
C(24)-C(25)	1.380(15)	C(33)-H(33)	0.9300
C(25)-C(26)	1.366(13)	C(34)-H(34)	0.9300
C(31)-C(32)	1.438(11)	C(36)-H(36)	0.9800
C(31)-C(35)	1.428(12)	C(37)-H(37A)	0.9600
C(37)-H(37B)	0.9600	C(45)-H(45)	0.9300
C(37)-H(37C)	0.9600	C(52)-H(52)	0.9300

C(38)-H(38A)	0.9600	C(53)-H(53)	0.9300
C(38)-H(38B)	0.9600	C(54)-H(54)	0.9300
C(38)-H(38C)	0.9600	C(55)-H(55)	0.9300
C(39)-H(39A)	0.9600	C(56)-H(56)	0.9300
C(39)-H(39B)	0.9600	C(62)-H(62)	0.9300
C(39)-H(39C)	0.9600	C(63)-H(63)	0.9300
C(42)-H(42)	0.9300	C(64)-H(64)	0.9300
C(43)-H(43)	0.9300	C(65)-H(65)	0.9300
C(44)-H(44)	0.9300	C(66)-H(66)	0.9300
P(1)-Au(1)-Cl(1)	175.41(10)	C(45)-Fe-C(33)	106.0(4)
P(2)-Au(2)-Cl(2)	174.01(10)	C(41)-Fe-C(33)	116.0(3)
C(45)-Fe-C(41)	41.7(4)	C(42)-Fe-C(33)	151.0(4)
C(45)-Fe-C(42)	69.5(4)	C(31)-Fe-C(33)	68.8(3)
C(41)-Fe-C(42)	41.4(3)	C(32)-Fe-C(33)	40.8(3)
C(45)-Fe-C(31)	147.5(4)	C(44)-Fe-C(33)	127.7(5)
C(41)-Fe-C(31)	169.9(3)	C(35)-Fe-C(33)	68.7(3)
C(42)-Fe-C(31)	130.5(3)	C(43)-Fe-C(33)	166.3(5)
C(45)-Fe-C(32)	113.7(4)	C(34)-Fe-C(33)	40.1(4)
C(41)-Fe-C(32)	148.0(3)	C(31)-P(1)-C(11)	107.8(4)
C(42)-Fe-C(32)	167.9(4)	C(31)-P(1)-C(21)	102.9(4)
C(31)-Fe-C(32)	41.1(3)	C(11)-P(1)-C(21)	105.3(4)
C(45)-Fe-C(44)	40.8(4)	C(31)-P(1)-Au(1)	117.1(3)
C(41)-Fe-C(44)	69.1(4)	C(11)-P(1)-Au(1)	110.3(3)
C(42)-Fe-C(44)	68.2(5)	C(21)-P(1)-Au(1)	112.5(3)
C(31)-Fe-C(44)	115.8(4)	C(41)-P(2)-C(51)	104.0(4)
C(32)-Fe-C(44)	106.0(5)	C(41)-P(2)-C(61)	108.3(4)
C(45)-Fe-C(35)	169.1(3)	C(51)-P(2)-C(61)	103.9(4)
C(41)-Fe-C(35)	131.0(4)	C(41)-P(2)-Au(2)	113.3(3)
C(42)-Fe-C(35)	110.3(4)	C(51)-P(2)-Au(2)	109.7(3)
C(31)-Fe-C(35)	40.8(3)	C(61)-P(2)-Au(2)	116.5(3)
C(32)-Fe-C(35)	68.9(4)	C(39)-N(1)-C(38)	112.0(9)
C(44)-Fe-C(35)	149.9(4)	C(39)-N(1)-C(36)	112.3(8)
C(45)-Fe-C(43)	67.6(4)	C(38)-N(1)-C(36)	115.0(8)
C(41)-Fe-C(43)	67.9(3)	C(16)-C(11)-C(12)	119.0(8)
C(42)-Fe-C(43)	39.9(4)	C(16)-C(11)-P(1)	122.5(7)
C(31)-Fe-C(43)	109.6(4)	C(12)-C(11)-P(1)	118.5(7)
C(32)-Fe-C(43)	129.2(4)	C(13)-C(12)-C(11)	120.4(9)
C(44)-Fe-C(43)	39.6(4)	C(13)-C(12)-H(12)	119.8
C(35)-Fe-C(43)	119.7(4)	C(11)-C(12)-H(12)	119.8
C(45)-Fe-C(34)	129.6(4)	C(14)-C(13)-C(12)	119.1(10)
C(41)-Fe-C(34)	109.6(4)	C(14)-C(13)-H(13)	120.4
C(42)-Fe-C(34)	120.1(4)	C(12)-C(13)-H(13)	120.4
C(31)-Fe-C(34)	67.8(3)	C(15)-C(14)-C(13)	121.4(10)
C(32)-Fe-C(34)	67.7(4)	C(15)-C(14)-H(14)	119.3
C(44)-Fe-C(34)	166.8(4)	C(13)-C(14)-H(14)	119.3
C(35)-Fe-C(34)	40.4(3)	C(14)-C(15)-C(16)	120.0(10)
C(43)-Fe-C(34)	153.1(5)	C(14)-C(15)-H(15)	120.0
C(16)-C(15)-H(15)	120.0	N(1)-C(36)-C(37)	115.4(8)
C(11)-C(16)-C(15)	120.0(9)	C(35)-C(36)-C(37)	112.1(8)
C(11)-C(16)-H(16)	120.0	N(1)-C(36)-H(36)	107.6
C(15)-C(16)-H(16)	120.0	C(35)-C(36)-H(36)	107.6
C(26)-C(21)-C(22)	118.8(9)	C(37)-C(36)-H(36)	107.6

C(26)-C(21)-P(1)	119.2(8)	C(36)-C(37)-H(37A)	109.5
C(22)-C(21)-P(1)	122.0(7)	C(36)-C(37)-H(37B)	109.5
C(23)-C(22)-C(21)	119.4(10)	H(37A)-C(37)-H(37B)	109.5
C(23)-C(22)-H(22)	120.3	C(36)-C(37)-H(37C)	109.5
C(21)-C(22)-H(22)	120.3	H(37A)-C(37)-H(37C)	109.5
C(22)-C(23)-C(24)	120.6(11)	H(37B)-C(37)-H(37C)	109.5
C(22)-C(23)-H(23)	119.7	N(1)-C(38)-H(38A)	109.5
C(24)-C(23)-H(23)	119.7	N(1)-C(38)-H(38B)	109.5
C(25)-C(24)-C(23)	120.7(10)	H(38A)-C(38)-H(38B)	109.5
C(25)-C(24)-H(24)	119.7	N(1)-C(38)-H(38C)	109.5
C(23)-C(24)-H(24)	119.7	H(38A)-C(38)-H(38C)	109.5
C(26)-C(25)-C(24)	119.0(11)	H(38B)-C(38)-H(38C)	109.5
C(26)-C(25)-H(25)	120.5	N(1)-C(39)-H(39A)	109.5
C(24)-C(25)-H(25)	120.5	N(1)-C(39)-H(39B)	109.5
C(25)-C(26)-C(21)	121.5(11)	H(39A)-C(39)-H(39B)	109.5
C(25)-C(26)-H(26)	119.3	N(1)-C(39)-H(39C)	109.5
C(21)-C(26)-H(26)	119.3	H(39A)-C(39)-H(39C)	109.5
C(35)-C(31)-C(32)	108.1(7)	H(39B)-C(39)-H(39C)	109.5
C(35)-C(31)-P(1)	126.9(6)	C(42)-C(41)-C(45)	106.4(8)
C(32)-C(31)-P(1)	125.0(7)	C(42)-C(41)-P(2)	130.6(8)
C(35)-C(31)-Fe	70.0(5)	C(45)-C(41)-P(2)	122.8(7)
C(32)-C(31)-Fe	69.5(5)	C(42)-C(41)-Fe	69.3(5)
P(1)-C(31)-Fe	125.4(4)	C(45)-C(41)-Fe	68.4(5)
C(33)-C(32)-C(31)	107.9(8)	P(2)-C(41)-Fe	131.0(5)
C(33)-C(32)-Fe	70.1(5)	C(43)-C(42)-C(41)	107.2(10)
C(31)-C(32)-Fe	69.3(5)	C(43)-C(42)-Fe	70.6(6)
C(33)-C(32)-H(32)	126.1	C(41)-C(42)-Fe	69.3(5)
C(31)-C(32)-H(32)	126.1	C(43)-C(42)-H(42)	126.4
Fe-C(32)-H(32)	126.1	C(41)-C(42)-H(42)	126.4
C(34)-C(33)-C(32)	107.1(8)	Fe-C(42)-H(42)	125.4
C(34)-C(33)-Fe	69.8(5)	C(44)-C(43)-C(42)	110.7(9)
C(32)-C(33)-Fe	69.1(5)	C(44)-C(43)-Fe	70.1(6)
C(34)-C(33)-H(33)	126.5	C(42)-C(43)-Fe	69.5(5)
C(32)-C(33)-H(33)	126.5	C(44)-C(43)-H(43)	124.6
Fe-C(33)-H(33)	126.1	C(42)-C(43)-H(43)	124.6
C(33)-C(34)-C(35)	110.1(9)	Fe-C(43)-H(43)	127.4
C(33)-C(34)-Fe	70.1(5)	C(43)-C(44)-C(45)	107.5(10)
C(35)-C(34)-Fe	69.7(5)	C(43)-C(44)-Fe	70.3(6)
C(33)-C(34)-H(34)	125.0	C(45)-C(44)-Fe	68.5(5)
C(35)-C(34)-H(34)	125.0	C(43)-C(44)-H(44)	126.2
Fe-C(34)-H(34)	126.9	C(45)-C(44)-H(44)	126.2
C(34)-C(35)-C(31)	106.8(8)	Fe-C(44)-H(44)	126.5
C(34)-C(35)-C(36)	128.7(9)	C(44)-C(45)-C(41)	108.1(9)
C(31)-C(35)-C(36)	124.3(7)	C(44)-C(45)-Fe	70.8(5)
C(34)-C(35)-Fe	69.9(5)	C(41)-C(45)-Fe	69.9(5)
C(31)-C(35)-Fe	69.2(5)	C(44)-C(45)-H(45)	125.9
C(36)-C(35)-Fe	129.4(6)	C(41)-C(45)-H(45)	125.9
N(1)-C(36)-C(35)	106.1(7)	Fe-C(45)-H(45)	125.0
C(52)-C(51)-C(56)	118.8(9)	C(62)-C(61)-C(66)	120.3(9)
C(52)-C(51)-P(2)	122.8(7)	C(62)-C(61)-P(2)	119.9(7)
C(56)-C(51)-P(2)	118.4(7)	C(66)-C(61)-P(2)	119.7(7)
C(53)-C(52)-C(51)	119.8(10)	C(61)-C(62)-C(63)	120.5(10)
C(53)-C(52)-H(52)	120.1	C(61)-C(62)-H(62)	119.8

C(51)-C(52)-H(52)	120.1	C(63)-C(62)-H(62)	119.8
C(54)-C(53)-C(52)	123.3(11)	C(64)-C(63)-C(62)	119.9(10)
C(54)-C(53)-H(53)	118.3	C(64)-C(63)-H(63)	120.1
C(52)-C(53)-H(53)	118.3	C(62)-C(63)-H(63)	120.1
C(53)-C(54)-C(55)	116.9(10)	C(65)-C(64)-C(63)	118.7(10)
C(53)-C(54)-H(54)	121.6	C(65)-C(64)-H(64)	120.7
C(55)-C(54)-H(54)	121.6	C(63)-C(64)-H(64)	120.7
C(54)-C(55)-C(56)	121.6(11)	C(64)-C(65)-C(66)	121.6(10)
C(54)-C(55)-H(55)	119.2	C(64)-C(65)-H(65)	119.2
C(56)-C(55)-H(55)	119.2	C(66)-C(65)-H(65)	119.2
C(55)-C(56)-C(51)	119.5(10)	C(61)-C(66)-C(65)	119.1(9)
C(55)-C(56)-H(56)	120.2	C(61)-C(66)-H(66)	120.5
C(51)-C(56)-H(56)	120.2	C(65)-C(66)-H(66)	120.5

Table B.1.3 Anisotropic displacement parameters ($Å^2$ x 10^3) for [$(AuCl)_2$(μ-dppf-$CH(CH_3)N(CH_3)_2$)]. The anisotropic displacement factor exponent takes the form: $-2\pi^2[h^2a^{*2}U11 + ... + 2hka^*b^*U12]$.

	U11	U22	U33	U23	U13	U12
Au(1)	45(1)	38(1)	51(1)	-7(1)	3(1)	11(1)
Au(2)	45(1)	31(1)	47(1)	-1(1)	19(1)	3(1)
Fe	38(1)	30(1)	39(1)	2(1)	4(1)	-2(1)
P(1)	31(1)	30(1)	41(2)	0(1)	6(1)	0(1)
P(2)	37(1)	27(1)	40(1)	-2(1)	10(1)	0(1)
N(1)	52(5)	53(5)	41(5)	-7(4)	14(4)	-4(4)
Cl(1)	101(3)	105(3)	97(3)	-42(2)	-13(2)	65(2)
Cl(2)	81(2)	43(1)	81(2)	-7(1)	40(2)	12(1)
C(11)	41(5)	35(5)	39(6)	9(4)	9(4)	-1(4)
C(12)	53(6)	44(5)	36(6)	-3(4)	13(5)	-5(5)
C(13)	66(8)	56(7)	52(7)	-8(5)	-1(6)	-13(6)
C(14)	55(7)	80(9)	52(8)	8(6)	-18(6)	-8(7)
C(15)	59(7)	63(8)	69(8)	24(6)	-7(6)	7(6)
C(16)	42(6)	38(5)	59(7)	4(5)	4(5)	-4(4)
C(21)	47(6)	35(5)	33(5)	0(4)	10(4)	-12(4)
C(22)	52(7)	61(7)	48(7)	-9(5)	13(5)	-7(5)
C(23)	71(8)	72(8)	65(8)	-15(6)	42(7)	-7(6)
C(24)	94(10)	61(7)	61(8)	-13(6)	46(8)	-30(7)
C(25)	104(10)	65(7)	39(7)	8(6)	24(7)	-22(8)
C(26)	63(7)	34(5)	51(7)	-1(5)	11(5)	-11(5)
C(31)	22(5)	38(5)	35(5)	-1(4)	4(4)	5(4)
C(32)	46(6)	44(6)	54(7)	-17(5)	21(5)	1(5)
C(33)	48(6)	41(5)	58(7)	-9(5)	4(5)	2(5)
C(34)	40(5)	28(5)	44(6)	10(4)	-3(5)	0(4)
C(35)	36(5)	27(5)	42(6)	2(4)	6(4)	9(4)
C(36)	40(5)	37(5)	44(6)	2(4)	14(5)	-4(4)
C(37)	61(7)	96(9)	55(7)	-14(6)	25(6)	-25(7)
C(38)	68(8)	100(10)	68(9)	0(7)	-2(7)	14(7)
C(39)	88(9)	82(8)	66(8)	-34(7)	22(7)	-24(7)
C(41)	36(5)	32(5)	37(6)	0(4)	-3(4)	-3(4)
C(42)	47(6)	44(6)	44(6)	-7(5)	-13(5)	10(5)
C(43)	55(7)	33(5)	80(9)	22(6)	-21(6)	-13(5)
C(44)	82(9)	68(8)	33(6)	18(6)	-2(6)	-17(7)
C(45)	59(7)	54(6)	31(6)	-3(5)	4(5)	-17(5)

C(51)	40(5)	36(5)	46(6)	0(5)	14(4)	-4(5)
C(52)	55(7)	45(6)	82(9)	-5(6)	-10(6)	2(5)
C(53)	68(9)	83(9)	68(9)	19(7)	-5(7)	-2(7)
C(54)	37(6)	88(9)	70(8)	5(7)	-7(6)	8(6)
C(55)	53(8)	92(10)	96(11)	11(8)	-12(7)	-4(7)
C(56)	58(7)	61(7)	65(8)	12(6)	-6(6)	-17(6)
C(61)	33(5)	34(5)	38(5)	6(4)	2(4)	4(4)
C(62)	61(7)	81(8)	44(7)	6(6)	18(6)	36(6)
C(63)	64(8)	76(8)	92(10)	-5(7)	37(8)	20(7)
C(64)	78(9)	96(9)	43(7)	-15(6)	28(6)	-4(7)
C(65)	67(8)	61(7)	38(7)	12(5)	4(5)	-11(6)
C(66)	45(6)	42(5)	44(6)	1(5)	11(5)	3(5)

Table B.1.4 Hydrogen coordinates (x 10^4) and isotropic displacement parameters (Å^2 x 10^3) for [$(AuCl)_2$(μ-dppf-$CH(CH_3)N(CH_3)_2$)].

	x	y	z	U(eq)
H(12)	2331	3822	3735	54
H(13)	3569	3945	4602	75
H(14)	4484	2355	4775	85
H(15)	4149	604	4161	84
H(16)	2903	446	3302	59
H(22)	2884	1333	2224	65
H(23)	3132	1482	1193	77
H(24)	2228	2516	292	80
H(25)	1037	3358	398	83
H(26)	818	3309	1438	61
H(32)	1550	-274	1897	56
H(33)	810	-2188	2069	62
H(34)	176	-1745	2978	49
H(36)	101	1425	3389	48
H(37A)	-256	371	4236	104
H(37B)	164	-814	4077	104
H(37C)	-622	-288	3531	104
H(38A)	1807	-462	4130	126
H(38B)	1505	-250	4763	126
H(38C)	2271	465	4700	126
H(39A)	728	2662	4291	118
H(39B)	1606	2388	4799	118
H(39C)	840	1672	4861	118
H(42)	-1371	922	2124	62
H(43)	-540	2292	1644	79
H(44)	-20	1152	833	79
H(45)	-559	-997	761	60
H(52)	-2507	116	539	82
H(53)	-3729	325	-291	95
H(54)	-4753	-1072	-458	85
H(55)	-4465	-2862	166	107
H(56)	-3237	-3117	1014	80
H(62)	-2838	-470	2036	74
H(63)	-3168	-450	3039	90
H(64)	-2506	-1772	3918	84
H(65)	-1541	-3101	3769	70

H(66)	-1211	-3118	2771	53

B.2 Crystal data of [(AuSCN)$_2$(μ-dppf-CH(CH$_3$)N(CH$_3$)$_2$)].

Table B.2.1 Atomic coordinates (x 10^4) and equivalent isotropic displacement parameters (Å^2 x 10^3) for [(AuSCN)$_2$(μ-dppf-CH(CH$_3$)N(CH$_3$)$_2$)]. U(eq) is defined as one third of the trace of the orthogonalized Uij tensor.

	x	y	z	U(eq)
Au(1)	5762(1)	4317(1)	3423(1)	35(1)
Au(2)	-985(1)	8829(1)	1474(1)	40(1)
P(1)	4442(3)	3837(2)	2487(1)	30(1)
P(2)	149(3)	8823(2)	2610(2)	36(1)
S(1)	7079(4)	4934(3)	4342(2)	55(1)
S(2)	-2204(4)	8932(2)	324(2)	60(1)
N(1)	5661(17)	7065(11)	4167(9)	102(5)
N(2)	-1186(15)	6939(10)	-395(7)	81(4)
N(3)	6680(8)	5041(6)	1559(5)	38(2)
Fe	1845(1)	6200(1)	2457(1)	29(1)
C(1)	6238(15)	6193(11)	4229(8)	64(3)
C(11)	5637(10)	2922(6)	1716(6)	33(2)
C(12)	7195(11)	2511(8)	1806(6)	44(2)
C(13)	8160(13)	1810(9)	1217(7)	56(3)
C(14)	7601(14)	1535(8)	562(7)	55(3)
C(15)	6067(14)	1949(9)	454(7)	55(3)
C(16)	5089(12)	2652(8)	1025(6)	43(2)
C(2)	-1590(13)	7724(9)	-69(7)	53(3)
C(21)	2960(10)	3246(7)	2968(6)	36(2)
C(22)	2123(13)	2742(8)	2546(7)	51(3)
C(23)	957(14)	2346(10)	2951(9)	66(3)
C(24)	661(15)	2435(10)	3758(9)	68(3)
C(25)	1484(16)	2938(11)	4184(8)	67(3)
C(26)	2633(13)	3319(9)	3793(6)	51(3)
C(31)	3424(10)	4917(7)	1951(5)	32(2)
C(32)	1971(9)	5045(7)	1650(5)	32(2)
C(33)	1607(10)	5986(7)	1262(5)	34(2)
C(34)	2803(10)	6472(7)	1322(5)	31(2)
C(35)	3927(10)	5821(6)	1750(5)	28(2)
C(36)	5484(10)	5976(7)	1899(6)	35(2)
C(37)	5713(11)	7014(8)	1597(7)	49(3)
C(38)	6793(13)	4901(9)	679(6)	52(3)
C(39)	8199(11)	4994(9)	1804(7)	55(3)
C(41)	706(10)	7584(7)	3023(6)	37(2)
C(42)	2004(12)	7087(7)	3423(5)	37(2)
C(43)	1831(13)	6127(8)	3687(6)	49(3)
C(44)	430(12)	6005(8)	3476(6)	48(3)
C(45)	-260(12)	6880(7)	3072(6)	43(2)
C(51)	-1164(17)	9604(9)	3425(8)	70(2)
C(52)	-1513(16)	9208(9)	4165(7)	70(2)
C(53)	-2557(17)	9791(9)	4731(8)	70(2)
C(54)	-3280(16)	10849(9)	4628(8)	70(2)

C(55)	-2977(17)	11206(9)	3875(8)	70(2)
C(56)	-1950(16)	10613(9)	3291(8)	70(2)
C(61)	1842(11)	9311(7)	2468(6)	39(2)
C(62)	2665(14)	9406(9)	3113(7)	55(3)
C(63)	4000(15)	9752(11)	2983(8)	67(3)
C(64)	4462(14)	10058(9)	2247(9)	63(3)
C(65)	3676(15)	9995(9)	1604(8)	57(3)
C(66)	2362(12)	9625(8)	1719(7)	46(2)

Table B.2.2 Bond lengths (Å) and angles (°) for [$(AuSCN)_2$(μ-dppf-$CH(CH_3)N(CH_3)_2$)].

Au(1)-P(1)	2.265(2)	Fe-C(33)	2.060(9)
Au(1)-S(1)	2.327(3)	C(11)-C(16)	1.392(14)
Au(2)-P(2)	2.260(3)	C(11)-C(12)	1.395(13)
Au(2)-S(2)	2.313(3)	C(12)-C(13)	1.402(14)
P(1)-C(31)	1.799(9)	C(12)-H(12)	0.9300
P(1)-C(11)	1.813(9)	C(13)-C(14)	1.348(17)
P(1)-C(21)	1.831(9)	C(13)-H(13)	0.9300
P(2)-C(41)	1.769(10)	C(14)-C(15)	1.383(16)
P(2)-C(61)	1.803(10)	C(14)-H(14)	0.9300
P(2)-C(51)	1.816(12)	C(15)-C(16)	1.389(15)
S(1)-C(1)	1.678(15)	C(15)-H(15)	0.9300
S(2)-C(2)	1.673(12)	C(16)-H(16)	0.9300
N(1)-C(1)	1.158(18)	C(21)-C(26)	1.369(14)
N(2)-C(2)	1.133(16)	C(21)-C(22)	1.386(14)
N(3)-C(39)	1.463(12)	C(22)-C(23)	1.401(16)
N(3)-C(38)	1.468(13)	C(22)-H(22)	0.9300
N(3)-C(36)	1.482(11)	C(23)-C(24)	1.339(18)
Fe-C(32)	2.023(9)	C(23)-H(23)	0.9300
Fe-C(45)	2.025(10)	C(24)-C(25)	1.380(19)
Fe-C(31)	2.029(9)	C(24)-H(24)	0.9300
Fe-C(35)	2.032(8)	C(25)-C(26)	1.369(16)
Fe-C(41)	2.036(9)	C(25)-H(25)	0.9300
Fe-C(42)	2.044(9)	C(26)-H(26)	0.9300
Fe-C(43)	2.053(10)	C(31)-C(35)	1.427(12)
Fe-C(34)	2.056(9)	C(31)-C(32)	1.429(12)
Fe-C(44)	2.057(10)	C(32)-C(33)	1.396(12)
C(32)-H(32)	0.9300	C(44)-H(44)	0.9300
C(33)-C(34)	1.412(13)	C(45)-H(45)	0.9300
C(33)-H(33)	0.9300	C(51)-C(52)	1.377(16)
C(34)-C(35)	1.418(12)	C(51)-C(56)	1.383(16)
C(34)-H(34)	0.9300	C(52)-C(53)	1.337(16)
C(35)-C(36)	1.522(12)	C(52)-H(52)	0.9300
C(36)-C(37)	1.535(13)	C(53)-C(54)	1.416(16)
C(36)-H(36)	0.9800	C(53)-H(53)	0.9300
C(37)-H(37A)	0.9600	C(54)-C(55)	1.366(17)
C(37)-H(37B)	0.9600	C(54)-H(54)	0.9300
C(37)-H(37C)	0.9600	C(55)-C(56)	1.354(16)
C(38)-H(38A)	0.9600	C(55)-H(55)	0.9300
C(38)-H(38B)	0.9600	C(56)-H(56)	0.9300
C(38)-H(38C)	0.9600	C(61)-C(66)	1.385(14)
C(39)-H(39A)	0.9600	C(61)-C(62)	1.403(14)
C(39)-H(39B)	0.9600	C(62)-C(63)	1.393(16)

C(39)-H(39C)	0.9600	C(62)-H(62)	0.9300
C(41)-C(42)	1.428(13)	C(63)-C(64)	1.347(18)
C(41)-C(45)	1.439(14)	C(63)-H(63)	0.9300
C(42)-C(43)	1.400(14)	C(64)-C(65)	1.370(17)
C(42)-H(42)	0.9300	C(64)-H(64)	0.9300
C(43)-C(44)	1.402(16)	C(65)-C(66)	1.393(16)
C(43)-H(43)	0.9300	C(65)-H(65)	0.9300
C(44)-C(45)	1.391(14)	C(66)-H(66)	0.9300
P(1)-Au(1)-S(1)	175.61(9)	C(35)-Fe-C(41)	128.3(4)
P(2)-Au(2)-S(2)	176.86(9)	C(32)-Fe-C(42)	166.3(4)
C(31)-P(1)-C(11)	105.6(4)	C(45)-Fe-C(42)	68.0(4)
C(31)-P(1)-C(21)	105.8(4)	C(31)-Fe-C(42)	128.0(4)
C(11)-P(1)-C(21)	107.1(4)	C(35)-Fe-C(42)	108.5(4)
C(31)-P(1)-Au(1)	112.7(3)	C(41)-Fe-C(42)	41.0(4)
C(11)-P(1)-Au(1)	114.4(3)	C(32)-Fe-C(43)	128.4(4)
C(21)-P(1)-Au(1)	110.6(3)	C(45)-Fe-C(43)	67.3(4)
C(41)-P(2)-C(61)	107.3(4)	C(31)-Fe-C(43)	107.5(4)
C(41)-P(2)-C(51)	103.6(5)	C(35)-Fe-C(43)	118.1(4)
C(61)-P(2)-C(51)	106.7(6)	C(41)-Fe-C(43)	68.5(4)
C(41)-P(2)-Au(2)	113.4(3)	C(42)-Fe-C(43)	40.0(4)
C(61)-P(2)-Au(2)	113.2(3)	C(32)-Fe-C(34)	67.7(4)
C(51)-P(2)-Au(2)	112.0(5)	C(45)-Fe-C(34)	130.0(4)
C(1)-S(1)-Au(1)	95.9(4)	C(31)-Fe-C(34)	68.5(4)
C(2)-S(2)-Au(2)	103.1(4)	C(35)-Fe-C(34)	40.6(3)
C(39)-N(3)-C(38)	110.7(8)	C(41)-Fe-C(34)	108.7(4)
C(39)-N(3)-C(36)	112.0(8)	C(42)-Fe-C(34)	119.6(4)
C(38)-N(3)-C(36)	114.2(8)	C(43)-Fe-C(34)	152.2(4)
C(32)-Fe-C(45)	117.3(4)	C(32)-Fe-C(44)	108.0(4)
C(32)-Fe-C(31)	41.3(3)	C(45)-Fe-C(44)	39.8(4)
C(45)-Fe-C(31)	150.1(4)	C(31)-Fe-C(44)	117.0(4)
C(32)-Fe-C(35)	68.9(3)	C(35)-Fe-C(44)	150.8(4)
C(45)-Fe-C(35)	167.9(4)	C(41)-Fe-C(44)	68.7(4)
C(31)-Fe-C(35)	41.1(3)	C(42)-Fe-C(44)	67.4(4)
C(32)-Fe-C(41)	151.0(3)	C(43)-Fe-C(44)	39.9(5)
C(45)-Fe-C(41)	41.5(4)	C(34)-Fe-C(44)	167.1(4)
C(31)-Fe-C(41)	166.6(4)	C(32)-Fe-C(33)	40.0(4)
C(45)-Fe-C(33)	109.2(4)	C(33)-C(32)-Fe	71.4(5)
C(31)-Fe-C(33)	68.4(3)	C(31)-C(32)-Fe	69.6(5)
C(35)-Fe-C(33)	68.2(3)	C(33)-C(32)-H(32)	125.5
C(41)-Fe-C(33)	118.5(4)	C(31)-C(32)-H(32)	125.5
C(42)-Fe-C(33)	152.7(4)	Fe-C(32)-H(32)	125.0
C(43)-Fe-C(33)	166.1(4)	C(32)-C(33)-C(34)	108.1(7)
C(34)-Fe-C(33)	40.1(4)	C(32)-C(33)-Fe	68.6(5)
C(44)-Fe-C(33)	129.0(4)	C(34)-C(33)-Fe	69.8(5)
N(1)-C(1)-S(1)	178.7(13)	C(32)-C(33)-H(33)	126.0
C(16)-C(11)-C(12)	118.9(9)	C(34)-C(33)-H(33)	126.0
C(16)-C(11)-P(1)	123.1(7)	Fe-C(33)-H(33)	127.2
C(12)-C(11)-P(1)	118.0(7)	C(33)-C(34)-C(35)	108.4(8)
C(11)-C(12)-C(13)	119.6(10)	C(33)-C(34)-Fe	70.1(5)
C(11)-C(12)-H(12)	120.2	C(35)-C(34)-Fe	68.8(5)
C(13)-C(12)-H(12)	120.2	C(33)-C(34)-H(34)	125.8
C(14)-C(13)-C(12)	120.7(10)	C(35)-C(34)-H(34)	125.8

C(14)-C(13)-H(13)	119.6	Fe-C(34)-H(34)	126.9
C(12)-C(13)-H(13)	119.6	C(34)-C(35)-C(31)	107.7(8)
C(13)-C(14)-C(15)	120.6(10)	C(34)-C(35)-C(36)	127.3(8)
C(13)-C(14)-H(14)	119.7	C(31)-C(35)-C(36)	124.6(8)
C(15)-C(14)-H(14)	119.7	C(34)-C(35)-Fe	70.6(5)
C(14)-C(15)-C(16)	119.9(10)	C(31)-C(35)-Fe	69.3(5)
C(14)-C(15)-H(15)	120.1	C(36)-C(35)-Fe	130.5(6)
C(16)-C(15)-H(15)	120.1	N(3)-C(36)-C(35)	106.6(7)
C(15)-C(16)-C(11)	120.3(10)	N(3)-C(36)-C(37)	115.7(8)
C(15)-C(16)-H(16)	119.9	C(35)-C(36)-C(37)	112.6(8)
C(11)-C(16)-H(16)	119.9	N(3)-C(36)-H(36)	107.2
N(2)-C(2)-S(2)	174.5(12)	C(35)-C(36)-H(36)	107.2
C(26)-C(21)-C(22)	117.7(9)	C(37)-C(36)-H(36)	107.2
C(26)-C(21)-P(1)	118.4(7)	C(36)-C(37)-H(37A)	109.5
C(22)-C(21)-P(1)	123.9(8)	C(36)-C(37)-H(37B)	109.5
C(21)-C(22)-C(23)	120.8(11)	H(37A)-C(37)-H(37B)	109.5
C(21)-C(22)-H(22)	119.6	C(36)-C(37)-H(37C)	109.5
C(23)-C(22)-H(22)	119.6	H(37A)-C(37)-H(37C)	109.5
C(24)-C(23)-C(22)	119.9(12)	H(37B)-C(37)-H(37C)	109.5
C(24)-C(23)-H(23)	120.0	N(3)-C(38)-H(38A)	109.5
C(22)-C(23)-H(23)	120.0	N(3)-C(38)-H(38B)	109.5
C(23)-C(24)-C(25)	119.7(12)	H(38A)-C(38)-H(38B)	109.5
C(23)-C(24)-H(24)	120.2	N(3)-C(38)-H(38C)	109.5
C(25)-C(24)-H(24)	120.2	H(38A)-C(38)-H(38C)	109.5
C(26)-C(25)-C(24)	120.7(12)	H(38B)-C(38)-H(38C)	109.5
C(26)-C(25)-H(25)	119.7	N(3)-C(39)-H(39A)	109.5
C(24)-C(25)-H(25)	119.7	N(3)-C(39)-H(39B)	109.5
C(25)-C(26)-C(21)	121.1(10)	H(39A)-C(39)-H(39B)	109.5
C(25)-C(26)-H(26)	119.5	N(3)-C(39)-H(39C)	109.5
C(21)-C(26)-H(26)	119.5	H(39A)-C(39)-H(39C)	109.5
C(35)-C(31)-C(32)	106.8(8)	H(39B)-C(39)-H(39C)	109.5
C(35)-C(31)-P(1)	125.8(7)	C(42)-C(41)-C(45)	105.1(8)
C(32)-C(31)-P(1)	127.4(7)	C(42)-C(41)-P(2)	132.1(7)
C(35)-C(31)-Fe	69.5(5)	C(45)-C(41)-P(2)	122.6(7)
C(32)-C(31)-Fe	69.1(5)	C(42)-C(41)-Fe	69.8(5)
P(1)-C(31)-Fe	125.9(5)	C(45)-C(41)-Fe	68.8(5)
C(33)-C(32)-C(31)	108.9(8)	P(2)-C(41)-Fe	129.2(5)
C(43)-C(42)-C(41)	108.9(9)	C(52)-C(53)-C(54)	122.5(12)
C(43)-C(42)-Fe	70.4(6)	C(52)-C(53)-H(53)	118.7
C(41)-C(42)-Fe	69.2(5)	C(54)-C(53)-H(53)	118.7
C(43)-C(42)-H(42)	125.5	C(55)-C(54)-C(53)	115.4(11)
C(41)-C(42)-H(42)	125.5	C(55)-C(54)-H(54)	122.3
Fe-C(42)-H(42)	126.5	C(53)-C(54)-H(54)	122.3
C(42)-C(43)-C(44)	108.6(9)	C(56)-C(55)-C(54)	122.1(11)
C(42)-C(43)-Fe	69.7(6)	C(56)-C(55)-H(55)	119.0
C(44)-C(43)-Fe	70.2(6)	C(54)-C(55)-H(55)	119.0
C(42)-C(43)-H(43)	125.7	C(55)-C(56)-C(51)	121.4(12)
C(44)-C(43)-H(43)	125.7	C(55)-C(56)-H(56)	119.3
Fe-C(43)-H(43)	126.0	C(51)-C(56)-H(56)	119.3
C(45)-C(44)-C(43)	108.0(10)	C(66)-C(61)-C(62)	117.4(9)
C(45)-C(44)-Fe	68.8(6)	C(66)-C(61)-P(2)	121.1(7)
C(43)-C(44)-Fe	69.9(6)	C(62)-C(61)-P(2)	121.5(8)
C(45)-C(44)-H(44)	126.0	C(63)-C(62)-C(61)	120.5(10)

C(43)-C(44)-H(44)	126.0	C(63)-C(62)-H(62)	119.7
Fe-C(44)-H(44)	126.8	C(61)-C(62)-H(62)	119.7
C(44)-C(45)-C(41)	109.4(10)	C(64)-C(63)-C(62)	120.2(11)
C(44)-C(45)-Fe	71.3(6)	C(64)-C(63)-H(63)	119.9
C(41)-C(45)-Fe	69.7(5)	C(62)-C(63)-H(63)	119.9
C(44)-C(45)-H(45)	125.3	C(63)-C(64)-C(65)	121.1(12)
C(41)-C(45)-H(45)	125.3	C(63)-C(64)-H(64)	119.4
Fe-C(45)-H(45)	125.3	C(65)-C(64)-H(64)	119.4
C(52)-C(51)-C(56)	117.5(11)	C(64)-C(65)-C(66)	119.3(12)
C(52)-C(51)-P(2)	122.5(9)	C(64)-C(65)-H(65)	120.4
C(56)-C(51)-P(2)	119.8(10)	C(66)-C(65)-H(65)	120.4
C(53)-C(52)-C(51)	120.6(11)	C(61)-C(66)-C(65)	121.4(10)
C(53)-C(52)-H(52)	119.7	C(61)-C(66)-H(66)	119.3
C(51)-C(52)-H(52)	119.7	C(65)-C(66)-H(66)	119.3

Table B.2.3 Anisotropic displacement parameters ($Å^2$ x 10^3) for [$(AuSCN)_2$(μ-dppf-$CH(CH_3)N(CH_3)_2$)]. The anisotropic displacement factor exponent takes the form: $-2\pi^2[h^2a^{*2}U11 + ... + 2hka^*b^*U12]$.

	U11	U22	U33	U23	U13	U12
Au(1)	33(1)	33(1)	42(1)	0(1)	-13(1)	-7(1)
Au(2)	43(1)	33(1)	41(1)	-2(1)	-12(1)	-3(1)
P(1)	24(1)	23(1)	40(1)	-1(1)	-8(1)	-1(1)
P(2)	40(1)	25(1)	38(1)	-4(1)	-9(1)	-1(1)
S(1)	56(2)	64(2)	53(2)	0(1)	-25(1)	-22(1)
S(2)	69(2)	50(2)	58(2)	-2(1)	-33(2)	-3(1)
N(1)	112(11)	66(9)	132(12)	-18(8)	-55(9)	-11(8)
N(2)	96(9)	81(9)	74(8)	-22(7)	-17(7)	-35(7)
N(3)	18(4)	40(4)	51(5)	-8(4)	-5(3)	-1(3)
Fe	23(1)	22(1)	38(1)	2(1)	-3(1)	-1(1)
C(1)	57(7)	72(9)	67(8)	-21(7)	-16(6)	-24(7)
C(11)	32(5)	21(4)	47(5)	2(4)	-5(4)	-6(3)
C(12)	32(5)	43(6)	54(6)	3(5)	-9(4)	-4(4)
C(13)	38(6)	46(6)	69(8)	-6(6)	4(5)	13(5)
C(14)	61(7)	30(5)	62(7)	1(5)	8(6)	0(5)
C(15)	69(8)	49(6)	50(6)	-6(5)	-10(5)	-21(6)
C(16)	43(6)	38(5)	45(6)	-5(4)	-4(4)	-5(4)
C(2)	52(7)	58(7)	53(7)	-6(6)	-22(5)	-17(5)
C(21)	31(5)	24(4)	58(6)	8(4)	-12(4)	-11(4)
C(22)	53(7)	39(6)	63(7)	9(5)	-15(5)	-13(5)
C(23)	47(7)	54(7)	103(11)	4(7)	-20(7)	-21(6)
C(24)	54(8)	65(8)	84(10)	11(7)	9(7)	-25(6)
C(25)	82(9)	77(9)	52(7)	1(6)	-6(6)	-39(7)
C(26)	61(7)	52(7)	47(6)	3(5)	-13(5)	-25(5)
C(31)	31(5)	28(4)	36(5)	-7(4)	-5(4)	-7(4)
C(32)	19(4)	26(4)	50(5)	-2(4)	-11(4)	0(3)
C(33)	22(4)	38(5)	39(5)	4(4)	-9(4)	-2(4)
C(34)	27(4)	33(5)	29(4)	7(4)	-7(3)	-1(4)
C(35)	24(4)	26(4)	32(4)	-1(3)	0(3)	-5(3)
C(36)	30(5)	31(5)	40(5)	-5(4)	-4(4)	-4(4)
C(37)	29(5)	38(5)	86(8)	10(5)	-12(5)	-20(4)
C(38)	41(6)	62(7)	48(6)	-8(5)	3(5)	-8(5)
C(39)	30(5)	61(7)	72(8)	-1(6)	-11(5)	-8(5)

C(41)	31(5)	30(5)	44(5)	-7(4)	-6(4)	2(4)
C(42)	44(6)	30(5)	34(5)	-2(4)	-4(4)	-3(4)
C(43)	57(7)	46(6)	35(5)	2(4)	-5(5)	0(5)
C(44)	42(6)	37(6)	53(6)	3(5)	13(5)	1(4)
C(45)	37(5)	36(5)	50(6)	1(4)	4(4)	-6(4)
C(51)	92(4)	37(3)	61(3)	3(2)	9(3)	10(2)
C(52)	92(4)	37(3)	61(3)	3(2)	9(3)	10(2)
C(53)	92(4)	37(3)	61(3)	3(2)	9(3)	10(2)
C(54)	92(4)	37(3)	61(3)	3(2)	9(3)	10(2)
C(55)	92(4)	37(3)	61(3)	3(2)	9(3)	10(2)
C(56)	92(4)	37(3)	61(3)	3(2)	9(3)	10(2)
C(61)	46(6)	22(4)	47(6)	-5(4)	-11(4)	-5(4)
C(62)	69(8)	63(7)	42(6)	11(5)	-12(5)	-31(6)
C(63)	63(8)	70(9)	78(9)	-10(7)	-28(7)	-26(7)
C(64)	49(7)	48(7)	93(10)	-1(6)	-10(7)	-14(5)
C(65)	62(8)	50(7)	57(7)	-3(5)	-5(6)	-12(6)
C(66)	46(6)	42(6)	53(6)	3(5)	-8(5)	-15(5)

Table B.2.4 Hydrogen coordinates (x 10^4) and isotropic displacement parameters (Å^2 x 10^3) for [$(AuSCN)_2$(μ-dppf-$CH(CH_3)N(CH_3)_2$)].

	x	y	z	U(eq)
H(12)	7592	2699	2254	53
H(13)	9198	1533	1278	68
H(14)	8251	1062	181	66
H(15)	5691	1758	-1	65
H(16)	4064	2944	946	52
H(22)	2339	2666	1986	61
H(23)	390	2022	2660	79
H(24)	-96	2160	4029	81
H(25)	1255	3018	4743	81
H(26)	3200	3633	4092	61
H(32)	1366	4578	1704	39
H(33)	730	6248	1008	41
H(34)	2846	7110	1116	37
H(36)	5500	5984	2486	42
H(37A)	6705	7077	1708	73
H(37B)	4911	7571	1869	73
H(37C)	5668	7043	1025	73
H(38A)	5791	4922	531	79
H(38B)	7502	4245	510	79
H(38C)	7161	5446	419	79
H(39A)	8941	4383	1567	82
H(39B)	8135	4973	2382	82
H(39C)	8516	5595	1624	82
H(42)	2830	7357	3496	45
H(43)	2529	5649	3956	58
H(44)	32	5439	3587	57
H(45)	-1200	6993	2865	51
H(52)	-1017	8529	4271	84
H(53)	-2819	9490	5212	84
H(54)	-3917	11272	5045	84
H(55)	-3493	11879	3761	84

H(56)	-1770	10890	2788	84
H(62)	2317	9237	3630	66
H(63)	4573	9772	3407	81
H(64)	5329	10315	2173	75
H(65)	4016	10197	1096	69
H(66)	1822	9589	1284	56

B.3 Crystal data of [$(AuCl)_2$(μ-dppf-$CH(CH_3)OAc$)].

Table B.3.1 Atomic coordinates (x 10^4) and equivalent isotropic displacement parameters ($Å^2$ x 10^3) for [$(AuCl)_2$(μ-dppf-$CH(CH_3)OAc$)]. U(eq) is defined as one third of the trace of the orthogonalized Uij tensor.

	x	y	z	U(eq)
C(221)	1501(4)	1592(3)	2074(2)	17(1)
C(211)	60(4)	2317(3)	1875(2)	17(1)
C(242)	355(4)	-447(3)	1515(2)	15(1)
C(132)	819(4)	5977(3)	804(2)	17(1)
C(144)	-858(4)	6941(3)	972(2)	23(2)
C(121)	-1456(4)	5171(3)	535(2)	16(1)
C(131)	108(4)	5718(3)	646(2)	15(1)
C(145)	-126(4)	7272(3)	1036(2)	16(1)
C(126)	-1538(4)	4804(3)	260(2)	23(2)
C(122)	-2054(4)	5608(3)	611(2)	22(2)
C(112)	690(4)	4393(3)	534(2)	19(1)
C(133)	1220(4)	6347(3)	562(2)	18(1)
C(234)	-1073(4)	335(3)	2060(2)	22(2)
C(116)	-398(4)	3858(3)	812(2)	22(2)
C(111)	-53(4)	4407(3)	705(2)	17(1)
C(134)	757(4)	6346(3)	265(2)	19(1)
C(142)	-512(4)	7444(3)	491(2)	17(1)
C(214)	-799(4)	3409(3)	1979(2)	24(2)
C(215)	-880(4)	2918(3)	2204(2)	23(2)
C(143)	-1093(4)	7053(3)	638(2)	22(1)
C(216)	-441(4)	2380(3)	2157(2)	21(1)
C(235)	-735(4)	748(3)	1822(2)	19(1)
C(115)	-13(5)	3303(3)	756(2)	26(2)
C(226)	2083(4)	1131(3)	2032(2)	19(1)
Cl(22)	-2303(1)	-1222(1)	850(1)	33(1)
C(261)	-1378(4)	-1289(3)	2175(2)	24(1)
C(251)	-259(4)	-2127(3)	1825(2)	17(1)
C(256)	-783(4)	-2632(3)	1843(2)	22(2)
C(262)	-2091(4)	-1024(3)	2129(2)	24(1)
C(161)	1372(4)	7922(3)	283(2)	19(1)
C(162)	905(5)	8088(3)	3(2)	23(2)
C(151)	635(4)	8868(3)	674(2)	19(1)
C(156)	-190(5)	9019(3)	630(2)	26(2)
C(252)	580(4)	-2217(3)	1850(2)	19(1)
C(152)	1205(5)	9337(3)	710(2)	24(2)
Cl(12)	2750(1)	7777(1)	1540(1)	28(1)
C(264)	-2233(4)	-1146(3)	2719(2)	24(1)

C(153)	983(5)	9943(3)	688(2)	26(2)
C(254)	358(5)	-3310(3)	1916(2)	28(2)
C(222)	1586(5)	1996(3)	2338(2)	27(2)
C(266)	-1006(4)	-1460(3)	2443(2)	24(1)
C(265)	-1443(4)	-1396(3)	2730(2)	24(1)
C(212)	127(4)	2809(3)	1649(2)	20(1)
C(253)	880(5)	-2812(3)	1900(2)	23(2)
C(113)	1070(5)	3833(3)	474(2)	25(2)
C(224)	2792(4)	1467(3)	2517(2)	25(2)
C(225)	2708(4)	1070(3)	2257(2)	26(2)
C(135)	67(4)	5955(3)	315(2)	17(1)
C(124)	-2804(5)	5311(4)	129(2)	32(2)
C(123)	-2727(4)	5676(3)	406(2)	29(2)
C(263)	-2538(4)	-946(3)	2418(2)	24(1)
C(223)	2235(4)	1945(3)	2553(2)	28(2)
C(213)	-299(4)	3349(3)	1706(2)	24(2)
C(255)	-477(5)	-3224(3)	1888(2)	25(2)
C(141)	97(4)	7585(3)	734(2)	18(1)
C(114)	725(5)	3286(3)	585(2)	29(2)
C(166)	2094(4)	7589(3)	237(2)	24(2)
C(125)	-2221(4)	4874(4)	58(2)	30(2)
C(155)	-418(5)	9645(3)	616(2)	30(2)
C(165)	2312(5)	7410(3)	-83(2)	32(2)
C(154)	166(5)	10102(3)	637(2)	35(2)
C(163)	1130(5)	7902(3)	-314(2)	32(2)
C(164)	1830(5)	7554(4)	-352(2)	37(2)
O(11)	1366(3)	5205(2)	1146(1)	20(1)
O(21)	-1542(3)	1489(2)	1552(1)	24(1)
C(13)	1399(4)	4913(3)	1440(2)	23(2)
C(12)	1794(4)	6259(3)	1262(2)	24(2)
C(21)	-1081(4)	917(3)	1493(2)	20(1)
C(11)	1101(4)	5852(3)	1154(2)	16(1)
C(23)	-1540(5)	1915(3)	1306(2)	32(2)
C(22)	-1656(5)	437(3)	1348(2)	40(2)
C(24)	-2023(5)	2462(3)	1390(2)	36(2)
C(14)	1674(5)	4267(3)	1395(2)	33(2)
O(22)	-1173(5)	1841(4)	1058(2)	89(3)
O(12)	1242(4)	5155(2)	1703(1)	36(1)
Au(21)	947(1)	1558(1)	1257(1)	17(1)
Au(22)	-1482(1)	-1297(1)	1307(1)	19(1)
Au(11)	-883(1)	5165(1)	1345(1)	17(1)
Au(12)	1883(1)	7925(1)	1102(1)	18(1)
Fe(11)	50(1)	6661(1)	651(1)	14(1)
Fe(21)	93(1)	78(1)	1931(1)	15(1)
P(21)	628(1)	1608(1)	1795(1)	15(1)
P(11)	-560(1)	5128(1)	807(1)	15(1)
Cl(21)	1276(1)	1588(1)	703(1)	28(1)
Cl(11)	-1249(1)	5147(1)	1893(1)	30(1)
P(12)	993(1)	8072(1)	693(1)	16(1)
P(22)	-728(1)	-1374(1)	1767(1)	16(1)
C(243)	1058(4)	-115(3)	1618(2)	19(1)
C(244)	1238(4)	-291(3)	1951(2)	18(1)
C(231)	-15(4)	1008(3)	1971(2)	15(1)

C(245)	653(4)	-724(3)	2056(2)	18(1)
C(232)	84(4)	746(3)	2293(2)	18(1)
C(241)	100(4)	-833(3)	1788(2)	15(1)
C(233)	-569(4)	324(3)	2344(2)	20(2)

Table B.3.2 Bond lengths (Å) and angles (°) for [$(AuCl)_2$(μ-dppf-$CH(CH_3)OAc$)].

C(221)-C(222)	1.383(9)	C(142)-C(143)	1.406(9)
C(221)-C(226)	1.389(9)	C(142)-C(141)	1.431(9)
C(221)-P(21)	1.817(7)	C(142)-Fe(11)	2.034(6)
C(211)-C(216)	1.405(9)	C(142)-H(142)	0.9300
C(211)-C(212)	1.405(8)	C(214)-C(213)	1.376(10)
C(211)-P(21)	1.824(6)	C(214)-C(215)	1.407(9)
C(242)-C(243)	1.418(9)	C(214)-H(214)	0.9300
C(242)-C(241)	1.443(8)	C(215)-C(216)	1.383(9)
C(242)-Fe(21)	2.069(6)	C(215)-H(215)	0.9300
C(242)-H(242)	0.9300	C(143)-Fe(11)	2.054(7)
C(132)-C(133)	1.420(9)	C(143)-H(143)	0.9300
C(132)-C(131)	1.439(8)	C(216)-H(216)	0.9300
C(132)-C(11)	1.510(9)	C(235)-C(231)	1.436(9)
C(132)-Fe(11)	2.040(6)	C(235)-C(21)	1.486(9)
C(144)-C(143)	1.418(9)	C(235)-Fe(21)	2.034(6)
C(144)-C(145)	1.419(9)	C(115)-C(114)	1.390(10)
C(144)-Fe(11)	2.061(7)	C(115)-H(115)	0.9300
C(144)-H(144)	0.9300	C(226)-C(225)	1.372(9)
C(121)-C(126)	1.370(9)	C(226)-H(226)	0.9300
C(121)-C(122)	1.395(9)	Cl(22)-Au(22)	2.2831(17)
C(121)-P(11)	1.831(7)	C(261)-C(266)	1.293(9)
C(131)-C(135)	1.429(8)	C(261)-C(262)	1.313(9)
C(131)-P(11)	1.802(6)	C(261)-P(22)	1.965(8)
C(131)-Fe(11)	2.045(6)	C(251)-C(252)	1.390(9)
C(145)-C(141)	1.439(8)	C(251)-C(256)	1.392(9)
C(145)-Fe(11)	2.057(6)	C(251)-P(22)	1.817(6)
C(145)-H(145)	0.9300	C(256)-C(255)	1.390(9)
C(126)-C(125)	1.389(10)	C(256)-H(256)	0.9300
C(126)-H(126)	0.9300	C(262)-C(263)	1.385(10)
C(122)-C(123)	1.383(9)	C(262)-H(262)	0.9300
C(122)-H(122)	0.9300	C(161)-C(166)	1.397(10)
C(112)-C(113)	1.384(9)	C(161)-C(162)	1.409(10)
C(112)-C(111)	1.398(9)	C(161)-P(12)	1.794(7)
C(112)-H(112)	0.9300	C(162)-C(163)	1.387(10)
C(133)-C(134)	1.418(9)	C(162)-H(162)	0.9300
C(133)-Fe(11)	2.064(7)	C(151)-C(152)	1.386(9)
C(133)-H(133)	0.9300	C(151)-C(156)	1.401(10)
C(234)-C(233)	1.410(10)	C(151)-P(12)	1.824(6)
C(234)-C(235)	1.424(9)	C(156)-C(155)	1.408(9)
C(234)-Fe(21)	2.054(7)	C(156)-H(156)	0.9300
C(234)-H(234)	0.9300	C(252)-C(253)	1.395(9)
C(116)-C(115)	1.376(9)	C(252)-H(252)	0.9300
C(116)-C(111)	1.384(9)	C(152)-C(153)	1.366(9)
C(116)-H(116)	0.9300	C(152)-H(152)	0.9300
C(111)-P(11)	1.817(6)	Cl(12)-Au(12)	2.2840(17)
C(134)-C(135)	1.425(9)	C(264)-C(263)	1.383(9)

C(134)-Fe(11)	2.055(6)	C(264)-C(265)	1.401(9)
C(134)-H(134)	0.9300	C(264)-H(264)	0.9300
C(153)-C(154)	1.395(11)	O(21)-C(21)	1.470(7)
C(153)-H(153)	0.9300	C(13)-O(12)	1.210(8)
C(254)-C(253)	1.378(10)	C(13)-C(14)	1.482(9)
C(254)-C(255)	1.383(10)	C(12)-C(11)	1.500(9)
C(254)-H(254)	0.9300	C(12)-H(12A)	0.9600
C(222)-C(223)	1.374(10)	C(12)-H(12B)	0.9600
C(222)-H(222)	0.9300	C(12)-H(12C)	0.9600
C(266)-C(265)	1.364(10)	C(21)-C(22)	1.517(9)
C(266)-H(266)	0.9300	C(21)-H(21)	0.9800
C(265)-H(265)	0.9300	C(11)-H(11)	0.9800
C(212)-C(213)	1.380(9)	C(23)-O(22)	1.178(10)
C(212)-H(212)	0.9300	C(23)-C(24)	1.464(10)
C(253)-H(253)	0.9300	C(22)-H(22A)	0.9600
C(113)-C(114)	1.386(10)	C(22)-H(22B)	0.9600
C(113)-H(113)	0.9300	C(22)-H(22C)	0.9600
C(224)-C(225)	1.362(10)	C(24)-H(24A)	0.9600
C(224)-C(223)	1.387(10)	C(24)-H(24B)	0.9600
C(224)-H(224)	0.9300	C(24)-H(24C)	0.9600
C(225)-H(225)	0.9300	C(14)-H(14A)	0.9600
C(135)-Fe(11)	2.041(6)	C(14)-H(14B)	0.9600
C(135)-H(135)	0.9300	C(14)-H(14C)	0.9600
C(124)-C(123)	1.371(11)	Au(21)-P(21)	2.2330(16)
C(124)-C(125)	1.375(11)	Au(21)-Cl(21)	2.2943(16)
C(124)-H(124)	0.9300	Au(22)-P(22)	2.2324(17)
C(123)-H(123)	0.9300	Au(11)-P(11)	2.2312(16)
C(263)-H(263)	0.9300	Au(11)-Cl(11)	2.2872(16)
C(223)-H(223)	0.9300	Au(12)-P(12)	2.2217(17)
C(213)-H(213)	0.9300	Fe(21)-C(245)	2.027(6)
C(255)-H(255)	0.9300	Fe(21)-C(231)	2.029(6)
C(141)-P(12)	1.812(7)	Fe(21)-C(244)	2.038(6)
C(141)-Fe(11)	2.031(6)	Fe(21)-C(232)	2.053(6)
C(114)-H(114)	0.9300	Fe(21)-C(241)	2.055(6)
C(166)-C(165)	1.392(10)	Fe(21)-C(233)	2.057(6)
C(166)-H(166)	0.9300	Fe(21)-C(243)	2.064(6)
C(125)-H(125)	0.9300	P(21)-C(231)	1.815(6)
C(155)-C(154)	1.380(11)	P(22)-C(241)	1.792(6)
C(155)-H(155)	0.9300	C(243)-C(244)	1.427(9)
C(165)-C(164)	1.374(12)	C(243)-H(243)	0.9300
C(165)-H(165)	0.9300	C(244)-C(245)	1.404(9)
C(154)-H(154)	0.9300	C(244)-H(244)	0.9300
C(163)-C(164)	1.379(12)	C(231)-C(232)	1.425(8)
C(163)-H(163)	0.9300	C(245)-C(241)	1.428(9)
C(164)-H(164)	0.9300	C(245)-H(245)	0.9300
O(11)-C(13)	1.342(8)	C(232)-C(233)	1.421(9)
O(11)-C(11)	1.466(7)	C(232)-H(232)	0.9300
O(21)-C(23)	1.351(8)	C(233)-H(233)	0.9300
C(222)-C(221)-C(226)	118.6(6)	C(243)-C(242)-C(241)	107.8(6)
C(222)-C(221)-P(21)	122.8(5)	C(243)-C(242)-Fe(21)	69.7(4)
C(226)-C(221)-P(21)	118.5(5)	C(241)-C(242)-Fe(21)	69.0(3)
C(216)-C(211)-C(212)	119.6(6)	C(243)-C(242)-H(242)	126.1

C(216)-C(211)-P(21)	121.4(5)	C(241)-C(242)-H(242)	126.1
C(212)-C(211)-P(21)	119.0(5)	Fe(21)-C(242)-H(242)	126.7
C(133)-C(132)-C(131)	107.0(5)	C(112)-C(111)-P(11)	121.8(5)
C(133)-C(132)-C(11)	126.8(6)	C(133)-C(134)-C(135)	107.7(5)
C(131)-C(132)-C(11)	126.1(6)	C(133)-C(134)-Fe(11)	70.2(4)
C(133)-C(132)-Fe(11)	70.7(4)	C(135)-C(134)-Fe(11)	69.1(3)
C(131)-C(132)-Fe(11)	69.6(3)	C(133)-C(134)-H(134)	126.2
C(11)-C(132)-Fe(11)	126.9(4)	C(135)-C(134)-H(134)	126.2
C(143)-C(144)-C(145)	108.3(6)	Fe(11)-C(134)-H(134)	126.1
C(143)-C(144)-Fe(11)	69.6(4)	C(143)-C(142)-C(141)	108.1(6)
C(145)-C(144)-Fe(11)	69.7(4)	C(143)-C(142)-Fe(11)	70.6(4)
C(143)-C(144)-H(144)	125.9	C(141)-C(142)-Fe(11)	69.3(3)
C(145)-C(144)-H(144)	125.9	C(143)-C(142)-H(142)	126.0
Fe(11)-C(144)-H(144)	126.4	C(141)-C(142)-H(142)	126.0
C(126)-C(121)-C(122)	120.0(6)	Fe(11)-C(142)-H(142)	125.7
C(126)-C(121)-P(11)	122.2(5)	C(213)-C(214)-C(215)	120.0(6)
C(122)-C(121)-P(11)	117.8(5)	C(213)-C(214)-H(214)	120.0
C(135)-C(131)-C(132)	107.9(5)	C(215)-C(214)-H(214)	120.0
C(135)-C(131)-P(11)	124.1(5)	C(216)-C(215)-C(214)	120.0(6)
C(132)-C(131)-P(11)	127.5(5)	C(216)-C(215)-H(215)	120.0
C(135)-C(131)-Fe(11)	69.4(3)	C(214)-C(215)-H(215)	120.0
C(132)-C(131)-Fe(11)	69.2(3)	C(142)-C(143)-C(144)	108.7(6)
P(11)-C(131)-Fe(11)	132.6(3)	C(142)-C(143)-Fe(11)	69.1(4)
C(144)-C(145)-C(141)	107.5(6)	C(144)-C(143)-Fe(11)	70.1(4)
C(144)-C(145)-Fe(11)	70.0(4)	C(142)-C(143)-H(143)	125.6
C(141)-C(145)-Fe(11)	68.4(3)	C(144)-C(143)-H(143)	125.6
C(144)-C(145)-H(145)	126.3	Fe(11)-C(143)-H(143)	126.7
C(141)-C(145)-H(145)	126.3	C(215)-C(216)-C(211)	119.8(6)
Fe(11)-C(145)-H(145)	126.9	C(215)-C(216)-H(216)	120.1
C(121)-C(126)-C(125)	119.3(7)	C(211)-C(216)-H(216)	120.1
C(121)-C(126)-H(126)	120.4	C(234)-C(235)-C(231)	106.5(6)
C(125)-C(126)-H(126)	120.4	C(234)-C(235)-C(21)	127.4(6)
C(123)-C(122)-C(121)	120.1(7)	C(231)-C(235)-C(21)	126.0(6)
C(123)-C(122)-H(122)	120.0	C(234)-C(235)-Fe(21)	70.4(4)
C(121)-C(122)-H(122)	120.0	C(231)-C(235)-Fe(21)	69.1(3)
C(113)-C(112)-C(111)	119.7(6)	C(21)-C(235)-Fe(21)	128.4(5)
C(113)-C(112)-H(112)	120.2	C(116)-C(115)-C(114)	120.2(6)
C(111)-C(112)-H(112)	120.2	C(116)-C(115)-H(115)	119.9
C(134)-C(133)-C(132)	109.3(6)	C(114)-C(115)-H(115)	119.9
C(134)-C(133)-Fe(11)	69.5(4)	C(225)-C(226)-C(221)	120.0(6)
C(132)-C(133)-Fe(11)	68.8(4)	C(225)-C(226)-H(226)	120.0
C(134)-C(133)-H(133)	125.4	C(221)-C(226)-H(226)	120.0
C(132)-C(133)-H(133)	125.4	C(266)-C(261)-C(262)	131.5(8)
Fe(11)-C(133)-H(133)	127.9	C(266)-C(261)-P(22)	114.5(6)
C(233)-C(234)-C(235)	109.3(6)	C(262)-C(261)-P(22)	113.7(5)
C(233)-C(234)-Fe(21)	70.0(4)	C(252)-C(251)-C(256)	119.6(6)
C(235)-C(234)-Fe(21)	68.9(4)	C(252)-C(251)-P(22)	123.5(5)
C(233)-C(234)-H(234)	125.4	C(256)-C(251)-P(22)	116.9(5)
C(235)-C(234)-H(234)	125.4	C(255)-C(256)-C(251)	120.7(7)
Fe(21)-C(234)-H(234)	127.3	C(255)-C(256)-H(256)	119.6
C(115)-C(116)-C(111)	120.8(7)	C(251)-C(256)-H(256)	119.6
C(115)-C(116)-H(116)	119.6	C(261)-C(262)-C(263)	113.7(7)
C(111)-C(116)-H(116)	119.6	C(261)-C(262)-H(262)	123.2

C(116)-C(111)-C(112)	119.3(6)	C(263)-C(262)-H(262)	123.2
C(116)-C(111)-P(11)	118.8(5)	C(166)-C(161)-C(162)	118.8(6)
C(166)-C(161)-P(12)	120.6(5)	C(134)-C(135)-H(135)	126.0
C(162)-C(161)-P(12)	120.3(5)	C(131)-C(135)-H(135)	126.0
C(163)-C(162)-C(161)	121.3(7)	Fe(11)-C(135)-H(135)	125.8
C(163)-C(162)-H(162)	119.3	C(123)-C(124)-C(125)	120.2(7)
C(161)-C(162)-H(162)	119.3	C(123)-C(124)-H(124)	119.9
C(152)-C(151)-C(156)	119.5(6)	C(125)-C(124)-H(124)	119.9
C(152)-C(151)-P(12)	118.2(5)	C(124)-C(123)-C(122)	119.7(7)
C(156)-C(151)-P(12)	122.3(5)	C(124)-C(123)-H(123)	120.1
C(151)-C(156)-C(155)	119.0(7)	C(122)-C(123)-H(123)	120.1
C(151)-C(156)-H(156)	120.5	C(264)-C(263)-C(262)	120.6(7)
C(155)-C(156)-H(156)	120.5	C(264)-C(263)-H(263)	119.7
C(251)-C(252)-C(253)	119.2(6)	C(262)-C(263)-H(263)	119.7
C(251)-C(252)-H(252)	120.4	C(222)-C(223)-C(224)	120.2(7)
C(253)-C(252)-H(252)	120.4	C(222)-C(223)-H(223)	119.9
C(153)-C(152)-C(151)	121.2(7)	C(224)-C(223)-H(223)	119.9
C(153)-C(152)-H(152)	119.4	C(214)-C(213)-C(212)	120.7(6)
C(151)-C(152)-H(152)	119.4	C(214)-C(213)-H(213)	119.6
C(263)-C(264)-C(265)	118.7(7)	C(212)-C(213)-H(213)	119.6
C(263)-C(264)-H(264)	120.7	C(254)-C(255)-C(256)	119.4(6)
C(265)-C(264)-H(264)	120.7	C(254)-C(255)-H(255)	120.3
C(152)-C(153)-C(154)	120.2(7)	C(256)-C(255)-H(255)	120.3
C(152)-C(153)-H(153)	119.9	C(142)-C(141)-C(145)	107.5(6)
C(154)-C(153)-H(153)	119.9	C(142)-C(141)-P(12)	128.7(5)
C(253)-C(254)-C(255)	120.2(6)	C(145)-C(141)-P(12)	123.8(5)
C(253)-C(254)-H(254)	119.9	C(142)-C(141)-Fe(11)	69.5(3)
C(255)-C(254)-H(254)	119.9	C(145)-C(141)-Fe(11)	70.4(3)
C(223)-C(222)-C(221)	120.7(7)	P(12)-C(141)-Fe(11)	126.1(4)
C(223)-C(222)-H(222)	119.7	C(113)-C(114)-C(115)	119.3(6)
C(221)-C(222)-H(222)	119.7	C(113)-C(114)-H(114)	120.3
C(261)-C(266)-C(265)	115.4(7)	C(115)-C(114)-H(114)	120.3
C(261)-C(266)-H(266)	122.3	C(165)-C(166)-C(161)	119.0(7)
C(265)-C(266)-H(266)	122.3	C(165)-C(166)-H(166)	120.5
C(266)-C(265)-C(264)	119.9(7)	C(161)-C(166)-H(166)	120.5
C(266)-C(265)-H(265)	120.1	C(124)-C(125)-C(126)	120.7(7)
C(264)-C(265)-H(265)	120.1	C(124)-C(125)-H(125)	119.6
C(213)-C(212)-C(211)	119.9(6)	C(126)-C(125)-H(125)	119.6
C(213)-C(212)-H(212)	120.1	C(154)-C(155)-C(156)	120.4(7)
C(211)-C(212)-H(212)	120.1	C(154)-C(155)-H(155)	119.8
C(254)-C(253)-C(252)	120.9(7)	C(156)-C(155)-H(155)	119.8
C(254)-C(253)-H(253)	119.5	C(164)-C(165)-C(166)	121.1(8)
C(252)-C(253)-H(253)	119.5	C(164)-C(165)-H(165)	119.4
C(112)-C(113)-C(114)	120.7(7)	C(166)-C(165)-H(165)	119.4
C(112)-C(113)-H(113)	119.7	C(155)-C(154)-C(153)	119.7(7)
C(114)-C(113)-H(113)	119.7	C(155)-C(154)-H(154)	120.2
C(225)-C(224)-C(223)	119.0(6)	C(153)-C(154)-H(154)	120.2
C(225)-C(224)-H(224)	120.5	C(164)-C(163)-C(162)	118.6(7)
C(223)-C(224)-H(224)	120.5	C(164)-C(163)-H(163)	120.7
C(224)-C(225)-C(226)	121.5(7)	C(162)-C(163)-H(163)	120.7
C(224)-C(225)-H(225)	119.3	C(165)-C(164)-C(163)	121.0(7)
C(226)-C(225)-H(225)	119.3	C(165)-C(164)-H(164)	119.5
C(134)-C(135)-C(131)	108.0(6)	C(163)-C(164)-H(164)	119.5

C(134)-C(135)-Fe(11)	70.2(3)	C(13)-O(11)-C(11)	116.3(5)
C(131)-C(135)-Fe(11)	69.7(3)	C(23)-O(21)-C(21)	117.2(5)
O(12)-C(13)-O(11)	123.9(6)	C(142)-Fe(11)-C(131)	148.3(2)
O(12)-C(13)-C(14)	125.6(7)	C(132)-Fe(11)-C(131)	41.2(2)
O(11)-C(13)-C(14)	110.5(6)	C(135)-Fe(11)-C(131)	40.9(2)
C(11)-C(12)-H(12A)	109.5	C(141)-Fe(11)-C(143)	68.4(3)
C(11)-C(12)-H(12B)	109.5	C(142)-Fe(11)-C(143)	40.2(3)
H(12A)-C(12)-H(12B)	109.5	C(132)-Fe(11)-C(143)	150.4(3)
C(11)-C(12)-H(12C)	109.5	C(135)-Fe(11)-C(143)	107.8(3)
H(12A)-C(12)-H(12C)	109.5	C(131)-Fe(11)-C(143)	117.1(3)
H(12B)-C(12)-H(12C)	109.5	C(141)-Fe(11)-C(134)	115.5(3)
O(21)-C(21)-C(235)	105.0(5)	C(142)-Fe(11)-C(134)	106.9(3)
O(21)-C(21)-C(22)	108.7(5)	C(132)-Fe(11)-C(134)	68.8(3)
C(235)-C(21)-C(22)	114.2(6)	C(135)-Fe(11)-C(134)	40.7(2)
O(21)-C(21)-H(21)	109.6	C(131)-Fe(11)-C(134)	68.6(2)
C(235)-C(21)-H(21)	109.6	C(143)-Fe(11)-C(134)	129.1(3)
C(22)-C(21)-H(21)	109.6	C(141)-Fe(11)-C(145)	41.2(2)
O(11)-C(11)-C(12)	110.1(5)	C(142)-Fe(11)-C(145)	68.9(2)
O(11)-C(11)-C(132)	104.0(5)	C(132)-Fe(11)-C(145)	109.1(2)
C(12)-C(11)-C(132)	113.4(5)	C(135)-Fe(11)-C(145)	169.2(2)
O(11)-C(11)-H(11)	109.7	C(131)-Fe(11)-C(145)	131.0(2)
C(12)-C(11)-H(11)	109.7	C(143)-Fe(11)-C(145)	68.0(3)
C(132)-C(11)-H(11)	109.7	C(134)-Fe(11)-C(145)	149.5(3)
O(22)-C(23)-O(21)	122.0(7)	C(141)-Fe(11)-C(144)	68.5(3)
O(22)-C(23)-C(24)	125.5(7)	C(142)-Fe(11)-C(144)	68.2(3)
O(21)-C(23)-C(24)	112.5(7)	C(132)-Fe(11)-C(144)	118.0(3)
C(21)-C(22)-H(22A)	109.5	C(135)-Fe(11)-C(144)	130.3(3)
C(21)-C(22)-H(22B)	109.5	C(131)-Fe(11)-C(144)	109.5(3)
H(22A)-C(22)-H(22B)	109.5	C(143)-Fe(11)-C(144)	40.3(3)
C(21)-C(22)-H(22C)	109.5	C(134)-Fe(11)-C(144)	168.1(3)
H(22A)-C(22)-H(22C)	109.5	C(145)-Fe(11)-C(144)	40.3(3)
H(22B)-C(22)-H(22C)	109.5	C(141)-Fe(11)-C(133)	108.5(3)
C(23)-C(24)-H(24A)	109.5	C(142)-Fe(11)-C(133)	129.7(3)
C(23)-C(24)-H(24B)	109.5	C(132)-Fe(11)-C(133)	40.5(2)
H(24A)-C(24)-H(24B)	109.5	C(135)-Fe(11)-C(133)	68.0(3)
C(23)-C(24)-H(24C)	109.5	C(131)-Fe(11)-C(133)	68.0(2)
H(24A)-C(24)-H(24C)	109.5	C(143)-Fe(11)-C(133)	167.7(3)
H(24B)-C(24)-H(24C)	109.5	C(134)-Fe(11)-C(133)	40.3(3)
C(13)-C(14)-H(14A)	109.5	C(145)-Fe(11)-C(133)	118.1(3)
C(13)-C(14)-H(14B)	109.5	C(144)-Fe(11)-C(133)	151.0(3)
H(14A)-C(14)-H(14B)	109.5	C(245)-Fe(21)-C(231)	150.6(3)
C(13)-C(14)-H(14C)	109.5	C(245)-Fe(21)-C(235)	165.1(3)
H(14A)-C(14)-H(14C)	109.5	C(231)-Fe(21)-C(235)	41.4(2)
H(14B)-C(14)-H(14C)	109.5	C(245)-Fe(21)-C(244)	40.4(2)
P(21)-Au(21)-Cl(21)	175.62(6)	C(231)-Fe(21)-C(244)	117.8(3)
P(22)-Au(22)-Cl(22)	177.55(7)	C(235)-Fe(21)-C(244)	154.3(3)
P(11)-Au(11)-Cl(11)	176.66(6)	C(245)-Fe(21)-C(232)	115.6(3)
P(12)-Au(12)-Cl(12)	177.34(7)	C(231)-Fe(21)-C(232)	40.9(2)
C(141)-Fe(11)-C(142)	41.2(2)	C(235)-Fe(21)-C(232)	69.2(3)
C(141)-Fe(11)-C(132)	130.0(3)	C(244)-Fe(21)-C(232)	104.8(3)
C(142)-Fe(11)-C(132)	168.6(3)	C(245)-Fe(21)-C(234)	126.1(3)
C(141)-Fe(11)-C(135)	147.9(2)	C(231)-Fe(21)-C(234)	68.3(3)
C(142)-Fe(11)-C(135)	114.9(2)	C(235)-Fe(21)-C(234)	40.8(3)

C(132)-Fe(11)-C(135)	69.3(2)	C(244)-Fe(21)-C(234)	161.7(3)
C(141)-Fe(11)-C(131)	169.8(3)	C(232)-Fe(21)-C(234)	67.8(3)
C(245)-Fe(21)-C(241)	40.9(2)	C(241)-P(22)-C(251)	105.2(3)
C(231)-Fe(21)-C(241)	167.3(2)	C(241)-P(22)-C(261)	108.0(3)
C(235)-Fe(21)-C(241)	128.9(3)	C(251)-P(22)-C(261)	101.9(3)
C(244)-Fe(21)-C(241)	68.2(2)	C(241)-P(22)-Au(22)	114.0(2)
C(232)-Fe(21)-C(241)	151.1(2)	C(251)-P(22)-Au(22)	113.9(2)
C(234)-Fe(21)-C(241)	109.7(3)	C(261)-P(22)-Au(22)	112.8(2)
C(245)-Fe(21)-C(233)	105.1(3)	C(242)-C(243)-C(244)	107.8(6)
C(231)-Fe(21)-C(233)	68.5(2)	C(242)-C(243)-Fe(21)	70.1(4)
C(235)-Fe(21)-C(233)	68.8(3)	C(244)-C(243)-Fe(21)	68.7(4)
C(244)-Fe(21)-C(233)	123.7(3)	C(242)-C(243)-H(243)	126.1
C(232)-Fe(21)-C(233)	40.5(3)	C(244)-C(243)-H(243)	126.1
C(234)-Fe(21)-C(233)	40.1(3)	Fe(21)-C(243)-H(243)	126.7
C(241)-Fe(21)-C(233)	118.6(2)	C(245)-C(244)-C(243)	108.7(6)
C(245)-Fe(21)-C(243)	68.4(3)	C(245)-C(244)-Fe(21)	69.4(4)
C(231)-Fe(21)-C(243)	108.4(2)	C(243)-C(244)-Fe(21)	70.6(4)
C(235)-Fe(21)-C(243)	121.5(3)	C(245)-C(244)-H(244)	125.6
C(244)-Fe(21)-C(243)	40.7(3)	C(243)-C(244)-H(244)	125.6
C(232)-Fe(21)-C(243)	125.6(3)	Fe(21)-C(244)-H(244)	125.9
C(234)-Fe(21)-C(243)	156.9(3)	C(232)-C(231)-C(235)	108.4(5)
C(241)-Fe(21)-C(243)	68.3(2)	C(232)-C(231)-P(21)	125.0(5)
C(233)-Fe(21)-C(243)	161.9(3)	C(235)-C(231)-P(21)	126.5(5)
C(245)-Fe(21)-C(242)	68.7(3)	C(232)-C(231)-Fe(21)	70.5(3)
C(231)-Fe(21)-C(242)	128.8(2)	C(235)-C(231)-Fe(21)	69.5(3)
C(235)-Fe(21)-C(242)	110.8(3)	P(21)-C(231)-Fe(21)	129.1(3)
C(244)-Fe(21)-C(242)	68.1(3)	C(244)-C(245)-C(241)	108.4(6)
C(232)-Fe(21)-C(242)	164.3(3)	C(244)-C(245)-Fe(21)	70.2(4)
C(234)-Fe(21)-C(242)	123.1(3)	C(241)-C(245)-Fe(21)	70.6(3)
C(241)-Fe(21)-C(242)	41.0(2)	C(244)-C(245)-H(245)	125.8
C(233)-Fe(21)-C(242)	155.1(3)	C(241)-C(245)-H(245)	125.8
C(243)-Fe(21)-C(242)	40.1(2)	Fe(21)-C(245)-H(245)	125.0
C(231)-P(21)-C(221)	101.7(3)	C(233)-C(232)-C(231)	107.7(6)
C(231)-P(21)-C(211)	103.9(3)	C(233)-C(232)-Fe(21)	69.9(4)
C(221)-P(21)-C(211)	108.0(3)	C(231)-C(232)-Fe(21)	68.7(3)
C(231)-P(21)-Au(21)	118.5(2)	C(233)-C(232)-H(232)	126.1
C(221)-P(21)-Au(21)	114.5(2)	C(231)-C(232)-H(232)	126.1
C(211)-P(21)-Au(21)	109.3(2)	Fe(21)-C(232)-H(232)	126.9
C(131)-P(11)-C(111)	104.6(3)	C(245)-C(241)-C(242)	107.2(5)
C(131)-P(11)-C(121)	103.6(3)	C(245)-C(241)-P(22)	128.4(5)
C(111)-P(11)-C(121)	106.0(3)	C(242)-C(241)-P(22)	124.2(5)
C(131)-P(11)-Au(11)	117.9(2)	C(245)-C(241)-Fe(21)	68.5(3)
C(111)-P(11)-Au(11)	110.9(2)	C(242)-C(241)-Fe(21)	70.0(3)
C(121)-P(11)-Au(11)	112.9(2)	P(22)-C(241)-Fe(21)	129.5(3)
C(161)-P(12)-C(141)	105.0(3)	C(234)-C(233)-C(232)	108.1(6)
C(161)-P(12)-C(151)	104.0(3)	C(234)-C(233)-Fe(21)	69.8(4)
C(141)-P(12)-C(151)	107.2(3)	C(232)-C(233)-Fe(21)	69.6(4)
C(161)-P(12)-Au(12)	115.4(2)	C(234)-C(233)-H(233)	126.0
C(141)-P(12)-Au(12)	112.3(2)	C(232)-C(233)-H(233)	126.0
C(151)-P(12)-Au(12)	112.2(2)	Fe(21)-C(233)-H(233)	126.1

Table B.3.3 Anisotropic displacement parameters ($Å^2$ x 10^3) for [$(AuCl)_2$(μ-dppf-$CH(CH_3)OAc$)]. The anisotropic displacement factor exponent takes the form: $-2\pi^2[h^2a^{*2}U11 + ... + 2hka^*b^*U12]$.

	U11	U22	U33	U23	U13	U12
C(211)	14(3)	12(3)	25(3)	-2(2)	-1(3)	0(3)
C(242)	15(3)	14(3)	17(3)	-1(2)	6(3)	2(2)
C(132)	19(4)	14(3)	19(3)	-5(2)	0(3)	-1(3)
C(144)	27(4)	19(3)	24(4)	-1(3)	9(3)	4(3)
C(121)	17(3)	15(3)	16(3)	5(2)	3(3)	-4(3)
C(131)	18(3)	10(3)	16(3)	-3(2)	0(3)	-1(3)
C(145)	21(4)	12(3)	16(3)	-3(2)	8(3)	3(3)
C(126)	18(4)	27(4)	24(3)	-2(3)	3(3)	2(3)
C(122)	23(4)	17(3)	27(4)	-1(3)	-1(3)	-3(3)
C(112)	22(4)	19(3)	16(3)	1(3)	-1(3)	4(3)
C(133)	16(3)	12(3)	27(4)	3(3)	5(3)	-3(3)
C(234)	18(4)	13(3)	35(4)	-2(3)	9(3)	-1(3)
C(116)	19(4)	16(3)	32(4)	-3(3)	-3(3)	0(3)
C(111)	26(4)	12(3)	12(3)	-2(2)	-8(3)	2(3)
C(134)	26(4)	13(3)	17(3)	1(2)	10(3)	2(3)
C(142)	18(4)	11(3)	22(3)	0(2)	-7(3)	1(3)
C(214)	25(4)	18(3)	30(4)	-3(3)	-3(3)	5(3)
C(215)	24(4)	22(3)	23(3)	-5(3)	1(3)	3(3)
C(143)	16(4)	20(3)	30(4)	-1(3)	-4(3)	1(3)
C(216)	20(4)	18(3)	25(4)	-5(3)	2(3)	-1(3)
C(235)	13(3)	15(3)	29(4)	-8(3)	1(3)	4(3)
C(115)	37(5)	12(3)	28(4)	2(3)	-9(3)	-3(3)
C(226)	21(4)	13(3)	21(3)	-2(2)	0(3)	0(3)
Cl(22)	30(1)	40(1)	28(1)	8(1)	-12(1)	-9(1)
C(261)	23(2)	15(1)	33(2)	-1(1)	-9(1)	2(1)
C(251)	26(4)	11(3)	14(3)	1(2)	-1(3)	2(3)
C(256)	27(4)	17(3)	22(3)	-2(3)	4(3)	2(3)
C(262)	23(2)	15(1)	33(2)	-1(1)	-9(1)	2(1)
C(161)	24(4)	11(3)	22(3)	0(2)	6(3)	-6(3)
C(162)	32(4)	18(3)	21(3)	2(3)	8(3)	-9(3)
C(151)	28(4)	10(3)	18(3)	5(2)	2(3)	2(3)
C(156)	30(4)	19(3)	28(4)	3(3)	-1(3)	3(3)
C(252)	25(4)	12(3)	21(3)	-4(2)	2(3)	-1(3)
C(152)	28(4)	23(4)	21(3)	2(3)	7(3)	-4(3)
Cl(12)	27(1)	23(1)	33(1)	1(1)	-12(1)	-1(1)
C(264)	23(2)	15(1)	33(2)	-1(1)	-9(1)	2(1)
C(153)	37(5)	17(3)	25(4)	-3(3)	9(3)	-7(3)
C(254)	49(5)	15(3)	19(3)	-2(3)	4(3)	9(3)
C(222)	29(4)	24(4)	28(4)	-5(3)	3(3)	3(3)
C(266)	23(2)	15(1)	33(2)	-1(1)	-9(1)	2(1)
C(265)	23(2)	15(1)	33(2)	-1(1)	-9(1)	2(1)
C(212)	15(3)	18(3)	25(3)	2(3)	0(3)	3(3)
C(253)	28(4)	20(3)	19(3)	-1(3)	0(3)	5(3)
C(113)	34(4)	20(3)	22(3)	-7(3)	0(3)	5(3)
C(224)	23(4)	30(4)	23(4)	7(3)	-8(3)	-4(3)
C(225)	21(4)	25(4)	30(4)	5(3)	4(3)	5(3)
C(135)	23(4)	13(3)	14(3)	-1(2)	0(3)	0(3)
C(124)	21(4)	46(5)	28(4)	11(3)	-6(3)	-7(4)

C(123)	20(4)	28(4)	39(4)	7(3)	-8(3)	0(3)
C(263)	23(2)	15(1)	33(2)	-1(1)	-9(1)	2(1)
C(223)	19(4)	42(4)	22(4)	-13(3)	-6(3)	0(3)
C(213)	27(4)	15(3)	30(4)	10(3)	2(3)	3(3)
C(255)	35(4)	11(3)	28(4)	6(3)	12(3)	-1(3)
C(141)	25(4)	8(3)	23(3)	4(2)	-2(3)	0(3)
C(114)	38(5)	23(4)	26(4)	-10(3)	-6(3)	12(3)
C(166)	28(4)	18(3)	27(4)	0(3)	8(3)	-12(3)
C(125)	26(4)	42(5)	20(4)	-3(3)	-1(3)	-7(4)
C(155)	36(5)	21(4)	32(4)	-1(3)	-5(3)	11(3)
C(165)	31(5)	22(4)	44(5)	2(3)	19(4)	-5(3)
C(154)	60(6)	14(3)	32(4)	3(3)	8(4)	9(4)
C(163)	42(5)	30(4)	24(4)	0(3)	2(3)	-10(4)
C(164)	54(6)	28(4)	29(4)	-12(3)	16(4)	-18(4)
O(11)	28(3)	13(2)	19(2)	-1(2)	-4(2)	6(2)
O(21)	23(3)	19(2)	30(3)	4(2)	-2(2)	3(2)
C(13)	27(4)	15(3)	26(4)	1(3)	-8(3)	-1(3)
C(12)	26(4)	21(3)	24(4)	-4(3)	-11(3)	-2(3)
C(21)	12(3)	21(3)	25(3)	-3(3)	-3(3)	4(3)
C(11)	18(3)	6(3)	24(3)	0(2)	0(3)	4(2)
C(23)	37(5)	30(4)	30(4)	9(3)	-6(4)	13(3)
C(22)	45(5)	23(4)	51(5)	-1(4)	-21(4)	-6(4)
C(24)	37(5)	30(4)	41(5)	9(3)	-15(4)	8(4)
C(14)	43(5)	20(4)	35(4)	10(3)	-9(4)	7(3)
O(22)	127(7)	103(6)	35(4)	43(4)	33(4)	79(6)
O(12)	55(4)	26(3)	27(3)	3(2)	-10(3)	3(3)
Au(21)	21(1)	14(1)	17(1)	0(1)	2(1)	0(1)
Au(22)	21(1)	18(1)	18(1)	2(1)	-3(1)	-3(1)
Au(11)	23(1)	14(1)	16(1)	0(1)	4(1)	-2(1)
Au(12)	20(1)	14(1)	22(1)	0(1)	-4(1)	-2(1)
Fe(11)	16(1)	11(1)	15(1)	1(1)	-1(1)	0(1)
Fe(21)	16(1)	11(1)	17(1)	-1(1)	1(1)	1(1)
P(21)	14(1)	13(1)	17(1)	0(1)	1(1)	0(1)
P(11)	19(1)	12(1)	14(1)	0(1)	2(1)	0(1)
Cl(21)	44(1)	20(1)	19(1)	0(1)	7(1)	-1(1)
Cl(11)	49(1)	23(1)	18(1)	0(1)	12(1)	-7(1)
P(12)	20(1)	12(1)	17(1)	-1(1)	1(1)	-2(1)
P(22)	18(1)	12(1)	19(1)	1(1)	-1(1)	0(1)
C(243)	19(4)	15(3)	24(3)	2(3)	6(3)	0(3)
C(244)	12(3)	16(3)	27(4)	-5(3)	-3(3)	2(3)
C(231)	18(3)	10(3)	17(3)	1(2)	4(3)	3(2)
C(245)	19(4)	13(3)	22(3)	3(3)	-7(3)	-2(3)
C(232)	20(4)	14(3)	20(3)	-4(2)	-2(3)	1(3)
C(241)	15(3)	8(3)	22(3)	0(2)	-2(3)	2(2)
C(233)	29(4)	11(3)	21(3)	2(2)	11(3)	5(3)

Table B.3.4 Hydrogen coordinates (x 10^4) and isotropic displacement parameters (Å^2 x 10^3) for [$(AuCl)_2$(μ-dppf-CH(CH_3)OAc)].

	x	y	z	U(eq)
H(242)	103	-420	1308	18
H(144)	-1136	6694	1123	28
H(145)	158	7284	1236	20

H(126)	-1141	4512	209	28
H(122)	-2001	5854	799	27
H(112)	927	4758	459	23
H(133)	1710	6556	595	22
H(234)	-1550	107	2033	26
H(116)	-897	3865	922	26
H(134)	881	6562	71	22
H(142)	-522	7586	273	20
H(214)	-1084	3775	2014	29
H(215)	-1228	2954	2386	28
H(143)	-1555	6894	535	26
H(216)	-477	2060	2310	25
H(115)	-247	2939	832	31
H(226)	2049	865	1852	22
H(256)	-1343	-2572	1824	26
H(262)	-2279	-901	1921	29
H(162)	437	8326	30	28
H(156)	-582	8710	611	31
H(252)	937	-1884	1834	23
H(152)	1749	9237	751	29
H(264)	-2545	-1115	2912	29
H(153)	1377	10251	707	31
H(254)	568	-3705	1947	33
H(222)	1200	2305	2370	32
H(266)	-477	-1617	2441	29
H(265)	-1218	-1518	2931	29
H(212)	457	2771	1463	23
H(253)	1440	-2874	1922	27
H(113)	1563	3823	359	30
H(224)	3218	1419	2668	31
H(225)	3081	750	2232	31
H(135)	-338	5869	160	20
H(124)	-3252	5359	-10	38
H(123)	-3126	5967	456	35
H(263)	-3048	-758	2409	29
H(223)	2300	2231	2723	33
H(213)	-247	3676	1557	29
H(255)	-830	-3560	1899	30
H(114)	985	2911	546	35
H(166)	2423	7488	417	29
H(125)	-2283	4623	-127	36
H(155)	-966	9751	592	36
H(165)	2793	7189	-116	39
H(154)	16	10515	618	42
H(163)	816	8011	-498	39
H(164)	1977	7414	-562	45
H(12A)	1945	6158	1486	36
H(12B)	1626	6683	1252	36
H(12C)	2254	6196	1118	36
H(21)	-636	997	1336	23
H(11)	641	5898	1308	19
H(22A)	-1853	577	1137	59
H(22B)	-2109	377	1497	59

H(22C)	-1368	54	1320	59
H(24A)	-1821	2811	1268	54
H(24B)	-1979	2543	1624	54
H(24C)	-2585	2392	1334	54
H(14A)	2258	4258	1372	49
H(14B)	1426	4097	1199	49
H(14C)	1517	4027	1585	49
H(243)	1350	167	1490	23
H(244)	1670	-144	2078	22
H(245)	631	-909	2264	22
H(232)	501	835	2442	22
H(233)	-650	84	2533	24

B.4 Crystal data of [(AuSCN)$_2$(μ-dppf-CH(CH$_3$)OAc)].

Table B.4.1 Atomic coordinates (x 10^4) and equivalent isotropic displacement parameters (Å^2 x 10^3) for [(AuSCN)$_2$(μ-dppf-CH(CH$_3$)OAc)]. U(eq) is defined as one third of the trace of the orthogonalized Uij tensor.

	x	y	z	U(eq)
S(2)	12038(3)	5031(2)	4332(1)	61(1)
S(1)	2417(4)	9324(2)	398(2)	79(1)
O(1)	10880(6)	5814(5)	1083(3)	57(2)
C(21)	3645(8)	9755(6)	3453(4)	41(2)
C(61)	10292(9)	3257(6)	1791(5)	42(2)
C(26)	2831(9)	10754(7)	3308(5)	52(2)
C(51)	7747(8)	3378(6)	3029(5)	41(2)
C(48)	12342(10)	5218(8)	1127(7)	63(3)
C(1)	3116(10)	8163(8)	39(5)	56(2)
O(2)	13004(7)	5073(7)	1708(5)	95(3)
C(12)	7135(9)	9878(7)	1811(5)	52(2)
C(25)	1841(10)	11320(7)	3861(6)	62(2)
C(16)	7506(9)	9577(7)	3173(5)	53(2)
C(66)	11898(9)	2835(7)	1878(5)	53(2)
C(2)	11134(11)	6291(10)	4245(6)	71(3)
C(11)	6635(9)	9557(6)	2553(4)	41(2)
C(47)	10154(10)	7384(7)	1802(6)	62(3)
C(56)	6883(10)	2865(7)	2619(5)	54(2)
C(46)	10080(8)	6284(7)	1802(5)	45(2)
C(62)	9623(10)	3065(8)	1118(5)	57(2)
C(52)	7493(10)	3401(7)	3817(5)	55(2)
C(13)	8475(10)	10257(8)	1713(5)	60(2)
C(24)	1650(11)	10863(8)	4590(6)	70(3)
C(15)	8850(11)	9967(8)	3070(6)	65(3)
C(55)	5776(11)	2421(8)	3009(7)	68(3)
C(14)	9336(11)	10284(8)	2343(6)	62(2)
N(1)	3552(11)	7400(8)	-252(6)	93(3)
C(65)	12804(12)	2235(8)	1311(6)	75(3)
C(63)	10575(13)	2444(8)	566(6)	74(3)
C(23)	2421(16)	9868(10)	4749(6)	108(5)
C(64)	12151(13)	2035(8)	658(6)	74(3)

C(49)	12946(11)	4774(8)	354(7)	87(4)
C(22)	3456(14)	9305(9)	4177(5)	91(4)
C(53)	6378(12)	2965(9)	4199(6)	72(3)
C(54)	5536(12)	2474(9)	3809(7)	77(3)
N(2)	10607(12)	7170(10)	4191(7)	109(4)
Au(2)	10632(1)	4503(1)	3418(1)	42(1)
Au(1)	3666(1)	9143(1)	1555(1)	46(1)
Fe	6527(1)	6424(1)	2554(1)	34(1)
P(2)	9140(2)	4064(2)	2541(1)	37(1)
P(1)	4893(2)	9038(2)	2674(1)	38(1)
C(41)	7971(8)	5178(6)	2032(4)	37(2)
C(31)	5478(8)	7757(6)	3090(4)	38(2)
C(42)	8417(8)	6110(6)	1772(4)	39(2)
C(32)	4514(9)	7049(7)	3173(5)	52(2)
C(44)	5907(9)	6299(7)	1450(5)	47(2)
C(43)	7138(8)	6781(6)	1416(4)	40(2)
C(35)	6914(9)	7244(7)	3461(4)	46(2)
C(45)	6387(8)	5318(6)	1831(5)	43(2)
C(34)	6761(11)	6245(7)	3743(5)	55(2)
C(33)	5285(10)	6134(7)	3580(5)	57(2)

Table B.4.2 Bond lengths (Å) and angles (°) for [$(AuSCN)_2$(μ-dppf-$CH(CH_3)OAc$)].

S(2)-C(2)	1.673(14)	C(48)-O(2)	1.176(12)
S(2)-Au(2)	2.317(2)	C(48)-C(49)	1.497(13)
S(1)-C(1)	1.659(11)	C(1)-N(1)	1.131(12)
S(1)-Au(1)	2.313(2)	C(12)-C(13)	1.390(11)
O(1)-C(48)	1.336(11)	C(12)-C(11)	1.395(11)
O(1)-C(46)	1.473(9)	C(12)-H(12)	0.9300
C(21)-C(26)	1.364(11)	C(25)-C(24)	1.375(14)
C(21)-C(22)	1.364(12)	C(25)-H(25)	0.9300
C(21)-P(1)	1.826(7)	C(16)-C(11)	1.363(11)
C(61)-C(66)	1.398(11)	C(16)-C(15)	1.402(11)
C(61)-C(62)	1.402(11)	C(16)-H(16)	0.9300
C(61)-P(2)	1.813(8)	C(66)-C(65)	1.375(11)
C(26)-C(25)	1.369(12)	C(66)-H(66)	0.9300
C(26)-H(26)	0.9300	C(2)-N(2)	1.150(15)
C(51)-C(52)	1.358(11)	C(11)-P(1)	1.826(8)
C(51)-C(56)	1.395(10)	C(47)-C(46)	1.488(11)
C(51)-P(2)	1.830(8)	C(47)-H(2A)	0.9600
C(47)-H(2B)	0.9600	C(54)-H(54)	0.9300
C(47)-H(2C)	0.9600	Au(2)-P(2)	2.2663(18)
C(56)-C(55)	1.374(12)	Au(1)-P(1)	2.2542(19)
C(56)-H(56)	0.9300	Fe-C(32)	2.014(8)
C(46)-C(42)	1.542(10)	Fe-C(45)	2.024(7)
C(46)-H(46)	0.9800	Fe-C(31)	2.033(7)
C(62)-C(63)	1.387(12)	Fe-C(42)	2.033(7)
C(62)-H(62)	0.9300	Fe-C(41)	2.038(7)
C(52)-C(53)	1.368(12)	Fe-C(44)	2.042(8)
C(52)-H(52)	0.9300	Fe-C(43)	2.047(7)
C(13)-C(14)	1.374(13)	Fe-C(35)	2.057(7)
C(13)-H(13)	0.9300	Fe-C(34)	2.062(8)
C(24)-C(23)	1.353(16)	Fe-C(33)	2.071(8)

C(24)-H(24)	0.9300	P(2)-C(41)	1.799(8)
C(15)-C(14)	1.365(13)	P(1)-C(31)	1.777(8)
C(15)-H(15)	0.9300	C(41)-C(45)	1.424(9)
C(55)-C(54)	1.378(14)	C(41)-C(42)	1.432(11)
C(55)-H(55)	0.9300	C(31)-C(32)	1.415(11)
C(14)-H(14)	0.9300	C(31)-C(35)	1.449(11)
C(65)-C(64)	1.369(14)	C(42)-C(43)	1.403(10)
C(65)-H(65)	0.9300	C(32)-C(33)	1.409(12)
C(63)-C(64)	1.373(14)	C(32)-H(32)	0.9300
C(63)-H(63)	0.9300	C(44)-C(43)	1.386(10)
C(23)-C(22)	1.406(12)	C(44)-C(45)	1.406(11)
C(23)-H(23)	0.9300	C(44)-H(44)	0.9300
C(64)-H(64)	0.9300	C(43)-H(43)	0.9300
C(49)-H(4A)	0.9600	C(35)-C(34)	1.425(12)
C(49)-H(4B)	0.9600	C(35)-H(35)	0.9300
C(49)-H(4C)	0.9600	C(45)-H(45)	0.9300
C(22)-H(22)	0.9300	C(34)-C(33)	1.393(12)
C(53)-C(54)	1.343(14)	C(34)-H(34)	0.9300
C(53)-H(53)	0.9300	C(33)-H(33)	0.9300
C(2)-S(2)-Au(2)	96.0(3)	O(1)-C(46)-C(42)	102.1(6)
C(1)-S(1)-Au(1)	101.9(3)	C(47)-C(46)-C(42)	115.4(7)
C(48)-O(1)-C(46)	117.7(7)	O(1)-C(46)-H(46)	109.7
C(26)-C(21)-C(22)	118.5(8)	C(47)-C(46)-H(46)	109.7
C(26)-C(21)-P(1)	119.8(7)	C(42)-C(46)-H(46)	109.7
C(22)-C(21)-P(1)	121.6(7)	C(63)-C(62)-C(61)	118.7(8)
C(66)-C(61)-C(62)	119.1(8)	C(63)-C(62)-H(62)	120.7
C(66)-C(61)-P(2)	119.1(6)	C(61)-C(62)-H(62)	120.7
C(62)-C(61)-P(2)	121.7(6)	C(51)-C(52)-C(53)	121.0(8)
C(21)-C(26)-C(25)	122.5(9)	C(51)-C(52)-H(52)	119.5
C(21)-C(26)-H(26)	118.8	C(53)-C(52)-H(52)	119.5
C(25)-C(26)-H(26)	118.8	C(14)-C(13)-C(12)	120.0(9)
C(52)-C(51)-C(56)	118.4(7)	C(14)-C(13)-H(13)	120.0
C(52)-C(51)-P(2)	119.0(5)	C(12)-C(13)-H(13)	120.0
C(56)-C(51)-P(2)	122.5(6)	C(23)-C(24)-C(25)	120.0(9)
O(2)-C(48)-O(1)	122.6(10)	C(23)-C(24)-H(24)	120.0
O(2)-C(48)-C(49)	126.9(9)	C(25)-C(24)-H(24)	120.0
O(1)-C(48)-C(49)	110.4(10)	C(14)-C(15)-C(16)	120.3(9)
N(1)-C(1)-S(1)	175.3(10)	C(14)-C(15)-H(15)	119.8
C(13)-C(12)-C(11)	119.9(8)	C(16)-C(15)-H(15)	119.8
C(13)-C(12)-H(12)	120.0	C(56)-C(55)-C(54)	119.8(9)
C(11)-C(12)-H(12)	120.0	C(56)-C(55)-H(55)	120.1
C(26)-C(25)-C(24)	118.9(9)	C(54)-C(55)-H(55)	120.1
C(26)-C(25)-H(25)	120.6	C(15)-C(14)-C(13)	120.1(8)
C(24)-C(25)-H(25)	120.6	C(15)-C(14)-H(14)	120.0
C(11)-C(16)-C(15)	120.0(8)	C(13)-C(14)-H(14)	120.0
C(11)-C(16)-H(16)	120.0	C(64)-C(65)-C(66)	120.7(10)
C(15)-C(16)-H(16)	120.0	C(64)-C(65)-H(65)	119.6
C(65)-C(66)-C(61)	120.3(9)	C(66)-C(65)-H(65)	119.6
C(65)-C(66)-H(66)	119.9	C(64)-C(63)-C(62)	121.6(9)
C(61)-C(66)-H(66)	119.9	C(64)-C(63)-H(63)	119.2
N(2)-C(2)-S(2)	175.5(10)	C(62)-C(63)-H(63)	119.2
C(16)-C(11)-C(12)	119.6(7)	C(24)-C(23)-C(22)	120.2(11)

C(16)-C(11)-P(1)	120.7(6)	C(24)-C(23)-H(23)	119.9
C(12)-C(11)-P(1)	119.6(6)	C(22)-C(23)-H(23)	119.9
C(46)-C(47)-H(2A)	109.5	C(65)-C(64)-C(63)	119.5(9)
C(46)-C(47)-H(2B)	109.5	C(65)-C(64)-H(64)	120.2
H(2A)-C(47)-H(2B)	109.5	C(63)-C(64)-H(64)	120.2
C(46)-C(47)-H(2C)	109.5	C(48)-C(49)-H(4A)	109.5
H(2A)-C(47)-H(2C)	109.5	C(48)-C(49)-H(4B)	109.5
H(2B)-C(47)-H(2C)	109.5	H(4A)-C(49)-H(4B)	109.5
C(55)-C(56)-C(51)	120.2(8)	C(48)-C(49)-H(4C)	109.5
C(55)-C(56)-H(56)	119.9	H(4A)-C(49)-H(4C)	109.5
C(51)-C(56)-H(56)	119.9	H(4B)-C(49)-H(4C)	109.5
O(1)-C(46)-C(47)	110.0(6)	C(21)-C(22)-C(23)	119.8(10)
C(21)-C(22)-H(22)	120.1	C(35)-Fe-C(33)	67.6(3)
C(23)-C(22)-H(22)	120.1	C(34)-Fe-C(33)	39.4(3)
C(54)-C(53)-C(52)	121.0(10)	C(41)-P(2)-C(61)	105.9(4)
C(54)-C(53)-H(53)	119.5	C(41)-P(2)-C(51)	106.1(3)
C(52)-C(53)-H(53)	119.5	C(61)-P(2)-C(51)	108.2(3)
C(53)-C(54)-C(55)	119.7(9)	C(41)-P(2)-Au(2)	112.3(2)
C(53)-C(54)-H(54)	120.1	C(61)-P(2)-Au(2)	113.2(3)
C(55)-C(54)-H(54)	120.1	C(51)-P(2)-Au(2)	110.8(3)
P(2)-Au(2)-S(2)	176.72(8)	C(31)-P(1)-C(11)	107.7(3)
P(1)-Au(1)-S(1)	177.51(9)	C(31)-P(1)-C(21)	103.6(3)
C(32)-Fe-C(45)	115.0(3)	C(11)-P(1)-C(21)	105.7(3)
C(32)-Fe-C(31)	40.9(3)	C(31)-P(1)-Au(1)	113.5(2)
C(45)-Fe-C(31)	149.1(3)	C(11)-P(1)-Au(1)	112.6(3)
C(32)-Fe-C(42)	166.4(4)	C(21)-P(1)-Au(1)	113.0(2)
C(45)-Fe-C(42)	68.5(3)	C(45)-C(41)-C(42)	106.2(7)
C(31)-Fe-C(42)	129.9(3)	C(45)-C(41)-P(2)	126.4(6)
C(32)-Fe-C(41)	149.4(3)	C(42)-C(41)-P(2)	127.3(5)
C(45)-Fe-C(41)	41.0(3)	C(45)-C(41)-Fe	68.9(4)
C(31)-Fe-C(41)	168.9(3)	C(42)-C(41)-Fe	69.2(4)
C(42)-Fe-C(41)	41.2(3)	P(2)-C(41)-Fe	125.0(4)
C(32)-Fe-C(44)	106.1(3)	C(32)-C(31)-C(35)	105.8(7)
C(45)-Fe-C(44)	40.5(3)	C(32)-C(31)-P(1)	124.6(6)
C(31)-Fe-C(44)	117.0(3)	C(35)-C(31)-P(1)	129.5(6)
C(42)-Fe-C(44)	67.5(3)	C(32)-C(31)-Fe	68.8(4)
C(41)-Fe-C(44)	68.3(3)	C(35)-C(31)-Fe	70.2(4)
C(32)-Fe-C(43)	127.4(3)	P(1)-C(31)-Fe	129.0(4)
C(45)-Fe-C(43)	67.8(3)	C(43)-C(42)-C(41)	108.3(6)
C(31)-Fe-C(43)	108.8(3)	C(43)-C(42)-C(46)	126.4(7)
C(42)-Fe-C(43)	40.2(3)	C(41)-C(42)-C(46)	125.1(7)
C(41)-Fe-C(43)	68.4(3)	C(43)-C(42)-Fe	70.4(4)
C(44)-Fe-C(43)	39.6(3)	C(41)-C(42)-Fe	69.6(4)
C(32)-Fe-C(35)	68.2(3)	C(46)-C(42)-Fe	130.7(5)
C(45)-Fe-C(35)	166.1(3)	C(33)-C(32)-C(31)	110.2(8)
C(31)-Fe-C(35)	41.5(3)	C(33)-C(32)-Fe	72.0(5)
C(42)-Fe-C(35)	111.7(3)	C(31)-C(32)-Fe	70.2(4)
C(41)-Fe-C(35)	129.9(3)	C(33)-C(32)-H(32)	124.9
C(44)-Fe-C(35)	153.3(3)	C(31)-C(32)-H(32)	124.9
C(43)-Fe-C(35)	122.0(3)	Fe-C(32)-H(32)	124.4
C(32)-Fe-C(34)	67.3(4)	C(43)-C(44)-C(45)	108.8(6)
C(45)-Fe-C(34)	126.8(4)	C(43)-C(44)-Fe	70.4(4)
C(31)-Fe-C(34)	68.9(3)	C(45)-C(44)-Fe	69.1(4)

C(42)-Fe-C(34)	122.1(3)	C(43)-C(44)-H(44)	125.6
C(41)-Fe-C(34)	108.9(3)	C(45)-C(44)-H(44)	125.6
C(44)-Fe-C(34)	163.3(4)	Fe-C(44)-H(44)	126.5
C(43)-Fe-C(34)	156.2(3)	C(44)-C(43)-C(42)	108.5(7)
C(35)-Fe-C(34)	40.5(3)	C(44)-C(43)-Fe	70.0(4)
C(32)-Fe-C(33)	40.3(3)	C(42)-C(43)-Fe	69.3(4)
C(45)-Fe-C(33)	105.6(4)	C(44)-C(43)-H(43)	125.8
C(31)-Fe-C(33)	68.7(3)	C(42)-C(43)-H(43)	125.8
C(42)-Fe-C(33)	153.1(3)	Fe-C(43)-H(43)	126.5
C(41)-Fe-C(33)	117.1(3)	C(34)-C(35)-C(31)	107.4(7)
C(44)-Fe-C(33)	125.9(4)	C(34)-C(35)-Fe	69.9(5)
C(43)-Fe-C(33)	163.7(3)	C(31)-C(35)-Fe	68.3(4)
C(34)-C(35)-H(35)	126.3	C(35)-C(34)-Fe	69.6(5)
C(31)-C(35)-H(35)	126.3	C(33)-C(34)-H(34)	125.4
Fe-C(35)-H(35)	127.0	C(35)-C(34)-H(34)	125.4
C(44)-C(45)-C(41)	108.2(7)	Fe-C(34)-H(34)	125.9
C(44)-C(45)-Fe	70.5(4)	C(34)-C(33)-C(32)	107.5(8)
C(41)-C(45)-Fe	70.0(4)	C(34)-C(33)-Fe	70.0(5)
C(44)-C(45)-H(45)	125.9	C(32)-C(33)-Fe	67.7(5)
C(41)-C(45)-H(45)	125.9	C(34)-C(33)-H(33)	126.3
Fe-C(45)-H(45)	125.2	C(32)-C(33)-H(33)	126.3
C(33)-C(34)-C(35)	109.1(8)	Fe-C(33)-H(33)	127.6
C(33)-C(34)-Fe	70.6(5)		

Table B.4.3 Anisotropic displacement parameters ($Å^2$ x 10^3) for [$(AuSCN)_2$(μ-dppf-$CH(CH_3)OAc$)]. The anisotropic displacement factor exponent takes the form: $-2\pi^2[h^2a^{*2}U11 + ... + 2hka^*b^*U12]$.

	U11	U22	U33	U23	U13	U12
S(2)	58(1)	83(2)	50(1)	2(1)	-22(1)	-31(1)
S(1)	106(2)	70(2)	55(2)	-14(1)	-40(2)	5(2)
O(1)	44(3)	67(4)	52(3)	-2(3)	12(3)	-5(3)
C(21)	41(4)	42(5)	37(4)	-7(4)	-4(3)	-4(3)
C(61)	48(4)	29(4)	46(4)	0(3)	-5(4)	-4(3)
C(26)	49(5)	45(5)	61(5)	-5(4)	3(4)	-12(4)
C(51)	39(4)	34(4)	53(5)	-8(4)	-10(4)	-12(3)
C(48)	35(5)	60(6)	92(8)	-1(6)	11(5)	-15(4)
C(1)	50(5)	67(6)	53(5)	7(5)	-17(4)	-13(5)
O(2)	40(4)	129(8)	113(7)	-24(6)	-14(4)	-6(4)
C(12)	50(5)	57(6)	49(5)	-1(4)	-5(4)	-10(4)
C(25)	55(5)	43(5)	80(7)	-3(5)	-3(5)	4(4)
C(16)	57(5)	60(6)	44(5)	-8(4)	-2(4)	-19(4)
C(66)	52(5)	52(5)	50(5)	-3(4)	-9(4)	-2(4)
C(2)	50(5)	106(9)	67(7)	-30(7)	-9(5)	-29(6)
C(11)	49(4)	40(4)	34(4)	-4(3)	0(4)	-9(4)
C(47)	54(5)	56(6)	80(7)	-1(5)	15(5)	-28(5)
C(56)	65(5)	47(5)	52(5)	3(4)	-11(4)	-18(4)
C(46)	37(4)	58(5)	42(4)	-1(4)	9(3)	-19(4)
C(62)	53(5)	73(7)	46(5)	-14(5)	-6(4)	-15(5)
C(52)	62(5)	62(6)	48(5)	-3(4)	-3(4)	-31(5)
C(13)	54(5)	75(7)	50(5)	7(5)	4(4)	-21(5)
C(24)	71(6)	67(7)	65(7)	-26(6)	10(5)	-5(5)
C(15)	69(6)	75(7)	60(6)	-8(5)	-18(5)	-31(5)

C(55)	61(6)	58(6)	95(8)	4(6)	-14(6)	-32(5)
C(14)	58(5)	67(6)	67(6)	-7(5)	5(5)	-28(5)
N(1)	90(7)	78(7)	108(8)	-31(6)	-34(6)	-1(5)
C(65)	71(6)	75(7)	63(6)	-8(6)	10(6)	5(5)
C(63)	99(8)	73(7)	54(6)	-17(5)	-5(6)	-28(6)
C(23)	171(12)	77(8)	45(6)	-14(6)	43(7)	14(8)
C(64)	84(7)	57(6)	68(7)	-5(5)	20(6)	-2(5)
C(49)	71(7)	70(7)	112(9)	-23(7)	56(7)	-15(6)
C(22)	143(10)	66(7)	34(5)	-8(5)	13(6)	24(7)
C(53)	85(7)	79(8)	59(6)	13(6)	1(6)	-38(6)
C(54)	69(6)	79(8)	88(8)	18(6)	-4(6)	-36(6)
N(2)	80(7)	109(9)	140(10)	-53(9)	-19(6)	-12(6)
Au(2)	39(1)	48(1)	41(1)	-1(1)	-11(1)	-14(1)
Au(1)	51(1)	50(1)	35(1)	-4(1)	-11(1)	-6(1)
Fe	32(1)	35(1)	36(1)	1(1)	-1(1)	-7(1)
P(2)	37(1)	35(1)	38(1)	-2(1)	-9(1)	-8(1)
P(1)	41(1)	41(1)	30(1)	-4(1)	-3(1)	-4(1)
C(41)	31(4)	37(4)	43(4)	-2(3)	-5(3)	-8(3)
C(31)	36(4)	46(5)	33(4)	-2(3)	5(3)	-13(3)
C(42)	44(4)	38(4)	34(4)	-13(3)	-2(3)	-4(3)
C(32)	36(4)	63(6)	56(5)	1(5)	9(4)	-13(4)
C(44)	34(4)	55(5)	47(5)	-6(4)	-12(3)	0(4)
C(43)	49(4)	33(4)	32(4)	4(3)	1(3)	0(3)
C(35)	50(4)	52(5)	34(4)	-4(4)	-6(4)	-9(4)
C(45)	41(4)	33(4)	56(5)	-4(4)	-17(4)	-6(3)
C(34)	66(5)	53(5)	34(4)	5(4)	3(4)	4(4)
C(33)	58(5)	55(6)	52(5)	7(4)	20(4)	-11(4)

Table B.4.4 Hydrogen coordinates (x 10^4) and isotropic displacement parameters (Å^2 x 10^3) for [$(AuSCN)_2$(μ-dppf-$CH(CH_3)OAc$)].

	x	y	z	U(eq)
H(26)	2954	11062	2814	62
H(12)	6572	9837	1381	63
H(25)	1307	12001	3746	75
H(16)	7208	9331	3665	63
H(66)	12355	2960	2321	63
H(2A)	11233	7417	1799	93
H(2B)	9588	7693	2261	93
H(2C)	9689	7752	1345	93
H(56)	7057	2823	2081	64
H(46)	10586	5900	2258	54
H(62)	8562	3348	1043	68
H(52)	8086	3718	4101	65
H(13)	8790	10493	1221	72
H(24)	989	11239	4974	84
H(15)	9413	10010	3498	78
H(55)	5192	2087	2735	82
H(14)	10250	10518	2275	74
H(65)	13873	1962	1372	89
H(63)	10136	2301	123	88
H(23)	2267	9556	5238	129
H(64)	12770	1624	279	88

H(4A)	14026	4397	382	131
H(4B)	12870	5324	-41	131
H(4C)	12329	4315	223	131
H(22)	4010	8628	4293	109
H(53)	6201	3010	4738	87
H(54)	4793	2171	4076	92
H(32)	3514	7169	2987	63
H(44)	4925	6579	1253	56
H(43)	7118	7437	1195	48
H(35)	7777	7517	3506	55
H(45)	5775	4844	1933	52
H(34)	7525	5747	3996	66
H(33)	4883	5562	3715	69

B.5 Crystal data of [$(AuSCN)_2$(μ-dppf)].

Table B.5.1 Atomic coordinates (x 10^4) and equivalent isotropic displacement parameters ($Å^2$ x 10^3) for [$(AuSCN)_2$(μ-dppf)]. U(eq) is defined as one third of the trace of the orthogonalized Uij tensor.

	x	y	z	U(eq)
C(31)	9488(2)	2747(2)	6550(2)	14(1)
C(32)	9395(2)	2005(2)	6622(2)	16(1)
C(51)	10473(2)	1050(2)	3772(2)	14(1)
C(25)	10602(2)	5008(2)	6986(2)	20(1)
C(35)	9076(2)	3091(2)	6952(2)	14(1)
C(33)	8924(2)	1905(2)	7055(2)	19(1)
C(42)	9020(2)	1865(2)	2517(2)	15(1)
C(41)	9390(2)	2194(2)	3139(2)	14(1)
C(44)	8923(2)	3061(2)	2357(2)	20(1)
C(43)	8728(2)	2404(2)	2044(2)	18(1)
C(45)	9327(2)	2944(2)	3032(2)	19(1)
C(61)	9111(2)	1387(2)	4196(2)	15(1)
C(62)	9391(2)	975(2)	4759(2)	23(1)
C(66)	8269(3)	1419(2)	3864(2)	31(1)
C(11)	9312(2)	3419(2)	5315(2)	16(1)
C(12)	9420(3)	4046(2)	5021(2)	24(1)
C(63)	8828(3)	604(2)	4976(2)	28(1)
C(64)	7989(3)	639(2)	4645(2)	32(1)
C(15)	8122(3)	3160(2)	4384(2)	30(1)
C(65)	7711(3)	1040(3)	4094(2)	43(1)
N(1)	11622(2)	630(2)	6996(2)	31(1)
C(1)	11678(2)	910(2)	6544(2)	21(1)
C(13)	8879(3)	4225(2)	4409(2)	28(1)
C(2)	11359(2)	4077(2)	4330(2)	23(1)
Fe(1)	10000	2460(1)	7500	11(1)
Au(1)	10926(1)	2258(1)	5918(1)	14(1)
Au(2)	10714(1)	2640(1)	4539(1)	15(1)
Fe(2)	10000	2484(1)	2500	13(1)
C(14)	8237(3)	3781(2)	4093(2)	28(1)
C(16)	8659(3)	2977(2)	4995(2)	25(1)
P(2)	9899(1)	1801(1)	3915(1)	13(1)

C(34)	8728(2)	2564(2)	7257(2)	16(1)
P(1)	10073(1)	3115(1)	6064(1)	12(1)
S(1)	11786(1)	1322(1)	5882(1)	24(1)
N(2)	11255(2)	4418(2)	3869(2)	36(1)
S(2)	11548(1)	3590(1)	5011(1)	27(1)
C(52)	11339(2)	1048(2)	3997(2)	16(1)
C(21)	10615(2)	3878(2)	6492(2)	14(1)
C(56)	10047(2)	471(2)	3433(2)	17(1)
C(22)	11481(2)	3872(2)	6744(2)	17(1)
C(23)	11903(2)	4426(2)	7129(2)	20(1)
C(55)	10486(3)	-88(2)	3297(2)	22(1)
C(24)	11457(2)	4987(2)	7251(2)	22(1)
C(26)	10181(2)	4454(2)	6612(2)	16(1)
C(53)	11775(2)	487(2)	3853(2)	19(1)
C(54)	11348(3)	-72(2)	3493(2)	23(1)

Table B.5.2 Bond lengths (Å) and angles (°) for [$(AuSCN)_2$(μ-dppf)].

C(31)-C(35)	1.435(5)	C(63)-C(64)	1.377(6)
C(31)-C(32)	1.437(5)	C(63)-H(63)	0.9300
C(31)-P(1)	1.800(4)	C(64)-C(65)	1.369(6)
C(31)-Fe(1)	2.037(3)	C(64)-H(64)	0.9300
C(32)-C(33)	1.424(5)	C(15)-C(14)	1.384(6)
C(32)-Fe(1)	2.044(3)	C(15)-C(16)	1.391(5)
C(32)-H(32)	0.9300	C(15)-H(15)	0.9300
C(51)-C(56)	1.394(5)	C(65)-H(65)	0.9300
C(51)-C(52)	1.395(5)	N(1)-C(1)	1.144(5)
C(51)-P(2)	1.812(4)	C(1)-S(1)	1.693(4)
C(25)-C(24)	1.381(5)	C(13)-C(14)	1.379(6)
C(25)-C(26)	1.385(5)	C(13)-H(13)	0.9300
C(25)-H(25)	0.9300	C(2)-N(2)	1.155(6)
C(35)-C(34)	1.429(5)	C(2)-S(2)	1.684(4)
C(35)-Fe(1)	2.034(3)	Fe(1)-C(35)#1	2.034(3)
C(35)-H(35)	0.9300	Fe(1)-C(31)#1	2.037(3)
C(33)-C(34)	1.404(5)	Fe(1)-C(32)#1	2.044(3)
C(33)-Fe(1)	2.066(4)	Fe(1)-C(34)#1	2.062(4)
C(33)-H(33)	0.9300	Fe(1)-C(34)	2.062(4)
C(42)-C(43)	1.423(5)	Fe(1)-C(33)#1	2.066(4)
C(42)-C(41)	1.436(5)	Au(1)-P(1)	2.2692(10)
C(42)-Fe(2)	2.048(4)	Au(1)-S(1)	2.3226(10)
C(42)-H(42)	0.9300	Au(1)-Au(2)	2.9798(7)
C(41)-C(45)	1.448(5)	Au(2)-P(2)	2.2611(10)
C(41)-P(2)	1.790(4)	Au(2)-S(2)	2.3281(11)
C(41)-Fe(2)	2.048(3)	Fe(2)-C(41)#2	2.048(3)
C(44)-C(43)	1.414(5)	Fe(2)-C(42)#2	2.048(4)
C(44)-C(45)	1.421(5)	Fe(2)-C(45)#2	2.057(4)
C(44)-Fe(2)	2.071(4)	Fe(2)-C(44)#2	2.071(4)
C(44)-H(44)	0.9300	Fe(2)-C(43)#2	2.074(4)
C(43)-Fe(2)	2.074(4)	C(14)-H(14)	0.9300
C(43)-H(43)	0.9300	C(16)-H(16)	0.9300
C(45)-Fe(2)	2.057(4)	C(34)-H(34)	0.9300
C(45)-H(45)	0.9300	P(1)-C(21)	1.813(4)
C(61)-C(66)	1.382(5)	C(52)-C(53)	1.391(5)

C(61)-C(62)	1.400(5)	C(52)-H(52)	0.9300
C(61)-P(2)	1.815(4)	C(21)-C(26)	1.391(5)
C(62)-C(63)	1.384(5)	C(21)-C(22)	1.397(5)
C(62)-H(62)	0.9300	C(56)-C(55)	1.386(5)
C(66)-C(65)	1.400(6)	C(56)-H(56)	0.9300
C(66)-H(66)	0.9300	C(22)-C(23)	1.394(5)
C(11)-C(16)	1.390(5)	C(22)-H(22)	0.9300
C(11)-C(12)	1.393(5)	C(23)-C(24)	1.383(6)
C(11)-P(1)	1.818(4)	C(23)-H(23)	0.9300
C(12)-C(13)	1.395(5)	C(55)-C(54)	1.387(6)
C(12)-H(12)	0.9300	C(55)-H(55)	0.9300
C(24)-H(24)	0.9300	C(53)-H(53)	0.9300
C(26)-H(26)	0.9300	C(54)-H(54)	0.9300
C(53)-C(54)	1.382(5)		
C(35)-C(31)-C(32)	107.1(3)	C(44)-C(43)-Fe(2)	69.9(2)
C(35)-C(31)-P(1)	129.7(3)	C(42)-C(43)-Fe(2)	68.8(2)
C(32)-C(31)-P(1)	123.2(3)	C(44)-C(43)-H(43)	125.6
C(35)-C(31)-Fe(1)	69.25(19)	C(42)-C(43)-H(43)	125.6
C(32)-C(31)-Fe(1)	69.65(19)	Fe(2)-C(43)-H(43)	127.2
P(1)-C(31)-Fe(1)	123.76(18)	C(44)-C(45)-C(41)	107.9(3)
C(33)-C(32)-C(31)	107.9(3)	C(44)-C(45)-Fe(2)	70.4(2)
C(33)-C(32)-Fe(1)	70.6(2)	C(41)-C(45)-Fe(2)	69.0(2)
C(31)-C(32)-Fe(1)	69.10(19)	C(44)-C(45)-H(45)	126.1
C(33)-C(32)-H(32)	126.0	C(41)-C(45)-H(45)	126.1
C(31)-C(32)-H(32)	126.0	Fe(2)-C(45)-H(45)	126.1
Fe(1)-C(32)-H(32)	125.9	C(66)-C(61)-C(62)	119.1(3)
C(56)-C(51)-C(52)	119.6(3)	C(66)-C(61)-P(2)	123.8(3)
C(56)-C(51)-P(2)	119.9(3)	C(62)-C(61)-P(2)	116.9(3)
C(52)-C(51)-P(2)	120.4(3)	C(63)-C(62)-C(61)	120.1(4)
C(24)-C(25)-C(26)	119.9(3)	C(63)-C(62)-H(62)	119.9
C(24)-C(25)-H(25)	120.0	C(61)-C(62)-H(62)	119.9
C(26)-C(25)-H(25)	120.0	C(61)-C(66)-C(65)	119.7(4)
C(34)-C(35)-C(31)	108.0(3)	C(61)-C(66)-H(66)	120.1
C(34)-C(35)-Fe(1)	70.7(2)	C(65)-C(66)-H(66)	120.1
C(31)-C(35)-Fe(1)	69.46(19)	C(16)-C(11)-C(12)	119.6(3)
C(34)-C(35)-H(35)	126.0	C(16)-C(11)-P(1)	118.6(3)
C(31)-C(35)-H(35)	126.0	C(12)-C(11)-P(1)	121.4(3)
Fe(1)-C(35)-H(35)	125.4	C(11)-C(12)-C(13)	120.0(4)
C(34)-C(33)-C(32)	108.7(3)	C(11)-C(12)-H(12)	120.0
C(34)-C(33)-Fe(1)	70.0(2)	C(13)-C(12)-H(12)	120.0
C(32)-C(33)-Fe(1)	68.9(2)	C(64)-C(63)-C(62)	120.6(4)
C(34)-C(33)-H(33)	125.7	C(64)-C(63)-H(63)	119.7
C(32)-C(33)-H(33)	125.7	C(62)-C(63)-H(63)	119.7
Fe(1)-C(33)-H(33)	127.1	C(65)-C(64)-C(63)	119.7(4)
C(43)-C(42)-C(41)	107.9(3)	C(65)-C(64)-H(64)	120.2
C(43)-C(42)-Fe(2)	70.8(2)	C(63)-C(64)-H(64)	120.2
C(41)-C(42)-Fe(2)	69.5(2)	C(14)-C(15)-C(16)	120.2(4)
C(43)-C(42)-H(42)	126.0	C(14)-C(15)-H(15)	119.9
C(41)-C(42)-H(42)	126.0	C(16)-C(15)-H(15)	119.9
Fe(2)-C(42)-H(42)	125.3	C(64)-C(65)-C(66)	120.8(4)
C(42)-C(41)-C(45)	107.1(3)	C(64)-C(65)-H(65)	119.6
C(42)-C(41)-P(2)	129.3(3)	C(66)-C(65)-H(65)	119.6

C(45)-C(41)-P(2)	123.5(3)	N(1)-C(1)-S(1)	178.6(4)
C(42)-C(41)-Fe(2)	69.5(2)	C(14)-C(13)-C(12)	120.0(4)
C(45)-C(41)-Fe(2)	69.7(2)	C(14)-C(13)-H(13)	120.0
P(2)-C(41)-Fe(2)	123.25(19)	C(12)-C(13)-H(13)	120.0
C(43)-C(44)-C(45)	108.4(3)	N(2)-C(2)-S(2)	177.9(4)
C(43)-C(44)-Fe(2)	70.2(2)	C(35)#1-Fe(1)-C(35)	107.4(2)
C(45)-C(44)-Fe(2)	69.3(2)	C(35)#1-Fe(1)-C(31)	115.71(14)
C(43)-C(44)-H(44)	125.8	C(35)-Fe(1)-C(31)	41.29(13)
C(45)-C(44)-H(44)	125.8	C(35)#1-Fe(1)-C(31)#1	41.29(13)
Fe(2)-C(44)-H(44)	126.3	C(35)-Fe(1)-C(31)#1	115.71(14)
C(44)-C(43)-C(42)	108.7(3)	C(31)-Fe(1)-C(31)#1	148.9(2)
C(35)#1-Fe(1)-C(32)	149.41(14)	C(42)-Fe(2)-C(45)	68.82(15)
C(35)-Fe(1)-C(32)	69.01(14)	C(42)#2-Fe(2)-C(45)	148.55(14)
C(31)-Fe(1)-C(32)	41.24(14)	C(41)#2-Fe(2)-C(45)#2	41.33(14)
C(31)#1-Fe(1)-C(32)	168.46(15)	C(41)-Fe(2)-C(45)#2	169.04(15)
C(35)#1-Fe(1)-C(32)#1	69.01(14)	C(42)-Fe(2)-C(45)#2	148.55(14)
C(35)-Fe(1)-C(32)#1	149.41(14)	C(42)#2-Fe(2)-C(45)#2	68.82(15)
C(31)-Fe(1)-C(32)#1	168.46(14)	C(45)-Fe(2)-C(45)#2	129.5(2)
C(31)#1-Fe(1)-C(32)#1	41.24(14)	C(41)#2-Fe(2)-C(44)#2	68.56(14)
C(32)-Fe(1)-C(32)#1	129.7(2)	C(41)-Fe(2)-C(44)#2	130.78(14)
C(35)#1-Fe(1)-C(34)#1	40.83(14)	C(42)-Fe(2)-C(44)#2	170.48(14)
C(35)-Fe(1)-C(34)#1	130.05(15)	C(42)#2-Fe(2)-C(44)#2	68.08(15)
C(31)-Fe(1)-C(34)#1	108.05(14)	C(45)-Fe(2)-C(44)#2	108.02(15)
C(31)#1-Fe(1)-C(34)#1	68.82(14)	C(45)#2-Fe(2)-C(44)#2	40.29(14)
C(32)-Fe(1)-C(34)#1	117.07(14)	C(41)#2-Fe(2)-C(44)	130.78(14)
C(32)#1-Fe(1)-C(34)#1	68.05(14)	C(41)-Fe(2)-C(44)	68.56(14)
C(35)#1-Fe(1)-C(34)	130.05(15)	C(42)-Fe(2)-C(44)	68.08(15)
C(35)-Fe(1)-C(34)	40.83(14)	C(42)#2-Fe(2)-C(44)	170.48(14)
C(31)-Fe(1)-C(34)	68.82(14)	C(45)-Fe(2)-C(44)	40.29(14)
C(31)#1-Fe(1)-C(34)	108.05(14)	C(45)#2-Fe(2)-C(44)	108.02(15)
C(32)-Fe(1)-C(34)	68.05(14)	C(44)#2-Fe(2)-C(44)	115.8(2)
C(32)#1-Fe(1)-C(34)	117.07(14)	C(41)#2-Fe(2)-C(43)#2	68.24(14)
C(34)#1-Fe(1)-C(34)	169.0(2)	C(41)-Fe(2)-C(43)#2	109.31(14)
C(35)#1-Fe(1)-C(33)	168.35(14)	C(42)-Fe(2)-C(43)#2	132.56(15)
C(35)-Fe(1)-C(33)	68.14(15)	C(42)#2-Fe(2)-C(43)#2	40.39(14)
C(31)-Fe(1)-C(33)	68.65(14)	C(45)-Fe(2)-C(43)#2	116.33(15)
C(31)#1-Fe(1)-C(33)	129.74(14)	C(45)#2-Fe(2)-C(43)#2	67.64(15)
C(32)-Fe(1)-C(33)	40.53(14)	C(44)#2-Fe(2)-C(43)#2	39.88(15)
C(32)#1-Fe(1)-C(33)	108.93(15)	C(44)-Fe(2)-C(43)#2	147.79(15)
C(34)#1-Fe(1)-C(33)	150.10(15)	C(41)#2-Fe(2)-C(43)	109.31(14)
C(34)-Fe(1)-C(33)	39.76(15)	C(41)-Fe(2)-C(43)	68.24(14)
C(35)#1-Fe(1)-C(33)#1	68.14(15)	C(42)-Fe(2)-C(43)	40.39(14)
C(35)-Fe(1)-C(33)#1	168.35(15)	C(42)#2-Fe(2)-C(43)	132.56(15)
C(31)-Fe(1)-C(33)#1	129.74(14)	C(45)-Fe(2)-C(43)	67.64(15)
C(31)#1-Fe(1)-C(33)#1	68.65(14)	C(45)#2-Fe(2)-C(43)	116.33(15)
C(32)-Fe(1)-C(33)#1	108.93(15)	C(44)#2-Fe(2)-C(43)	147.79(15)
C(32)#1-Fe(1)-C(33)#1	40.53(14)	C(44)-Fe(2)-C(43)	39.88(15)
C(34)#1-Fe(1)-C(33)#1	39.76(15)	C(43)#2-Fe(2)-C(43)	171.5(2)
C(34)-Fe(1)-C(33)#1	150.10(16)	C(13)-C(14)-C(15)	120.2(4)
C(33)-Fe(1)-C(33)#1	118.3(2)	C(13)-C(14)-H(14)	119.9
P(1)-Au(1)-S(1)	173.21(3)	C(15)-C(14)-H(14)	119.9
P(1)-Au(1)-Au(2)	94.69(2)	C(11)-C(16)-C(15)	120.0(4)
S(1)-Au(1)-Au(2)	91.89(3)	C(11)-C(16)-H(16)	120.0

P(2)-Au(2)-S(2)	170.13(3)	C(15)-C(16)-H(16)	120.0
P(2)-Au(2)-Au(1)	106.35(3)	C(41)-P(2)-C(51)	107.29(16)
S(2)-Au(2)-Au(1)	83.51(3)	C(41)-P(2)-C(61)	107.91(17)
C(41)#2-Fe(2)-C(41)	148.6(2)	C(51)-P(2)-C(61)	101.81(16)
C(41)#2-Fe(2)-C(42)	116.24(14)	C(41)-P(2)-Au(2)	106.59(12)
C(41)-Fe(2)-C(42)	41.06(14)	C(51)-P(2)-Au(2)	113.69(12)
C(41)#2-Fe(2)-C(42)#2	41.06(14)	C(61)-P(2)-Au(2)	118.96(12)
C(41)-Fe(2)-C(42)#2	116.24(14)	C(33)-C(34)-C(35)	108.3(3)
C(42)-Fe(2)-C(42)#2	109.6(2)	C(33)-C(34)-Fe(1)	70.3(2)
C(41)#2-Fe(2)-C(45)	169.04(15)	C(35)-C(34)-Fe(1)	68.5(2)
C(41)-Fe(2)-C(45)	41.33(14)	C(33)-C(34)-H(34)	125.8
C(35)-C(34)-H(34)	125.8	C(23)-C(22)-H(22)	119.9
Fe(1)-C(34)-H(34)	126.9	C(21)-C(22)-H(22)	119.9
C(31)-P(1)-C(21)	107.41(16)	C(24)-C(23)-C(22)	119.5(4)
C(31)-P(1)-C(11)	106.08(17)	C(24)-C(23)-H(23)	120.3
C(21)-P(1)-C(11)	107.50(17)	C(22)-C(23)-H(23)	120.3
C(31)-P(1)-Au(1)	107.01(12)	C(56)-C(55)-C(54)	120.3(4)
C(21)-P(1)-Au(1)	114.07(12)	C(56)-C(55)-H(55)	119.9
C(11)-P(1)-Au(1)	114.27(12)	C(54)-C(55)-H(55)	119.9
C(1)-S(1)-Au(1)	95.24(13)	C(25)-C(24)-C(23)	120.6(4)
C(2)-S(2)-Au(2)	97.12(14)	C(25)-C(24)-H(24)	119.7
C(53)-C(52)-C(51)	120.0(3)	C(23)-C(24)-H(24)	119.7
C(53)-C(52)-H(52)	120.0	C(25)-C(26)-C(21)	120.5(3)
C(51)-C(52)-H(52)	120.0	C(25)-C(26)-H(26)	119.8
C(26)-C(21)-C(22)	119.1(3)	C(21)-C(26)-H(26)	119.8
C(26)-C(21)-P(1)	121.2(3)	C(54)-C(53)-C(52)	119.9(4)
C(22)-C(21)-P(1)	119.6(3)	C(54)-C(53)-H(53)	120.0
C(55)-C(56)-C(51)	119.8(4)	C(52)-C(53)-H(53)	120.0
C(55)-C(56)-H(56)	120.1	C(53)-C(54)-C(55)	120.2(4)
C(51)-C(56)-H(56)	120.1	C(53)-C(54)-H(54)	119.9
C(23)-C(22)-C(21)	120.3(3)	C(55)-C(54)-H(54)	119.9

Symmetry transformations used to generate equivalent atoms: #1 (-x+2,y,-z+3/2), #2 (-x+2,y,-z+1/2).

Table B.5.3 Anisotropic displacement parameters ($Å^2$ x 10^3) for $[(AuSCN)_2(\mu\text{-dppf})]$. The anisotropic displacement factor exponent takes the form: $-2\pi^2[h^2a^{*2}U11 + ... + 2hka^*b^*U12]$.

	U11	U22	U33	U23	U13	U12
C(31)	14(2)	18(2)	8(2)	-2(1)	2(1)	-2(1)
C(32)	20(2)	15(2)	11(2)	-2(1)	3(1)	-2(1)
C(51)	19(2)	14(2)	7(2)	3(1)	4(1)	1(1)
C(25)	30(2)	14(2)	20(2)	0(2)	14(2)	1(2)
C(35)	15(2)	17(2)	10(2)	-1(1)	2(1)	3(1)
C(33)	21(2)	22(2)	14(2)	-4(2)	4(2)	-7(2)
C(42)	16(2)	16(2)	12(2)	0(1)	4(1)	-1(1)
C(41)	21(2)	15(2)	9(2)	0(1)	7(1)	1(1)
C(44)	28(2)	19(2)	13(2)	4(2)	9(2)	9(2)
C(43)	20(2)	24(2)	11(2)	4(2)	6(2)	5(2)
C(45)	30(2)	16(2)	13(2)	1(1)	12(2)	4(2)
C(61)	21(2)	15(2)	11(2)	-1(1)	9(1)	1(1)
C(62)	16(2)	34(2)	14(2)	6(2)	0(2)	-1(2)
C(66)	24(2)	43(3)	23(2)	17(2)	6(2)	5(2)

C(11)	19(2)	19(2)	11(2)	1(1)	7(1)	7(2)
C(12)	26(2)	28(2)	15(2)	7(2)	2(2)	-1(2)
C(63)	31(2)	33(2)	17(2)	11(2)	5(2)	-4(2)
C(64)	26(2)	45(3)	29(2)	13(2)	14(2)	-6(2)
C(15)	27(2)	38(2)	17(2)	-4(2)	-3(2)	-1(2)
C(65)	14(2)	71(4)	42(3)	29(3)	5(2)	3(2)
N(1)	35(2)	31(2)	28(2)	8(2)	14(2)	10(2)
C(1)	21(2)	18(2)	24(2)	0(2)	6(2)	6(2)
C(13)	33(2)	32(2)	18(2)	14(2)	7(2)	9(2)
C(2)	17(2)	18(2)	32(2)	-4(2)	7(2)	0(2)
Fe(1)	15(1)	12(1)	7(1)	0	4(1)	0
Au(1)	19(1)	15(1)	9(1)	0(1)	6(1)	3(1)
Au(2)	21(1)	17(1)	8(1)	-2(1)	6(1)	-3(1)
Fe(2)	21(1)	11(1)	7(1)	0	6(1)	0
C(14)	29(2)	41(3)	13(2)	7(2)	4(2)	15(2)
C(16)	28(2)	25(2)	18(2)	2(2)	3(2)	-1(2)
P(2)	19(1)	13(1)	7(1)	0(1)	5(1)	1(1)
C(34)	11(2)	24(2)	12(2)	0(2)	2(1)	-2(1)
P(1)	17(1)	13(1)	7(1)	1(1)	4(1)	2(1)
S(1)	29(1)	26(1)	21(1)	2(1)	14(1)	11(1)
N(2)	34(2)	26(2)	44(2)	9(2)	8(2)	5(2)
S(2)	31(1)	30(1)	17(1)	-7(1)	6(1)	-13(1)
C(52)	22(2)	17(2)	11(2)	2(1)	6(2)	-2(2)
C(21)	21(2)	13(2)	9(2)	0(1)	6(1)	-2(1)
C(56)	23(2)	18(2)	10(2)	3(1)	4(2)	1(2)
C(22)	22(2)	18(2)	14(2)	1(1)	10(2)	1(2)
C(23)	18(2)	26(2)	17(2)	0(2)	6(2)	-6(2)
C(55)	30(2)	18(2)	15(2)	-2(2)	1(2)	2(2)
C(24)	28(2)	20(2)	18(2)	-5(2)	9(2)	-7(2)
C(26)	18(2)	15(2)	17(2)	1(1)	10(2)	1(1)
C(53)	21(2)	22(2)	15(2)	4(2)	9(2)	3(2)
C(54)	31(2)	22(2)	17(2)	1(2)	8(2)	10(2)

Table B.5.4 Hydrogen coordinates (x 10^4) and isotropic displacement parameters (Å^2 x 10^3) for [$(AuSCN)_2$(μ-dppf)].

	x	y	z	U(eq)
H(32)	9606	1653	6422	19
H(25)	10309	5395	7059	24
H(35)	9041	3573	7004	17
H(33)	8771	1474	7184	23
H(42)	8979	1385	2437	18
H(44)	8806	3496	2155	24
H(43)	8455	2335	1602	22
H(45)	9517	3288	3349	22
H(62)	9956	950	4987	27
H(66)	8073	1690	3489	37
H(12)	9855	4345	5234	29
H(63)	9018	328	5348	33
H(64)	7614	392	4796	39
H(15)	7685	2864	4170	36
H(65)	7145	1061	3869	52
H(13)	8950	4644	4214	34

H(14)	7879	3899	3683	34
H(16)	8582	2559	5189	30
H(34)	8423	2643	7540	19
H(52)	11626	1422	4243	20
H(56)	9469	460	3300	21
H(22)	11779	3497	6654	20
H(23)	12479	4417	7304	24
H(55)	10202	-474	3072	27
H(24)	11736	5353	7514	26
H(26)	9605	4467	6439	19
H(53)	12353	488	3998	22
H(54)	11639	-439	3383	28